WOMEN IN SCIENCE - OPHTHALMOLOGY 2021

EDITED BY: Menaka Chanu Thounaojam
PUBLISHED IN: Frontiers in Medicine

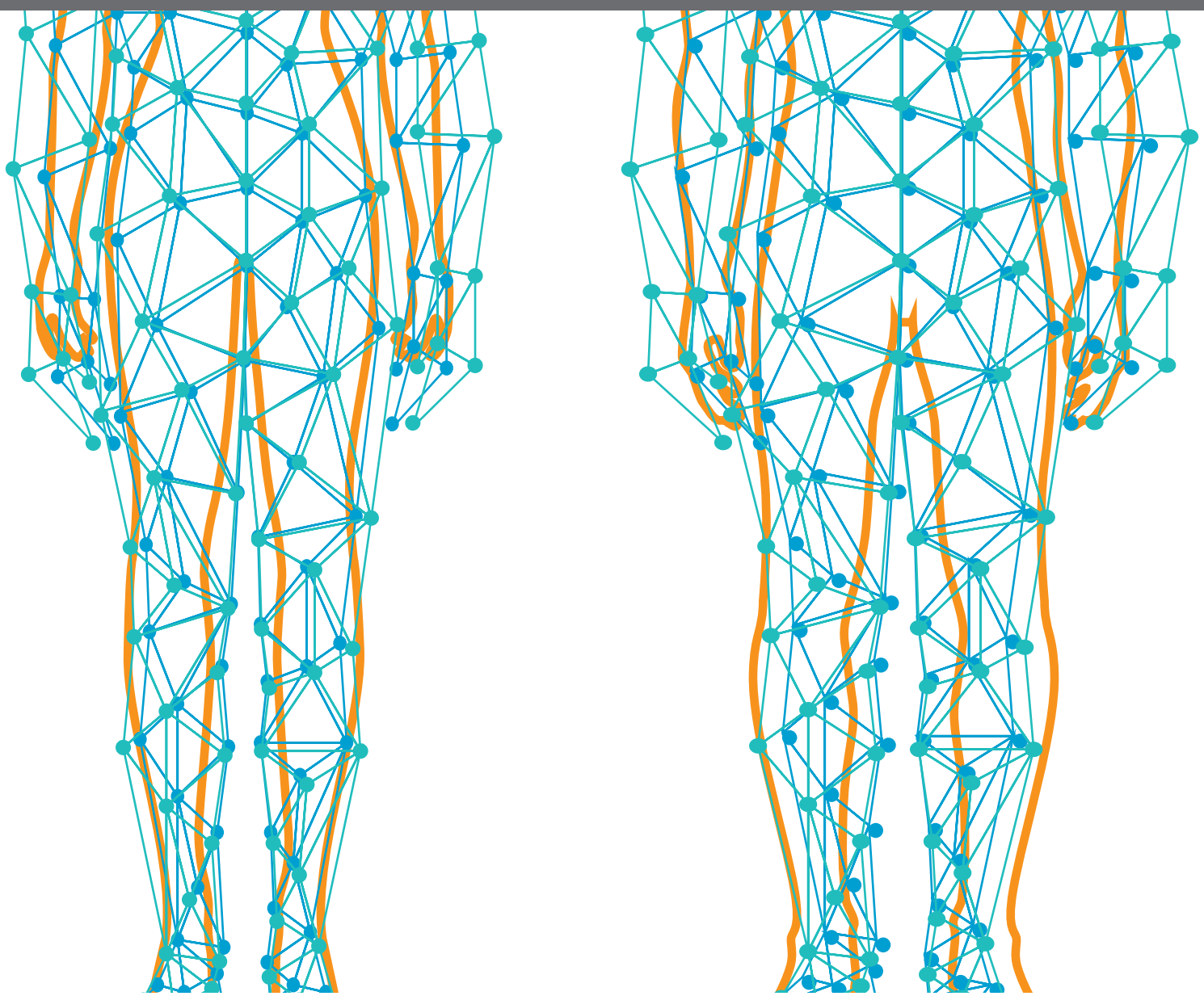

frontiers Research Topics

frontiers

ISSN 1664-8714
ISBN 978-2-88976-634-5
DOI 10.3389/978-2-88976-634-5

About Frontiers

Frontiers is more than just an open-access publisher of scholarly articles: it is a pioneering approach to the world of academia, radically improving the way scholarly research is managed. The grand vision of Frontiers is a world where all people have an equal opportunity to seek, share and generate knowledge. Frontiers provides immediate and permanent online open access to all its publications, but this alone is not enough to realize our grand goals.

Frontiers Journal Series

The Frontiers Journal Series is a multi-tier and interdisciplinary set of open-access, online journals, promising a paradigm shift from the current review, selection and dissemination processes in academic publishing. All Frontiers journals are driven by researchers for researchers; therefore, they constitute a service to the scholarly community. At the same time, the Frontiers Journal Series operates on a revolutionary invention, the tiered publishing system, initially addressing specific communities of scholars, and gradually climbing up to broader public understanding, thus serving the interests of the lay society, too.

Dedication to Quality

Each Frontiers article is a landmark of the highest quality, thanks to genuinely collaborative interactions between authors and review editors, who include some of the world's best academicians. Research must be certified by peers before entering a stream of knowledge that may eventually reach the public - and shape society; therefore, Frontiers only applies the most rigorous and unbiased reviews.
Frontiers revolutionizes research publishing by freely delivering the most outstanding research, evaluated with no bias from both the academic and social point of view. By applying the most advanced information technologies, Frontiers is catapulting scholarly publishing into a new generation.

What are Frontiers Research Topics?

Frontiers Research Topics are very popular trademarks of the Frontiers Journals Series: they are collections of at least ten articles, all centered on a particular subject. With their unique mix of varied contributions from Original Research to Review Articles, Frontiers Research Topics unify the most influential researchers, the latest key findings and historical advances in a hot research area! Find out more on how to host your own Frontiers Research Topic or contribute to one as an author by contacting the Frontiers Editorial Office: frontiersin.org/about/contact

WOMEN IN SCIENCE - OPHTHALMOLOGY 2021

Topic Editor:
Menaka Chanu Thounaojam, Augusta University, United States

Citation: Thounaojam, M. C., ed. (2022). Women in Science - Ophthalmology 2021. Lausanne: Frontiers Media SA. doi: 10.3389/978-2-88976-634-5

Table of Contents

frontiers | Frontiers in Medicine

EDITORIAL
published: 30 June 2022
doi: 10.3389/fmed.2022.966392

Editorial: Women in Science - Ophthalmology 2021

Menaka C. Thounaojam [1,2]*

[1] Department of Ophthalmology, Medical College of Georgia, Augusta University, Augusta, GA, United States, [2] James and Jean Culver Vision Discovery Institute, Medical College of Georgia, Augusta University, Augusta, GA, United States

Keywords: Ophthalmology, UNESCO, stem, public health, medicine

Editorial on the Research Topic

Women in Science - Ophthalmology 2021

According to 2016 data from the UNESCO Institute for Statistics (UIS), women make up fewer than 30% of science, technology, engineering, and mathematics (STEM) researchers. Although, at the undergraduate level, the proportion of women and men studying STEM is roughly equal, women are underrepresented in top positions in medicine[1]. Nevertheless, many extremely influential and accomplished women in the field of Ophthalmology are contributing to the field and solving important questions. On the other hand, female scientists continue to be underrepresented in various facets of academic life. Several initiatives to promote the visibility of women in science have lately been launched (e.g., awards for women in STEM). Under-representation, income disparities, and increased career-related problems continue to be obstacles for women in scientific disciplines. Despite decades of progress, the COVID-19 pandemic has exacerbated these issues, emphasizing the so-called "leaky pipeline," a model that depicts how women in science, technology, engineering, and mathematics (STEM) have missed opportunities due to gender bias and structural barriers (1). The COVID-19 pandemic also widened the gender divide in academic publishing (2). Even though female academic participation in Ophthalmology has increased in past decades, recent findings demonstrate that COVID-19 has reversed this trend. During the pandemic, women's contributions to COVID-19 Ophthalmology scholarship were much lower than predicted, particularly in senior roles (2). This Research Topic is aimed to create the frame for promoting and recognizing the scientific achievements of women researchers in Medicine, specifically in the field of Ophthalmology. Herein, we discuss 11 accepted articles wherein either the first or corresponding author identifies as female, collectively representing multiple countries worldwide.

Consistent with the theme of this Research Topic, Cao et al. evaluated the extent of the gender gap in citations in Ophthalmology literature between August 2015 and July 2020. This study suggested that despite the increase in female-led papers from August 2015 to July 2020, the proportion was still found to be much lower than that of the male-led papers. With the recent worldwide SARS-CoV-2 pandemic, several papers developed novel diagnostic tools for COVID-19 based on either molecular or imaging data. Hohberger et al. used Optical coherence tomography angiography (OCT-A) to evaluate the changes in the retinal vasculature and proposed that OCT-A observations could be correlated with systemic microcirculation and serve as clinical markers of severity of COVID-19 disease.

[1] http://uis.unesco.org/en/topic/women-science

OPEN ACCESS

Edited and reviewed by:
Jodhbir Mehta, Singapore National Eye Center, Singapore

***Correspondence:**
Menaka C. Thounaojam
mthounaojam@augusta.edu

Specialty section:
This article was submitted to Ophthalmology, a section of the journal Frontiers in Medicine

Received: *10 June 2022*
Accepted: *20 June 2022*
Published: *30 June 2022*

Citation:
Thounaojam MC (2022) Editorial: Women in Science - Ophthalmology 2021. Front. Med. 9:966392. doi: 10.3389/fmed.2022.966392

This Research Topic also included two case reports on two genetic conditions, a congenital disorder of glycosylation-Ia and CAFDADD syndrome (Cardiac, facial, and digital anomalies with developmental delay). A case presented by Midena and Pilotto confirmed the essential role of multimodal retinal imaging, a non-invasive way to provide new insights into the retinal involvement of patients affected by CDG-Ia. Additionally, multimodal retinal imaging associated CDG-Ia with multiple, bilateral, calcific retinal astrocytic hamartomas. A case report by Paprocka et al. detected *de novo* variant c.1708C>G [p.(His570Asp)] in TRAF7 in two pediatric patients with the very rare CAFDADD syndrome. Their studies indicated that a TRAF7 mutation should be evaluated in patients with characteristic dysmorphic features, especially within the palpebral fissure (blepharophimosis and/or ptosis), congenital defects of the heart and skeleton, and psychomotor delay.

Two of the articles on the utility and proper clinical usage of pattern electroretinogram and *in vivo* confocal microscopy for better patient data interpretation were also included in this Research Topic. Firstly, a study by Friedel et al. evaluated potentially more feasible procedures for PERG recordings in daily diagnostics in psychiatry. The authors were able to methodologically improve the recording procedure by demonstrating the suitability of a higher stimulation frequency for recordings and introducing an interpersonal normalization approach for the PERG signals, further enhancing the sensitivity of the method. Next, a study by Zhang et al. reported that to minimize the likelihood of under-sampling at the participant level of a study, the average cell density value from quantifying 12 random, non-overlapping IVCM images ($400 \times 400\,\mu m$) should be used for corneal epithelial IC density estimates for the central cornea, and seven equivalent images should be used for the peripheral cornea instead of the traditional "three representative images" approach.

Three more clinical studies with significant findings for myopia, primary open-angle glaucoma, and diabetic retinopathy were published. In China, vitamin D insufficiency is far more common than in other countries. Li et al. conducted a study to see if vitamin D is linked to myopia in these two groups of participants, who had different vitamin D levels due to various diets and sun exposure. They discovered that total serum vitamin D content does not affect myopia growth in Chinese children and adolescents, which suggests that the links between outdoor exposure and myopia progression should be investigated further. Improved medication adherence in the days leading up to clinic visits is referred to as whitecoat adherence. Poleon et al. conducted research to assess and identify parameters linked to whitecoat adherence. Within 3 days of the clinic appointment, they noticed a considerable increase in adherence. According to the authors, patients with higher levels of adherence may also have higher levels of healthcare engagement, prompting them to focus more significantly on their adherence, particularly before the clinic appointment. Tear fluid biomarkers may provide a non-invasive technique for diagnosing diabetic patients at risk of developing diabetic retinopathy (DR), improving diagnostic accuracy and understanding of the disease's etiology. Amorim et al. looked at the tear fluid of non-diabetic individuals, diabetic patients with no DR, and diabetic patients with non-proliferative DR (NPDR) or proliferative DR (PDR) to see if there were any potential biomarkers for DR diagnosis and staging. They discovered alterations in many proteins in tear fluid linked to various biological processes related to DR, such as oxidative stress, immunological response, and inflammation. The authors also urged that their findings be validated in a more extensive study with a larger sample size and suggested that the identification of a set of biomarkers could improve the early diagnosis of DR and assure quick treatment for this vision-threatening disease.

Finally, two review pieces were published in this Research Topic. To begin, Adamus examined the role of immunological reactions in the course of retinal degeneration caused by gene mutations. Inherited retinal diseases (IRDs) are a group of clinically and genetically diverse uncommon disorders that cause retinal malfunction and photoreceptor cell death, resulting in blindness. Retinitis pigmentosa (RP), which affects 1 in every 4,000 people worldwide, is one of the most common and severe forms of these retinopathies. This review paper meticulously assembled pertinent research and offers insight into the present function of autoimmunity/immunity in RP pathogenesis. Ocriplasmin is a recombinant protease that can be injected into the vitreous cavity to treat this illness; however, there is still debate about its efficacy and safety, especially regarding patient selection. Chen et al. conducted a comprehensive analysis of articles published before August 2020 to determine the efficacy and safety of ocriplasmin treatment on symptomatic vitreomacular adhesion (sVMA). The authors concluded that ocriplasmin is a viable treatment option for sVMA based on evidence from five randomized controlled trials and 50 cohort studies.

While the pandemic has reformed the workspaces and increased challenges in female authorship, more efforts are required to bridge the gender gap. In this regard, this Research Topic is a small effort to acknowledge the contribution of excellent female scientists worldwide in the field of Ophthalmology.

AUTHOR CONTRIBUTIONS

The author confirms being the sole contributor of this work and has approved it for publication.

ACKNOWLEDGMENTS

With great pleasure and respect, we extend our thanks to the reviewers for the critical assessment of each paper, their constructive criticisms, and timely response that made this Research Topic possible.

REFERENCES

1. Shah A, Lopez I, Surner B, Sarkar S, Duthely LM, Pillai A, et al. Turning the tide for academic women in STEM: a postpandemic vision for supporting female scientists. *ACS Nano*. (2021) 15:18647–52. doi: 10.1021/acsnano.1c09686
2. Nguyen AX, Trinh XV, Kurian J, Wu AY. Impact of COVID-19 on longitudinal ophthalmology authorship gender trends. *Graefes Arch Clin Exp Ophthalmol*. (2021) 259:733–44. doi: 10.1007/s00417-021-05085-4

Conflict of Interest: The author declares that the research was conducted in the absence of any commercial or financial relationships that could be construed as a potential conflict of interest.

Publisher's Note: All claims expressed in this article are solely those of the authors and do not necessarily represent those of their affiliated organizations, or those of the publisher, the editors and the reviewers. Any product that may be evaluated in this article, or claim that may be made by its manufacturer, is not guaranteed or endorsed by the publisher.

frontiers in Medicine

ORIGINAL RESEARCH
published: 09 July 2021
doi: 10.3389/fmed.2021.676554

Retinal Microcirculation as a Correlate of a Systemic Capillary Impairment After Severe Acute Respiratory Syndrome Coronavirus 2 Infection

Bettina Hohberger[1†], Marion Ganslmayer[2†], Marianna Lucio[3], Friedrich Kruse[1], Jakob Hoffmanns[1], Michael Moritz[1], Lennart Rogge[1], Felix Heltmann[1], Charlotte Szewczykowski[1], Julia Fürst[2], Maximilian Raftis[1], Antonio Bergua[1], Matthias Zenkel[1], Andreas Gießl[1], Ursula Schlötzer-Schrehardt[1], Paul Lehmann[1], Richard Strauß[2‡], Christian Mardin[1‡] and Martin Herrmann[4‡]*

[1] Department of Ophthalmology, University of Erlangen-Nürnberg, Friedrich-Alexander-University of Erlangen-Nürnberg, Erlangen, Germany, [2] Department of Internal Medicine 1, University of Erlangen-Nürnberg, Friedrich-Alexander-University of Erlangen-Nürnberg, Erlangen, Germany, [3] Research Unit Analytical BioGeoChemistry, Helmholtz Zentrum München-German Research Center for Environmental Health, Neuherberg, Germany, [4] Department of Internal Medicine 3, University of Erlangen-Nürnberg, Friedrich-Alexander-University of Erlangen-Nürnberg, Erlangen, Germany

OPEN ACCESS

Edited by:
Masaru Takeuchi, National Defense Medical College, Japan

Reviewed by:
Carlo Gesualdo, Università della Campania Luigi Vanvitelli, Italy
Folami Powell, Augusta University, United States

***Correspondence:**
Bettina Hohberger
bettina.hohberger@uk-erlangen.de

[†]These authors share first authorship

[‡]These authors share senior authorship

Specialty section:
This article was submitted to Ophthalmology, a section of the journal Frontiers in Medicine

Received: *05 March 2021*
Accepted: *08 June 2021*
Published: *09 July 2021*

Citation:
Hohberger B, Ganslmayer M, Lucio M, Kruse F, Hoffmanns J, Moritz M, Rogge L, Heltmann F, Szewczykowski C, Fürst J, Raftis M, Bergua A, Zenkel M, Gießl A, Schlötzer-Schrehardt U, Lehmann P, Strauß R, Mardin C and Herrmann M (2021) Retinal Microcirculation as a Correlate of a Systemic Capillary Impairment After Severe Acute Respiratory Syndrome Coronavirus 2 Infection. Front. Med. 8:676554. doi: 10.3389/fmed.2021.676554

Severe acute respiratory syndrome coronavirus 2 (SARS-CoV-2), which causes coronavirus disease 2019 (COVID-19), affects the pulmonary systems via angiotensin-converting enzyme-2 (ACE-2) receptor, being an entry to systemic infection. As COVID-19 disease features ACE-2 deficiency, a link to microcirculation is proposed. Optical coherence tomography angiography (OCT-A) enables non-invasive analysis of retinal microvasculature. Thus, an impaired systemic microcirculation might be mapped on retinal capillary system. As recent OCT-A studies, analyzing microcirculation in two subdivided layers, yielded contrary results, an increased subdivision of retinal microvasculature might offer an even more fine analysis. The aim of the study was to investigate retinal microcirculation by OCT-A after COVID-19 infection in three subdivided layers (I). In addition, short-term retinal affections were monitored during COVID-19 disease (II). Considering (I), a prospective study (33 patients$_{post-COVID}$ and 28 controls) was done. Macula and peripapillary vessel density (VD) were scanned with the Spectralis II. Macula VD was measured in three layers: superficial vascular plexus (SVP), intermediate capillary plexus (ICP), and deep capillary plexus (DCP). Analysis was done by the EA-Tool, including an Anatomical Positioning System and an analysis of peripapillary VD by implementing Bruch's membrane opening (BMO) landmarks. Overall, circular (c_1, c_2, and c_3) and sectorial VD (s_1-s_{12}) was analyzed. Considering (II), in a retrospective study, 29 patients with severe complications of COVID-19 infection, hospitalized at the intensive care unit, were monitored for retinal findings at bedside during hospitalization. (I) Overall ($p = 0.0133$) and circular (c_1, $p = 0.00257$; c_2, $p = 0.0067$; and c_3, $p = 0.0345$). VD of the ICP was significantly reduced between patients$_{post-COVID}$ and controls, respectively. Overall ($p = 0.0179$) and circular (c_1, $p = 0.0189$)

peripapillary VD was significantly reduced between both groups. Subgroup analysis of hospitalized vs. non-hospitalized patients$_{post-COVID}$ yielded a significantly reduced VD of adjacent layers (DCP and SVP) with increased severity of COVID-19 disease. Clinical severity parameters showed a negative correlation with VD (ICP) and peripapillary VD. (II) Funduscopy yielded retinal hemorrhages and cotton wool spots in 17% of patients during SARS-CoV-2 infection. As VD of the ICP and peripapillary regions was significantly reduced after COVID-19 disease and showed a link to clinical severity markers, we assume that the severity of capillary impairment after COVID-19 infection is mapped on retinal microcirculation, visualized by non-invasive OCT-A.

Keywords: OCT-angiography, COVID-19, SARS-CoV-2, retina, macula, optic nerve head, microcirculation

INTRODUCTION

In December 2019, several cases of a severe and unknown pneumonia were diagnosed in Wuhan (1). Severe acute respiratory syndrome coronavirus 2 (SARS-CoV-2) was identified as a disease causative agent, and clinical features were summarized as coronavirus disease 2019 (COVID-19). Ranking to a worldwide healthcare problem, COVID-19 pandemic was declared on March 11, 2020. On the molecular basis, SARS-CoV-2 enters human cells via the angiotensin-converting enzyme-2 (ACE-2) receptor (2, 3). After binding via receptor-binding domain of the spike protein, a target cell protease splits the spike, enabling virus entry mediated by the spike fusion peptide (4–6). The natural target of the ACE-2 receptor, ACE-2, was first discovered in 2000 (7). ACE-2, part of the renin–angiotensin system (RAS), converts angiotensin II (Ang II) to angiotensin (Ang)-1-7. ACE-2 and Ang-1-7 are assumed to prevent atherosclerosis and protect endothelial cells via inhibition of inflammation (8). The latter one was seen to reduce oxidative stress via the MAS receptor (9, 10). Several studies have suggested a link of ACE-2 to vascular diseases (11, 12). Considering this, ACE-2 deficiency consecutively was observed to cause vascular inflammation and atherosclerosis (8, 13). In addition, e.g., expression of adhesion molecules (e.g., VCAM), monocyte chemoattractant protein-1 (MCP-1), and interleukin 6 (IL-6) were significantly increased (8, 14, 15). It is hypothesized that SARS-CoV-2 targeting the ACE-2 receptor features molecular characteristics of ACE-2 deficiency (16, 17).

Data on ACE-2 and its receptor in human retina are rare in literature up to now. The ACE-2 protein was detected in human retina by Western blotting analysis (18). Structural analysis in animal models (rodent and porcine) indicated that ACE-2 is present in the inner granular and nuclear layers (19, 20). Thus, it is assumed that involvement of SARS-CoV-2 might also be present in the retina itself. If we assume that SARS-CoV-2 infection might mimic an ACE-2 deficiency, we hypothesize that retinal microcirculation might be affected, especially, in the inner granular and nuclear layers. In addition, during COVID-19, the circulating neutrophils are activated, and the population of low-density granulocytes is highly increased. These cells are prone to form neutrophil extracellular traps (NETs). The latter have been shown to occlude pulmonary vessels in active COVID-19, which is referred to as immunothrombosis. Hepatic and glomerular vessels were also affected (21–23). We hypothesized that this kind of vasculopathy may also affect retinal microvasculature.

Optical coherence tomography angiography (OCT-A) is a non-invasive technique, visualizing retinal microcirculation. Several devices can be used right now, most of them analyzing vessel density (VD) and characteristics of microcirculation in two different retinochoroidal layers (superior vs. deep). Up to now, there is only one device available (Spectralis II; Heidelberg Engineering, Heidelberg, Germany) enabling analysis of retinal microcirculation in three layers with high resolution: superficial vascular plexus (SVP), intermediate capillary plexus (ICP), and deep capillary plexus (DCP). Those three layers correlate well with human anatomy (24). The SVP correlates with the ganglion cell layer (GCL) and part of the inner plexiform layer (IPL), the ICP with part of the IPL and inner nuclear layer (INL), and the DCP with part of the INL and outer plexiform layer (OPL), respectively (**Figure 1A**). This more fine resolution of OCT-A data enables an even more detailed analysis of retinal microcirculation. Recent studies investigated changes in retinal microcirculation early after COVID-19 infection (2 weeks until 1 month) by OCT-A devices, subdividing the OCT-A scan into two layers (superficial retinal capillary plexus and deep retinal capillary plexus) (25, 26). Thus, it was the aim of the present study to investigate retinal microvasculature of the macula, subdivided into three retinal layers, and peripapillary region in patients after long-term COVID-19 infection as compared with control eyes. In addition, short-term alterations of retinal findings and clinical outcome were monitored in patients with severe COVID-19 complications.

METHODS

Subjects

Long-Term Effect of Coronavirus Disease 2019 Infection on Retinal Microcirculation

A prospective study was done analyzing long-term effects of COVID-19 infection on retinal microcirculation: 61 eyes of 61 persons were included: 33 eyes of patients$_{post-COVID}$ (13 females and 20 males) and 28 control eyes (20 females and 8 males).

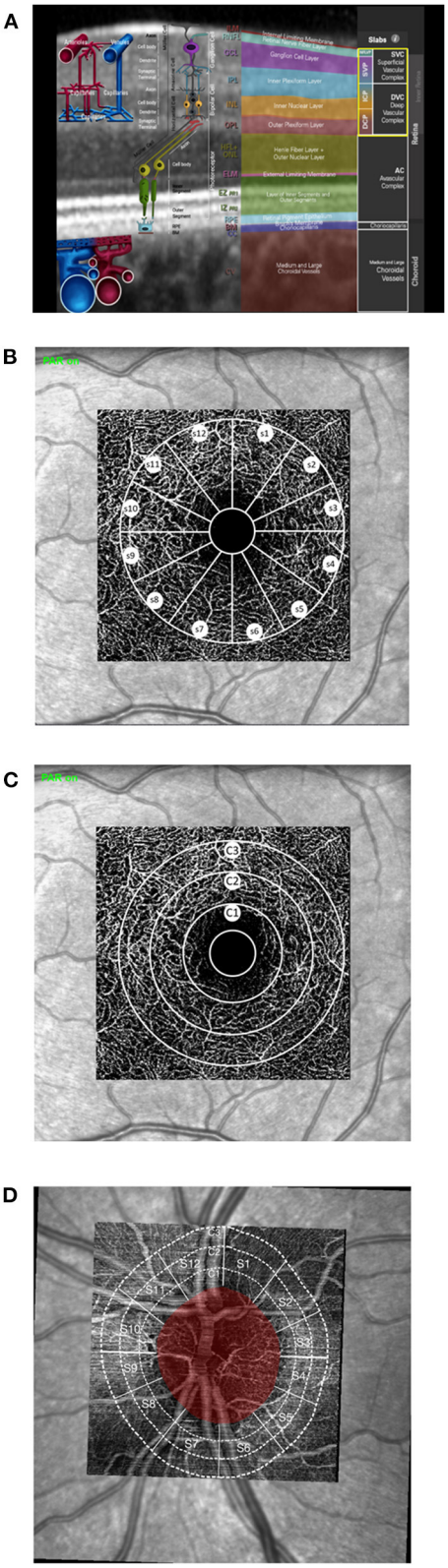

FIGURE 1 | Morphometric and quantitative analyses of optical coherence tomography angiography (OCT-A): **(A)** anatomic correlation of retinal layers to superficial capillary plexus (SVP), intermediate capillary plexus (ICP), and deep *(Continued)*

FIGURE 1 | capillary plexus (DCP; image courtesy by Heidelberg Engineering, Heidelberg, Germany). **(B–D)** Schematic sketch of quantitative OCT-A analysis of the macula **(B,C)** and peripapillary scans **(D)** with the Erlangen Angio Tool: circular (**B**; c_1, c_2, and c_3) and sectorial VD (**C**; 12 sectors, s_1-s_{12}; à 30°).

Infection of COVID-19 was confirmed by a positive result of real-time, reverse transcription–polymerase chain reaction (PCR). $Patients_{post-COVID}$ were recruited after hospitalization in the Department of Internal Medicine 1, University of Erlangen-Nürnberg, and from local residents, which were not hospitalized for COVID-19 infection. Time after positive SARS-CoV-2 PCR test was 138.13 ± 70.67 days (range 34–281 days). All eyes had no history of a previously known retinal or papillary disorder. No ocular laser therapy or surgery has been performed. Control eyes did not show ocular disorders or had a history of laser therapy or ocular surgery. All patients and subjects underwent measurement of best-corrected visual acuity (BCVA) and intraocular pressure (IOP). Axial length was measured by IOLMaster (Zeiss, Oberkochen, Germany). Demographic data can be seen in **Table 1**. The study has been approved by the local ethics committee and performed in accordance with the tenets of the Declaration of Helsinki.

Short-Term Effect of Severe Coronavirus Disease 2019 Infection on Retinal Microcirculation

Short-term effects of severe COVID-19 infection on retinal microcirculation were assessed retrospectively: 29 patients with severe complications of COVID-19 infection, hospitalized at the intensive care unit at the University of Erlangen, were monitored by an ophthalmologist for retinal findings. Mean age was 60.9 ± 15 years. Infection of SARS-CoV-2 was confirmed by a positive result of real-time, reverse transcription-PCR. Funduscopy was done at bedside during hospitalization.

Optical Coherence Tomography Angiography and Erlangen-Angio-Tool (Version 3.0)

Macula and peripapillary VD was scanned with the Heidelberg Spectralis II (Heidelberg, Germany). Macula VD was measured in three microvascular layers: SVP (thickness: 80 µm), ICP (thickness: 50 µm), and DCP (thickness: 40 µm). The scans were based on an angle of 15° × 15° and the highest commercially available lateral resolution of 5.7 µm/pixel. Scan size was 2.9 × 2.9 mm (total scan size 8.41 mm^2; diameter of inner ring: 0.8 mm; diameter of outer ring: 2.9 mm). All scans were analyzed by the EA-Tool (version 3.0), which was coded in Matlab (The MathWorks, Inc., Natick, USA, R2017b). This software tool enables quantification of macula and peripapillary VD with high reliability and reproducibility (27).

EA-Tool version 3.0 is an advanced quantification software, including an Anatomical Positioning System (APS; part of Glaucoma Module Premium Edition [GMPE], Heidelberg Engineering, Heidelberg, Germany) allowing alignment of OCT-A scans to each patient's individual FoBMOC (Fovea-to-Bruch's

TABLE 1 | Demographic data of the prospective study cohort for long-term effects of coronavirus disease 2019 (COVID-19) infection: gender, age, best-corrected visual acuity (BCVA), intraocular pressure (IOP), and axial length in patients after COVID-19 infection ($patients_{post-COVID}$) and controls.

	Gender (f/m)	Age [years]	BCVA	IOP [mmHg]	Axial length [mm]
$Patients_{post-COVID}$	12/20	43.7 ± 19	0.9 ± 0.2	14 ± 3	23.7 ± 1.1
Controls	20/8	29.2 ± 12	1.2 ± 0.2	15 ± 3	23.9 ± 0.8

Membrane Opening-Center) axis, during scan acquisition or retrospectively ("APS-ify"). In addition, peripapillary VD can be analyzed by implementing the BMO landmarks (BMO-based peripapillary VD). APS and BMO coordinates were exported by SP-X1902 software (prototype software, Heidelberg Engineering, Heidelberg, Germany) (28). After manual checking for correct segmentation and artifacts, the analysis was performed. Overall, circular (c_1, c_2, and c_3) and sectorial VD (12 sectors, s_1-s_{12}; à 30°) of the macula and peripapillary scans were analyzed (**Figure 1**). In addition, analysis of the foveal avascular zone (FAZ) was done.

Statistical Analysis

For the variable VD of the SVP, ICP, and DCP, we applied a mixed model analysis with sectors as repetition measures. The variables gender and age were introduced in the model as covariates. The model has a random intercept and 12 time measurements defined as repetitions. The interactions between diagnosis and sectors were also calculated together with the *p*-values of the multiple comparisons (after the Tukey–Kramer adjustment). The 95% CI was reported together with the *p*-values. As the experimental design was unbalanced, we estimated the least squares (LS)-means that correspond to the specified effects for the linear predictor part of the model, and the relative confidence limits. LS-means are closer to reality and represent even more real data, when cofactors occur, compared with means. Moreover, we calculated the within-subjects effects using the interactions between the variables ($patients_{post-COVID}$ and controls) * sectors.

For the variables c_1, c_2, and c_3 of the SVP, ICP, and DCP, we applied a covariance analysis (where gender and age were set in the model as covariates). The diagnosis was set as a class variable with two levels ($patients_{post-COVID}$ and controls). Type III SS test of the multiple comparisons (adjusted with Tukey–Kramer) and 95% CI were reported to evaluate the contribution of the factor. The LS-means were calculated. All the statistical elaborations were done using SAS version 9.3 (SAS Institute Inc., Cary, NC, USA).

RESULTS

Long-Term Effect of Coronavirus Disease 2019 Infection on Retinal Macula Microcirculation

The covariance models were done with age and gender as covariates. The *p*-values were adjusted with Tukey's test. In addition, a mixed model with the sector's variables as repeated measures, age and gender as covariates, and patients' group as variables ($patients_{post-COVID}$ vs. controls) was performed.

LS-mean macula VD was 30.25 ± 0.5 (SVP), 22.74 ± 0.5 (ICP), and 24.02 ± 0.6 (DCP) in controls. LS-mean macula VD was 29.51 ± 0.5 (SVP), 21.02 ± 0.4 (ICP), and 23.08 ± 0.5 (DCP) in $patients_{post-COVID}$. Mixed model analysis yielded a significant age effect on macula VD in the SVP ($p = 0.0015$), ICP ($p = 0.0002$), and DCP ($p = 0.0028$). After age correction of the VD data, additional regional variations (i.e., sectorial effect) of macula VD were observed in the SVP ($p < 0.0001$), ICP ($p < 0.0001$), and DCP ($p < 0.0001$). Gender did not affect macula VD in all three microvascular layers ($p > 0.05$).

After age correction of VD data, overall macula VD was significantly reduced in the ICP between $patients_{post-COVID}$ and controls ($p = 0.0133$). Yet overall macula VD of the SVP and DCP was not significantly different between $patients_{post-COVID}$ and controls ($p > 0.05$), respectively.

After age correction of VD data, subgroup analysis of the three peri-macula circles (c_1, c_2, and c_3) yielded a significant reduction of VD of c_1, c_2, and c_3 of the ICP in $patients_{post-covid}$ compared with controls ($p = 0.00257$; $p = 0.0067$; and $p = 0.0345$). No significant differences of macula VD were observed in c_1, c_2, and c_3 of the SVP ($p > 0.05$) and DCP ($p > 0.05$). In addition to the analysis of peri-macula VD, a sectorial analysis was done, showing significant interactions between $patients_{post-COVID}$ and controls in the ICP (**Figure 2**). Color-coded numbers of all significant interactions between each sector are shown in **Figure 2** for the SVP, ICP, and DCP (number of significant interactions: red, $n \geq 8$; pink, $n = 6$–7; orange, $n = 5$; yellow, $n = 4$; green, $n = 2$–3; and gray, $n = 0$–1).

Long-Term Effect of Coronavirus Disease 2019 Infection on Retinal Peripapillary Microcirculation

Peripapillary LS-mean VD was 42.12 ± 0.8 (controls) and 39.37 ± 0.7 ($patients_{post-COVID}$). Type 3 tests of fixed effects showed a significant influence of age ($p = 0.0013$), yet no gender effect on peripapillary VD ($p > 0.05$). After age correction of VD data, an additional sectorial effect was observed ($p < 0.0001$). After age correction of VD data, overall peripapillary VD was significantly reduced between $patients_{post-COVID}$ and controls ($p = 0.0179$). In addition, c_1 was significantly lowered in $patients_{post-COVID}$ compared with controls ($p = 0.0189$), yet not c_2 and c_3 ($p > 0.05$).

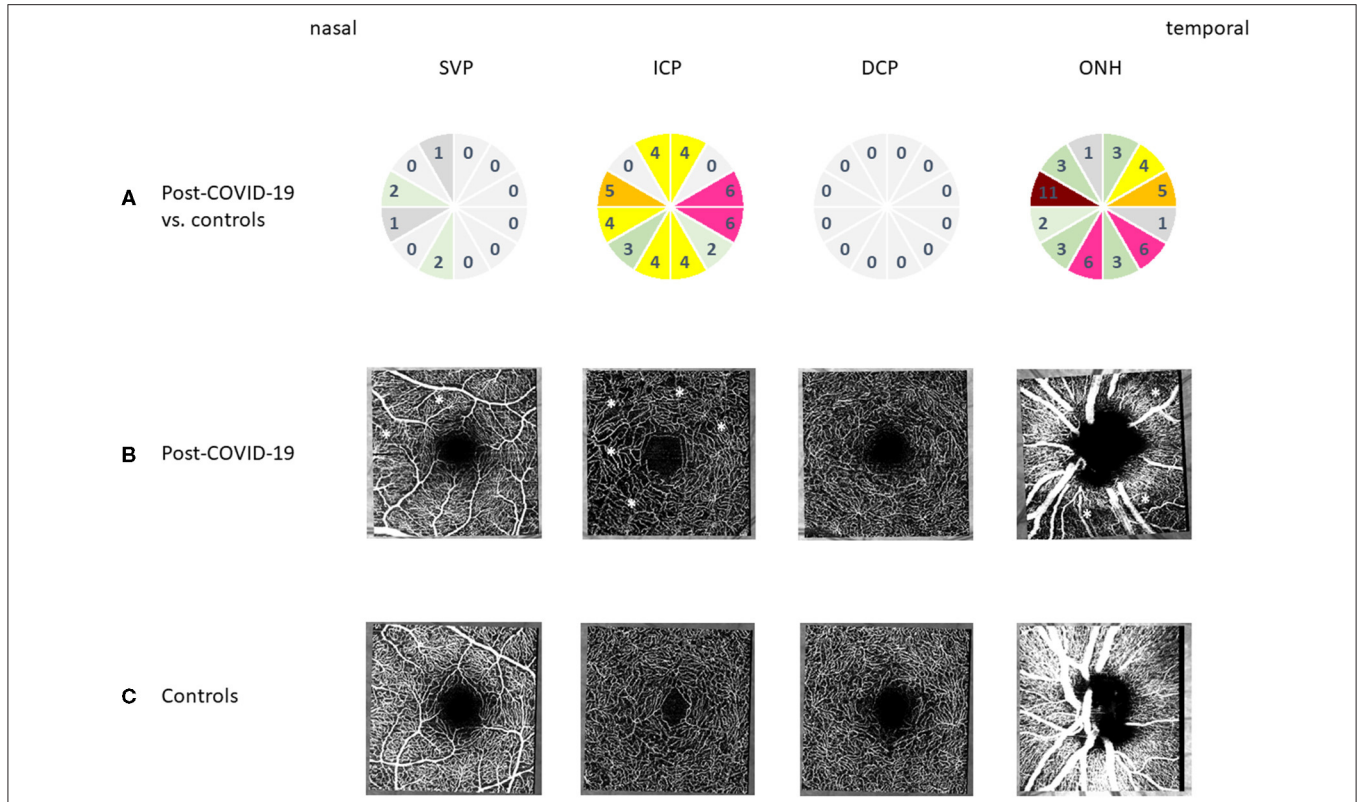

FIGURE 2 | Microcirculation of the macula and peripapillary regions after coronavirus disease 2019 (COVID-19) infection compared to controls: **(A)** qualitative analysis of the number of significant interactions between vessel density of each sector (s_1-s_{12}) of macula optical coherence tomography angiography (OCT-A) in superficial vascular plexus (SVP), intermediate capillary plexus (ICP), and deep capillary plexus (DCP) and optic nerve head (ONH) by color coding (red, $n \geq 8$; pink, $n = 6$–7; orange, $n = 5$; yellow, $n = 4$; green, $n = 2$–3; gray, $n = 0$–1) between controls and post-COVID-19 eyes. **(B)** Representative OCT-A scans of the macula (SVP, ICP, and DCP) and peripapillary regions after COVID-19 infection (*Areas of reduced vessel density). **(C)** Representative OCT-A scans of the macula (SVP, ICP, and DCP) and peripapillary region in controls.

Considering the sectorial effect with localized and fine alterations of microcirculation, a distinct analysis of each single sector (s_1-s_{12}) was added. **Figure 2** shows a color-coded number of significant interactions between each hour in $patients_{post-COVID}$ and controls (number of significant interactions: red, $n \geq 8$; pink, $n = 6$–7; orange, $n = 5$; yellow, $n = 4$; green, $n = 2$–3; gray, $n = 0$–1).

Long-Term Effect of Coronavirus Disease 2019 Infection on Foveal Avascular Zone Characteristics

FAZ was 0.28 ± 0.02 (SVP), 0.19 ± 0.02 (ICP), and 0.27 ± 0.07 (DCP) in controls. $Patients_{post-COVID}$ showed a FAZ of 0.24 ± 0.02 (SVP), 0.16 ± 0.015 (ICP), and 0.35 ± 0.06 (DCP). Mixed model analysis yielded no age effect on FAZ of the SVP, ICP, and DCP ($p > 0.05$). Gender did affect FAZ in the ICP significantly ($p = 0.042$), yet not in the SVP ($p > 0.05$) and DCP ($p > 0.05$). No significant differences were observed between $patients_{post-COVID}$ and controls for FAZ in all three microvascular layers ($p > 0.05$).

Analysis of Long-Term Effect of Coronavirus Disease 2019 Infection Between Hospitalized and Non-hospitalized Patients

We applied the same model (mixed model) to find differences in the SVP, ICP, DCP, and peripapillary region between the $patients_{post-COVID}$ being hospitalized and non-hospitalized during SARS-CoV-2 infection. These groups showed overall LS-mean of 30.00 ± 0.9 (non-hospitalized) and 28.12 ± 0.9 (hospitalized) in the SVP, 21.43 ± 0.8 (non-hospitalized) and 19.58 ± 0.8 (hospitalized) in the ICP, and 24.23 ± 0.9 (non-hospitalized) and 21.00 ± 0.9 (hospitalized) in the DCP. Peripapillary LS-mean VD was 39.51 ± 1.3 (non-hospitalized) and 37.84 ± 1.3 (hospitalized).

A significantly reduced overall LS-mean VD was observed in the DCP of hospitalized $patients_{post-COVID}$ compared with non-hospitalized ones ($p = 0.0304$, **Table 2A**). Contrarily, overall LS-mean of the SVP and ICP was similar between both groups ($p > 0.05$). LS-mean VD of the SVP, ICP, and DCP of $patients_{post-COVID}$ who were hospitalized and

TABLE 2 | Overall (A) and c_3 of (B) vessel density of deep capillary plexus (DCP) of patients$_{post-COVID}$ who were hospitalized and non-hospitalized during COVID-19 infection: (A) mixed model analysis showed a significantly reduced overall LS-mean vessel density (VD) for hospitalized (coded as 1) compared with non-hospitalized patients (coded as 0); (B) general linear model (non-hospitalized, hospitalized patients$_{post-COVID}$ and controls) showed a significantly reduced VD of c_3 of DCP for hospitalized < non-hospitalized < controls.

(A)

Type 3 tests of fixed effects of vessel density of DCP

Effect	Num DF	Den DF	F value	Pr > F
Hospitalized	1	29	5.18	0.0304
Gender	1	29	2.58	0.1188
Age	1	29	0.06	0.8099
Sector	11	352	2.92	0.001

Least squares means of vessel density of DCP

Effect	Groups	Estimate	Standard error	DF	*t*	Pr > |t|	Alpha	Lower	Upper
Hospitalized	**0**	24.23	0.8928	29	27.14	<0.0001	0.05	22.404	26.06
Hospitalized	**1**	21.003	0.9006	29	23.32	<0.0001	0.05	19.161	22.85

Differences of least squares means of vessel density of DCP

Effect	Group	Group	Estimate	Standard Err.	DF	*t* Value	Pr > |t|	Adj p	Alpha	Lower	Upper	Adj lower	Adj Upper
Hospitalized	**0**	**1**	3.23	1.42	29	2.28	0.03	0.03	0.05	0.33	6.13	0.33	6.13

(B)

Least squares means of c_3 of DCP for effect groups

t for H0: LS-mean(i) = LS-mean(j)/Pr > |t|
Dependent Variable: c_3 of DCP

i/j	Non-hospitalized	Hospitalized	Control
Non-hospitalized		2.822824	0.124304
		0.0178	0.9915
Hospitalized	−2.82282		−2.72584
	0.0178		0.0229
Control	−0.1243	2.725835	
	0.9915	0.0229	

non-hospitalized during SARS-CoV-2 infection can be seen in **Table 3**. Considering fine variations of VD, a circular analysis was done: VD of c_2 ($p = 0.0468$) and c_3 of the DCP ($p = 0.0232$) and VD of c_1 of the SVP ($p = 0.0465$) were significantly reduced in patients$_{post-COVID}$ being hospitalized vs. non-hospitalized during SARS-CoV-2 infection. Comparing this two subgroups of patients$_{post-COVID}$ with controls, VD of c_3 of the DCP was significantly reduced in hospitalized < non-hospitalized < controls ($p = 0.015$), yet not c_2 (DCP) and c_1 (SVP, $p > 0.05$). The comparison of each group with its respective *p*-value can be seen in **Table 2B**. In addition, no differences were observed for c_1 (DCP); c_2 and c_3 (SVP); c_1, c_2, and c_3 (ICP); and c_1, c_2, and c_3 (peripapillary) of hospitalized vs. non-hospitalized patients$_{post-COVID}$ ($p > 0.05$).

Correlation of Clinical Data During Hospitalization and Optical Coherence Tomography Angiography Parameters

Clinical characteristics of the hospitalized patients$_{post-COVID}$ ($n = 17$) during their hospitalization can be seen in **Table 4**. The non-hospitalized patients$_{post-COVID}$ ($n = 16$; six females and 10 males) were at home during their SARS-CoV-2 infection without the necessity of being inpatients. Only few preexisting conditions were monitored in the non-hospitalized group: asthma (1/16, 6%) and status after cardiac ablation (1/16, 16%). The correlation of VD of each microvascular layer (SVP, ICP, and DCP) with clinical parameters during hospitalization can be seen in **Table 5**. Interestingly, negative correlations

TABLE 3 | Long-term effect of COVID-19 infection on circular vessel density (c_1, c_2, and c_3) of SVP, ICP, DCP, and peripapillary region between hospitalized (coded as 1) and non-hospitalized (coded as 0) patients: LS-mean, 95% confidence limits.

		Groups	LS-mean	95% confidence limits	
SVP	c_1	0	25.50	23.23	27.76
		1	21.84	19.55	24.12
	c_2	0	30.58	28.68	32.48
		1	29.03	27.11	30.95
	c_3	0	32.01	30.10	33.91
		1	30.39	28.47	32.31
ICP	c_1	0	19.25	17.60	20.91
		1	18.32	16.65	19.99
	c_2	0	21.40	19.79	23.01
		1	19.84	18.21	21.46
	c_3	0	22.60	20.85	24.36
		1	19.98	18.21	21.75
DCP	c_1	0	19.76	17.64	21.88
		1	16.65	14.51	18.79
	c_2	0	24.86	23.17	26.54
		1	22.14	20.44	23.84
	c_3	0	26.00	23.95	28.05
		1	22.18	20.11	24.25
Peripapillary	c_1	0	40.36	37.14	43.58
		1	39.74	36.50	42.99
	c_2	0	38.85	35.19	42.51
		1	37.43	33.74	41.13
	c_3	0	30.46	25.86	35.07
		1	33.35	28.70	38.00

COVID-19, coronavirus disease 2019; SVP, superficial vascular plexus; ICP, intermediate capillary plexus; DCP, deep capillary plexus.

were observed for the highest level of D-dimer and the highest level of Glutamat-Pyruvat-Transaminase (GPT) with peripapillary VD (circular analysis, c_1 and c_2). In addition, stage at diagnosis correlated negatively with VD in the ICP (overall, c_1-c_3), peripapillary region (overall, c_1-c_3), and SVP (overall, c_2 and c_3). Thus, the worse the COVID-19 infection had been, the more reduced the VD was measured in OCT-A.

Short-Term Effect of Severe Coronavirus Disease 2019 Infection on Retinal Microcirculation

Twenty-nine persons with severe complications of COVID-19 infection were monitored for retinal finding during hospitalization in the intensive care unit: six persons (first wave, until August 31, 2020) and 23 persons (second wave). None of them showed an involvement of the cornea, anterior chamber, and vitreous body in terms of infection. Retinal findings (e.g., retinal bleedings and cotton wool spots) were observed in 17% (5/29 persons, **Figure 3**).

DISCUSSION

COVID-19 infection had reached to a pandemic healthcare problem during 2020. Next to pulmonary complications, microcirculation (e.g., vasculitis and thromboembolism) is impaired during SARS-CoV-2 infection (16, 31). Endothelial cells, attacked by SARS-CoV-2, were observed to show either inclusion bodies of the endothelial cells or an endotheliitis (32). The inflammation itself or microthrombosis can consecutively be the starting point on an impaired capillary microcirculation and afterwards an endothelial dysfunction (32). An immunological component has been proposed for the microthrombosis (immune thrombosis) (33). The data of the present study emphasized that capillary microcirculation is restricted even in patients after COVID-19 infection. Especially, the retinal microvascular layer (ICP), showing ACE-2 receptor in animal models (inner nuclear and inner plexiform layer), was affected in patients$_{post-COVID}$ and showed significantly reduced VD. The worse the stage at diagnosis was, the worse the VD of the ICP was observed even after a period after COVID-19 infection. In addition, peripapillary VD was significantly reduced after SARS-CoV-2 infection. Considering severity of COVID-19 disease, the more increased the level of D-dimers and GPT were observed during hospitalization, the more reduced the peripapillary VD was measured in OCT-A scans. This effect was emphasized by the finding that patients$_{post-COVID}$ who were hospitalized during COVID-19 infection showed even significantly reduced VD in the adjacent microvascular layers next to the ICP (i.e., SVP, and DCP) than the patients$_{post-COVID}$ who did not need hospitalization during COVID-19 infection, and even when compared with controls (c_3 of DCP). These results argue for a critical impairment of retinal microcirculation after COVID-19 infection, accented in the ICP, yet affecting additional adjacent microvascular layers after even worse COVID-19 infections.

An ocular involvement of COVID-19 infection has been described for several times. Patients' symptoms vary from normal till blurred vision with accompanying epiphora, discharge, or itching (34–36). Clinical findings can be summarized as follicular conjunctivitis (35), pseudomembranous or hemorrhagic conjunctivitis (37), or keratoconjunctivitis (38). Data of animal models showed that SARS-CoV-2 might affect uveal (e.g., anterior pyogranulomatous uveitis and choroiditis) or neuronal tissue (e.g., retinitis or optic neuritis) (39–43). *In vivo* data of the present study yielded that none of the patients showed signs of uveitis or vasculitis. Yet self-limiting bleedings or cotton wool spots were monitored, being a marker of an impaired retinal microcirculation. This sign of capillary restriction was observed in even 17% of the COVID-19 patients during their hospitalization at the intensive care unit. To the best of our knowledge, the data of the present study show this high percentage of short-term affections of retinal findings during COVID-19 infection for the first time. The only data available in literature up to now offer percentages of 12.9–22% in patients after COVID-19 infection (26, 44).

TABLE 4 | Clinical data of hospitalized patients with coronavirus disease 2019 (COVID-19) infection ($n = 17$): preexisting condition, immunosuppressive medication (past 3 months), smoker, systemic therapy, thrombosis prophylaxis, clinical follow-up during hospitalization at the intensive care unit, and body mass index (BMI) ($n = 13$).

Clinical characteristics		
	11 males (65%)	**6 females (35%)**
Stage at diagnosis	Non-severe	14 (82%)
	Severe	2 (12%)
	Critical	1 (6%)
Median hospital stay	8 days (range 3–46 days)	
Preexisting condition	Chronic heart failure	1 (6%)
	Peripheral artery occlusive disease	1 (6%)
	Hypertension	4 (24%)
	Diabetes	1 (6%)
	Chronic kidney disease	1 (6%)
	Rheumatic disorder	1 (6%)
	Atrial fibrillation	1 (6%)
	Immunosuppression	3 (18%)
	Chemotherapy	2 (12%)
COVID treatment	Hydroxychloroquine	12 (63%)
	Steroids	1 (6%)
	Reconvalescent plasma	1 (6%)
Thrombosis prophylaxis(e.g., heparin or low-molecular-weight heparin prophylactic dose)		15 (88%)
Heparin therapeutic dose		1 (6%)

Clinical data were collected using REDCap electronic data capture tools hosted at University Hospital Erlangen (29). Clinical phases were defined according to the definition of stages proposed by the LEOSS registry (30). Severe phase was mainly characterized by need of oxygen supplementation; critical phase was mainly defined by need of mechanical ventilation.

TABLE 5 | Correlation analysis of clinical data during hospitalization and vessel density in SVP, ICP, and DCP: time between positive SARS-CoV-2 test and OCT-A; stage at diagnosis (non-severe, severe, and critical) and the highest level of D-dimer and Glutamat-Pyruvat-Transaminase (GPT) during hospitalization.

		Time [positive SARS-CoV-2 test until OCT-A; days]	**Stage at diagnosis [non-severe (1), severe (2), critical (3)]**	**Highest level of D-dimer [ng/ml] during hospitalization**	**Highest level of GPT[U/L] during hospitalization**
SVP	Overall	0.15	−0.10	0.45	0.26
	c_1	0.34	0.23	0.51	0.33
	c_2	0.09	−0.12	0.45	0.24
	c_3	0.08	−0.21	0.34	0.20
ICP	Overall	0.10	−0.11	0.46	0.14
	c_1	0.18	−0.02	0.47	0.28
	c_2	0.11	−0.06	0.51	0.14
	c_3	0.07	−0.17	0.39	0.08
DCP	Overall	0.12	0.12	0.29	0.03
	c_1	0.22	0.22	0.34	0.09
	c_2	0.08	0.08	0.26	0.00
	c_3	0.11	0.11	0.27	0.03
Peripapillary	Overall	0.26	−0.38	0.09	0.11
	c_1	0.28	−0.43	−0.21	−0.10
	c_2	0.01	−0.50	−0.23	−0.13
	c_3	0.24	−0.28	0.18	0.11

Severe phase was mainly characterized by need of oxygen supplementation; critical phase was mainly defined by need of mechanical ventilation; Pearson's correlations: negative value represent a worsening of VD with increasing clinical parameter.

SVP, superficial vascular plexus; ICP, intermediate capillary plexus; DCP, deep capillary plexus; SARS-CoV-2, severe acute respiratory syndrome coronavirus 2; OCT-A, optical coherence tomography angiography; VD, vessel density.

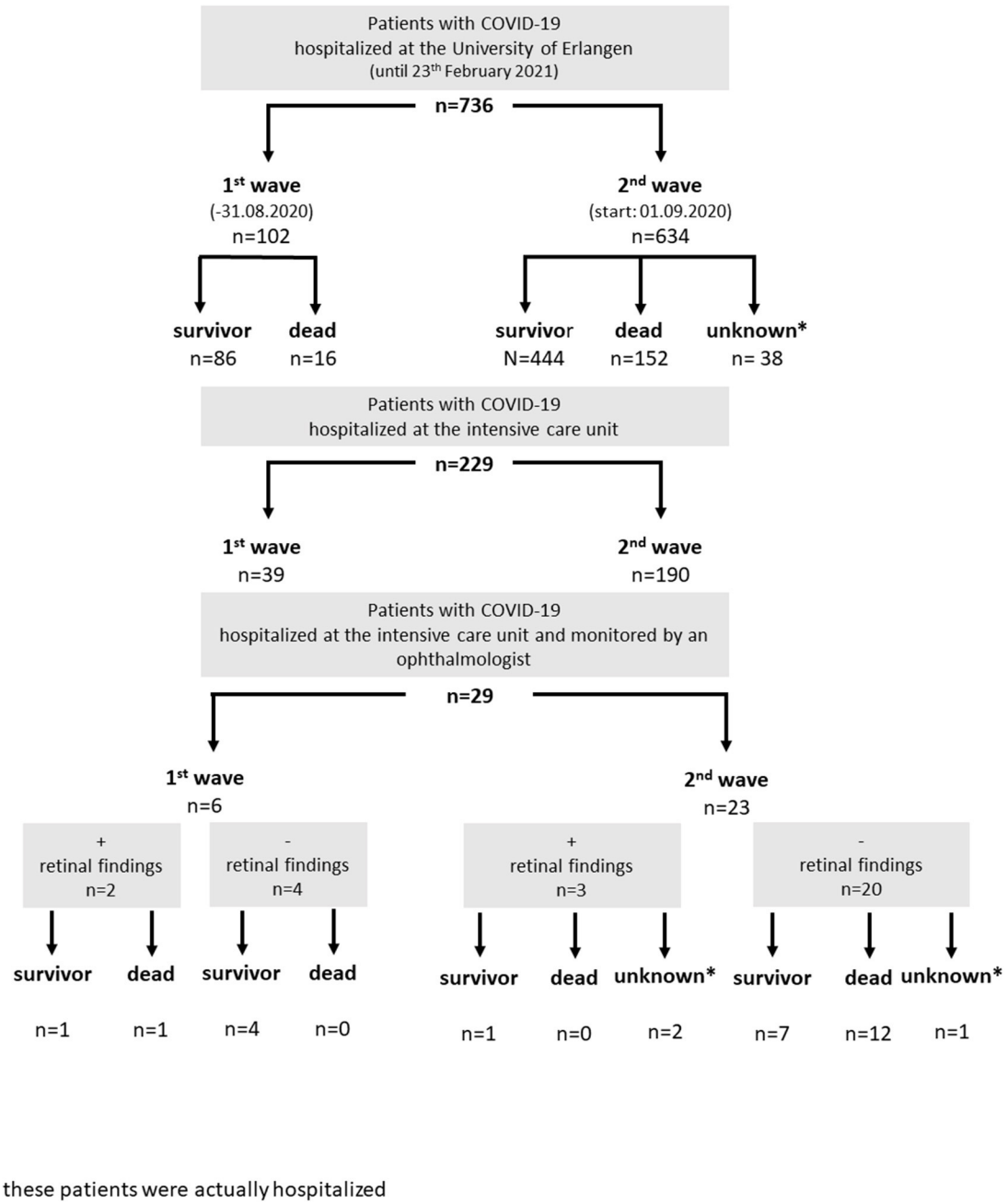

FIGURE 3 | Hospitalized patients with coronavirus disease 2019 (COVID-19) infection at the University of Erlangen (status February 23, 2021): a subgroup of patients of the intensive care unit was monitored by an ophthalmologist for retinal findings (subdivided by their clinical outcome).

Yet the percentage of an affected retinal microcirculation seemed to be even higher as OCT-A results suggest. Retinal microcirculation can be monitored by non-invasive OCT-A technology with a high resolution of the scanned structures. There are only two previous clinical studies up to now, investigating microvasculature of the macula with OCT-A after COVID-19 infection, yet showing contrary results. As one study yielded a significant reduction of VD in the superficial capillary plexus and DCP (25), the other one showed no alterations in OCT-A characteristics, yet funduscopic retinal alterations (e.g., cotton wool spots) (26). The data of the present study yielded that especially the intermediate layer (ICP) is affected after COVID-19 infections. Only if COVID-19 disease had shown an even worse clinical progress during SARS-CoV-2 infection were the adjacent retinal microvascular layers affected as well (SVP and DCP). Thus, the present data might explain why the two previous

studies showed "contrary" results. Thus, if mild forms of COVID-19 infections would be monitored by OCT-A scans and these devices do not divide the retina into three microvascular layers (the previous studies subdivided into two layers), then mild or moderate affections of microcirculation in the ICP might be masked by the two adjacent unaffected microvascular layers, as the ICP is not scanned by its one. Furthermore, the data of the present study showed a significant impairment of peripapillary VD after COVID-19 disease. To the best of our knowledge, this is the first clinical study on BMO-based APSified peripapillary VD analysis after SARS-CoV-2 infection.

In addition to its diagnostic impact, the results of the present study might be the basis for subsequent analysis of pathophysiological aspects. As VD was reduced significantly even after 138.13 ± 70.67 days, we hypothesize that retinal microcirculation, being a correlate of systemic capillary microcirculation, is affected even long after SARS-CoV-2 infection. As viral SARS-CoV-2 particles were less present in tears and conjunctiva samples (0–7.14%) (45, 46), it might be suggested that clinical retinal findings were triggered by systemic factors during COVID-19 infection. We know that the transition of SARS-CoV-2 from the alveolus to the lung capillaries is crucial for systemic infection and distribution. The endocytosis via ACE-2 receptor is established as the key functional pathway not only for initial infection but also for organ dysfunction (47). However, SARS-CoV-2 is able to cross the border between alveolus and the remaining systems via lung capillaries. A high level of ACE-2 receptor is expressed on endothelial cells being a probable entry to human blood cells. From there, a distribution into any other organs may occur. This pathway is the postulated principal route for the entry into the central nervous system (CNS), leading to neurological symptoms such as dizziness or loss of taste (48). Similarly, COVID-19 enters the liver and may infect hepatocytes, cholangiocytes, and liver endothelium with a high expression of ACE-2 receptor (49). However, infection of endothelial cells is not only an entry way but also an important mediator of organ dysfunction itself. Disruption of the endothelial integrity leads to an activation of the coagulation panel, the downregulation of anti-thrombotic mechanisms (Ang 1-7/MAS 1-R), and the activation of platelets (50). This explains the high risk of thrombosis in large arterial or venous vessels leading to cerebral ischemia (arterial system) or lung emboli. In addition, similar mechanisms of activated coagulation systems have been described in septic shock or systemic inflammatory response syndrome (SIRS). Here, microthrombosis in any capillary system is common. We postulate a similar mechanism due to SARS-CoV-2 in any solid organ with an extensive microvessel system (e.g., retina). Microthrombosis leads to necrotic tissue and deterioration of organ function. This hypothesis is confirmed by the findings of microthrombosis and necrosis in histological studies (51). In addition, alterations of the complete blood count (CBC) might contribute to this pathomechanism. Neutrophilia and lymphopenia, observed in sera of COVID-19 patients, were associated with disease severity (52–55). Going along with an increased number of neutrophils, NET formation occludes the microvessels (immunothrombosis) (21–23, 56). Another important fact is the cross-link between the endothelium and the immune system. Any activation of the coagulation panel leads to a chemotaxis of neutrophils and macrophages with a high cytokine release (57). We observed an overactivation of the immune system in some COVID-19 patients with undulating levels of acute phase proteins and interleukins. Dexamethasone, an overall immunosuppressing drug, shows significant benefit on the prognosis of those patients who no longer suffer from the primary infection but from the secondary problems. Consequently, the exact evaluation of the beginning, quantity, and recovery of micro-vessel thrombosis or rarefication of the capillaries may offer an additional approach to the prediction of organ failure and immunological features such as hemolysis.

A limitation of the study is the very heterogeneous COVID-19-affected population due the disease *per se*, the small number of the cohort, and the relatively young population of controls. Sato et al. could not find a correlation between superficial macular VD and age in the TAIWA study (58). In addition, Park et al. could find no significant difference in parafoveal VD between the age group 20–30 years and age group 40–50 years (59). So we would postulate that the significant difference between the control and post-COVID-19 group was independent of the age difference in the present study, even as the results in the ICP were still significant after age correction of the data. We hypothesize that the severity of capillary impairment after COVID-19 infection is mapped on retinal microcirculation. Thus, the systemic affection of microcirculation might become visible by non-invasive OCT-A technique. As retinal microcirculation is a finely regulated and complex system, analysis of regional alterations of VD might extend the overall VD data. We could observe that the more severe the COVID-19 infection had been, the more alterations in the circular SVP and DCP could be observed, yet not in the overall SVP or overall DCP. These results suggest that next to measurements of overall VD in three retinal micro-vascular layers, regional analysis might increase the diagnostic value of OCT-A in diseases with impaired microcirculation for initial diagnosis and follow-ups.

CONCLUSION

Retinal microcirculation may offer a window to the systemic micro-vessel system. We found a remarkable duration of the changed VD in patients who had suffered at COVID-19 infection. The retinal micro-vascular layer in OCT-A imaging (ICP), correlating with the inner nuclear and inner plexiform layers, showed significantly lower microcirculation parameters after SARS-CoV-2 infection compared with healthy eyes, correlating with clinical marker of severity of COVID-19 disease. Future studies regarding the impact of baseline thrombosis prophylaxis might show a clinical impact of these data.

DATA AVAILABILITY STATEMENT

The original contributions presented in the study are included in the article, further inquiries can be directed to the corresponding authors.

ETHICS STATEMENT

The studies involving human participants were reviewed and approved by Ethics Committee of Erlangen, 295_20B. The patients/participants provided their written informed consent to participate in this study.

AUTHOR CONTRIBUTIONS

BH, MG, RS, CM, and MH had the idea. BH, MG, RS, CM, MH, FK, and AB were involved in construction of the study. JH, MM, LR, FH, CS, and MR performed the clinical trial for long-term effects. BH performed the clinical monitoring for short-term effects. LM performed statistical analysis. JF, MM, JH, LR, FH, and CS acquired clinical data. LR, FH, and MR analyzed the OCT-A scans. PL was involved in generation of the draft of the manuscript. BH, CM, MG, MH, RS, MZ, AG, and US-S discussed and interpreted results. BH, MG, and LM were responsible for the draft of the manuscript. All authors contributed to the article and approved the submitted version.

REFERENCES

1. Zhu H, Wei L, Niu P. The novel coronavirus outbreak in Wuhan, China. *Glob Health Res Policy.* (2020) 5:6. doi: 10.1186/s41256-020-00135-6
2. Lan J, Ge J, Yu J, Shan S, Zhou H, Fan S, et al. Structure of the SARS-CoV-2 spike receptor-binding domain bound to the ACE2 receptor. *Nature.* (2020) 581:215–20. doi: 10.1038/s41586-020-2180-5
3. Yan R, Zhang Y, Li Y, Xia L, Guo Y, Zhou Q. Structural basis for the recognition of SARS-CoV-2 by full-length human ACE2. *Science.* (2020) 367:1444–8. doi: 10.1126/science.abb2762
4. Belouzard S, Chu VC, Whittaker GR. Activation of the SARS coronavirus spike protein via sequential proteolytic cleavage at two distinct sites. *Proc Natl Acad Sci USA.* (2009) 106:5871–6. doi: 10.1073/pnas.0809524106
5. Bertram S, Glowacka I, Muller MA, Lavender H, Gnirss K, Nehlmeier I, et al. Cleavage and activation of the severe acute respiratory syndrome coronavirus spike protein by human airway trypsin-like protease. *J Virol.* (2011) 85:13363–72. doi: 10.1128/JVI.05300-11
6. Simmons G, Zmora P, Gierer S, Heurich A, Pohlmann S. Proteolytic activation of the SARS-coronavirus spike protein: cutting enzymes at the cutting edge of antiviral research. *Antiviral Res.* (2013) 100:605–14. doi: 10.1016/j.antiviral.2013.09.028
7. Donoghue M, Hsieh F, Baronas E, Godbout K, Gosselin M, Stagliano N, et al. A novel angiotensin-converting enzyme-related carboxypeptidase (ACE2) converts angiotensin I to angiotensin 1-9. *Circ Res.* (2000) 87:E1–9. doi: 10.1161/01.RES.87.5.e1
8. Zhang YH, Zhang YH, Dong XF, Hao QQ, Zhou XM, Yu QT, et al. ACE2 and Ang-(1-7) protect endothelial cell function and prevent early atherosclerosis by inhibiting inflammatory response. *Inflamm Res.* (2015) 64:253–60. doi: 10.1007/s00011-015-0805-1
9. Fletcher EL, Phipps JA, Ward MM, Vessey KA, Wilkinson-Berka JL. The renin-angiotensin system in retinal health and disease: Its influence on neurons, glia and the vasculature. *Prog Retin Eye Res.* (2010) 29:284–311. doi: 10.1016/j.preteyeres.2010.03.003
10. Simoes E, Silva AC, Silveira KD, Ferreira AJ, Teixeira MM. ACE2, angiotensin-(1-7) and Mas receptor axis in inflammation and fibrosis. *Br J Pharmacol.* (2013) 169:477–92. doi: 10.1111/bph.12159
11. Patel VB, Zhong JC, Grant MB, Oudit GY. Role of the ACE2/Angiotensin 1-7 axis of the renin-angiotensin system in heart failure. *Circ Res.* (2016) 118:1313–26. doi: 10.1161/CIRCRESAHA.116.307708
12. Santisteban MM, Qi Y, Zubcevic J, Kim S, Yang T, Shenoy V, et al. Hypertension-Linked Pathophysiological alterations in the gut. *Circ Res.* (2017) 120:312–23. doi: 10.1161/CIRCRESAHA.116.309006
13. Lovren F, Pan Y, Quan A, Teoh H, Wang G, Shukla PC, et al. Angiotensin converting enzyme-2 confers endothelial protection and attenuates atherosclerosis. *Am J Physiol Heart Circ Physiol.* (2008) 295:H1377–84. doi: 10.1152/ajpheart.00331.2008
14. Jin HY, Song B, Oudit GY, Davidge ST, Yu HM, Jiang YY, et al. ACE2 deficiency enhances angiotensin II-mediated aortic profilin-1 expression, inflammation and peroxynitrite production. *PLoS ONE.* (2012) 7:e38502. doi: 10.1371/journal.pone.0038502
15. Thatcher SE, Gupte M, Hatch N, Cassis LA. Deficiency of ACE2 in bone-marrow-derived cells increases expression of TNF-alpha in adipose stromal cells and augments glucose intolerance in obese C57BL/6 mice. *Int J Hypertens.* (2012) 2012:762094. doi: 10.1155/2012/762094
16. Gan R, Rosoman NP, Henshaw DJE, Noble EP, Georgius P, Sommerfeld N. COVID-19 as a viral functional ACE2 deficiency disorder with ACE2 related multi-organ disease. *Medical Hypotheses.* (2020) 144:110024. doi: 10.1016/j.mehy.2020.110024
17. Verdecchia P, Cavallini C, Spanevello A, Angeli F. The pivotal link between ACE2 deficiency and SARS-CoV-2 infection. *Eur J Intern Med.* (2020) 76:14–20. doi: 10.1016/j.ejim.2020.04.037
18. Senanayake P, Drazba J, Shadrach K, Milsted A, Rungger-Brandle E, Nishiyama K, et al. Angiotensin II and its receptor subtypes in the human retina. *Invest Ophthalmol Vis Sci.* (2007) 48:3301–11. doi: 10.1167/iovs.06-1024
19. Tikellis C, Johnston CI, Forbes JM, Burns WC, Thomas MC, Lew RA, et al. Identification of angiotensin converting enzyme 2 in the rodent retina. *Curr Eye Res.* (2004) 29:419–27. doi: 10.1080/02713680490517944
20. Luhtala S, Vaajanen A, Oksala O, Valjakka J, Vapaatalo H. Activities of angiotensin-converting enzymes ACE1 and ACE2 and inhibition by bioactive peptides in porcine ocular tissues. *J Ocul Pharmacol Ther.* (2009) 25:23–8. doi: 10.1089/jop.2008.0081
21. Leppkes M, Knopf J, Naschberger E, Lindemann A, Singh J, Herrmann I, et al. Vascular occlusion by neutrophil extracellular traps in COVID-19. *EBioMedicine.* (2020) 58:102925. doi: 10.1016/j.ebiom.2020.102925
22. Staats LAN, Pfeiffer H, Knopf J, Lindemann A, Fürst J, Kremer AE, et al. IgA2 antibodies against SARS-CoV-2 correlate with NET formation and fatal outcome in severely diseased COVID-19 patients. *Cells.* (2020) 9:2676. doi: 10.3390/cells9122676
23. Janiuk K, Jablonska E, Garley M. Significance of NETs formation in COVID-19. *Cells.* (2021) 10:151. doi: 10.3390/cells10010151
24. Campbell J, Zhang M, Hwang T, Bailey S, Wilson D, Jia Y, et al. Detailed vascular anatomy of the human retina by projection-resolved optical coherence tomography angiography. *Sci Rep.* (2017) 7:42201. doi: 10.1038/srep42201
25. Abrishami M, Emamverdian Z, Shoeibi N, Omidtabrizi A, Daneshvar R, Saeidi Rezvani T, et al. Optical coherence tomography angiography analysis of the retina in patients recovered from COVID-19: a case-control study. *Can J Ophthalmol.* (2021) 56:24–30. doi: 10.1016/j.jcjo.2020.11.006
26. Savastano MC, Gambini G, Cozzupoli GM, Crincoli E, Savastano A, De Vico U, et al. Retinal capillary involvement in early post-COVID-19 patients: a healthy controlled study. *Graefes Arch Clin Exp Ophthalmol.* (2021) 1–9. doi: 10.1007/s00417-020-05070-3
27. Hosari S, Hohberger B, Theelke L, Sari H, Lucio M, Mardin CY. OCT Angiography: measurement of retinal macular microvasculature with spectralis II OCT angiography-reliability and reproducibility. *Ophthalmologica.* (2020) 243:75–84. doi: 10.1159/000502458
28. Christian Mardin JS, Andreas M, Sebastian FD, Mülle M, Hohberger B. *APSifyed Bruch's Membrane Opening (BMO) Based Peripapillary OCT-A Analysis*. In: *ARVO*. IOVS (2021).
29. Harris PA, Taylor R, Minor BL, Elliott V, Fernandez M, O'neal L, et al. The REDCap consortium: building an international community

of software platform partners. *J Biomed Inform.* (2019) 95:103208. doi: 10.1016/j.jbi.2019.103208
30. Cremer S, Jakob C, Berkowitsch A, Borgmann S, Pilgram L, Tometten L, et al. Elevated markers of thrombo-inflammatory activation predict outcome in patients with cardiovascular comorbidities and COVID-19 disease: insights from the LEOSS registry. *Clin Res Cardiol.* (2020) 1–12. doi: 10.1007/s00392-020-01769-9
31. Albini A, Di Guardo G, Noonan DM, Lombardo M. The SARS-CoV-2 receptor, ACE-2, is expressed on many different cell types: implications for ACE-inhibitor- and angiotensin II receptor blocker-based cardiovascular therapies. *Intern Emerg Med.* (2020) 15:759–66. doi: 10.1007/s11739-020-02364-6
32. Varga Z, Flammer AJ, Steiger P, Haberecker M, Andermatt R, Zinkernagel AS, et al. Endothelial cell infection and endotheliitis in COVID-19. *Lancet.* (2020) 395:1417–8. doi: 10.1016/S0140-6736(20)30937-5
33. Middleton EA, He XY, Denorme F, Campbell RA, Ng D, Salvatore SP, et al. Neutrophil extracellular traps contribute to immunothrombosis in COVID-19 acute respiratory distress syndrome. *Blood.* (2020) 136:1169–79. doi: 10.1182/blood.2020007008
34. Chen L, Deng C, Chen X, Zhang X, Chen B, Yu H, et al. Ocular manifestations and clinical characteristics of 535 cases of COVID-19 in Wuhan, China: a cross-sectional study. *Acta Ophthalmol.* (2020) 98:e951–9. doi: 10.1111/aos.14472
35. Chen L, Liu M, Zhang Z, Qiao K, Huang T, Chen M, et al. Ocular manifestations of a hospitalised patient with confirmed 2019 novel coronavirus disease. *Br J Ophthalmol.* (2020) 104:748–51. doi: 10.1136/bjophthalmol-2020-316304
36. Zhou Y, Duan C, Zeng Y, Tong Y, Nie Y, Yang Y, et al. Ocular findings and proportion with conjunctival SARS-COV-2 in COVID-19 patients. *Ophthalmology.* (2020) 127:982–3. doi: 10.1016/j.ophtha.2020.04.028
37. Navel V, Chiambaretta F, Dutheil F. Haemorrhagic conjunctivitis with pseudomembranous related to SARS-CoV-2. *Am J Ophthalmol Case Rep.* (2020) 19:100735. doi: 10.1016/j.ajoc.2020.100735
38. Cheema M, Aghazadeh H, Nazarali S, Ting A, Hodges J, Mcfarlane A, et al. Keratoconjunctivitis as the initial medical presentation of the novel coronavirus disease 2019 (COVID-19). *Can J Ophthalmol.* (2020) 55:e125–9. doi: 10.1016/j.jcjo.2020.03.003
39. Doherty MJ. Ocular manifestations of feline infectious peritonitis. *J Am Vet Med Assoc.* (1971) 159:417–24.
40. Robbins SG, Detrick B, Hooks JJ. Retinopathy following intravitreal injection of mice with MHV strain JHM. *Adv Exp Med Biol.* (1990) 276:519–24. doi: 10.1007/978-1-4684-5823-7_72
41. Shindler KS, Kenyon LC, Dutt M, Hingley ST, Das Sarma J. Experimental optic neuritis induced by a demyelinating strain of mouse hepatitis virus. *J Virol.* (2008) 82:8882–6. doi: 10.1128/JVI.00920-08
42. Burgos-Blasco B, Guemes-Villahoz N, Donate-Lopez J, Vidal-Villegas B, Garcia-Feijoo J. Optic nerve analysis in COVID-19 patients. *J Med Virol.* (2021) 93:190–1. doi: 10.1002/jmv.26290
43. Marinho PM, Marcos AA, Romano AC, Nascimento H, Belfort R. Retinal findings in patients with COVID-19. *Lancet.* (2020) 395:1610. doi: 10.1016/S0140-6736(20)31014-X
44. Landecho MF, Yuste JR, Gandara E, Sunsundegui P, Quiroga J, Alcaide AB, et al. COVID-19 retinal microangiopathy as an in vivo biomarker of systemic vascular disease? *J Intern Med.* (2021) 289:116–20. doi: 10.1111/joim.13156
45. Seah IYJ, Anderson DE, Kang AEZ, Wang L, Rao P, Young BE, et al. Assessing viral shedding and infectivity of tears in coronavirus disease 2019 (COVID-19) patients. *Ophthalmology.* (2020) 127:977–9. doi: 10.1016/j.ophtha.2020.03.026
46. Wu P, Duan F, Luo C, Liu Q, Qu X, Liang L, et al. Characteristics of ocular findings of patients with coronavirus disease 2019 (COVID-19) in Hubei Province, China. *JAMA Ophthalmol.* (2020) 138:575–8. doi: 10.1001/jamaophthalmol.2020.1291
47. Bourgonje AR, Abdulle AE, Timens W, Hillebrands JL, Navis GJ, Gordijn SJ, et al. Angiotensin-converting enzyme 2 (ACE2), SARS-CoV-2 and the pathophysiology of coronavirus disease 2019 (COVID-19). *J Pathol.* (2020) 251:228–48. doi: 10.1002/path.5471
48. Zhou Z, Kang H, Li S, Zhao X. Understanding the neurotropic characteristics of SARS-CoV-2: from neurological manifestations of COVID-19 to potential neurotropic mechanisms. *J Neurol.* (2020) 267:2179–84. doi: 10.1007/s00415-020-09929-7
49. Wang Y, Liu S, Liu H, Li W, Lin F, Jiang L, et al. SARS-CoV-2 infection of the liver directly contributes to hepatic impairment in patients with COVID-19. *J Hepatol.* (2020) 73:807–16. doi: 10.1016/j.jhep.2020.05.002
50. Kumar A, Narayan RK, Kumari C, Faiq MA, Kulandhasamy M, Kant K, et al. SARS-CoV-2 cell entry receptor ACE2 mediated endothelial dysfunction leads to vascular thrombosis in COVID-19 patients. *Med Hypotheses.* (2020) 145:110320. doi: 10.1016/j.mehy.2020.110320
51. Rapkiewicz AV, Mai X, Carsons SE, Pittaluga S, Kleiner DE, Berger JS, et al. Megakaryocytes and platelet-fibrin thrombi characterize multi-organ thrombosis at autopsy in COVID-19: a case series. *EClinicalMedicine.* (2020) 24:100434. doi: 10.1016/j.eclinm.2020.100434
52. Agbuduwe C, Basu S. Haematological manifestations of COVID-19: from cytopenia to coagulopathy. *Eur J Haematol.* (2020) 105:540–6. doi: 10.1111/ejh.13491
53. Henry BM, De Oliveira MHS, Benoit S, Plebani M, Lippi G. Hematologic, biochemical and immune biomarker abnormalities associated with severe illness and mortality in coronavirus disease 2019 (COVID-19): a meta-analysis. *Clin Chem Lab Med.* (2020) 58:1021–8. doi: 10.1515/cclm-2020-0369
54. Huang W, Berube J, Mcnamara M, Saksena S, Hartman M, Arshad T, et al. Lymphocyte subset counts in COVID-19 patients: a meta-analysis. *Cytometry A.* (2020) 97:772–6. doi: 10.1002/cyto.a.24172
55. Pozdnyakova O, Connell NT, Battinelli EM, Connors JM, Fell G, Kim AS. Clinical Significance of CBC and WBC morphology in the diagnosis and clinical course of COVID-19 infection. *Am J Clin Pathol.* (2021) 155:364–75. doi: 10.1093/ajcp/aqaa231
56. Ackermann M, Anders HJ, Bilyy R, Bowlin GL, Daniel C, De Lorenzo R, et al. Patients with COVID-19: in the dark-NETs of neutrophils. *Cell Death Differ.* (2021) 1–15. doi: 10.1038/s41418-021-00805-z
57. Karakike E, Giamarellos-Bourboulis EJ. Macrophage activation-like syndrome: a distinct entity leading to early death in sepsis. *Front Immunol.* (2019) 10:55. doi: 10.3389/fimmu.2019.00055
58. Sato R, Kunikata H, Asano T, Aizawa N, Kiyota N, Shiga Y, et al. Quantitative analysis of the macula with optical coherence tomography angiography in normal Japanese subjects: the Taiwa Study. *Sci Rep.* (2019) 9:8875. doi: 10.1038/s41598-019-45336-3
59. Park SH, Cho H, Hwang SJ, Jeon B, Seong M, Yeom H, et al. Changes in the retinal microvasculature measured using optical coherence tomography angiography according to age. *J Clin Med.* (2020) 9:883. doi: 10.3390/jcm9030883

Conflict of Interest: The authors declare that the research was conducted in the absence of any commercial or financial relationships that could be construed as a potential conflict of interest.

frontiers in Medicine

CASE REPORT
published: 26 August 2021
doi: 10.3389/fmed.2021.708717

Case Report: Blepharophimosis and Ptosis as Leading Dysmorphic Features of Rare Congenital Malformation Syndrome With Developmental Delay – New Cases With *TRAF7* Variants

Justyna Paprocka[1], Magdalena Nowak[2], Maria Nieć[2], Izabela Janik[2], Małgorzata Rydzanicz[3], Śmigiel Robert[4], Magdalena Klaniewska[4], Karolina Rutkowska[3], Rafał Płoski[3] and Aleksandra Jezela-Stanek[5]**

[1] Department of Pediatric Neurology, Faculty of Medical Sciences in Katowice, Medical University of Silesia, Katowice, Poland, [2] Students' Scientific Society, Department of Pediatric Neurology, Faculty of Medical Sciences in Katowice, Medical University of Silesia, Katowice, Poland, [3] Department of Medical Genetics, Medical University of Warsaw, Warsaw, Poland, [4] Department of Paediatrics, Division of Propaedeutic of Paediatrics and Rare Disorders, Wroclaw Medical University, Wroclaw, Poland, [5] Department of Genetics and Clinical Immunology, National Institute of Tuberculosis and Lung Diseases, Warsaw, Poland

Germline variants in tumor necrosis factor receptor-associated factor 7 (TRAF7) gene have recently been described in about 50 patients with developmental delay and cardiac, facial, and digital anomalies (CAFDADD). We aimed to depict further the clinical and genetic spectrum associated with *TRAF7* germline variants in two additional patients, broaden the mutational spectrum, and support the characteristic clinical variety to facilitate the diagnostics of the syndrome among physician involved in the evaluation of patients with developmental delay/congenital malformations.

Keywords: blepharophimosis, ptosis, developmental delay, *TRAF7* variants, facial features, dysmorphic features

OPEN ACCESS

Edited by:
Filippo M. Santorelli, Fondazione Stella Maris (IRCCS), Italy

Reviewed by:
Diego Lopergolo, University of Siena, Italy
Arzu Taskiran Comez, Çanakkale Onsekiz Mart University, Turkey

****Correspondence:***
Justyna Paprocka
jpaprocka@sum.edu.pl
Aleksandra Jezela-Stanek
jezela@gmail.com

Specialty section:
This article was submitted to Ophthalmology, a section of the journal Frontiers in Medicine

Received: *12 May 2021*
Accepted: *27 July 2021*
Published: *26 August 2021*

Citation:
Paprocka J, Nowak M, Nieć M, Janik I, Rydzanicz M, Robert Ś, Klaniewska M, Rutkowska K, Płoski R and Jezela-Stanek A (2021) Case Report: Blepharophimosis and Ptosis as Leading Dysmorphic Features of Rare Congenital Malformation Syndrome With Developmental Delay – New Cases With TRAF7 Variants. Front. Med. 8:708717. doi: 10.3389/fmed.2021.708717

INTRODUCTION

TRAF7 (Tumor necrosis factor receptor-associated factor 7) is a multifunctional intracellular protein belonging to the TRAF family (tumor necrosis factor receptor - TNF-R), which consists of seven proteins (TRAF1-7) (1, 2). It is encoded by a homonymous gene - *TRAF7* – encompassing 21 exons, located within the chromosomal region 16p13.3 (2). A modular structure characterizes all members of the TRAF family. TRAF7 670-amino acid protein contains an N-terminal RING finger domain (aa 125–160), a zinc finger domain (aa 221–287) and a coiled-coil domain, but instead of the classical TRAF domain, it has seven WD40 repeats at the C-terminus (1, 3).

TRAF proteins are active in many biological processes, including embryonic development, tissue homeostasis as well as innate and adaptive humoral immune responses (4, 5). *TRAF7* is involved in the process of protein ubiquitination. It is one of the critical mediators of NF-κB (nuclear factor-κB) and MAPK (mitogen-activated protein kinase) signaling pathways. It, therefore, plays an important role in many cellular processes (1–3, 6). The interaction of TRAF7 and MEKK3 (mitogen-activated protein kinase kinase kinase 3) through the WD40 domain leads to the activation of JNK and p38 MAP signaling pathways, which are responsible for cell survival, proliferation and differentiation

(1–3). *TRAF7* also plays a specific role in muscle function. Reduced *TRAF7* expression under the influence of MyoD1 in growing myoblasts causes a decrease in NF-κB ubiquitination, exit from the cell cycle and acceleration of myogenesis (3, 6).

As a result of research conducted toward a closer understanding of TRAF7, a relationship between the protein and the development of neoplasms was demonstrated. Somatic mutations in *TRAF7* have been described in meningiomas, mesotheliomas, perineural tumors of soft tissues, as well as in glandular neoplasms of the genital tract (1, 7–9). In turn, germline mutations in this gene have been described in the neurodevelopmental syndrome, encompassing cardiac, facial, and digital anomalies with developmental delay, thus termed CAFDADD (OMIM #6181640), characterized by facial dysmorphism with specific anomalies within the eyes (ptosis, epicanthic folds), congenital defects of the heart (aortic coarctation, hypoplastic left heart, double outlet right ventricle) and skeletal system (distal contractures, overlapping digits), and psychomotor delay. The described to date germline variants are heterozygous missense mutations, including frequently repeated c.1964G>A (p. Arg655Gln) and occur *de novo* (2, 5, 10).

We present two patients with characteristic facial dysmorphic features in whom, as a result of performed Whole Exome Sequencing (WES), heterozygous *de novo* variants were detected in *TRAF7* gene: the c.1708C>G (p.His570Asp) in case 1 and c.1783C>G (p.Leu595Val) in case 2. Our aim is to delineate the phenotype and to underline the specific ocular findings that may facilitate the clinical diagnosis.

PATIENTS' DESCRIPTIONS

Case 1

A 2-month-old boy was admitted to the Department of Pediatric Neurology for the diagnosis of dysmorphic and ophthalmoplegic features. The boy was born in the 41st week of an uncomplicated pregnancy with the Apgar score of 10, bodyweight of 3,100 g and head circumference of 32 cm. The examination revealed a short two-vessel umbilical cord. He developed neonatal jaundice, which was treated with phototherapy. Transfontanelle ultrasound showed an asymmetric ventricular system. The patient's family history was unremarkable.

The child was diagnosed with facial dysmorphism, including swollen eyelids, small sunken eyes, which initially opened only 2–3 mm, as well as a wide nose with an upturned tip, a receding mandible and asymmetrical auricles; head circumference was 36 cm (<3rd percentile) and the frontal fontanel, sized 2 × 3 cm, was below the level of the skull bone. Moreover, the physical examination revealed a narrow chest with widely spaced nipples and significant binary stenosis (**Figure 1**).

Correct tendon-periosteal reflexes and symmetrical posture reflexes were found. Positional asymmetry with shortening of the left side and reduced muscle tension in the head-torso axis were revealed, and, for this reason, physical rehabilitation was recommended. Ophthalmoplegia was diagnosed by an ophthalmologist. The results of basic laboratory tests (morphology, urinalysis, capillary gasometry, liver function assessment, ionogram) were within the normal range.

MRI of the head and eye sockets was performed, which showed no abnormalities apart from the asymmetry of the bones of the skull cover. Suspecting the myogenic background of the described ptosis, the diagnostics was extended to include an electrostimulation test for measuring muscle fatigue, during which the right axillary nerve was stimulated with the registration of a response from the right deltoid muscle. No decrease in amplitude was found; therefore, the test result was determined as negative. In addition, the test for antibodies against acetylcholine receptors was performed, and the result was normal.

Echocardiography showed patent foramen ovale/atrial septal defect (PFO/ASD II) and patent ductus arteriosus (PDA) with a left-right shunt. The ultrasound of the abdomen and retroperitoneal space was also performed, which visualized the enlarged caliceal-pelvic system of the left kidney. *E. Coli* 10^4 was obtained from the urine culture, and therefore a nephrological consultation was recommended. The patient was discharged with recommendations for further care in specialist units: cardiology, nephrology, ophthalmology, genetic counseling and physical rehabilitation clinics.

The patient was consulted by a geneticist, who recommended an array comparative genomic hybridization (aCGH) test. The result was normal. Thus, whole-exome sequencing (WES) was recommended for the suspected blepharophimosis, ptosis, epicanthus in vs. syndrome (BPES).

Case 2

An almost 2-year-old boy is currently under the care of the Genetic Clinic because of a delay in psychomotor development and facial dysmorphic features. The boy was born by cesarean section at 40 weeks of gestation, with Apgar score of 8 points and birth weight of 4,120 g. The pregnancy was complicated by maternal infection and threatened preterm delivery. Family history was unremarkable.

After birth, no malformations of internal organs were found. Conductive hearing loss on the left side was identified. Due to clubfoot, the boy was referred to orthopedic consultation. The feet were successively plastered and splinted with good results. Cardiac ultrasound showed a bicuspid tricuspid valve. Ultrasound of the abdominal cavity showed a left-sided duplication of the caliceal-pelvic system. Cerebral NMR and angio-NMR showed hypoplasia of the middle and anterior segment of the sagittal sinus with peripheral venous circulation and slight dilatation of the supra-ventricular system as well as dilatation of brain fissures in the frontal and temporal regions and basal cisterns. TSH and CPK levels were normal. There were no abnormalities in the ophthalmological examination.

Physical examination at the age of 16 months revealed specific features of craniofacial dysmorphia such as increased head circumference (OFC 50 cm – 97 percentile), prominent forehead and prominent veins on the forehead, two hair whirls as well as wide nasal bridge, short palpebral fissures, blepharophimosis and mild ptosis of both eyelids (**Figure 2**).

Palms and fingers were normal; however, the toes overlap. At 16 months of life, the weight was 10kg (25 percentile) and height 78 cm (25–50 percentile). Hypotonia was also found. The boy is intensively rehabilitated. He sat up by himself at the age of 12

FIGURE 1 | The facial phenotype of Case 1 at 11 months. Note the significant short palpebral fissures, ptosis, epicanthic folds and high forehead with flat, broad nasal bridge.

months and started walking at the age of 2 years. He does not speak; however, according to his parents, he understands speech.

Cytogenetic examination showed normal male karyotype. Array CGH did not reveal any chromosomal aberrations. Clinically dysmorphic syndrome belonging to the RASopathies group was suspected in the child. Therefore, a whole-exome sequencing (WES) was performed.

For both probands, WES analysis was performed using SureSelectXT Human kit All Exon v7 - Case 1 and v5 – Case 2 (Agilent, Agilent Technologies, Santa Clara, CA). Enriched libraries were paired-end sequenced (2 × 100 bp) on HiSeq 1,500 (Illumina, San Diego, CA, USA) and analyzed as previously described (11). In brief, raw sequence readouts were initially analyzed with *bcl2fastq* software (Illumina) to generate reads in fastq format. After the quality control steps, including adapter trimming and low-quality read removal, reads were aligned to the GRCh38 (hg38) reference genome with Burrows-Wheeler Alignment Tool (http://bio-bwa.sourceforge.net/), and processed further by Picard (http://broadinstitute.github.io/picard/) and Genome Analysis Toolkit (https://software.broadinstitute.org/gatk/). Identified variants were annotated with functional information, frequency in population (including gnomAD (http://gnomad.broadinstitute.org/), and an in-house database of >3,500 Polish exomes), and known association with clinical

FIGURE 2 | The facial phenotype of Case 2 and 16 months. Not the high and broad forehead, flat nasal bridge, short palpebral fissures and ptosis, thin lips.

phenotypes, based on both ClinVar (https://www.ncbi.nlm.nih.gov/clinvar/) and HGMD (http://www.hgmd.cf.ac.uk) databases. *In silico* pathogenicity prediction was performed based on Varsome pathogenicity and conservation scores (12) and by MetaSVM (13).

Variants passing a default quality were further filtered to include only those with <1% minor allele frequency in all tested databases (gnomAD, in house database of >3,500 Polish exomes), and to exclude deep intronic variants. The final list of variants were screened against known pathogenic mutations listed in ClinVar an dHGMD databases, and then searched for biallelic mutations consistent with autosomal recessive inheritance and monoallelic variants potentially causative of an autosomal dominant. All prioritized variants were manually inspected with Integrative Genomics Viewer (14).

Enriched libraries were paired-end sequenced (2 × 100 bp) on HiSeq 1,500 (Illumina, San Diego, CA, USA). Raw sequencing data and variants prioritization were performed as previously described (11). For variants considered as disease-causing segregation analysis in probands' families was performed by amplicon deep sequencing (ADS) performed by Nextera XT Kit (Illumina) and sequenced as described for WES.

In Case 1, ultra-rare variants in *LEMD3*, *RAI1* and *TRAF7* genes were prioritized for further validation. Variants in *LEMD3*, *RAI1* were found to be inherited from proband's

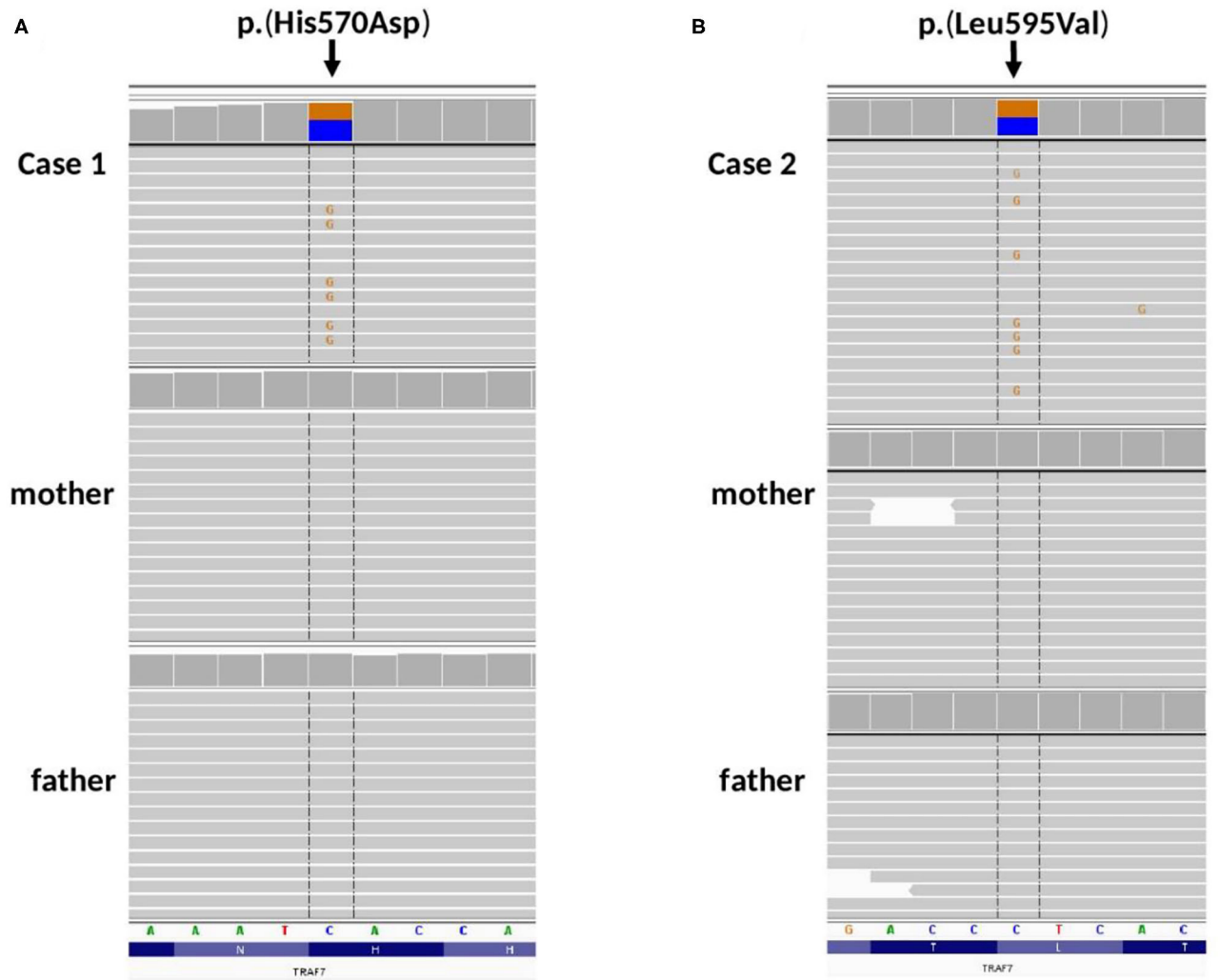

FIGURE 3 | Amplicon deep sequencing validation of TRAF7 gene variants identified by WES in **(A)** Case 1, *de novo* p.(His570Asp), **(B)** Case 2, *de novo* p.(Leu595Val). Integrative Genomic Viewer screenshots are presented.

healthy mother and were classified as benign (data not shown). Whereas, missense heterozygous variant in *TRAF7* gene [(hg38, chr16:g.002175915-C>G, NM_032271.3: c.1708C>G, p.(His570Asp)] was absent in both parents (**Figure 3A**) and considered as *de novo* event.

In Case 2, ultra-rare variants in *CHD1*, *NAV2*, *KIF3B* and *TRAF7* genes were prioritized for segregation study. Variants in *CHD1*, *NAV2*, *KIF3B* were inherited from healthy parents (*CHD1* from a father, *NAV2*, *KIF3B* from a mother, date not shown) and were considered as benign. Missense heterozygous variant in *TRAF7* gene [(hg38, chr16:g.002176085-C>G, NM_032271.3: c.1783C>G, p.(His595Asp)] was absent in both parents (**Figure 3B**) and considered as *de novo* event.

Both p.(His570Asp) and p.(Leu595Val) have 0 frequency in all tested databases (including the in-house database of >4,500 Polish individuals examined by WES). According to ACMG classification (15) p.(His570Asp) variant is classified as "Likely Pathogenic," while p.(Leu595Val) as "Variant of Unknown Significance." Additionally, c.1783C>G (p.Leu595Val) was predicted as damaging/pathogenic by 16 out of 21 pathogenicity predictors implemented by Varsome (including MutationTaster, SIFT, FATHMM), and as damaging by MetaSVM.

DISCUSSION

Germline mutations in *TRAF7* and the associated clinical symptoms were first described in 2018 by Tokita et al. *De novo* missense mutations in *TRAF7* were found in 7 patients with diagnosed developmental delay, congenital defects and

dysmorphic features (2). Castilla-Vallmanya et al., on the basis of the identification of 45 patients, defined this disease entity as *TRAF7* syndrome characterized by specific features of facial dysmorphia, especially eyelid fissure defects, congenital heart and skeletal defects, as well as motor retardation and intellectual disability (10). To date, 54 cases of patients with a germline mutation in *TRAF7* have been described in the literature (2, 5, 10).

De novo variant p.(His570Asp) identified in Case 1 was previously reported in two independent CAFDADD patients (10). While p.(Leu595Val) identified in Case 2 has not been described in the literature so far.

We present a case of a patient with a *de novo* heterozygous *TRAF7* mutation. The pathogenic nature of this variant and its participation in the clinical picture of the patient is indicated by the characteristic clinical symptoms consistent with the phenotypes of patients with diagnosed *TRAF7* germinal mutations (2, 10), the applied bioinformatics programs and the exclusion of its occurrence in both parents.

The phenotype revealed in the patient, and primarily the occurrence of blepharophimosis and epicanthic folds, highlight the intensity of dysmorphic features within the eyes, which is characteristic of the CAFDADD syndrome. In addition, the described features such as broad nasal base, short neck, dysmorphic, asymmetrically placed auricles, and a retracted mandible (retrognathia) complete the picture of typical phenotype features characteristic of *TRAF7* germline mutations (2, 10). The skeletal defects, manifested by significant bilateral narrowing of the skull, raise the suspicion of craniosynostosis, which is one of the most frequently described skull defects in patients with *TRAF7* mutations (5, 10). Therefore, the CAFDADD syndrome should be included in the spectrum of genetic defect syndromes, in which the neurosurgical assessment of the patient and constant monitoring of their condition and development is of key importance in order to avoid possible complications of craniosynostosis through properly implemented treatment (16–18). The patent ductus arteriosus and patent foramen ovale diagnosed in the patient are typical cardiac manifestations of the CAFDADD syndrome, which indicates the need for constant cardiological supervision (2, 10). Due to the previously described developmental disorders such as psychomotor retardation, intellectual disability and speech disorders, the support of early child development as well as physical rehabilitation, aimed at compensating for frequently occurring muscle tension disorders, is of key importance (2, 5, 10).

Primarily, the CAFDADD syndrome phenotype includes distinctive dysmorphic features in the eye area, which can often be the first abnormalities noticed. Thus, it is of importance for child ophthalmologists to keep the syndrome in mind during the evaluation of the patients with such features having other developmental anomalies (physical as well as delayed psychomotor milestones). The patient's disorders of eye-opening indicated a clinical picture characteristic of ophthalmic forms of myasthenia gravis (19). The exclusion of myasthenia gravis by means of a negative result of the electrostimulation-induced muscle fatigue test led to further diagnostics toward a genetic syndrome with severe ptosis, narrow eyelid cracks and epicanthic folds.

Initially, the blepharophimosis-ptosis-epicanthus invertus syndrome (BPES) was suspected in the presented Case 1. BPES is a complex eyelid defect syndrome characterized by four main features: blepharophimosis, eyelid ptosis, epicanthus invertus and telecanthus (BPES II), as well as premature ovarian failure in BPES I (20). In both BPES and CAFDADD, a palpebral fissure defect is one of the characteristic clinical features. If BPES is suspected, it is necessary to exclude CAFDADD, in which there are both systemic complications, especially the heart and skeletal defects, as well as possible predisposition to cancer development and premature aging, absent in BPES.

In patients with a suspected *TRAF7* mutation in the differential diagnosis, Ohdo's syndrome, which is characterized by blepharophimosis, ptosis, congenital disorders of the heart and limbs, and developmental delay, should also be considered (21, 22). In previously described patients, RASopathy group diseases were also suspected, e.g., Noonan syndrome and Costello syndrome (2, 5, 10). Of note, the RASopathy was initially suspected in presented Case 2. The common pathomechanism of RASopathy associated with dysregulation of the Ras/MAPK signaling pathways causes a characteristic clinical picture: features of craniofacial dysmorphia, heart defects, ocular and musculoskeletal disorders (23). The overlapping phenotypes of RASopathy and the CAFDADD syndrome and the suspected involvement of *TRAF7* in the regulation of MAPK signaling pathways suggest a possible correlation in the pathomechanisms (1, 2, 5).

Somatic mutations in *TRAF7* have been detected in such neoplasms as meningiomas, mesotheliomas, perineural tumors of soft tissues or glandular neoplasms of the genital tract (1, 23). Most of them are missense mutations located within the WD40 domain. The germline mutations in *TRAF7* are also mostly clustered within the WD40 domain (1, 10). For this reason, constant supervision in aging patients is required to determine whether they have a higher risk of cancer development and should be included in the oncological surveillance (10).

CONCLUSIONS

The detected *de novo* variant c.1708C>G [p.(His570Asp)] in *TRAF7* and the described phenotype correlating with it allow to extend of the genetic spectrum of the very rare CAFDADD syndrome (Cardiac, facial and digital anomalies with developmental delay). Moreover, the presented known variant - c.1783C>G, p.(His595Asp) – support the previous findings concerning the phenotypic spectrum of *TRF7* germline variants. A *TRAF7* mutation should be suspected in patients with characteristic dysmorphic features, especially within the palpebral fissure (blepharophimosis and/or ptosis), congenital defects of the heart and skeleton, and psychomotor delay. As we proved herein, the clinical manifestation may differ and overlaps with other, more frequent genetic condition

as Noonan syndrome (RASopathies). Constant ophthalmic, neurological and cardiological assessment, as well as early development support and motor rehabilitation, are essential in the management of patients with the syndrome resulting from variants in *TRAF7*.

DATA AVAILABILITY STATEMENT

The original contributions presented in the study are included in the article/supplementary materials, further inquiries can be directed to the corresponding author/s.

ETHICS STATEMENT

Written informed consent was obtained from the parents for the publication of any potentially identifiable images or data included in this article.

AUTHOR CONTRIBUTIONS

Conceptualization was performed by JP and AJ-S. Methodology, formal analysis, investigation, resources, data curation, and project administration were performed by JP, MNo, MNi, IJ, MR, ŚR, RP, and AJ-S. Software by validation was performed by JP, MNo, MNi, IJ, and AJ-S. Writing-original draft preparation, writing-review and editing, and visualization were performed by JP, MNo, MNi, IJ, MR, ŚR, MK, KR, RP, and AJ-S. Supervision was performed by AJ-S. Funding acquisition was performed by JP. All authors have read and agreed to the published version of the manuscript.

ACKNOWLEDGMENTS

The authors would like to thank the patients and their parents for their cooperation in this study.

REFERENCES

1. Zotti T, Scudiero I, Vito P, Stilo R. The emerging role of TRAF7 in tumor development. *J Cell Physiol.* (2017) 232:1233–8. doi: 10.1002/jcp.25676
2. Tokita MJ, Chen CA, Chitayat D, Macnamara E, Rosenfeld JA, Hanchard N, et al. De novo missense variants in TRAF7 cause developmental delay, congenital anomalies, and dysmorphic features. *Am J Hum Genet*. (2018) 103:154–62. doi: 10.1016/j.ajhg.2018.06.005
3. Zotti T, Vito P, Stilo R. The seventh ring: exploring TRAF7 functions. *J Cell Physiol.* (2012) 227:1280–4. doi: 10.1002/jcp.24011
4. Park HH. Structure of TRAF family: current understanding of receptor recognition. *Front Immunol*. (2018) 9:1999. doi: 10.3389/fimmu.2018.01999
5. Accogli A, Scala M, Pavanello M, Severino M, Gandolfo C, De Marco P, et al. Sinus pericranii, skull defects, and structural brain anomalies in TRAF7-related disorder. *Birth Defects Res*. (2020) 112:1085–92. doi: 10.1002/bdr2.1711
6. Tsikitis M, Acosta-Alvear D, Blais A, Campos EI, Lane WS, Sánchez I, et al. Traf7, a MyoD1 transcriptional target, regulates nuclear factor-κ B activity during myogenesis. *EMBO Rep.* (2010) 11:969–76. doi: 10.1038/embor.2010.154
7. Klein CJ, Wu Y, Jentoft ME, Mer G, Spinner RJ, Dyck PJ, et al. Genomic analysis reveals frequent TRAF7 mutations in intraneural perineuriomas. *Ann Neurol*. (2017) 81:316–21. doi: 10.1002/ana.24854
8. Clark VE, Erson-Omay EZ, Serin A, Yin J, Cotney J, Ozduman K, et al. Genomic analysis of non-NF2 meningiomas reveals mutations in TRAF7, KLF4, AKT1, and SMO. *Science*. (2013) 339:1077–80. doi: 10.1126/science.1233009
9. Scudiero I, Zotti T, Ferravante A, Vessichelli M, Reale C, Masone MC, et al. Tumor necrosis factor (TNF) receptor-associated factor 7 is required for TNFα-induced Jun NH2-terminal kinase activation and promotes cell death by regulating polyubiquitination and lysosomal degradation of c-FLIP protein. *J Biol Chem.* (2012) 287:6053–61. doi: 10.1074/jbc.M111.300137
10. Castilla-Vallmanya L, Selmer KK, Dimartino C, Rabionet R, Blanco-Sánchez B, Yang S, et al. Phenotypic spectrum and transcriptomic profile associated with germline variants in TRAF7. *Genet Med.* (2020) 22:1215–26. doi: 10.1038/s41436-020-0792-7
11. Smigiel R, Biela M, Szmyd K, Błoch M, Szmida E, Skiba P, et al. Rapid whole-exome sequencing as a diagnostic tool in a neonatal/pediatric intensive care unit. *J Clin Med.* (2020) 9:2220. doi: 10.3390/jcm9072220
12. Kopanos C, Tsiolkas V, Kouris A, Chapple CE, Albarca Aguilera M, Meyer R, et al. VarSome: the human genomic variant search engine. *Bioinformatics.* (2019) 35:1978–80. doi: 10.1093/bioinformatics/bty897
13. Dong C, Wei P, Jian X, Gibbs R, Boerwinkle E, Wang K, et al. Comparison and integration of deleteriousness prediction methods for nonsynonymous SNVs in whole exome sequencing studies. *Hum Mol Genet.* (2015) 24:2125–37. doi: 10.1093/hmg/ddu733
14. Thorvaldsdottir H, Robinson JT, Mesirov JP. Integrative genomics viewer (IGV): high-performance genomics data visualization and exploration. *Brief Bioinform.* (2013) 14:178–92. doi: 10.1093/bib/bbs017
15. Tavtigian SV, Greenblatt MS, Harrison SM, Nussbaum RL, Prabhu SA, Boucher KM, et al. Modeling the ACMG/AMP variant classification guidelines as a bayesian classification framework. *Genet Med.* (2018) 20:1054–60. doi: 10.1038/gim.2017.210
16. Kimonis V, Gold JA, Hoffman TL, Panchal J, Boyadjiev SA. Genetics of craniosynostosis. *Semin Pediatr Neurol.* (2007) 14:150–61. doi: 10.1016/j.spen.2007.08.008
17. Kajdic N, Spazzapan P, Velnar T. Craniosynostosis-recognition, clinical characteristics, and treatment. *Bosn J Basic Med Sci.* (2018) 18:110–6. doi: 10.17305/bjbms.2017.2083
18. Governale LS. Craniosynostosis. *Pediatr Neurol.* (2015) 53:394–401. doi: 10.1016/j.pediatrneurol.2015.07.006
19. Nair AG, Patil-Chhablani P, Venkatramani DV, Gandhi RA. Ocular myasthenia gravis: a review. *Indian J Ophthalmol.* (2014) 62:985–91. doi: 10.4103/0301-4738.145987
20. Méjécase C, Nigam C, Moosajee M, Bladen JC. The genetic and clinical features of FOXL2-related blepharophimosis, ptosis and epicanthus inversus syndrome. *Genes.* (2021) 12:1–14. doi: 10.3390/genes12030364
21. Verloes A, Bremond-Gignac D, Isidor B, David A, Baumann C, Leroy MA, et al. Blepharophimosis-mental retardation (BMR) syndromes: a proposed clinical classification of the so-called ohdo syndrome, and delineation of two new BMR syndromes, one X-linked and one autosomal recessive.

Am J Med Genet Part A. (2006) 140:1285–96. doi: 10.1002/ajmg.a.31270
22. Campeau PM, Lu JT, Dawson BC, Fokkema IFAC, Robertson SP, Gibbs RA, et al. The KAT6B-related disorders genitopatellar syndrome and Ohdo/SBBYS syndrome have distinct clinical features reflecting distinct molecular mechanisms. *Hum Mutat.* (2012) 33:1520–5. doi: 10.1002/humu.22141
23. Rauen KA. The RASopathies. *Annu Rev Genomics Hum Genet.* (2013) 14:355–69. doi: 10.1146/annurev-genom-091212-153523

Conflict of Interest: The authors declare that the research was conducted in the absence of any commercial or financial relationships that could be construed as a potential conflict of interest.

Publisher's Note: All claims expressed in this article are solely those of the authors and do not necessarily represent those of their affiliated organizations, or those of the publisher, the editors and the reviewers. Any product that may be evaluated in this article, or claim that may be made by its manufacturer, is not guaranteed or endorsed by the publisher.

frontiers in Medicine

ORIGINAL RESEARCH
published: 29 October 2021
doi: 10.3389/fmed.2021.732222

Replication of Reduced Pattern Electroretinogram Amplitudes in Depression With Improved Recording Parameters

Evelyn B. N. Friedel[1,2,3†], Ludger Tebartz van Elst[1†], Céline Schmelz[4], Dieter Ebert[1], Simon Maier[1], Dominique Endres[1], Kimon Runge[1], Katharina Domschke[1,5], Emanuel Bubl[1], Jürgen Kornmeier[1,6], Michael Bach[2], Sven P. Heinrich[2] and Kathrin Nickel[1]*

[1] Department of Psychiatry and Psychotherapy, Medical Center—University of Freiburg, Faculty of Medicine, University of Freiburg, Freiburg, Germany, [2] Eye Center, Medical Center—University of Freiburg, Faculty of Medicine, University of Freiburg, Freiburg, Germany, [3] Faculty of Biology, University of Freiburg, Freiburg, Germany, [4] Pfalzklinikum—Clinic for Psychiatry and Neurology, Klingenmünster, Germany, [5] Center for Basics in Neuromodulation, Faculty of Medicine, University of Freiburg, Freiburg, Germany, [6] Institute for Frontier Areas of Psychology and Mental Health, Freiburg, Germany

OPEN ACCESS

Edited by:
Jason C. Park, University of Illinois at Chicago, United States

Reviewed by:
Jan Kremers, University Hospital Erlangen, Germany
Shresta Patangay, University of Illinois at Chicago, United States

****Correspondence:***
Ludger Tebartz van Elst
tebartzvanelst@uniklinik-freiburg.de

†These authors share first authorship

Specialty section:
This article was submitted to Ophthalmology, a section of the journal Frontiers in Medicine

Received: *28 June 2021*
Accepted: *06 October 2021*
Published: *29 October 2021*

Citation:
Friedel EBN, Tebartz van Elst L, Schmelz C, Ebert D, Maier S, Endres D, Runge K, Domschke K, Bubl E, Kornmeier J, Bach M, Heinrich SP and Nickel K (2021) Replication of Reduced Pattern Electroretinogram Amplitudes in Depression With Improved Recording Parameters. Front. Med. 8:732222. doi: 10.3389/fmed.2021.732222

Background: The retina has gained increasing attention in non-ophthalmological research in recent years. The pattern electroretinogram (PERG), a method to evaluate retinal ganglion cell function, has been used to identify objective correlates of the essentially subjective state of depression. A reduction in the PERG contrast gain was demonstrated in patients with depression compared to healthy controls with normalization after remission. PERG responses are not only modulated by stimulus contrast, but also by check size and stimulation frequency. Therefore, the rationale was to evaluate potentially more feasible procedures for PERG recordings in daily diagnostics in psychiatry.

Methods: Twenty-four participants (12 patients with major depression (MDD) and 12 age- and sex-matched healthy controls) were examined in this pilot study. We investigated PERG amplitudes for two steady-state pattern reversal frequencies (12.5/18.75 rps) and four sizes of a checkerboard stimulus (0.8°, 1.6°, 3.2°, and 16°) to optimize the PERG recordings in MDD patients.

Results: Smaller PERG amplitudes in MDD patients were observed for all parameters, whereby the extent of the reduction appeared to be stimulus-specific. The most pronounced decline in the PERG of MDD patients was observed at the higher stimulation frequency and the finest pattern, whilst responses for the largest check size were less affected. Following the PERG ratio protocol for early glaucoma, where similar stimulus dependent modulations have been reported, we calculated PERG ratios (0.8°/16°) for all participants. At the higher frequency (18.75 rps), significantly reduced ratios were observed in MDD patients.

Conclusion: The "normalization" of the PERG responses—via building a ratio—appears to be a very promising approach with regard to the development of an objective biomarker of the depressive state, facilitating inter-individual assessments of PERG recordings in patients with psychiatric disorders.

Keywords: pattern electroretinogram, PERG, depression, check size, dopamine

INTRODUCTION

As an ontogenetic part of the brain, the retina exhibits high levels of many neurotransmitters of the central nervous system, including dopamine (1). Since the retina represents a more accessible structure than the brain itself for related measurements, it recently gained increasing attention in other, non-ophthalmological research fields, such as neurology or psychiatry (2).

Indeed, previous studies indicate alterations in visual processing in diseases which are associated with a disturbance in the central dopaminergic homeostasis. These include Parkinson's disease (3–5), schizophrenia (6, 7) and major depressive disorder (MDD) (8–10).

Bubl et al. (8) initially reported higher contrast detection thresholds in patients suffering from MDD. In further research, they took advantage of a more objective electrophysiological approach from ophthalmology, the pattern electroretinogram (PERG), to demonstrate objective correlates of the essentially subjective state of depression (9).

The electroretinogram (ERG) uses corneal electrodes to measure the electrical activity of the retina in response to visual stimulation (11). The PERG is mostly generated by the retinal ganglion cells (12) which are stimulated by local contrast changes in black/white reversing pattern stimuli, like checkerboards (13, 14). The PERG allows both, an assessment of the macular function and a direct measurement of the retinal ganglion cell integrity (15). Therefore, it is—so far—primarily applied in ophthalmology for detecting early glaucomatous dysfunction (16–18).

In recent years, PERG has become increasingly important in psychiatric research as a possibility to map the integrity of the cerebral dopaminergic system indirectly via retinal ganglion cell function with minimal invasiveness (3, 19–22).

Bubl et al. (9), for instance, observed a remarkable reduction in the PERG contrast gain (corresponding to the increase in amplitude with ascending stimulus contrast) of about 50% in patients with MDD compared to healthy controls, with a significant negative correlation of contrast gain with depression severity. Moreover, with remission of the depressive symptoms, a normalization of the reduced retinal signals was observed (10). Therefore, it was postulated that the PERG could be a meaningful measurement tool for psychiatric disorders with the contrast gain as a state marker for depression (10). **Table 1** lists preliminary and present investigations focusing on the contrast sensitivity and the PERG-based contrast gain in MDD patients.

The International Society for Clinical Electrophysiology of Vision (ISCEV) published the current PERG standards in 2012 with recommendations for measurement parameters, calibrations and settings of PERG recordings (14). Various parameters have to be considered when recording the PERG signal.

For the standard PERG, a symmetrical black/white reversing checkerboard pattern with a constant mean luminance should be presented at a standard (15°) or large field size (≈ 30°). A check size of 0.8° (±0.2°), a reversal rate of approximately 16 rps (8 Hz) ±20% (for steady state stimulation) and a high stimulus contrast (> 80%) is recommended in the current guidelines (14). As the PERG amplitude increases almost linearly with increasing stimulus contrast (13), the PERG contrast gain can be calculated from a linear regression line (PERG contrast transfer function) as described by Bubl et al. (9). The slope of this regression line is modulated by the stimulus frequency as well as by the check sizes presented. Higher frequencies lead to a steeper slope of the PERG contrast transfer function, whereas the use of larger patterns (≈ 4°) seems to counteract this effect (25).

Aims of the Study

The recommended standard recording parameters of the ISCEV (14) for clinical PERG assessment have been adapted for ophthalmologic patients. However, it has not yet been investigated whether they are equally suitable for PERG recordings in psychiatric patients.

The aim of the current study was (1) to replicate the findings of reduced PERG responses in patients with depression (9, 10) in an independent sample and (2) to improve the PERG protocols for this patient group with a specific focus on check size and stimulus frequency.

Check Size

It is known that the PERG amplitudes attenuate with poor visual acuity (26). Proper refraction is thus mandatory for PERG recordings, but difficult to implement in non-ophthalmological settings. This effect can be bypassed by using very coarse checkerboard patterns for the stimulation, which are clearly above the visual acuity threshold. In the present study, we investigated the PERG in response to a whole set of black/white reversal checkerboards with the following check sizes: 0.8°, 1.6°, 3.2°, and 16°.

Frequency

In previous studies about PERG effects in patients with depression, a stimulation frequency of 12.5 rps was applied. Higher reversal frequencies have been reported to be capable to increase the sensitivity for detecting ophthalmological diseases like glaucoma (27, 28). In the present study, we compared PERG amplitudes for two steady-state frequencies for pattern reversals (12.5 and 18.75 rps) to assess whether they can be applied equivalently.

MATERIALS AND METHODS

Participants

The study was approved by the ethics committee of the University Medical Center Freiburg (Approval ID: 93/04) and was conducted in accordance with the Declaration of Helsinki. All participants gave their written informed consent. Patients were recruited at the Department of Psychiatry and Psychotherapy, University of Freiburg. The diagnosis of a major depressive episode was established by an experienced specialist in psychiatry according to DSM-5 criteria. A depressive episode in the context of bipolar disorder, the presence of psychotic symptoms, and comorbid alcohol abuse were defined as exclusion criteria. Initially, 17 patients with a diagnosis of major depressive

TABLE 1 | Previous studies on contrast sensitivity and/or PERG responses in patients with major depression.

References	*N* (Patients/HC)	Age (years) mean (SD)	Measurement parameters (e.g., pattern size, reversal rate, contrast level)	Results (Patients/HC)
1. Bubl et al. (8)	28 MDD 21 HC	31.8 (9.5) 33.1 (10)	Gabor patches: Size: 2 cpd Contrasts: 1, 3, 10, 20, 30, 40, 50%	Elevated contrast discrimination threshold in MDD
2. Bubl et al. (9) [see technical note in Bubl et al. (23)]	40 MDD (20 medicated, 20 without medication) 40 HC	43.2 (6.3) 44.6 (4.5) 41.8 (4.5) 43.3 (6.3)	PERG Check size: 0.51° Reversal rate: 12.5 rps Contrasts: 3.2, 7.3, 16.2, 36, 80%	Reduced PERG contrast gain in MDD (∼50% reduction in MDD)
3. Bubl et al. (10)	14 MDD (10 remitted, 4 not remitted) 40 HC	40.3 (12.8) 48.8 (9.8) 43.3 (12.7)	PERG Check size: 0.51° Reversal rate: 12.5 rps Contrasts: 3.2, 7.3, 16.2, 36, 80%	Normalization of reduced PERG-based contrast gain in MDD with remission
4. Fam et al. (24)	20 MDD 20 HC	44.5 (9.8) 43.7 (9.7)	(1) PERG Check size: 0.8° Reversal rate: 12 rps Contrasts: 7, 21, 42, 56, 68% (2) ffERG: flashes 0.01/3.0 cd·s/m²) (3) Contrast sensitivity (FrACT)	Normal signals in MDD for (1) PERG contrast gain and (2) ffERG; (3) Reduced contrast sensitivity in MDD which were correlated with BDI-symptoms

BDI, beck depression inventory; cpd, cycles per degree; ffERG, full-field electroretinogram; HC, healthy controls; MDD, major depressive disorder; N, number; PERG, pattern electroretinogram; rps, reversals per second; SD, standard deviation.

disorder (MDD) were recruited. PERG measurement was performed within the first few weeks after starting antidepressant medication, without clinical response. The intake of neuroleptics, methylphenidate, or the antidepressant bupropion were defined as exclusion criteria.

In addition, 17 healthy controls without current or a history of psychiatric or neurological diseases were recruited. They had to score within the normal range of the Beck Depression Inventory [BDI; (29)] and the Hamilton Depression Rating Scale [HDRS; (30)]. The matching procedure controlled for effects of sex and age.

Exclusion criteria for both groups were defined as an age > 65 years, the presence of neurological or ophthalmological diseases or an uncorrectable low visual acuity (< 0.8).

The following questionnaires were collected from both patients and control participants: the Beck Depression Inventory [BDI; (29)] to assess the severity of depressive symptoms and the Wender-Utah Rating Scale [WURS-k; (31)] for ADHD symptoms in childhood. In addition, the Hamilton Depression Rating Scale [HDRS; (30)] was applied as third-party assessment questionnaire.

Data Acquisition

Before examination, visual acuity of each participant was assessed monocularly with the Freiburg Visual Acuity and Contrast Test [FrACT; (32)] and, if necessary, corrected with refraction. A minimum of 0.8 decimal visual acuity was required for each eye.

DTL (Dawson, Trick, and Litzkow)-like electrodes (33), placed at the lower limbus of each eye were used for PERG recordings. Gold-cup electrodes positioned at each ipsilateral eye-canthus served as reference, an ear-clip as ground.

The EP2000 system was used for stimulation and initial data collection (https://michaelbach.de/sci/stim/ep2000/index.html; retrieval date 15.10.2021). Pattern stimuli were presented at an observer distance of 57 cm on a CRT monitor with 75 Hz frame rate in 800 x 600 pixel resolution, covering a field size of $32° \times 27°$. Symmetrical black/white reversal checkerboards with a mean luminance of 45 cd/m² and a Michelson contrast of 80% served as pattern stimuli. Four different check sizes (0.8°, 1.6°, 3.2°, 16°) were presented using two different reversal frequencies (12.5 and 18.75 rps) in the steady state range. Every check size was presented for a duration of 10 sweeps with a constant sweep length for both frequencies (960 ms), starting with the lower reversal rate, followed by the higher one. Blocks for the different pattern sizes were shown in ascending manner (stepwise increasing check size: 0.8°, 1.6°, 3.4°, 16°). This sequence was repeated in 10 equal cycles, with a short break in between. Responses exceeding a threshold of 120 μV were automatically rejected as artifacts. A minimum of 100 artifact free sweeps were recorded per condition and submitted to stimulus-synchronized averaging.

Data Analysis

First off-line data processing was performed in Igor Pro 7 (Wave Metrics) with the "EP2000" module. To eliminate mains hum artifacts, averaged response traces were digitally low pass filtered (40 Hz). A Fourier analysis was performed after any linear trend (e.g., due to baseline drifts) had been removed (34). PERG amplitudes were extracted from the Fourier spectra at the respective stimulation frequencies (12.5 and 18.75 Hz) and noise-corrected [as described in (34)]. The average magnitude from the direct adjacent frequencies served as noise estimate (35). Additionally, phases were extracted from the Fourier transformation.

Statistical Analysis

Statistical analysis was carried out in "R" (36) with RStudio (37) using the "tidyverse" package (38) for data handling. For the

TABLE 2 | Demographic and psychometric data.

	Characteristic	Controls, $N = 12$	Patients, $N = 12$	p-value [a]
Sex	Male	5/12 (42%)	5/12 (42%)	
	Female	7/12 (58%)	7/12 (58%)	
Age	Mean (SD)	29 (8)	26 (9)	0.087
	Range	20–51	19–51	
Medication	Medicated	0/12 (0%)	11/12 (92%)	
	Unmedicated	12/12 (100%)	1/12 (8.3%)	
WURS-k	Mean (SD)	11 (6)	23 (13)	0.003
	Median (IQR)	8 (7, 15)	18 (16, 27)	
BDI	Mean (SD)	3 (3)	25 (8)	<0.001
	Median (IQR)	3 (1, 5)	25 (18, 32)	
	(Missing)	0	1	
HDRS	Mean (SD)	1 (1)	22 (4)	<0.001
	Median (IQR)	1 (0, 1)	22 (20, 26)	

[a] *Statistical test: Wilcoxon rank-sum test. BDI, Beck Depression Inventory; HDRS, Hamilton Depression Rating Scale; IQR, interquartile range; N, number; SD, standard deviation; WURS-k, Wender-Utah Rating Scale; y, years.*

8 stimulus conditions (4 check sizes and 2 frequencies) PERG amplitudes from both eyes were averaged for every participant separately. Psychometric data comparisons and initial testing for differences between the groups or stimulation parameters were established using Wilcoxon rank sum tests ["rstatix" package (39)]. Response times (in ms) were calculated from the extracted phase values (40). The fully crossed factorial design was analyzed with a mixed analysis of variance (ANOVA) for repeated measures ["afex" package (41)]. The factors group, check size and stimulation frequency, as well as their interactions, were evaluated for their impact on PERG amplitudes or response times. The factors check size and frequency were considered as repeated measures factors for each subject. *Post-hoc* analysis was limited to group comparisons ["emmeans" package (42)] with equal variance assumed. Hedge corrected (43) Cohen's d was calculated as effect size estimation for unpaired samples ["rstatix" package (39)]. Significance levels were determined by applying the Bonferroni-Holm procedure for a familywise α of 0.05 (44).

RESULTS

Demographic and Psychometric Data

Of the originally measured 17 patients, five had to be excluded. The reasons for exclusion were intolerance of the electrodes, the intake of neuroleptic medication, regular somatic medication, subsequently diagnosed psychiatric comorbidity and substance abuse. Finally, 12 patients between 19 and 51 years of age could be included in the final analysis. Four patients suffered from a first severe depressive episode, while 8 patients had a recurrent severe depressive episode. Of the 17 control participants measured, 12 were matched by sex and age to the included patients and considered in the final analysis. The psychometric data of the patient and the control groups are presented in **Table 2**.

Pattern Electroretinogram (PERG)

Group Averaged PERG Responses

In both groups, measures of one eye of each of two participants had to be excluded due to electrode displacement during the experiment. Except for these cases, the responses of both eyes were averaged before further analysis.

Figure 1 illustrates the mean PERG amplitudes for patients and controls for all stimulus conditions.

The overall average of the PERG response of patients suffering from MDD was significantly lower compared to the control group ($p = 0.017$, unpaired, one-sided Wilcoxon test assuming lower PERG for MDD; data pooled across stimulus parameters), with a similar signal to noise ratio for both groups ($p = 0.242$, unpaired, two-sided Wilcoxon test, data averaged across stimulus parameters).

Although the average PERG amplitude in response to the higher frequency (18.75 rps) was significantly lower ($p < 0.001$; paired, one-sided Wilcoxon test assuming lower PERG at 18.75 rps; data averaged across groups and check sizes), the signal-to-noise ratio was comparable for both frequencies ($p = 0.121$; paired, two-sided Wilcoxon test, data pooled across groups and check sizes). Further visual inspection suggests largest amplitudes in response to the smallest check size with a slight attenuation toward coarser patterns.

The overall average of PERG response time was significantly reduced in patients with MDD compared to healthy controls ($p < 0.001$, unpaired, two-sided Wilcoxon test, data pooled across stimulus parameters).

Mixed ANOVA Results

With a mixed ANOVA, PERG amplitudes were evaluated for (between) group differences and influences from check size or stimulation frequency, both considered as subject-wise repeated measures (within). Possible interaction effects were included.

The ANOVA revealed a significant effect for the between factor group [$F_{(1, 22)} = 6.53$, $p = 0.018$] and the within factors check size [$F_{(1.52, 33.41)} = 55.42$, $p < 0.001$] and stimulation frequency [$F_{(1, 22)} = 53.02$, $p < 0.001$], as well as a significant interaction between the two stimulus parameters [$F_{(1.79, 39.38)} = 19.24$, $p < 0.001$] on the PERG amplitudes. Interactions between stimulus conditions and the factor group were not observed.

A separate ANOVA calculated for response times showed significant effects for the factors group [$F_{(1, 22)} = 14.70$, $p < 0.001$], frequency [$F_{(1, 22)} = 88.14$, $p < 0.001$] and size [$F_{(1.48, 32.51)} = 1313.83, p < 0.001$].

Post-hoc Analysis for Group Differences

A subsequent *post-hoc* comparison of the two groups indicated significantly reduced PERG amplitudes in the MDD group for almost all stimulus parameters (**Table 3**), considering the uncorrected results. After correcting significance levels for multiple comparisons according to the Bonferroni-Holm procedure, group differences remained significant only for the finest pattern (0.8°). At 18.75 rps, the decline of PERG in MDD (**Table 3**) apparently scales with the check size of the stimulus.

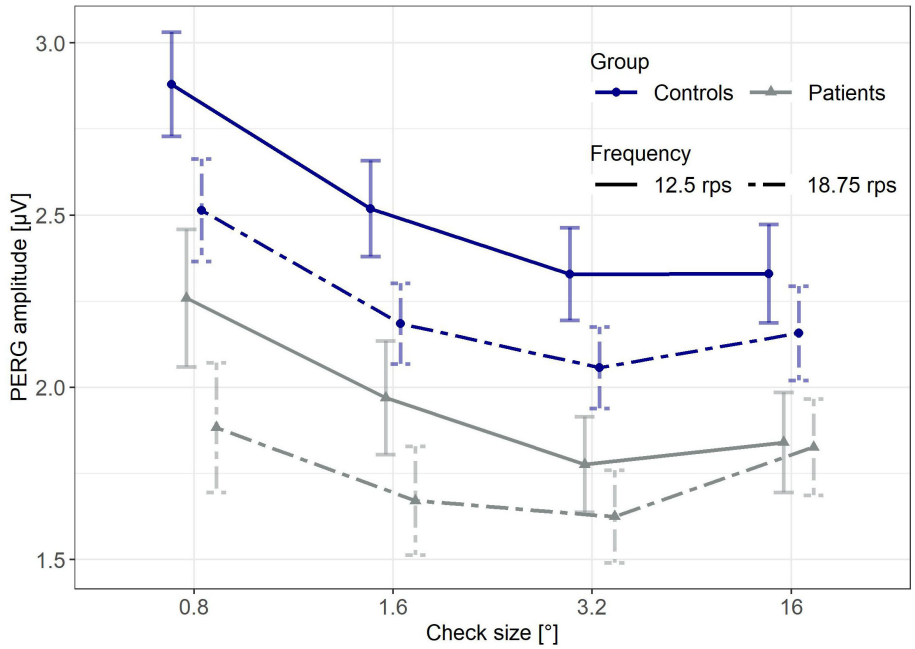

FIGURE 1 | Mean PERG amplitudes for both groups and all stimulus conditions. Error bars indicate the standard error of the mean (SE).

TABLE 3 | Results from the *post-hoc* analysis for PERG amplitudes (in µV).

Check Size [°]	Frequency [rps]	Controls mean (SD)	Patients mean (SD)	Differences of estimated marginal means (SE)	*P*-value (significance level Holm adjusted)	Hedge corrected Cohen's d
0.8	12.5	2.9 (0.5)	2.3 (0.7)	0.621 (0.21)	0.007 (*)	0.98
1.6	12.5	2.5 (0.5)	2 (0.6)	0.549 (0.21)	0.015 (ns)	1.00
3.2	12.5	2.3 (0.5)	1.8 (0.5)	0.553 (0.21)	0.014 (ns)	1.13
16	12.5	2.3 (0.5)	1.8 (0.5)	0.490 (0.21)	0.028 (ns)	0.95
0.8	18.75	2.5 (0.5)	1.9 (0.7)	0.630 (0.21)	0.006 (*)	1.04
1.6	18.75	2.2 (0.4)	1.7 (0.5)	0.514 (0.21)	0.022 (ns)	1.03
3.2	18.75	2.1 (0.4)	1.6 (0.5)	0.431 (0.21)	0.051 (ns)	0.95
16	18.75	2.2 (0.5)	1.8 (0.5)	0.331 (0.21)	0.127 (ns)	0.67

*Pairwise group comparisons (contrast: controls–patients) for all stimulus conditions with the corresponding differences in the estimated marginal means (SE included), the arithmetic mean and standard deviation (SD) for patients and controls as well as the effect size estimation (Cohen's d Hedge corrected) for group differences. Significance levels were adjusted according to Bonferroni-Holm procedure. *significant; ns, not significant.*

In an additional *post-hoc* analysis, we detected shorter response times for patients with MDD compared to healthy controls for all stimulus parameter combinations (**Table 4**).

Cohen's d Effect Size Estimation for Stimulus Parameter Combinations

Figure 2 shows that, at a stimulation frequency of 18.75 rps, the PERG response difference between patients and healthy controls is gradually smaller with increasing check size. The most prominent decay in patients' PERG amplitudes was observed with the finest pattern (0.8°) (25%, $d = 1.04$), while the PERG amplitudes at the coarsest checkerboard (16°) seemed to be least affected (15%, $d = 0.67$). Interestingly, this PERG response pattern is reminiscent of the conditions observed in early glaucoma (16, 17, 45).

PERG Check Size Ratio

Based on the "PERG ratio protocol" in early glaucoma (17, 46, 47), check size ratios for the PERG amplitudes were established for both groups and frequencies according to formula (1).

$$PERG\ ratio = \frac{PERG\ amplitude\ at\ 0.8^{\circ}}{PERG\ amplitude\ at\ 16^{\circ}}. \quad (1)$$

With regard to the application of PERG response as an objective biomarker, the calculation of PERG ratios for every subject has the advantage of minimizing inter-individual

TABLE 4 | Results from the *post-hoc* analysis for calculated response times (in ms).

Check size [°]	Frequency [rps]	Controls mean (SD)	Patients mean (SD)	Differences of estimated marginal means (SE)	*P*-value (significance level Holm adjusted)	Hedge corrected Cohen's d
0.8	12.5	55.2 (2.9)	51.9 (3)	3.37 (0.96)	0.002 (*)	1.09
1.6	12.5	51.7 (2.6)	48.3 (2.8)	3.42 (0.96)	0.001 (*)	1.22
3.2	12.5	48.9 (2.2)	45.3 (2.4)	3.58 (0.96)	0.001 (*)	1.53
16	12.5	44.7 (2.1)	41.5 (2.4)	3.22 (0.96)	0.002 (*)	1.36
0.8	18.75	56.4 (1.8)	53.2 (2.5)	3.19 (0.96)	0.003 (*)	1.41
1.6	18.75	53.4 (2)	49.6 (2.3)	3.79 (0.96)	0.001 (*)	1.69
3.2	18.75	50.4 (2.1)	46.5 (2)	3.87 (0.96)	<0.0001 (*)	1.84
16	18.75	46.5 (2.1)	43 (1.8)	3.52 (0.96)	0.001 (*)	1.72

*Pairwise group comparisons (contrast: controls–patients) for all stimulus conditions with the corresponding differences in the estimated marginal means (SE included), the arithmetic mean and standard deviation (SD) for patients and controls as well as the effect size estimation (Cohen's d Hedge corrected) for group differences. Significance levels were adjusted according to Bonferroni-Holm procedure. *significant; ns, not significant.*

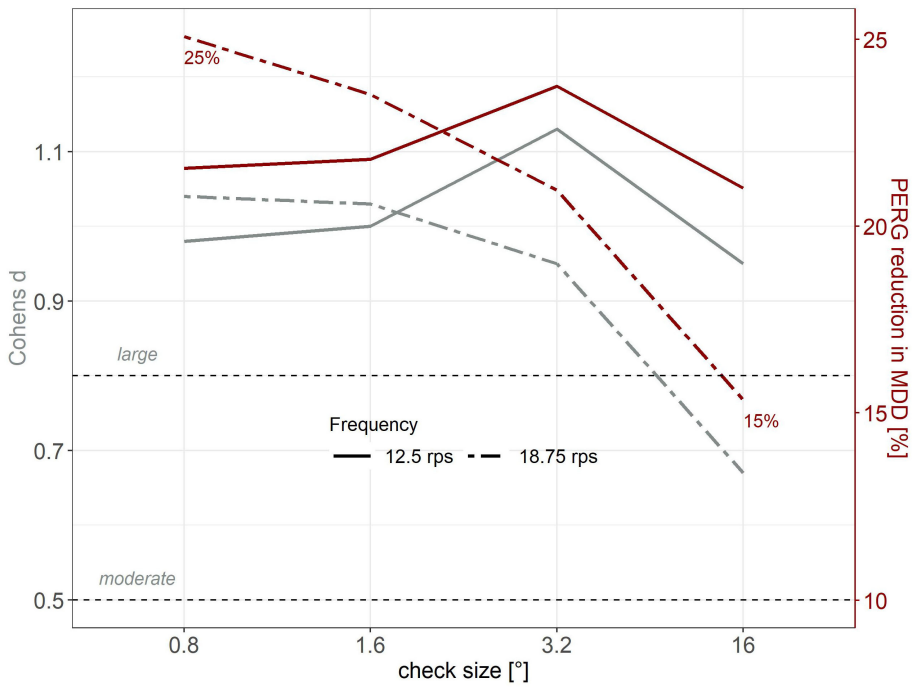

FIGURE 2 | Cohen's d (gray, left axis) as effect size estimation and mean relative PERG reduction (red, right axis, %) in MDD patients compared to healthy controls as a function of check size. Continuous lines depict 12.5 rps, dashed lines represent 18.75 rps.

variability by amplitude normalization. **Figure 3** depicts the normalized PERG amplitudes for the patient and the control group.

A second mixed ANOVA with the between factor group, the within-factor stimulation frequency and the PERG ratio as dependent variable revealed a significant influence of stimulus frequency on the PERG ratio [$F_{(1, 22)} = 29.23$, $p < 0.001$], no overall-group differences [$F_{(1, 22)} = 3.33$, $p = 0.082$], but a significant interaction effect between group and stimulus frequency [$F_{(1, 22)} = 6.96$, $p = 0.015$].

Post-hoc evaluation exhibited that the PERG ratios in the MDD group, in response to a stimulation frequency of 18.75 rps, were significantly reduced ($p = 0.008$, $d = 1.07$), whereas with the lower reversal rate (12.5 rps), PERG ratios did not differ between groups ($p = 0.674$, $d = 0.18$).

DISCUSSION

The aims of the present study were (1) the replication of the PERG amplitude effect in patients with MDD and (2) the evaluation of different stimulus conditions to further improve PERG recording procedures for this patient group. Four check sizes (0.8°, 1.6°, 3.2°, and 16°) were compared to analyze if PERG signals in MDD, in response to coarser patterns, are affected to the same extent as to smaller check

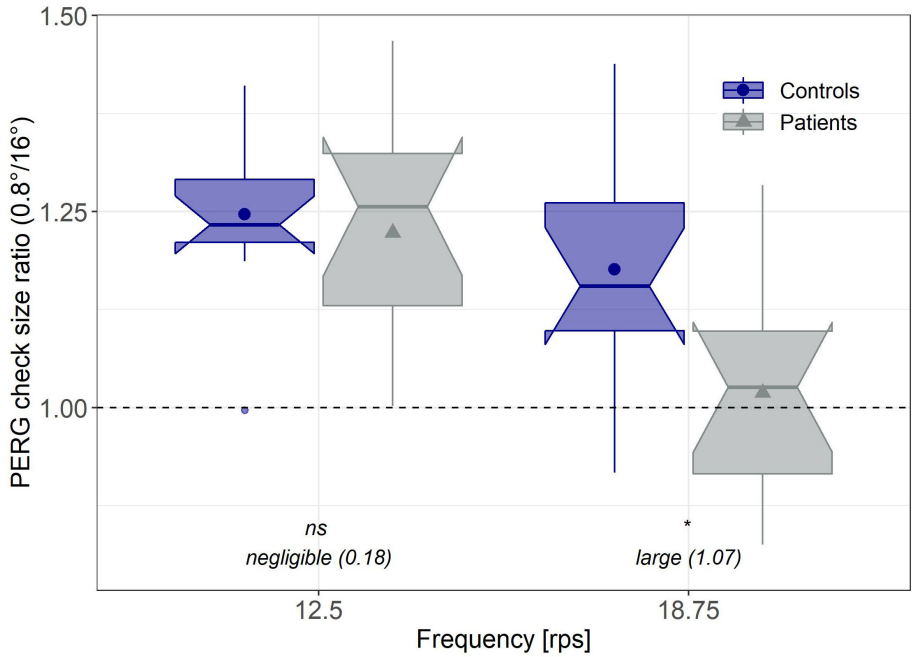

FIGURE 3 | Normalized PERG amplitudes. Individual PERG ratios (0.8°/16°) corresponding to the "PERG ratio protocol" for early glaucoma (17) for both groups and frequencies. Significance levels were Bonferroni-Holm corrected. Effect sizes were estimated based on Hedge's corrected Cohen's d. *significant; ns, not significant.

sizes used in previous studies. The application of coarser patterns would be beneficial by eliminating influences due to refraction errors. In addition, two frequencies (12.5 and 18.75 rps) for checkerboard reversals were investigated in order to test if PERG responses were similarly affected at higher stimulation frequencies.

Group Comparisons for the Different Parameter Combinations

Overall, we discerned smaller PERG amplitudes in patients with MDD compared to matched healthy control participants, which replicates earlier findings with an independent sample of patients and controls (9). After correction for multiple testing, statistically reliable reductions in the PERG in MDD were only indicated with the smallest check size (0.8°).

This effect was not only present for the lower (12.5 rps), as previously reported (9, 10), but also for the higher stimulation frequency (18.75 rps) with a comparable signal-to-noise ratio for both frequencies. A follow-up study should address, whether a higher frequency can provide the opportunity to reduce total recording time. A shorter measurement time would be particularly advantageous for psychiatric patients with depressive symptoms and limited ability to uphold attention.

The higher rate for checkerboard reversals (18.75 rps) is additionally beneficial by fine-tuning group differences between MDD and control subjects through check size dependent modulations, which allow for a normalization of PERG responses via the calculation of check size ratios, similar to those used for the detection of early glaucoma (17).

Besides, our observations are not in line with the results of Fam et al. (24), who reported normal PERG contrast gain in MDD patients applying a stimulation frequency of 12 rps and the check size of 0.8°. This could possibly be due to differences in the technical implementation of the measurement protocol.

Since the PERG amplitude reduction in patients with MDD was only significant with the smallest check size (0.8°), we cannot recommend a recording paradigm which uses exclusively larger check sizes (1.6°, 3.2°, or 16°) in the context of psychiatric disorders, which would render the correction of refractive anomalies unnecessary.

Considering the dopamine-dependent regulation of the receptive field sizes in the retina (48) and the assumption of a disturbed dopamine homeostasis in MDD (49, 50), check size specific PERG alterations in MDD patients seem convincing. Particularly, dopamine is known for its modulatory role in the light adaptation of the retina, favoring daylight vision with high acuity, a mechanism provided by the decoupling of horizontal cells in the retina, thereby shrinking the antagonistic surround structures of the receptive fields (48). A disturbed dopamine homeostasis probably results in alterations in the PERG signals in response to different check sizes as it was similarly described for patients suffering from Parkinson's disease (4, 5).

Moreover, shortened response times were observed in patients with MDD for all stimulus conditions. As described in transient stimulations (51), the effect of a shorter response time with larger check sizes is observed in both groups. In patients with glaucoma, not only reduced amplitudes but also shorter response

times have been similarly described by Bode and colleagues (40). At this point, the authors discuss an effect observed by Viswanathan et al. (52) that leads to a shortening of the P50 peak time when N95 is eliminated. Whether such a differential change between the N95 and the P50, which both contribute to the PERG signal, occurs in MDD and can explain the observed changes in the steady-state response time would need to be addressed in future studies.

PERG Ratio

While it would have been useful to find strong effects of depression with the very large check sizes, which would have obviated refraction, one can turn the relative constancy of these amplitudes into our favor by using them for individual normalization. Inspired by the PERG ratio protocol in early glaucoma (16, 17, 45), we compared the standardized PERG amplitudes, i.e., the amplitude ratio over the two check sizes (0.8° and 16°), between groups for both stimulation frequencies. The advantage of this "PERG ratio" approach is that it reduces inter-individual variability. We observed a significantly reduced PERG ratio in MDD patients compared to healthy controls for the high stimulation frequency (18.75 rps), but not for the low stimulation frequency (12.5 rps). This alternative analysis approach is promising since it increases interpersonal comparability and statistical power, which is particularly important for an objective biomarker. Moreover, higher stimulation frequencies could possibly reduce the time required for recording, which should be addressed in a follow-up study.

Methodological Issues and Limitations

The present study provides promising perspectives for the optimization of PERG recording procedures in psychiatric settings. However, some limitations have to be mentioned.

Due to the small number of patients, the results of the current study must be considered preliminary. Follow-up studies with larger samples sizes could yield further information about the adaptation of stimulation frequency and check size for PERG recordings in psychiatric patients. It should be noted, however, that the PERG ratio is feasible to minimize inter-individual differences.

At the time of measurement, patients had already been taking antidepressant medication for a few days or weeks. In a previous study by Bubl et al. (9), however, a reduction in contrast gain was detected in both medicated and un-medicated depressed patients. Another limitation is that smoking status was not considered as a matching factor between patients and controls. This could also have a confounding effect on results, as it could have an impact on dopamine neurotransmission (53). Lastly, the MDD group also exhibited elevated ADHD symptoms in childhood according to the WURS-k questionnaire compared to the control group. Since the PERG amplitudes from patients suffering from ADHD have been reported to be unaffected (54), we regard influences from ADHD symptoms as rather unlikely. Particularly since the so-called PERG noise, which has been shown to be elevated in ADHD patients (55), was not affected in our MDD patients ($p = 0.94$, one-sided Wilcoxon test comparing PERG noise between groups, data pooled across stimulus parameters).

Summary

In summary, in this methodological pilot study we could reproduce earlier findings of reduced PERG amplitudes in patients with depression as a potentially objective biomarker signal of the essentially subjective state of depression. In addition, we were able to methodologically improve the recording procedure by demonstrating the suitability of a higher stimulation frequency for recordings along with the introduction of an interpersonal normalization approach for the PERG signals, which further enhances the sensitivity of the method.

DATA AVAILABILITY STATEMENT

The original contributions presented in the study are included in the article, further inquiries can be directed to the corresponding author/s.

ETHICS STATEMENT

The studies involving human participants were reviewed and approved by the Ethics Committee of the University Medical Center Freiburg (Approval ID: 93/04). The patients/participants provided their written informed consent to participate in this study.

AUTHOR CONTRIBUTIONS

KN and EF wrote the paper. EF, KN, CS, and SM performed the data and statistical analysis. LTvE, KN, DEb, MB, and EF organized the study and created the study design. KN, DEb, and DEn recruited the patients and established the diagnosis. MB and SH supported the methodological and technical realization for the collection of the electrophysiological data. CS and EF performed the measurements. LTvE, KD, SM, DEb, DEn, KR, EB, MB, JK, and SH revised the manuscript critically focusing on clinical and statistical aspects. All authors were critically involved in the theoretical discussion, composition of the manuscript, and read and approved the final version of the manuscript.

FUNDING

Part of the study was funded by the DFG (HE 3504/11-1 | TE 280/24-1). The article processing charge was funded by the Baden-Wuerttemberg Ministry of Science, Research and Art and the University of Freiburg in the funding programme Open Access Publishing.

REFERENCES

1. Nguyen CTO, Hui F, Charng J, Velaedan S, van Koeverden AK, Lim JKH, et al. Retinal biomarkers provide 'insight' into cortical pharmacology and disease. *Pharmacol Therapeut.* (2017) 175:151–77. doi: 10.1016/j.pharmthera.2017.02.009
2. Almonte MT, Capellàn P, Yap TE, Cordeiro MF. Retinal correlates of psychiatric disorders. *Therapeut Adv Chronic Dis.* (2020) 11:1–21. doi: 10.1177/2040622320905215
3. Tebartz van Elst L, Greenlee MW, Foley JM, Lücking CH. Contrast detection, discrimination and adaptation in patients with Parkinson's disease and multiple system atrophy. *Brain J Neurol.* (1997) 120(Pt 12):2219–28.
4. Brandies R, Yehuda S. The possible role of retinal dopaminergic system in visual performance. *Neurosci Biobehav Rev.* (2008) 32:611–56. doi: 10.1016/j.neubiorev.2007.09.004
5. Armstrong RA. Visual symptoms in Parkinson's disease. *Parkinsons Dis.* (2011) 2011:e908306. doi: 10.4061/2011/908306
6. Silverstein S, Keane BP, Blake R, Giersch A, Green M, Kéri S. Vision in schizophrenia: why it matters. *Front Psychol.* (2015) 6:41. doi: 10.3389/fpsyg.2015.00041
7. Silverstein SM, Fradkin SI, Demmin DL. Schizophrenia and the retina: towards a 2020 perspective. *Schizophrenia Res.* (2020) 219:84–94. doi: 10.1016/j.schres.2019.09.016
8. Bubl E, Tebartz van Elst L, Gondan M, Ebert D, Greenlee MW. Vision in depressive disorder. *World J Biol Psychiatry.* (2009) 10 (4 Pt 2):377–84. doi: 10.1080/15622970701513756
9. Bubl E, Kern E, Ebert D, Bach M, Tebartz van Elst L. Seeing gray when feeling blue? Depression can be measured in the eye of the diseased. *Biol Psychiatry.* (2010) 68:205–8. doi: 10.1016/j.biopsych.2010.02.009
10. Bubl E, Ebert D, Kern E, Tebartz van Elst L, Bach M. Effect of antidepressive therapy on retinal contrast processing in depressive disorder. *Brit J Psychiatry.* (2012) 201:151–8. doi: 10.1192/bjp.bp.111.100560
11. Robson AG, Nilsson J, Li S, Jalali S, Fulton AB, Tormene AP, et al. ISCEV guide to visual electrodiagnostic procedures. *Document Ophthalmol.* (2018) 136:1–26. doi: 10.1007/s10633-017-9621-y
12. Luo X, Frishman LJ. Retinal pathway origins of the pattern electroretinogram (PERG). *Investig Ophthalmol Visual Sci.* (2011) 52:8571–84. doi: 10.1167/iovs.11-8376
13. Bach M, Hoffmann MB. The origin of the pattern electroretinogram. In: Heckenlively JR, Arden GB, editors. *Principles Practice of Clinical Electrophysiology of Vision*. 2nd ed. Cambridge, MA: MIT Press (2006), p. 185–96.
14. Bach M, Brigell MG, Hawlina M, Holder GE, Johnson MA, McCulloch DL, et al. ISCEV standard for clinical pattern electroretinography (PERG): 2012 update. *Document Ophthalmol.* (2012) 124:1–13. doi: 10.1007/s10633-012-9353-y
15. Holder GE. Pattern electroretinography (PERG) and an integrated approach to visual pathway diagnosis. *Prog Retinal Eye Res.* (2001) 20:531–61. doi: 10.1016/S1350-9462(00)00030-6
16. Bach M. Electrophysiological approaches for early detection of glaucoma. *Eur J Ophthalmol Suppl.* (2001) 11 (Suppl 2):S41–9. doi: 10.1177/112067210101102s05
17. Bach M, Hoffmann MB. Update on the pattern electroretinogram in glaucoma. *Optomet Vision Sci.* (2008) 85:386–95. doi: 10.1097/OPX.0b013e318177ebf3
18. Bach M, Ramharter-Sereinig A. Pattern electroretinogram to detect glaucoma: comparing the PERGLA and the PERG ratio protocols. *Document Ophthalmol.* (2013) 127:227–38. doi: 10.1007/s10633-013-9412-z
19. Langheinrich T, Tebartz van Elst L, Lagrèze WA, Bach M, Lücking CH, Greenlee MW. Visual contrast response functions in Parkinson's disease: evidence from electroretinograms, visually evoked potentials and psychophysics. *Clin Neurophysiol.* (2000) 111:66–74. doi: 10.1016/s1388-2457(99)00223-0
20. Lavoie J, Illiano P, Sotnikova TD, Gainetdinov RR, Beaulieu J-M, Hébert M. The electroretinogram as a biomarker of central dopamine and serotonin: potential relevance to psychiatric disorders. *Biological Psychiatry.* (2014) 75:479–86. doi: 10.1016/j.biopsych.2012.11.024
21. Lavoie J, Maziade M, Hébert M. The brain through the retina: the flash electroretinogram as a tool to investigate psychiatric disorders. *Prog Neuropsychopharmacol Biol Psychiatry.* (2014) 48:129–34. doi: 10.1016/j.pnpbp.2013.09.020
22. Schwitzer T, Schwan R, Bubl E, Lalanne L, Angioi-Duprez K, Laprevote V. Looking into the brain through the retinal ganglion cells in psychiatric disorders: a review of evidences. *Prog Neuropsychopharmacol Biol Psychiatry.* (2017) 76:155–62. doi: 10.1016/j.pnpbp.2017.03.008
23. Bubl E, Kern E, Ebert D, Riedel A, Tebartz van Elst L, Bach M. Retinal dysfunction of contrast processing in major depression also apparent in cortical activity. *Eur Arch Psychiatry Clin Neurosci.* (2015) 265:343–50. doi: 10.1007/s00406-014-0573-x
24. Fam J, Rush AJ, Haaland B, Barbier S, Luu C. Visual contrast sensitivity in major depressive disorder. *J Psychosom Res.* (2013) 75:83–6. doi: 10.1016/j.jpsychores.2013.03.008
25. Ben-Shlomo G, Bach M, Ofri R. Temporal and spatial frequencies interact in the contrast transfer function of the pattern electroretinogram. *Vision Res.* (2007) 47:1992–9. doi: 10.1016/j.visres.2007.04.009
26. Bach M, Mathieu M. Different effect of dioptric defocus vs. light scatter on the pattern electroretinogram (PERG). *Document Ophthalmol.* (2004) 108:99–106. doi: 10.1023/b:doop.0000018415.00285.56
27. Trick GL. Retinal potentials in patients with primary open-angle glaucoma: physiological evidence for temporal frequency tuning deficits. *Investig Ophthalmol Visual Sci.* (1985) 26:1750–58.
28. Hiss P, Fahl G. [Changes in the pattern electroretinogram in glaucoma and ocular hypertension are dependent on stimulus frequency]. *Fortschritte Der Ophthalmologie Zeitschrift Der Deutschen Ophthalmologischen Gesellschaft.* (1991) 88:562–65.
29. Beck AT, Ward CH, Mendelson M, Mock J, Erbaugh J. An inventory for measuring depression. *Arch Gen Psychiatry.* (1961) 4:561–71.
30. Hamilton M. A rating scale for depression. *J Neurol Neurosurg Psychiatry.* (1960) 23:56–62. doi: 10.1136/jnnp.23.1.56
31. Retz-Junginger P, Retz W, Blocher D, Weijers H-G, Trott E, Wender PH, et al. Wender Utah Rating Scale (WURS-k) Die deutsche Kurzform zur retrospektiven Erfassung des hyperkinetischen Syndroms bei Erwachsenen. *Der Nervenarzt.* (2002) 73:830–38. doi: 10.1007/s00115-001-1215-x
32. Bach M. The Freiburg visual acuity test–automatic measurement of visual acuity. *Optometry Vision Sci.* (1996) 73:49–53. doi: 10.1097/00006324-199601000-00008
33. Dawson WW, Trick GL, Litzkow CA. Improved electrode for electroretinography. *Invest Ophthalmol Vis Sci.* (1979) 18:988–91.
34. Bach M, Meigen T. Do's and don'ts in Fourier analysis of steady-state potentials. *Doc Ophthalmol.* (1999) 99:69–82. doi: 10.1023/A:1002648202420
35. Meigen T, Bach M. On the statistical significance of electrophysiological steady-state responses. *Doc Ophthalmol.* (1999) 98:207–32. doi: 10.1023/A:1002097208337
36. R Core Team. *R: A Language and Environment for Statistical Computing*. Vienna: R Foundation for Statistical Computing (2020). Available online at: https://www.R-project.org/
37. RStudio Team. *RStudio: Integrated Development Environment for R.* Boston, MA: RStudio, PBC (2020). Available online at: http://www.rstudio.com/
38. Wickham H, Averick M, Bryan J, Chang W, McGowan L, François R, et al. Welcome to the Tidyverse. *J Open Source Softw.* (2019) 4:1686. doi: 10.21105/joss.01686
39. Kassambara A. *Rstatix: Pipe-Friendly Framework for Basic Statistical Tests* (2020). Available online at: https://CRAN.R-project.org/package=rstatix
40. Bode SFN, Jehle T, Bach M. Pattern electroretinogram in glaucoma suspects: new findings from a longitudinal study. *Investig Opthalmol Visual Sci.* (2011) 52:4300. doi: 10.1167/iovs.10-6381
41. Singmann H, Bolker B, Westfall J, Aust F, Ben-Shachar MS. *Afex: Analysis of Factorial Experiments* (2020). Available online at: https://CRAN.R-project.org/package=afex
42. Lenth RV. *Emmeans: Estimated Marginal Means, Aka Least-Squares Means* (2020). Available online at: https://CRAN.R-project.org/package=emmeans

43. Hedges LV, Olkin I. Statistical methods for meta-analysis. In: *CHAPTER 5 - Estimation of a Single Effect Size: Parametric and Nonparametric Methods*. Orlando, FL: Academic Press (1985). p. 75–106. doi: 10.1016/C2009-0-03396-0
44. Holm S. A simple sequentially rejective multiple test procedure. *Scand J Statist*. (1979) 6:65–70.
45. Bach M, Unsoeld AS, Philippin H, Staubach F, Maier P, Walter HS, et al. Pattern ERG as an early glaucoma indicator in ocular hypertension: a long-term, prospective study. *Investig Ophthalmol Visual Sci*. (2006) 47:4881–7. doi: 10.1167/iovs.05-0875
46. Poloschek CM, Bach M. [Electrophysiological examination methods in glaucoma diagnostics]. *Der Ophthalmologe: Zeitschrift Der Deutschen Ophthalmologischen Gesellschaft*. (2012) 109:358–63. doi: 10.1007/s00347-012-2546-7
47. Anders L-M, Heinrich SP, Lagrèze WA, Joachimsen L. Little effect of 0.01% atropine eye drops as used in myopia prevention on the pattern electroretinogram. *Document Ophthalmol*. (2019) 138:85–95. doi: 10.1007/s10633-019-09671-0
48. Roy S, Field GD. Dopaminergic modulation of retinal processing from starlight to sunlight. *J Pharmacol Sci*. (2019) 140:86–93. doi: 10.1016/j.jphs.2019.03.006
49. Ebert D, Lammers C-H. Das zentrale dopaminerge System und die Depression. *Der Nervenarzt*. (1997) 68:545–55. doi: 10.1007/s001150050159
50. Dunlop BW, Nemeroff CB. The role of dopamine in the pathophysiology of depression. *Arch Gen Psychiatry*. (2007) 64:327. doi: 10.1001/archpsyc.64.3.327
51. Bach M, Holder GE. Check size tuning of the pattern electroretingoram: a reappraisal. *Document Ophthalmol*. (1996) 92:193–202. doi: 10.1007/BF02583290
52. Viswanathan S, Frishman LJ, Robson JG. The uniform field and pattern ERG in macaques with experimental glaucoma: removal of spiking activity. *Investig Ophthalmol Visual Sci*. (2000) 41:2797–810.
53. Dani JA. Roles of dopamine signaling in nicotine addiction. *Mol Psychiatry*. (2003) 8:255–6. doi: 10.1038/sj.mp.4001284
54. Bubl E, Dörr M, Philipsen A, Ebert D, Bach M, Tebartz van Elst L. Retinal contrast transfer functions in adults with without ADHD. *PLoS ONE*. (2013) 8:e61728. doi: 10.1371/journal.pone.0061728
55. Werner AL, Tebartz van Elst L, Ebert D, Friedel E, Bubl A, Clement HW, et al. Normalization of increased retinal background noise after ADHD treatment: a neuronal correlate. *Schizophr Res*. (2019) 219:77–83. doi: 10.1016/j.schres.2019.04.013

Conflict of Interest: LTvE Advisory boards, lectures, or travel grants within the last three years: Roche, Eli Lilly, Janssen-Cilag, Novartis, Shire, UCB, GSK, Servier, Janssen, and Cyberonics. KD member of the "Steering Committee Neurosciences," Janssen Pharmaceuticals, Inc.

The remaining authors declare that the research was conducted in the absence of any commercial or financial relationships that could be construed as a potential conflict of interest.

Publisher's Note: All claims expressed in this article are solely those of the authors and do not necessarily represent those of their affiliated organizations, or those of the publisher, the editors and the reviewers. Any product that may be evaluated in this article, or claim that may be made by its manufacturer, is not guaranteed or endorsed by the publisher.

frontiers in Medicine

REVIEW
published: 02 December 2021
doi: 10.3389/fmed.2021.672444

Importance of Autoimmune Responses in Progression of Retinal Degeneration Initiated by Gene Mutations

*Grazyna Adamus**

Ocular Immunology Laboratory, Casey Eye Institute, School of Medicine, Oregon Health and Science University, Portland, OR, United States

Inherited retinal diseases (IRDs) are clinically and genetically heterogeneous rare disorders associated with retinal dysfunction and death of retinal photoreceptor cells, leading to blindness. Among the most frequent and severe forms of those retinopathies is retinitis pigmentosa (RP) that affects 1:4,000 individuals worldwide. The genes that have been implicated in RP are associated with the proteins present in photoreceptor cells or retinal pigment epithelium (RPE). Asymmetric presentation or sudden progression in retinal disease suggests that a gene mutation alone might not be responsible for retinal degeneration. Immune responses could directly target the retina or be site effect of immunity as a bystander deterioration. Autoantibodies against retinal autoantigens have been found in RP, which led to a hypothesis that autoimmunity could be responsible for the progression of photoreceptor cell death initiated by a genetic mutation. The other contributory factor to retinal degeneration is inflammation that activates the innate immune mechanisms, such as complement. If autoimmune responses contribute to the progression of retinopathy, this could have an implication on treatment, such as gene replacement therapy. In this review, we provide a perspective on the current role of autoimmunity/immunity in RP pathophysiology.

Keywords: autoimmunity, retinal degeneration, inflammation, retinitis pigmentosa, autoantibodies, complement

OPEN ACCESS

Edited by:
Gemmy Cheung, Singapore National Eye Center, Singapore

Reviewed by:
Dimitra Athanasiou, University College London, United Kingdom
Carmela Rinaldi, University of Messina, Italy
Alecia K. Gross, University of Alabama at Birmingham, United States

***Correspondence:**
Grazyna Adamus
adamusg@ohsu.edu

Specialty section:
This article was submitted to Ophthalmology, a section of the journal Frontiers in Medicine

Received: *11 May 2021*
Accepted: *01 November 2021*
Published: *02 December 2021*

Citation:
Adamus G (2021) Importance of Autoimmune Responses in Progression of Retinal Degeneration Initiated by Gene Mutations. Front. Med. 8:672444. doi: 10.3389/fmed.2021.672444

INTRODUCTION

Inherited retinal diseases (IRDs) are clinically and genetically heterogeneous rare disorders associated with the retinal dysfunction and death of retinal photoreceptor cells. An incidence of IRD is estimated for 1 in 2,000–3,000 individuals, affecting about 2 million people in the world (1). The disease progresses over several decades of patient life and could be a rapid evolution over two decades, or a slow progression that never leads to complete blindness. A dysfunction or death of photoreceptor cells may cause vision loss and blindness. The prognosis of vision loss is difficult to determine because the disease symptoms may depend on a type of inheritance (autosomal dominant, autosomal recessive, or X-linked) and retinal regions involved that includes the periphery, the macula, and both the macula and periphery (2, 3). Furthermore, considering retinal cell contribution to pathology, IRDs can be divided into rod-dominant defect, cone-dominant defect, macular dystrophy, dysfunction of photoreceptors, and bipolar cells, vitreoretinopathies, and hereditary choroidal diseases (3). Among the most frequent and severe forms of those

retinopathies is retinitis pigmentosa (RP) which affects 1:4,000 individuals worldwide (1, 4). The objective of this review is to provide a perspective on the current knowledge on the role of autoimmunity/immunity in retinal degeneration initiated by a genetic mutation.

RETINITIS PIGMENTOSA

The retina consists of two types of photoreceptor cells, rods that are responsible for night vision, and cones for daytime vision and color vision. RP is characterized by degeneration of rods and cones caused initially by the gene mutations, typically affecting rods. Vision loss occurs when the primary rods deteriorate and are eliminated, which usually causes healthy cones to decline next, resulting in blindness (5). The age of RP onset differs and depends on the gene mutations. The rod dysfunction affects the peripheral retina and loss of central vision is the consequence of cone dysfunction, which occurs usually later in life. In addition, when cone degeneration occurs first, it leaves rods mostly unaffected but can cause a severe loss of visual acuity and daylight vision. Early-onset RP is diagnosed when the symptoms of mid-stage RP are already present at 2 years of age and late-onset RP is diagnosed when the symptoms are clinically apparent at or after midlife.

More than 250 genes with about 4,500 causative mutations are identified in different IRD-related diseases (RetNet—Retinal Information Network, http://www.sph.uth.edu/retnet) (6, 7). The genes that have been implicated in syndromic and non-syndromic disease are mostly associated with photoreceptors or RPE, and they involve phototransduction, visual cycle cascade, photoreceptor transcription, and structure (2, 7, 8). Although various genetic mutations have been identified in the patients with RP, the mechanisms by which, these mutations lead to photoreceptor apoptosis, remain mostly unknown (9, 10).

Non-syndromic RP usually involves the peripheral visual field loss, pigment deposits in the fundus, loss of photoreceptor cells as shown at optical coherence tomography (OCT) of the retina, and decreased or absent rod functional responses evaluated by electroretinography (ERG) (11–13). Pigmented deposits, called bone spicules found in the periphery of the retina are a result of photoreceptor cell degeneration. Other classic triads of RP that include intra-retinal pigment migration, optic nerve pallor, and attenuated vessels are not always present on the initial examination. Death of rods can be a direct consequence of genetic mutations; however, death of cones may be caused by the initial death of rods, not to mutations in the cone proteins. Therefore, the period between the onset of rod degeneration and a patient's legal blindness often spans decades (14). To add to the complexity of RP, 20–30% of patients may have an associated non-ocular condition (15).

Most information on the IRD degenerative mechanisms was obtained from the animal models that mimic photoreceptor cell degeneration phenotypes but the knowledge of molecular signaling pathways associated with RP pathogenesis is still incomplete (16, 17). Increasing evidence shows that immune/autoimmune processes may also contribute to the pathogenesis of RP, causing additional retinal degeneration (18). Immune responses could directly target the retina or be a site effect of immunity as a bystander deterioration (19).

The retina has a unique immune defense system, consisting of innate immune cells and the complement system. The sequestration of the eye from the immune system is part of the phenomenon known as an immune privilege (20). Under normal physiological conditions, the retina resides behind the protective blood-retinal barriers, and circulating immune cells are not able to enter the retina (21). In immunologically privileged sites, such as the eye, brain, and testis, autoreactive T cells and B cells can cross from the periphery into the tissue and remain inactive due to the sequestration of antigens behind those barriers (22). However, the sequestration of retinal antigens can be broken by infectious agents or other causes of tissue damage, which may lead to disease development (23). Such an event is dependent on several factors, such as the nature and dose of an antigen, number of exposures, frequency of activated T cells, upregulation of the major histocompatibility complex (MHC), and costimulatory molecules in the affected tissues (24).

AUTOIMMUNITY IN RETINAL DEGENERATION

Autoimmunity develops when the immune responses react against the own body, causing inflammation, degeneration, tissue destruction, and organ failure. Autoimmune responses resemble normal immune responses to the pathogens but they are activated by self-antigens or autoantigens. Immune mediated destruction of self-tissue could occur through specific recognition of autoantigens or could be a byproduct of non-specific inflammation (25, 26). Autoimmune diseases have high prevalence (∼7–9%) in the population, mostly affecting women, and can cause major illness and death (22). There are different triggers and pathways involved in the pathogenesis of autoimmune diseases (27). The most important feature of an autoimmune disease is the knowledge of an autoantigen involved in the pathogenic process. The retina contains a number of potent autoantigens that are expressed in the thymus and secondary lymphoid tissue, where immunologic tolerance and prevention of autoimmune disease is maintained by a variety of processes, such as clonal deletion and anergy (28–30). Thymic expression is a common feature for all the tissue-specific antigens and their levels of expression play a role in determining the susceptibility to autoimmunity against these molecules.

The other contributory factor to retinal degeneration is inflammation that activates innate immune mechanisms, such as toll-like receptors, inflammasome receptors, and complement components that initiate complex cellular cascades by recognizing or sensing different pathogen and damage-associated molecular patterns (31, 32).

Some observations corroborate that a gene mutation alone might not be responsible for retinal degeneration, e.g., sudden acceleration in photoreceptor decline does not explain degeneration caused by a gene mutation but is an indication that some other processes may be involved. The gene mutations may

initiate a stress of photoreceptor cells, secretion of chemokines, and recruitment of microglia to the outer retina, which in effect induces immune (inflammatory cells, cytokines, and chemokines) and autoimmune responses (autoantibodies, autoreactive B cells, and T cells) (33–35). Accumulated microglia secrete cytokines that can cause an increase photoreceptor cell death, disruption of the blood-retina barrier, and attraction of macrophages into the retina (33). Cell death, deposition of debris into subretinal space, and antigens released from dying cells/debris may trigger an autoantibody production (32). The presence of autoantibodies (AAbs) is the consequence of breakdown of tolerance and they are an important serological feature of autoimmune diseases. Initially, circulating AAbs and minor tissue infiltrates may appear without clinical consequences, but later in life, the autoantigens released from the damaged organ may be recognized as foreign substances by the immune system and, in effect, develop pathogenic autoimmunity (autoimmune disease) (19, 26). Altogether, in RP, autoimmunity is likely to be responsible for the progression of photoreceptor cell death that was initiated by a defective gene.

In recent years, a new entity of retinal degenerative disease has been recognized as "autoimmune retinopathy" (AR). AR is often mistaken for RP, because of the overlapping clinical findings and subacute vision loss (36, 37). However, AR has distinctive features that include *progressive* vision loss, often sudden onset later in life, photopsias, and unique visual field defects in the patients without familiar history of RP. In addition, AR is characterized by lack of pigment deposits that often distinguish AR from RP. ARs may present as paraneoplastic syndromes, such as cancer-associated retinopathy and melanoma-associated retinopathy (38–40). Additionally, AR may present without underlying malignancy but have clinical and immunological findings similar to paraneoplastic retinopathies (36, 41, 42). The hallmark of the syndrome are serum AAbs against retinal proteins that may be involved in the pathogenic processes (43–45). Anti-retinal AAbs can persist over the evolution of retinal degeneration and perpetuate the condition (19). Furthermore, cellular immunity is involved in the condition as increased number of memory T cells, NK cells, and decreased regulatory B cell subsets were found in many patients with AR compared with normal controls (37). The role of many different pathways of the immune system in the pathogenesis and progression of AR is under investigation to help with AR diagnosis (46). However, the evidence that the immune system is involved in AR pathogenesis helps with successful treatment of the patients with AR with immunosuppressive drugs, IVIg, and rituximab (42, 47).

PATHWAYS CONTRIBUTING TO THE DEATH OF PHOTORECEPTORS

The extent of the immune system activation during RP is still unknown. One can argue that the loss of controlling mechanisms contributes to tissue damage and activation of pro-apoptotic pathways in the retina, ultimately leading to cell death (48–50). To understand its pathology, the immune and autoimmune responses must be examined when a patient first presents some aspects of visual loss. However, the age at onset varies since some patients develop symptomatic visual loss in early childhood, whereas others can remain relatively asymptomatic until mid-adulthood. In addition, the failing photoreceptor cells are phagocytized by microglia to avoid the initiation of inflammation (51, 52). Several studies emphasized that the molecular mechanisms of cell death depends on the caspase-dependent or -independent apoptotic mitochondrial pathway, involving the Bcl-2 family of proteins (53–56). Besides, anti- and pro-apoptotic Bcl-2 protein members exist in retinal cells, suggesting their role in retinal disorders (9, 57). The animal models of retinal degeneration showed that different cell-death pathways could be activated and some of them were genotype-specific (58).

In addition, degeneration of rod photoreceptor cells can be caused by an impairment of autophagy, the process which participates in cell death possibly by initiating apoptosis (59–61). Degradation of proteins by autophagy to prevent the formation of protein aggregates seems to be a necessary process to prevent retinal degeneration (62). Therefore, it is essential to identify all the steps in RP cell death pathways to provide targets for treatment unrelated to the genetic mutations (63). Findings from the animal models have shown that photoreceptor cell death occurred in mice- and rats-expressing mutant rhodopsin in a similar pattern as in humans and the animals manifest clinical signs of autosomal dominant retinitis pigmentosa (ADRP) (64).

The inflammatory cells contribute to retinal degeneration through their cytotoxic effects on photoreceptors (65). Increased levels of pro-inflammatory cytokines and chemokines, in addition to anti-retinal AAbs and immune cells, were detected in sera, aqueous humor, and vitreous of the patients with RP (18, 31, 37, 66, 67) and in the rodent disease models (68, 69). Usually, there is a significant upregulation of the inflammatory markers [interleukin (IL)-1β, IL-6, tumor necrosis factor α (TNF-α), monocyte chemoattractant protein-1 (MCP-1), and ionized calcium binding adaptor molecule 1 (IBA1)] by intraocular cells to start the inflammatory processes (70, 71). In fact, the pro-inflammatory Th1 cytokines (IL-1α, IL-1β, IL-2, IL-6, and INF-γ) characteristic of a cytotoxic response, along with anti-inflammatory Th2 cytokines (IL-4 and IL-10) were found in aqueous humor and vitreous fluid of the patients with RP (31, 66). The vitreous in patients with RP predominantly contained CD4 and CD8 T cells, as well as human leukocyte antigen (HLA)-DR activated cells and some B cells. Moreover, serum high-sensitivity C-reactive protein (hs-CRP) was significantly increased in the patients with RP, and higher hs-CRP was associated with faster deterioration of central visual function (72). The patients with an increased number of inflammatory cells showed reduced visual function (reduced visual acuity and visual fields). All those factors may contribute to the progression of the retinal degeneration, and systemic and local inflammation can change overtime with the progression of tissue degeneration in RP (31, 37).

AUTOANTIBODIES IN RETINITIS PIGMENTOSA

Autoantibodies (AAbs) are frequently found in RP and in healthy individuals. High-affinity pathogenic AAbs are produced by

antigen-stimulated B cells that undergo somatic hypermutation to become long-lived plasma cells as a result of the self-tolerance breakdown (73, 74). Serum IgG autoantibody profiles are unique to an individual and may be remarkably stable over time (75). Presence of circulating AAbs specific for photoreceptor antigens raises the possibility of their pathogenic role (19).

In recent years, significant progress has been made in understanding the role of anti-retinal AAbs in pathogenesis, diagnosis, and management of AR, such as paraneoplastic retinopathies (45, 76–78). Since the ocular findings in ARs are similar to those found in many forms of RP, especially those that do not have family history of retinal degeneration, one could hypothesize that an underlying autoimmunity could cause, or at least contribute to, the progression of retinal disease. In early studies, the high levels of anti-retinal IgG and IgM antibodies were found in various cohorts of the patients with RP (79–81). However, specificities of those AAbs have not been determined by the investigators. Later studies showed ∼2% sera of simplex patients with RP possessed anti-recoverin AAbs, which let the authors to hypothesis that anti-recoverin AAbs exacerbate the underlying RP disease (76). This is in an agreement with the recent study that showed the patients with RP over 50 years old with identified gene mutation and history of cancer, had serum anti-recoverin AAbs (82). Such AAbs occurred more likely in the patients with RP with cancer than in the patients without cancer. This suggests that anti-recoverin AAbs were generated in response to cancer rather than to degenerating retina due to the gene mutation, because the mutations in the tumor genome can cause tumors to express mutant proteins, such as recoverin, that is normally expressed on the retina. Moreover, anti-retinal AAbs were reported secondary to the gene defects in the patients with RP (18, 66, 72) but their role have not been fully explained.

Autoantibody Targets Are the Same Proteins as Mutated Gene Products in RP

The likely sequence of events in the generation of anti-retinal AAbs in RP is the death of photoreceptor cells induced by a gene mutation, which causes the release of antigenic proteins that are then captured by the potential antigen-presenting cells (e.g., macrophages), and breakdown of the blood-retinal barrier during that process (83). An abnormal gene may lead to an abnormal protein or an abnormal amount of a normal protein, and mutated proteins can cause pathology by misfolding and aggregation. Those proteins can be targets of the autoimmune response, especially when mutation leads to photoreceptor degeneration (69). When photoreceptors die, it would be expected that the immune system targets freed proteins from failing outer segments and elicits AAbs against those autoantigens with the help of macrophages. Some patients with RP may have serum AAbs against retinal proteins that were subject to disease-causing mutation (8, 39). For example, AAbs against arrestin were detected in the patients with RP as well in the patients with autoimmune uveitis or autoimmune retinopathy (84, 85). However, the degree of immune reactivity against arrestin and the severity of disease in the patients with RP are not strongly correlated. This observation suggests that the immune responses to the retinal autoantigens are regulated by factors other than the level of retinal damage and the release of antigens from the affected tissues. The systemic autoimmune responses may play a bigger role in formation of AAbs.

The presence of AAbs in RP led to a hypothesis that autoimmunity could be responsible for the progression of photoreceptor cell death initiated by a genetic mutation. A majority of causative mutations in RP involve proteins that participate in the phototransduction cascade, such as rhodopsin (RHO), the catalytic unit and subunits of PDE6 (PDE6A and PDE6B, respectively), the subunit of the rod cyclic nucleotide gated channel (CNGA1), and arrestin (SAG) (86). The patients with AR have AAbs against phototransduction proteins (77). Detection of anti-retinal AAbs suggests a generation of AAbs started against mutant proteins in RP. However, whether AAbs are made to a wild-type protein or mutant protein has yet to be determined. The explanation of the role of specific mutations as etiological causes for RP must mostly depend on their ability to induce the pathogenic mutant proteins that cause structural and functional changes in the cell, leading to retinal pathology (87).

Recent studies on neurodegeneration in multiple sclerosis (MS) showed that both, mutant and wild myelin protein PLP1 were able to generate the immune responses (88). Using wild type and mutant peptide microarrays, several serum AAbs against multiple mutated PLP1 have been found in those patients. Anti-mutant PLP1 autoantibody responses provided evidence that PLP1 mutations conceivably elicit the immune-mediated destruction of myelin (88). We postulate that the retinal proteins altered by a gene mutation in RP, act as new autoantigens, thus AAbs may be generated with similar specificities as to native proteins. It is not easy to determine whether the patients have autoimmunity to a native or mutant protein. Explaining the specific role of mutations as etiological factors for RP relies on their ability to induce the structural changes in proteins that have pathophysiological consequences (87). Changes in the net charge of a protein may lead to conformational modifications in the tertiary and quaternary structure of that protein, and alters the interaction with other proteins, especially human HLA molecules. This would apply only to the mutations that change the amino acid sequences in such a way that influence the structure and function of proteins (89). The mutant-proteins accumulate during retinal degeneration and can be seen by the immune system as a new and amplify the autoimmune response, eventually leading to autoimmune pathology. Also, the posttranslational modifications, such as a protein citrullination can trigger the activation of the immune system, both locally and systemically for AAbs production, contributing to disease pathogenesis in RP (35, 90, 91). These findings suggest that the presence of mutations and associated immune response could be part of the pathogenesis of RP.

Few years ago, it has been proposed that the genes encoding for the proteins that become autoantigens could have a fundamental propensity toward mutation (92). According

to the study, the autoantigens contain significantly more single nucleotide polymorphisms (SNP) than other human genes do. The SNPs may represent an essential requirement for the primary generation of an autoimmune response. Structural features of a given autoantigen can be prerequisite to determine whether such an antigen is suitable to induce autoimmune response (89). Thus, the autoantibody repertoire to the retinal antigens is represented by pro-inflammatory and immunological properties of autoantigens (93, 94). The ability of new antigens released from the damaged cells and tissues may act as chemoattractants for leukocytes, which is an important step in promoting inflammation and favoring the development of autoimmunity (93). In fact, two retina-specific proteins, arrestin and interphotoreceptor retinoid-binding protein (IRBP) were found to be chemoattractants for lymphocytes and immature dendritic cells (95). These autoantigens, which have no primary or secondary structural homology to chemokines, induce cell migration by interacting with specific chemokine receptors. IRBP interacts with chemokine receptors CXCR5 and CXCR3, and arrestin interacts with CXCR3, and both the proteins can facilitate retinal damage by inflammatory and immune responses, and potentially contribute to the development of autoimmune diseases, such as autoimmune uveitis (95). Moreover, during the course of disease, specific AAbs bind stronger with the target antigens in the later stage than those occurring in the beginning (96).

Association Between Cystoid Macular Edema With Anti-retinal Autoantibodies

The patients with RP experience central vision loss in the form of cystoid macular edema (CME), which can form at any stage of RP, in one or both the eyes, and in any genetic form but is more often associated with Crumbs homolog (cell polarity complex component) (CRB1) mutations (97). The origin of macular edema remains poorly understood. CME is a major cause of vision loss in uveitis (98). Anti-retinal AAbs, vitreous traction, retinal pigment epithelium dysfunction, and Müller cell edema can contribute to the pathology of CME (97). AAbs against two enzymes, carbonic anhydrase II and enolase were detected in the patients with bilateral CME and RP, suggesting that these two enzymes play an important role in foveal function (99). The high prevalence of anti-CAII and anti-enolase AAbs in the patients with CME have also been found in a German group of patients with CME (100). The authors proposed that blocking of CAII and enolase activity by AAbs in the RPE may be a major cause of edema formation. Independently, our laboratory has also found the presence of anti-CAII AAbs in the patients with PR with CME, further corroborating their role in pathology of edema (101). In addition, the higher levels of intraocular cytokines, such as IL-2 have been found in the patients with CME, impaling their role of inflammation (66). This suggests that inflammatory mediators as well as AAbs may contribute to the development of inflammatory CME, but the exact mechanism for the CME development and its persistence is still unknown.

HLA AND RETINITIS PIGMENTOSA

A strong association between the HLA region and autoimmune disease has been established over 50 years. The HLA molecules are responsible for the induction and regulation of immune responses, and selection of T cell repertoire (102). The class II molecules, such as HLA-DR, DP, and DQ present exogenous peptides that are expressed on antigen-presenting cells (dendritic cells, macrophages, and B cells) and activated T cells. The likely mechanisms, by which HLA polymorphisms could contribute to the development of RP, may be related to the presentation of autoantigens, the shared epitope, and molecular mimicry. The only studies of HLA association and RP were performed over 30 years ago (103). HLA serological typing study of 173 patients with autosomal dominant and recessive RP was not different than the frequency of HLA antigens in control population (103). Then, the study of 10 patients with autosomal recessive RP showed a significant increase in the frequency of the antigens Cw4, Cw6, and DR11 (104). In other retinal diseases, the patients with severe diabetic retinopathy had frequent alleles on the DR3-DQ2 haplotype, such as DRB1*0301, DQA1*0501, and DQB1*0201 (105). The association between acute retinal necrosis syndrome and certain HLA specificities suggested immune predisposition to the disease (106). RPE cells phagocytose and recycle autoantigen-rich retinal rod outer segments and co-express HLA DR and DQ Class II antigens in response to IFN-gamma stimulation (107). This suggests that the RPE cells may play an immunoregulatory function in autoimmunity to the retinal antigens as primary inducers and/or as suppressors of retinal inflammation (108). Further studies are needed to understand whether the HLA polymorphism influence the development of RP.

INNATE RESPONSES—CONTRIBUTORY FACTOR?

There is some evidence that chronic inflammation is associated with the pathogenesis of RP (109, 110). The indications of chronic inflammation in the patients with RP and the rodent models include the presence of serum retinal AAbs, immune cells in the vitreous cavity of affected individuals, and increased levels of pro-inflammatory cytokines and chemokines in aqueous humor and vitreous fluid of the patients with RP (31, 32).

The retina has a unique immune defense system, consisting of innate immune cells and the complement system. Microglia that includes microglia (resident macrophages), perivascular macrophages, and dendritic cells play an important role in the retinal immune defense (111, 112). They are located behind the blood-retina barriers within an immune-privileged microenvironment in the inner layers of the retina, such as the ganglion layer, inner plexiform layer, and outer plexiform layer (113, 114).

Under normal physiological conditions, microglia are resting but in the disease state, the activated microglia change their shape and perform several important functions in the retina that includes phagocytosis of debris and apoptotic cells,

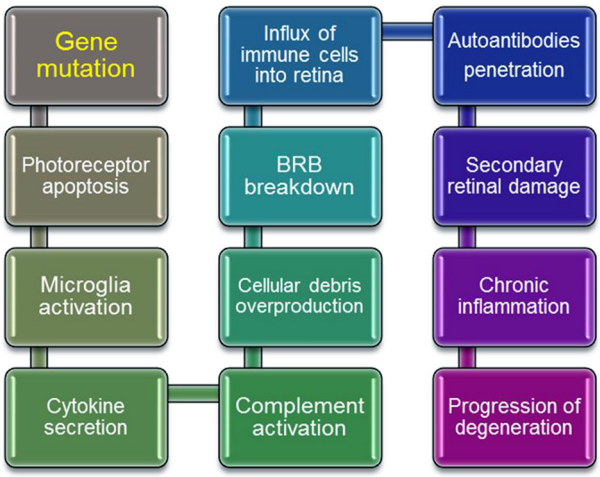

FIGURE 1 | Schematic steps in progressive retinal degeneration. Mutant-proteins accumulate during retinal degeneration and can be seen as new, which can amplify the autoimmune response, ultimately leading to autoimmune pathology. Activation of immune cells by overproduction of cellular debris due to photoreceptor death results in the inner Blood Retina Barrier (BRB) breakdown, which invites systemic macrophages into the retina. Resident and circulating macrophages can contribute to secondary retinal damage from inflammation, and in effect ameliorate retinal degeneration.

maintenance of synapses, and response to inflammation (114). Phagocytosis may actively induce apoptosis and those apoptotic photoreceptors are selectively eliminated from the outer nuclear layer to the subretinal space, and then phagocytosed by monocyte-derived macrophages (115). The activation of microglia contributes to retinal damage and disease progression (69, 116, 117). Microglia have different functions depending on the underlying cause of retinal degeneration (118, 119). In RP, the death of rod photoreceptors may attract resident microglia that become activated, depending on the local and systemic cytokines secretion, then migrate to the outer retina to phagocytose rod cell debris from dying cells (1, 48). Infiltrating microglia secrete pro-inflammatory cytokines that stimulate photoreceptor apoptosis (34, 63). Increased secretion of TNF-α and IL-1b was found shortly after disease onset (120). The studies from our laboratory, examining the evolution of autoimmune responses against retina in naive dystrophic RCS rats over the course of their retinal degeneration, linked the occurrence of anti-retinal autoantibodies to the entry of activated macrophage/microglia, suggesting their role in neurodegeneration (69). Microglial activation is independent of the underlying genetic defect, and it is not a side effect of hereditary photoreceptor dystrophies, but can arise by the availability of endogenous retinal proteins from the dying photoreceptors (121).

In addition, microglia are the source of complement and complement-regulatory factors that are markedly up-regulated in the human retinas with RP (122). The complement system has an integral role in maintaining immune surveillance and homeostasis in the eye microenvironment but overstimulation of the complement system can induce retinal pathology and ocular inflammation (32, 122). Complement mediates a wide range of functions in the tissue and can be activated by three distinct pathways: classical, alternative, and lectin. The studies using the animal models of RP showed an involvement of complement proteins in retinal degeneration (123). For example, in the rd10 mouse that is caused by a spontaneous mutation in Pde6β gene, at the stage when rod photoreceptors have completely degenerated, there was an increase in many classical and alternative complement pathway components, such as C1q, C1r, C3, and C4 (124). However, photoreceptor degeneration in the rd1 mouse with a naturally occurring null mutation within the gene encoding Pdeβ was unaffected by C1q component (125). In contrast, the levels of C1q progressively increased over the course of photoreceptor degeneration in the Rho−/− mouse when the mice lost all the rods over 3-month period by apoptosis. The C3 and its receptor CR3 signaling regulate the microglia–photoreceptor interactions. The deficiency of C3–CR3 lead to decrease microglial phagocytosis of apoptotic photoreceptors and increase microglial neurotoxicity to photoreceptor cells in RP (123). Another complement protein C1q is shown to be the primary component of cone photoreceptor survival factor (126). In the normal adult RPE–choroid, the choroidal cells are the predominant local source of most alternative complement pathway components and regulators (127). Moreover, the occurrence of reactive complement proteins on the surface of RPE cells may accelerate lipofuscin accumulation by inhibiting their clearance (128). These findings have potential implications for the pathological mechanisms independent of genetic mutation and new targets for therapy of retinal degeneration. Targeting the microglia (e.g., minocycline) may reduce the production of several pro-inflammatory mediators thus may result in broader beneficial effects than just inhibition of single cytokines (129).

FINAL REMARKS

Inherited retinal diseases represent a highly heterogeneous group of disorders that have one common element: abnormal visual function originating at the death of retinal photoreceptors. The gene defects can initiate death of retinal cells that can progress further to symptomatic changes mediated by immune and autoimmune responses (**Figure 1**). An initial gene mutation followed by sudden loss and progressive nature of retinal degeneration suggests the involvement of autoimmune responses. Since there are a variety of genes and mutations that cause retinal degeneration, gene replacement therapy approaches that are currently in development may be time-consuming and cost-prohibitive for treatment of all forms of RP. If the autoimmune responses contribute to the progression of retinopathy this could have implication on development of retinal degeneration and success of gene replacement therapy. Alternative approaches can be based on the immunological pathways that cause retinal degeneration in different forms of RP. In such cases, immunomodulatory and biologic drugs targeting B cells could be beneficial in slowing retinal degeneration caused

by a gene mutation. More studies are needed to fully establish the role of autoimmunity in different forms of retinal degenerations.

AUTHOR CONTRIBUTIONS

The sole author is responsible for the design and writing of the review.

FUNDING

This study was supported by grant P30 EY010572 from the National Institutes of Health (Bethesda, MD, USA) and by unrestricted departmental funding from the Research to Prevent Blindness (New York, NY, USA).

REFERENCES

1. Hartong DT, Berson EL, Dryja TP. Retinitis pigmentosa. *Lancet.* (2006) 368:1795–809. doi: 10.1016/S0140-6736(06)69740-7
2. Wang DY, Chan WM, Tam POS, Baum L, Lam DSC, Chong KKL, et al. Gene mutations in retinitis pigmentosa and their clinical implications. *Clinica Chimica Acta.* (2005) 351:5–16. doi: 10.1016/j.cccn.2004.08.004
3. Hohman TC. Hereditary retinal dystrophy. In: Whitcup SM, Azar DT, editors, *Pharmacologic Therapy of Ocular Disease*. Cham: Springer International Publishing (2017). p. 337–67. doi: 10.1007/164_2016_91
4. Hamel C. Retinitis pigmentosa. *Orphanet J Rare Dis.* (2006) 1:40. doi: 10.1186/1750-1172-1-40
5. Campochiaro PA, Mir TA. The mechanism of cone cell death in Retinitis Pigmentosa. *Prog Retin Eye Res.* (2018) 62:24–37. doi: 10.1016/j.preteyeres.2017.08.004
6. Sorrentino FS, Gallenga CE, Bonifazzi C, Perri PA. Challenge to the striking genotypic heterogeneity of retinitis pigmentosa: a better understanding of the pathophysiology using the newest genetic strategies *Eye.* (2016) 30:1542–8. doi: 10.1038/eye.2016.197
7. Farrar GJ, Carrigan M, Dockery A, Millington-Ward S, Palfi A, Chadderton N, et al. Toward an elucidation of the molecular genetics of inherited retinal degenerations. *Hum Mol Genet.* (2017) 26:R2–11. doi: 10.1093/hmg/ddx185
8. Birtel J, Gliem M, Mangold E, Muller PL, Holz FG, Neuhaus C, et al. Next-generation sequencing identifies unexpected genotype-phenotype correlations in patients with retinitis pigmentosa. *PLoS ONE.* (2018) 13:e0207958. doi: 10.1371/journal.pone.0207958
9. Sancho-Pelluz J, Arango-Gonzalez B, Kustermann S, Romero F, van Veen T, Zrenner E, et al. Photoreceptor cell death mechanisms in inherited retinal degeneration. *Mol Neurobiol.* (2008) 38:253–69. doi: 10.1007/s12035-008-8045-9
10. Ferrari S, Di Iorio E, Barbaro V, Ponzin D, Sorrentino FS, Parmeggiani F. Retinitis pigmentosa: genes and disease mechanisms. *Curr Genomics.* (2011) 12:238–49. doi: 10.2174/138920211795860107
11. Verbakel SK, van Huet RAC, Boon CJF, den Hollander AI, Collin RWJ, Klaver CCW, et al. Non-syndromic retinitis pigmentosa. *Progr Retinal Eye Res.* (2018) 3:5. doi: 10.1016/j.preteyeres.2018.03.005
12. Granse L, Ponjavic V, Andreasson S. Full-field ERG, multifocal ERG and multifocal VEP in patients with retinitis pigmentosa and residual central visual fields. *Acta Ophthalmol Scand.* (2004) 82:701–6. doi: 10.1111/j.1600-0420.2004.00362.x
13. Birch DG, Anderson JL, Fish GE. Yearly rates of rod and cone functional loss in retinitis pigmentosa and cone-rod dystrophy. *Ophthalmology.* (1999) 106:258–68. doi: 10.1016/S0161-6420(99)90064-7
14. Lobanova ES, Finkelstein S, Li J, Travis AM, Hao Y, Klingeborn M, et al. Increased proteasomal activity supports photoreceptor survival in inherited retinal degeneration. *Nat Commun.* (2018) 9:1738. doi: 10.1038/s41467-018-04117-8
15. Werdich XQ, Place EM, Pierce EA. Systemic diseases associated with retinal dystrophies. *Semin Ophthalmol.* (2014) 29:319–28. doi: 10.3109/08820538.2014.959202
16. Collin GB, Gogna N, Chang B, Damkham N, Pinkney J, Hyde LF, et al. Mouse models of inherited retinal degeneration with photoreceptor cell loss. *Cells.* (2020) 9:931. doi: 10.3390/cells9040931
17. Newton F, Megaw R. Mechanisms of photoreceptor death in retinitis pigmentosa. *Genes.* (2020) 11:1120. doi: 10.3390/genes11101120
18. McMurtrey JJ, Tso MOM. A review of the immunologic findings observed in retinitis pigmentosa. *Survey Ophthalmol.* (2018) XX:1–13. doi: 10.1016/j.survophthal.2018.03.002
19. Adamus G. Are anti-retinal autoantibodies a cause or a consequence of retinal degeneration in autoimmune retinopathies? *Front Immunol.* (2018) 9:765. doi: 10.3389/fimmu.2018.00765
20. Taylor AW. Ocular immune privilege. *Eye.* (2009) 23:1885–9. doi: 10.1038/eye.2008.382
21. Greenwood J. Mechanisms of blood-brain barrier breakdown. *Neuroradiology.* (1991) 33:95–100. doi: 10.1007/BF00588242
22. Theofilopoulos AN, Kono DH, Baccala R. The multiple pathways to autoimmunity. *Nat Immunol.* (2017) 18:716–24. doi: 10.1038/ni.3731
23. Stein-Streilein J, Caspi RR. Immune privilege and the philosophy of immunology. *Front Immunol.* (2014) 5:110. doi: 10.3389/fimmu.2014.00110
24. Gery I, Caspi RR. Tolerance induction in relation to the eye. *Front Immunol.* (2018) 9:2304. doi: 10.3389/fimmu.2018.02304
25. Forrester JV, Kuffova L, Dick AD. Autoimmunity, autoinflammation and infection in uveitis. *Am J Ophthalmol.* (2018) 2:19. doi: 10.1016/j.ajo.2018.02.019
26. Lleo A, Invernizzi P, Gao B, Podda M, Gershwin ME. Definition of human autoimmunity - autoantibodies versus autoimmune disease. *Autoimmunity Rev.* (2010) 9:A259–66. doi: 10.1016/j.autrev.2009.12.002
27. Lifeng W, Fu-Sheng W, Eric GM. Human autoimmune diseases: a comprehensive update. *J Internal Med.* (2015) 278:369–95. doi: 10.1111/joim.12395
28. Egwuagu CE, Charukamnoetkanok P, Gery I. Thymic expression of autoantigens correlates with resistance to autoimmune disease. *J Immunol.* (1997) 159:3109–12.
29. Charukamnoetkanok P, Fukushima A, Whitcup SM, Gery I, Egwuagu CE. Expression of ocular autoantigens in the mouse thymus. *Curr Eye Res.* (1998) 17:788–92. doi: 10.1080/02713689808951259
30. Voigt V, Wikstrom ME, Kezic JM, Schuster IS, Fleming P, Makinen K, et al. Ocular antigen does not cause disease unless presented in the context of inflammation. *Sci Rep.* (2017) 7:14226. doi: 10.1038/s41598-017-14618-z
31. Yoshida N, Ikeda Y, Notomi S, Ishikawa K, Murakami Y, Hisatomi T, et al. Clinical evidence of sustained chronic inflammatory reaction in retinitis pigmentosa. *Ophthalmology.* (2013) 120:100–5. doi: 10.1016/j.ophtha.2012.07.006
32. Sudharsan R, Beiting DP, Aguirre GD, Beltran WA. Involvement of innate immune system in late stages of inherited photoreceptor degeneration. *Sci Rep.* (2017) 7:17897. doi: 10.1038/s41598-017-18236-7
33. Cuenca N, Fernández-Sánchez L, Campello L, Maneu V, De la Villa P, Lax P, et al. Cellular responses following retinal injuries and therapeutic approaches for neurodegenerative diseases. *Prog Ret Eye Res.* (2014) 43:17–75. doi: 10.1016/j.preteyeres.2014.07.001
34. Zhao L, Zabel MK, Wang X, Ma W, Shah P, Fariss RN, et al. Microglial phagocytosis of living photoreceptors contributes to inherited retinal degeneration. *EMBO Molec Med.* (2015) 7:1179–97. doi: 10.15252/emmm.201505298
35. Hollingsworth TJ, Gross AK. Innate and autoimmunity in the pathogenesis of inherited retinal dystrophy. *Cells.* (2020) 9:630. doi: 10.3390/cells9030630
36. Heckenlively J, Ferreyra H. Autoimmune retinopathy: a review and summary. *Semin Immunopathol.* (2008) 30:127–34. doi: 10.1007/s00281-008-0114-7
37. Heckenlively JR, Lundy SK. Autoimmune retinopathy: an immunologic cellular-driven disorder. In: Ash J, Anderson R, LaVail M, Bowes Rickman C, Hollyfield J, Grimm C, editors, *Retinal Degenerative Diseases. Advances*

in Experimental Medicine and Biology. Cham: Springer International Publishing (2018). p. 193–201. doi: 10.1007/978-3-319-75402-4_24
38. Thirkill CE, Roth AM, Keltner JL. Cancer-associated retinopathy. *Archiv Ophthalmol.* (1987) 105:372–5. doi: 10.1001/archopht.1987.01060030092033
39. Adamus G. Paraneoplastic retinal degeneration. In: Levin L, Albert DM, editor, *Ocular Disease: Mechanisms and Management*. Saunders Elsevier, Inc. (2010). p. 599–608. doi: 10.1016/B978-0-7020-2983-7.00076-0
40. Lu Y, Jia L, He S, Hurley MC, Leys MJ, Jayasundera T, et al. Melanoma-associated retinopathy: a paraneoplastic autoimmune complication. *Arch Ophthalmol.* (2009) 127:1572–80. doi: 10.1001/archophthalmol.2009.311
41. Mizener JB, Kimura AE, Adamus G, Thirkill CE, Goeken JA, Kardon RH. Autoimmune retinopathy in the absence of cancer. *Am J Ophthalmol.* (1997) 123:607–18. doi: 10.1016/S0002-9394(14)71073-6
42. Fox AR, Gordon LK, Heckenlively JR, Davis JL, Goldstein DA, Lowder CY, et al. Consensus on the diagnosis and management of nonparaneoplastic autoimmune retinopathy using a modified delphi approach. *Am J Ophthalmol.* (2016) 168:183–90. doi: 10.1016/j.ajo.2016.05.013
43. Adamus G, Ren G, Weleber RG. Autoantibodies against retinal proteins in paraneoplastic and autoimmune retinopathy. *BMC Ophthalmol.* (2004) 4:5. doi: 10.1186/1471-2415-4-5
44. Adamus G. Latest updates on antiretinal autoantibodies associated with vision loss and breast cancer. *Invest Ophthalmol Vis Sci.* (2015) 56:1680–8. doi: 10.1167/iovs.14-15739
45. Adamus G, Champaigne R, Yang S. Occurrence of major anti-retinal autoantibodies associated with paraneoplastic autoimmune retinopathy. *Clin Immunol.* (2020) 210:108317. doi: 10.1016/j.clim.2019.108317
46. Sobrin L. Progress toward precisely diagnosing autoimmune retinopathy. *Am J Ophthalmol*. (2018) 188:xiv-xv. doi: 10.1016/j.ajo.2018.01.002
47. Davoudi S, Ebrahimiadib N, Yasa C, Sevgi DD, Roohipoor R, Papavasilieou E, et al. Outcomes in autoimmune retinopathy patients treated with rituximab. *Am J Ophthalmol*. (2017) 180:124–32. doi: 10.1016/j.ajo.2017.04.019
48. Gupta N, Brown KE, Milam AH. Activated microglia in human retinitis pigmentosa, late-onset retinal degeneration, and age-related macular degeneration. *Exp Eye Res*. (2003) 76:463–71. doi: 10.1016/S0014-4835(02)00332-9
49. Karlstetter M, Ebert S, Langmann T. Microglia in the healthy and degenerating retina: Insights from novel mouse models. *Immunobiology*. (2010) 215:685–691. doi: 10.1016/j.imbio.2010.05.010
50. Noailles A, Maneu V, Campello L, Gómez-Vicente V, Lax P, Cuenca N. Persistent inflammatory state after photoreceptor loss in an animal model of retinal degeneration. *Sci Rep*. (2016) 6:33356. doi: 10.1038/srep33356
51. Nagata S, Hanayama R, Kawane K. Autoimmunity and the clearance of dead cells. *Cell*. (2010) 140:619–30. doi: 10.1016/j.cell.2010.02.014
52. Okunuki Y, Mukai R, Pearsall EA, Klokman G, Husain D, Park DH, et al. Microglia inhibit photoreceptor cell death and regulate immune cell infiltration in response to retinal detachment. *Proc Natl Acad Sci USA*. (2018) 115:E6264–73. doi: 10.1073/pnas.1719601115
53. Portera-Cailliau C, Sung CH, Nathans J, Adler R. Apoptotic photoreceptor cell death in mouse models of retinitis pigmentosa. *Proc Natl Acad Sci USA*. (1994) 91:974–8. doi: 10.1073/pnas.91.3.974
54. Cottet S, Schorderet DF. Mechanisms of apoptosis in retinitis pigmentosa. *Curr Mol Med*. (2009) 9:375–83. doi: 10.2174/156652409787847155
55. Arango-Gonzalez B, Trifunovic D, Sahaboglu A, Kranz K, Michalakis S, Farinelli P, et al. Identification of a common non-apoptotic cell death mechanism in hereditary retinal degeneration. *PLoS ONE.* (2014) 9:e112142. doi: 10.1371/journal.pone.0112142
56. Hamann Sv, Schorderet DF, Cottet S. Bax-induced apoptosis in leber's congenital amaurosis: a dual role in rod and cone degeneration. *PLoS ONE*. (2009) 4:e6616. doi: 10.1371/journal.pone.0006616
57. Vargas A, Kim HS, Baral E, Yu WQ, Craft CM, Lee EJ. Protective effect of clusterin on rod photoreceptor in rat model of retinitis pigmentosa. *PLoS ONE*. (2017) 12:e0182389. doi: 10.1371/journal.pone.0182389
58. Viringipurampeer IA, Metcalfe AL, Bashar AE, Sivak O, Yanai A, Mohammadi Z, et al. NLRP3 inflammasome activation drives bystander cone photoreceptor cell death in a P23H rhodopsin model of retinal degeneration. *Hum Mol Genet*. (2016) 25:1501–16. doi: 10.1093/hmg/ddw029
59. Kunchithapautham K, Rohrer B. Autophagy is one of the multiple mechanisms active in photoreceptor degeneration. *Autophagy*. (2007) 3:65–66. doi: 10.4161/auto.3431
60. Zhou Z, Doggett TA, Sene A, Apte RS, Ferguson TA. Autophagy supports survival and phototransduction protein levels in rod photoreceptors. *Cell Death Different*. (2015) 22:488. doi: 10.1038/cdd.2014.229
61. Moreno ML, Merida S, Bosch-Morell F, Miranda M, Villar VM. Autophagy dysfunction and oxidative stress, two related mechanisms implicated in retinitis pigmentosa. *Front Physiol*. (2018) 9:1008. doi: 10.3389/fphys.2018.01008
62. Yao J, Jia L, Feathers K, Lin C, Khan NW, Klionsky DJ, Ferguson TA, Zacks DN. Autophagy-mediated catabolism of visual transduction proteins prevents retinal degeneration. *Autophagy*. (2016) 12:2439–2450. doi: 10.1080/15548627.2016.1238553
63. Marigo V. Programmed cell death in retinal degeneration: targeting apoptosis in photoreceptors as potential therapy for retinal degeneration. *Cell Cycle*. (2007) 6:652–655. doi: 10.4161/cc.6.6.4029
64. Athanasiou D, Aguila M, Bellingham J, Li W, McCulley C, Reeves PJ, et al. The molecular and cellular basis of rhodopsin retinitis pigmentosa reveals potential strategies for therapy. *Prog Retin Eye Res*. (2018) 62:1–23. doi: 10.1016/j.preteyeres.2017.10.002
65. Zhao B, Chen W, Jiang R, Zhang R, Wang Y, Wang L, et al. Expression profile of IL-1 family cytokines in aqueous humor and sera of patients with HLA-B27 associated anterior uveitis and idiopathic anterior uveitis. *Exp Eye Res*. (2015) 138:80–6. doi: 10.1016/j.exer.2015.06.018
66. Ten Berge JC, Fazil Z, van den Born I, Wolfs RCW, Schreurs MWJ, Dik WA, et al. Intraocular cytokine profile and autoimmune reactions in retinitis pigmentosa, age-related macular degeneration, glaucoma and cataract. *Acta Ophthalmol*. (2019) 97:185–92. doi: 10.1111/aos.13899
67. Lu B, Yin H, Tang Q, Wang W, Luo C, Chen X, et al. Multiple cytokine analyses of aqueous humor from the patients with retinitis pigmentosa. *Cytokine*. (2020) 127:154943. doi: 10.1016/j.cyto.2019.154943
68. Nakamura T, Fujisaka Y, Tamura Y, Tsuji H, Matsunaga N, Yoshida S, et al. Large cell neuroendocrine carcinoma of the lung with cancer-associated retinopathy. *Case Rep Oncol.* (2015) 8:153–8. doi: 10.1159/000380943
69. Kyger M, Worley A, Adamus G. Autoimmune responses against photoreceptor antigens during retinal degeneration and their role in macrophage recruitment into retinas of RCS rats. *J Neuroimmunol*. (2013) 254:91–100. doi: 10.1016/j.jneuroim.2012.10.007
70. Gorbatyuk M, Gorbatyuk O. Review: retinal degeneration: focus on the unfolded protein response. *Mol Vis*. (2013) 19:1985.
71. Rana T, Shinde VM, Starr CR, Kruglov AA, Boitet ER, Kotla P, et al. An activated unfolded protein response promotes retinal degeneration and triggers an inflammatory response in the mouse retina. *Cell Death Dis*. (2014) 5:e1578. doi: 10.1038/cddis.2014.539
72. Murakami Y, Ikeda Y, Nakatake S, Fujiwara K, Tachibana T, Yoshida N, et al. C-Reactive protein and progression of vision loss in retinitis pigmentosa. *Acta Ophthalmol.* (2018) 96:e174–9. doi: 10.1111/aos.13502
73. Panda S, Ding JL. Natural antibodies bridge innate and adaptive immunity. *J Immunol*. (2015) 194:13–20. doi: 10.4049/jimmunol.1400844
74. Zhang Y, Garcia-Ibanez L, Toellner KM. Regulation of germinal center B-cell differentiation. *Immunol Rev*. (2016) 270:8–19. doi: 10.1111/imr.12396
75. Nagele EP, Han M, Acharya NK, DeMarshall C, Kosciuk MC, Nagele RG. Natural IgG autoantibodies are abundant and ubiquitous in human sera, and their number is influenced by age, gender, and disease. *PLoS ONE*. (2013) 8:e60726. doi: 10.1371/journal.pone.0060726
76. Heckenlively JR, Fawzi AA, Oversier J, Jordan BL, Aptsiauri N. Autoimmune retinopathy: patients with antirecoverin immunoreactivity and panretinal degeneration. *Arch Ophthalmol.* (2000) 118:1525–1533. doi: 10.1001/archopht.118.11.1525
77. Adamus G. Autoantibody targets and their cancer relationship in the pathogenicity of paraneoplastic retinopathy. *Autoimmun Rev*. (2009) 8:410–4. doi: 10.1016/j.autrev.2009.01.002
78. Maeda T, Maeda A, Maruyama I, Ogawa KI, Kuroki Y, Sahara H, et al. Mechanisms of photoreceptor cell death in cancer-associated retinopathy. *Invest Ophthalmol Vis Sci*. (2001) 42:705–12.

79. Brinkman CJ, Pinckers AJ, Broekhuyse RM. Immune reactivity to different retinal antigens in patients suffering from retinitis pigmentosa. *Invest Ophthalmol Vis Sci*. (1980) 19:743–50.
80. Heckenlively JR, Solish AM, Chant SM, Meyers-Elliott RH. Autoimmunity in hereditary retinal degenerations. II. Clinical studies: antiretinal antibodies and fluorescein angiogram findings. *Br J Ophthalmol*. (1985) 69:758–64. doi: 10.1136/bjo.69.10.758
81. Broekhuyse RM, van Herck M, Pinckers AJ, Winkens HJ, van Vugt AH, Ryckaert S, et al. Immune responsiveness to retinal S-antigen and opsin in serpiginous choroiditis and other retinal diseases. *Doc Ophthalmol*. (1988) 69:83–93. doi: 10.1007/BF00154420
82. Sato T, Nishiguchi KM, Fujita K, Miya F, Inoue T, Sasaki E, et al. Serum anti-recoverin antibodies is found in elderly patients with retinitis pigmentosa and cancer. *Acta Ophthalmol*. (2020) 98:e722–9. doi: 10.1111/aos.14373
83. Tamm SA, Whitcup SM, Gery I, Wiggert B, Nussenblatt RB, Kaiser-Kupfer MI. Immune response to retinal antigens in patients with gyrate atrophy and other hereditary retinal dystrophies. *Ocul Immunol Inflamm*. (2001) 9:75–84. doi: 10.1076/ocii.9.2.75.3972
84. Heredia Garcia CD, Garcia Calderon PA. Evolution time and longitudinal studies of the anti-S-antigen antibody titers in retinitis pigmentosa. *Retina*. (1989) 9:237–241. doi: 10.1097/00006982-198909030-00013
85. Doekes G, Luyendijk L, Gerritsen MJ, Kijlstra A. Anti-retinal S-antigen antibodies in human sera: a comparison of reactivity in ELISA with human or bovine S-antigen. *Int Ophthalmol*. (1992) 16:147–152. doi: 10.1007/BF00916433
86. Berson EL, Rosner B, Weigel-DiFranco C, Dryja TP, Sandberg MA. Disease progression in patients with dominant retinitis pigmentosa and rhodopsin mutations. *Invest Ophthalmol Vis Sci*. (2002) 43:3027–36.
87. Maryam A, Vedithi SC, Khalid RR, Alsulami AF, Torres PHM, Siddiqi AR, et al. The molecular organization of human cGMP specific phosphodiesterase 6 (PDE6): structural implications of somatic mutations in cancer and retinitis pigmentosa. *Comput Struct Biotechnol J*. (2019) 17:378–89. doi: 10.1016/j.csbj.2019.03.004
88. Qendro V, Bugos GA, Lundgren DH, Glynn J, Han MH, Han DK. Integrative proteomics, genomics, and translational immunology approaches reveal mutated forms of Proteolipid Protein 1 (PLP1) and mutant-specific immune response in multiple sclerosis. *Proteomics*. (2017) 17:322. doi: 10.1002/pmic.201600322
89. Plotz PH. The autoantibody repertoire: searching for order. *Nat Rev Immunol*. (2003) 3:nri976. doi: 10.1038/nri976
90. Iannaccone A, Radic MZ. Increased protein citrullination as a trigger for resident immune system activation, intraretinal inflammation, and promotion of anti-retinal autoimmunity: intersecting paths in retinal degenerations of potential therapeutic relevance. *Adv Exp Med Biol*. (2019) 1185:175–9. doi: 10.1007/978-3-030-27378-1_29
91. Hollingsworth TJ, Hubbard MG, Levi HJ, White W, Wang X, Simpson R, et al. Proinflammatory pathways are activated in the human Q344X rhodopsin knock-in mouse model of retinitis pigmentosa. *Biomolecules*. (2021) 11:1163. doi: 10.3390/biom11081163
92. Stadler M, Arnold D, Frieden S, Luginbuhl S, Stadler B. Single nucleotide polymorphisms as a prerequisite for autoantigens. *Eur J Immunol*. (2005) 35:eji.200425481. doi: 10.1002/eji.200425481
93. Oppenheim JJ, Dong HF, Plotz P, Caspi RR, Dykstra M, Pierce S, et al. Autoantigens act as tissue-specific chemoattractants. *J Leukoc Biol*. (2005) 77:854–61. doi: 10.1189/jlb.1004623
94. Bei R, Masuelli L, Palumbo C, Modesti M, Modesti A. A common repertoire of autoantibodies is shared by cancer and autoimmune disease patients: inflammation in their induction and impact on tumor growth. *Cancer Lett*. (2009) 281:8–23. doi: 10.1016/j.canlet.2008.11.009
95. Howard OMZ, Dong HF, Su SB, Caspi RR, Chen X, Plotz P, et al. Autoantigens signal through chemokine receptors: uveitis antigens induce CXCR3- and CXCR5-expressing lymphocytes and immature dendritic cells to migrate. *Blood*. (2005) 105:4207–14. doi: 10.1182/blood-2004-07-2697
96. Bachmaier K, Krawczyk C, Kozieradzki I, Kong YY, Sasaki T, Oliveira-dos-Santos A, et al. Negative regulation of lymphocyte activation and autoimmunity by the molecular adaptor Cbl-b. *Nature*. (2000) 403:211–6. doi: 10.1038/35003228
97. Strong S, Liew G, Michaelides M. Retinitis pigmentosa-associated cystoid macular oedema: pathogenesis and avenues of intervention. *Br J Ophthalmol*. (2017) 101:31–7. doi: 10.1136/bjophthalmol-2016-309376
98. Rothova A. Inflammatory cystoid macular edema. *Curr Opin Ophthalmol*. (2007) 18:487–92. doi: 10.1097/ICU.0b013e3282f03d2e
99. Heckenlively JR, Jordan BL, Aptsiauri N. Association of antiretinal antibodies and cystoid macular edema in patients with retinitis pigmentosa. *Am J Ophthalmol*. (1999) 127:565–73. doi: 10.1016/S0002-9394(98)00446-2
100. Wolfensberger TJ, Aptsiauri N, Godley B, Downes S, Bird AC. Antiretinal antibodies associated with cystoid macular edema. *Klin Monbl Augenheilkd*. (2000) 216:283–5. doi: 10.1055/s-2000-10561
101. Grover S, Adamus G, Fishman GA. Is there an association of anti-retinal antibodies and cystoid macular edema in patients with retinitis pigmentosa? *Invest. Ophthalmol. Vis. Sci.* (2006) 47:5795.
102. Mosaad YM. Clinical role of human leukocyte antigen in health and disease. *Scand J Immunol*. (2015) 82:283–306. doi: 10.1111/sji.12329
103. Heckenlively JR, Bastek JV, Pearlman JT, Gladden J, Terasaki P. HLA typing in retinitis pigmentosa. *Br J Ophthalmol*. (1981) 65:131–2. doi: 10.1136/bjo.65.2.131
104. Castagna I, Fama F, Pettinato G, Palamara F, Trombetta CJ. HLA typing and retinitis pigmentosa. *Ophthalmologica*. (1996) 210:152–4. doi: 10.1159/000310696
105. Agardh D, Gaur LK, Agardh E, Landin-Olsson M, Agardh C-D, Lernmark Å. HLA-DQB1*0201/0302 is associated with severe retinopathy in patients with IDDM. *Diabetologia*. (1996) 39:1313–7. doi: 10.1007/s001250050575
106. Holland GN, Cornell PJ, Park MS, Barbetti A, Yuge J, Kreiger AE, et al. An association between acute retinal necrosis syndrome and HLA-DQw7 and phenotype Bw62,DR4. *Am J Ophthalmol*. (1989) 108:370–4. doi: 10.1016/S0002-9394(14)73303-3
107. Liversidge JM, Sewell HF, Forrester JV. Human retinal pigment epithelial cells differentially express MHC class II (HLA, DP, DR and DQ) antigens in response to *in vitro* stimulation with lymphokine or purified IFN-gamma. *Clin Exp Immunol*. (1988) 73:489–94.
108. Caspi RR, Chan CC, Grubbs BG, Silver PB, Wiggert B, Parsa CF, et al. Endogenous systemic IFN-gamma has a protective role against ocular autoimmunity in mice. *J Immunol*. (1994) 152:890–9.
109. Nagasaka Y, Ito Y, Ueno S, Terasaki H. Number of hyperreflective foci in the outer retina correlates with inflammation and photoreceptor degeneration in retinitis pigmentosa. *Ophthalmol Retina*. (2018) 2:726–34. doi: 10.1016/j.oret.2017.07.020
110. Massengill MT, Ahmed CM, Lewin AS, Ildefonso CJ. *Neuroinflammation in Retinitis Pigmentosa, Diabetic Retinopathy, and Age-Related Macular Degeneration: A Minireview*. Cham: Springer International Publishing (2018). p. 185–91. doi: 10.1007/978-3-319-75402-4_23
111. Forrester JV, Xu H, Kuffová L, Dick AD, McMenamin PG. Dendritic cell physiology and function in the eye. *Immunol Rev*. (2010) 234:282–304. doi: 10.1111/j.0105-2896.2009.00873.x
112. Xu H, Chen M, Forrester JV. Para-inflammation in the aging retina. *Progr Retinal Eye Res*. (2009) 28:348–68. doi: 10.1016/j.preteyeres.2009.06.001
113. Chen M, Xu H. Parainflammation, chronic inflammation, and age-related macular degeneration. *J Leukocyte Biol*. (2015) 98:713–25. doi: 10.1189/jlb.3RI0615-239R
114. Chinnery HR, McMenamin PG, Dando SJ. Macrophage physiology in the eye. *Pflügers Archiv*. (2017) 5:1–15. doi: 10.1007/s00424-017-1947-5
115. Hisatomi T, Sakamoto T, Sonoda K-h, Tsutsumi C, Qiao H, Enaida H, et al. Clearance of apoptotic photoreceptors. *Am J Pathol*. (2003) 162:1869–79. doi: 10.1016/S0002-9440(10)64321-0
116. Karlstetter M, Scholz R, Rutar M, Wong WT, Provis JM, Langmann T. Retinal microglia: just bystander or target for therapy? *Prog Retin Eye Res*. (2015) 45:4. doi: 10.1016/j.preteyeres.2014.11.004
117. Blank T, Goldmann T, Koch M, Amann L, Schön C, Bonin M, et al. Early microglia activation precedes photoreceptor degeneration in a mouse model of CNGB1-linked retinitis pigmentosa. *Front Immunol*. (2017) 8:1930. doi: 10.3389/fimmu.2017.01930
118. Langmann T. Microglia activation in retinal degeneration. *J Leukoc Biol*. (2007) 81:1345–51. doi: 10.1189/jlb.0207114
119. Rashid K, Akhtar-Schaefer I, Langmann T. Microglia in retinal degeneration. *Front Immunol*. (2019) 10:1975. doi: 10.3389/fimmu.2019.01975

120. Sivakumar V, Foulds WS, Luu CD, Ling E-A, Kaur C. Retinal ganglion cell death is induced by microglia derived pro-inflammatory cytokines in the hypoxic neonatal retina. *J Pathol*. (2011) 224:245–60. doi: 10.1002/path.2858
121. Kohno H, Chen Y, Kevany BM, Pearlman E, Miyagi M, Maeda T, et al. Photoreceptor proteins initiate microglial activation *via* toll-like receptor 4 in retinal degeneration mediated by all-trans-retinal. *J Biol Chem*. (2013) 288:15326–41. doi: 10.1074/jbc.M112.448712
122. Xu H, Chen M. Targeting the complement system for the management of retinal inflammatory and degenerative diseases. *Eur J Pharmacol*. (2016) 787:94–104. doi: 10.1016/j.ejphar.2016.03.001
123. Silverman SM, Ma W, Wang X, Zhao L, Wong WT. C3- and CR3-dependent microglial clearance protects photoreceptors in retinitis pigmentosa. *J Exp Med*. (2019) 216:1925–43. doi: 10.1084/jem.20190009
124. Uren PJ, Lee JT, Doroudchi MM, Smith AD, Horsager A. A profile of transcriptomic changes in the rd10 mouse model of retinitis pigmentosa. *Mol Vis*. (2014) 20:1612–28.
125. Rohrer B, Demos C, Frigg R, Grimm C. Classical complement activation and acquired immune response pathways are not essential for retinal degeneration in the rd1 mouse. *Exp Eye Res*. (2007) 84:82–91. doi: 10.1016/j.exer.2006.08.017
126. Humphries MM, Kenna PF, Campbell M, Tam LCS, Nguyen ATH, Farrar GJ, et al. C1q enhances cone photoreceptor survival in a mouse model of autosomal recessive retinitis pigmentosa. *Eur J Hum Genet*. (2012) 20:64–8. doi: 10.1038/ejhg.2011.151
127. Anderson DH, Radeke MJ, Gallo NB, Chapin EA, Johnson PT, Curletti CR, et al. The pivotal role of the complement system in aging and age-related macular degeneration: hypothesis re-visited. *Prog Retin Eye Res*. (2010) 29:95–112. doi: 10.1016/j.preteyeres.2009.11.003
128. Radu RA, Hu J, Yuan Q, Welch DL, Makshanoff J, Lloyd M, et al. Complement system dysregulation and inflammation in the retinal pigment epithelium of a mouse model for Stargardt macular degeneration. *J Biol Chem*. (2011) 286:18593–601. doi: 10.1074/jbc.M110.191866
129. Yang L, Kim J-H, Kovacs KD, Arroyo JG, Chen DF. Minocycline inhibition of photoreceptor degeneration. *Arch Ophthalmol*. (2009) 127:1475–80. doi: 10.1001/archophthalmol.2009.288

Conflict of Interest: The author declares that the research was conducted in the absence of any commercial or financial relationships that could be construed as a potential conflict of interest.

Publisher's Note: All claims expressed in this article are solely those of the authors and do not necessarily represent those of their affiliated organizations, or those of the publisher, the editors and the reviewers. Any product that may be evaluated in this article, or claim that may be made by its manufacturer, is not guaranteed or endorsed by the publisher.

frontiers in Medicine

SYSTEMATIC REVIEW
published: 13 January 2022
doi: 10.3389/fmed.2021.759311

Efficacy and Safety of Ocriplasmin Use for Vitreomacular Adhesion and Its Predictive Factors: A Systematic Review and Meta-Analysis

Xi Chen[1*†], *Min Li*[2†], *Ran You*[1], *Wei Wang*[1] *and Yanling Wang*[1*]

[1] *Department of Ophthalmology, Beijing Friendship Hospital, Capital Medical University, Beijing, China,* [2] *Clinical Epidemiology and Evidence-Based Medicine (EBM) Unit, National Clinical Research Center for Digestive Disease, Beijing Friendship Hospital, Capital Medical University, Beijing, China*

OPEN ACCESS

Edited by:
Menaka Chanu Thounaojam, Augusta University, United States

Reviewed by:
Koenraad Blot, Xintera BV, Belgium
Fangchao Liu, Capital Medical University, China
Yong Liu, Army Medical University, China
Huihui Yu, China Medical University, China

***Correspondence:**
Xi Chen
xichen@ccmu.edu.cn
Yanling Wang
wangyanling999@vip.sina.com

†These authors have contributed equally to this work

Specialty section:
This article was submitted to Ophthalmology, a section of the journal Frontiers in Medicine

Received: *16 August 2021*
Accepted: *13 December 2021*
Published: *13 January 2022*

Citation:
Chen X, Li M, You R, Wang W and Wang Y (2022) Efficacy and Safety of Ocriplasmin Use for Vitreomacular Adhesion and Its Predictive Factors: A Systematic Review and Meta-Analysis. Front. Med. 8:759311. doi: 10.3389/fmed.2021.759311

Symptomatic vitreomacular adhesion (sVMA) impedes visual acuity and quality. Ocriplasmin is a recombinant protease, which may be injected into the vitreous cavity to treat this condition, yet controversy remains with respect to its effectiveness and safety, particularly its patient selection standard. In this systematic review, the PubMed, Embase, and the Cochrane Library were searched to identify studies published prior to August 2020 on the impact of ocriplasmin treatment on VMA release, macular hole (MH) closure, and/or related adverse events (AEs). Data were pooled using a random-effects model. Risk ratios (RRs) with 95% CIs were calculated. Of 1,186 articles reviewed, 5 randomized controlled trials and 50 cohort studies were ultimately included, representing 4,159 patients. Ocriplasmin significantly increased the rate of VMA release (RR, 3.61; 95% CI, 1.99–6.53; 28 days after treatment) and MH closure (RR, 3.84; 95% CI, 1.62–9.08; 28 days after treatment) and was associated with visual function improvement. No increased risk for overall AEs was seen in ocriplasmin treatment. The proportion of VMA release and MH closure in patients was 0.50 and 0.36, respectively. VMA release was more likely in patients with absence of epiretinal membrane (ERM). Patients with smaller MH diameter were more likely to achieve MH closure. Evidence from included studies suggests that ocriplasmin is a suitable and safe approach for treating sVMA. ERM and MH status are important factors when considering ocriplasmin treatment.

Keywords: ocriplasmin, symptomatic vitreomacular adhesion/vitreomacular traction, macular hole (MH), meta-analysis (as topic), individual participant data analysis

INTRODUCTION

Symptomatic vitreomacular adhesion (sVMA) typically occurs with incomplete posterior vitreous detachment (PVD) and leads to subsequent loss or distortion of vision (1–3). sVMA can further result in the occurrence of vitreomacular traction (VMT), often coinciding with macular hole (MH) and epiretinal membrane (ERM).

Based on its etiology, treatment of sVMA requires the release of vitreous body traction on the retina. The current standard management option for treating these adhesions is pars plana vitrectomy (PPV),which involves removing the vitreous surgically (4, 5). However, even small-gauge procedure PPV can lead to serious complications including retinal detachment, retinal

tears, endophthalmitis, and postoperative cataract formation. A biological agent for non-invasive treatment of VMA known as ocriplasmin (Jetrea; ThromboGenics NV, Leuven, Belgium, UK) was approved as the first drug of its kind by the US Food and Drug Administration on October 17, 2012 (6, 7). Ocriplasmin is composed of the catalytic domain of human plasmin with proteolytic activity against protein components of the vitreous body and vitreoretinal interface. It dissolves the protein matrix responsible for VMA. The approval of ocriplasmin for clinical use was based on the MIVI-TRUST study (8). Since then, randomized controlled trials (RCTs) including MIVI-IIT and OASIS (9, 10), prospective cohort studies, and observational studies including INJECT, ORBIT, and OVIID-1 (11–13) have analyzed the efficacy of and adverse reactions to ocriplasmin. Resulting data show that non-surgical induction of PVD using ocriplasmin can offer the benefits of VMA release and MH closure while eliminating the risks associated with a surgical procedure.

Subgroup analyses on pharmacologic VMA resolution showed that subjects with certain baseline characteristics had higher VMA resolution rate included absence of ERM, presence of MH, small adhesion diameter, phakic lens status, gender, and age (11, 13, 14). Meta-analysis of Jackson et al. further demonstrated that presence of ERM and broad VMA, increasing age, and male gender were associated with decreased treatment response in RCT reports (15).

This study includes a complete search for existing data in this meta-analysis to evaluate the efficacy and safety profile of ocriplasmin for the treatment of sVMA with/without MH, across subgroups defined by the presence of ERM and MH, and also to identify factors which may affect the effectiveness of ocriplasmin including MH diameter, age, gender, and others. Based on our findings, we proposed the optimal profile of patient for treatment with ocriplasmin.

MATERIALS AND METHODS

This study is fully compliant with the Preferred Reporting Items for Systematic Reviews and Meta-analyses (PRISMA) statement (16). This study was registered with the International Prospective Register of Systematic Reviews (PROSPERO) (CRD42021228893).

Data Sources and Search Strategy

The PubMed, Embase, and the Cochrane Library were searched from inception to August 1, 2020. In addition, we checked the websites of the Association for Research in Vision and Ophthalmology (https://www.arvo.org) and the European Society of Ophthalmology (https://soevision.org/organisation) for annual conference abstracts published from inception to August 1, 2020 and the reference lists of all the relevant articles to identify additional studies. Full details of the search strategy and results are given in **Supplementary File 1**.

Study Selection

Randomized controlled trials and cohort studies were eligible for inclusion, if they met the following criteria: (1) participants were patients diagnosed with VMA and/or MH and (2) the effectiveness of ocriplasmin on VMA release, MH closure, or vision improvement was reported. For papers reporting data from the same participants with common authors, research centers, and overlapping enrollment periods, the most comprehensive of these was included. Reviews, editorials, letters, guidelines, and protocols as well as articles describing studies with fewer than 10 participants or focused on basic research were excluded.

Data Extraction and Quality Assessment

Two investigators (XC and ML) independently assessed the eligibility of studies and extracted data in duplicate. Any disagreement on study inclusion or interpretation of data was resolved by consulting the senior investigator (YW). The extracted data included study information (first author, publication year, sample size, region of study, and study design), characteristics of participants (age and gender), treatment details (dose), and disease characteristics (definition of cases, presence of ERM, diameter of VMA, and size of MH).

Study quality was assessed using the Cochrane Collaboration risk of bias tool for RCTs and a published quality appraisal checklist for cohort studies (17). This checklist examines the main domains including study design, population, intervention, outcome measures, statistical analysis, results/conclusions, competing interests, and sources of financial support.

Statistical Analysis

Characteristics of included studies were described. Heterogeneity between studies was quantified by the I^2-test. An I^2 statistic above 50% was considered to indicate substantial heterogeneity. Random-effects models were used for all the meta-analyses due to clinical heterogeneity inherent in the data. In case of zero event appeared in included studies, 0.5 was added to the event number, as Haldane–Anscombe correction referred.

Pooled risk ratios (RRs) with 95% CIs were calculated to estimate the impact of ocriplasmin vs. placebo/sham for participants with VMA and/or MH in increasing the rate of VMA release, MH closure, vision improvement, associated vitrectomy, or adverse events (AEs). Pooled proportions of eyes with VMA resolution and MH closure after ocriplasmin injection were calculated. Subgroup analyses were performed to examine whether the rate of VMA resolution after ocriplasmin injection was modified by preplanned variables including wet age-related macular degeneration (wAMD), diabetic retinopathy (DR), and retinal vein occlusion (RVO). Further, to reveal the factors associated with VMA release/MH closure, pooled mean difference/odds ratios (ORs) with 95% CIs for each potential factor were estimated as appropriate. The Begg's and Egger's tests and a funnel plot were used to evaluate publication bias.

All the data from included studies whose authors had provided the raw data were included in the individual participant data analysis (IPD) analysis. The receiver operating characteristic (ROC) curves were plotted and the area under the ROCs (AUROCs) were calculated to determine the predict ability of characteristics of participants including age, gender, VMA diameter, and ERM formation for VMA release after ocriplasmin injection. Those characteristics were included in

the multivariable logistic regression models and a final model selection was performed using a backward selection process. The maximum Youden index was used to define the optimal cutoff values. Sensitivity and specificity were used to evaluate the predicted performance of each cutoff value.

P-values (two-tailed) of <0.05 were considered as statistically significant. All the analyses were conducted using the meta package of R software, version 3.6.2.

RESULTS

Characteristics of the Included Studies

The search described above yielded 1,186 publications from the PubMed, Embase, and the Cochrane Library databases, of which 235 publications were duplicates. Of the 951 remaining articles, 784 irrelevant articles were identified by reviewing titles and abstracts and were excluded. The full text of the remaining 167 articles were reviewed, after which 110 articles were excluded due to a lack of outcomes with attention, papers reporting data from the same cohort, or participants smaller than 10. Finally, a total of 55 studies (5 RCTs and 50 cohort studies in 57 publishing articles) with 4,159 participants were included in this meta-analysis (**Figure 1**). All the included studies were conducted in North American and European countries, except one from Australia. The recommended ocriplasmin dose is 125 μg for single intravitreal injection and this was the intervention strategy applied in our included studies (**Supplementary Table 1**; **Supplementary File 2** for full included studies list).

Therapeutic Effect of Ocriplasmin Injection in RCTs

Overall, the RR for nonsurgical VMA release was 3.61 [95% CI: 1.99–6.53; $I^2 = 44\%$; $P_{het} = 0.15$ (*p*-value for heterogeneity); **Figure 2A**] in non-wAMD participants at 28 days after treatment, which was higher than reported in wAMD [(18); RR: 2.03; 95% CI: 0.65–6.31]. MH closure was achieved more frequently with ocriplasmin than in the control group (RR 3.84, 95% CI: 1.62–9.08; $I^2 = 0\%$; $P_{het} = 0.68$; **Figure 2B**) at 28 days after treatment, consistent with the OASIS trial that reported the number of participants achieving MH closure at 24 months after ocriplasmin treatment was higher than sham (RR: 1.95; 95% CI: 0.72–5.28).

Best corrected visual acuity (BCVA) improvement of at least three lines at 6 months after treatment was more likely in participants undergoing ocriplasmin treatment than with sham injection (RR: 1.97; 95% CI: 1.08–3.57; $I^2 = 0\%$; $P_{het} = 0.39$; **Figure 2C**). Also, we observed that the OASIS trial reported ≥2-line improvement in BCVA (RR: 1.27; 95% CI: 0.92–1.75). Moreover, comparison of the 25-item National Eye Institute Visual Function Questionnaire-25 (VFQ-25) composite score between ocriplasmin and control treatment data showed that a larger percentage of participants treated with ocriplasmin experienced a ≥5-point (clinically meaningful) improvement in VFQ-25 composite score at 6 months after treatment (RR: 1.33; 95% CI: 1.02–1.73) in MIVI 006 and 007 trials. Accordingly, the percentage of participants with ≥ 5-point worsening was lower with ocriplasmin at 6 months after treatment (RR: 0.62; 95% CI: 0.44–0.86) in MIVI 006 and 007 trials. The OASIS trial reported that the participants receiving ocriplasmin with ≥ 5-point improvement in VFQ-25 composite score at 24 months were also more than control (RR: 1.72; 95% CI: 1.17–2.52) and participants with ≥ 5-point worsening were lower than control (RR: 0.64; 95% CI: 0.31–1.34).

In addition, fewer participants who required PPV were in the ocriplasmin group than were in the sham group at 6 months after treatment (RR: 0.67; 95% CI: 0.50–0.91; $I^2 = 0\%$; $P_{het} = 0.73$; **Figure 2D**), consistent with the OASIS trial that reported the number of participants requiring PPV at 24 months after ocriplasmin treatment was less than control (RR: 0.76; 95% CI: 0.53–1.07).

Incidence of AEs After Receiving Ocriplasmin Therapy

The proportion of participants experiencing at least one AE was comparable between the ocriplasmin and control groups (RR: 1.13; 95% CI: 0.95–1.34; $I^2 = 71\%$; $P_{het} < 0.01$; **Supplementary Figure 1A**). No significant difference between ocriplasmin and control was found in the incidence of serious AEs (RR: 1.38; 95% CI: 0.44–4.32; $I^2 = 64\%$; $P_{het} = 0.10$; **Supplementary Figure 1B**) and serious ocular AEs (RR: 0.88; 95% CI: 0.58–1.33; $I^2 = 12\%$; $P_{het} = 0.33$; **Supplementary Figure 1D**). It is worth noting, however, that ocular AEs of ocriplasmin therapy were slightly higher than control (RR: 1.20; 95% CI: 1.05–1.37; $I^2 = 36\%$; $P_{het} = 0.18$; **Supplementary Figure 1C**), suggesting that while ocriplasmin therapy did not raise the risk of overall AEs, it may carry a higher risk of ocular AEs.

Proportion of Ocriplasmin Therapy in Cohort Studies

In cohort studies, the overall proportion of eyes achieving non-surgical VMA release was 0.50 (95% CI: 0.47–0.53; $I^2 = 48\%$; $P_{het} < 0.01$; **Figure 3**). In participants without ERM at baseline, the proportion of VMA release (0.58, 95% CI: 0.53–0.63; $I^2 = 58\%$; $P_{het} < 0.01$; **Figure 4A**) was higher than those with ERM (0.34, 95% CI: 0.25–0.44; $I^2 = 0\%$; $P_{het} = 0.51$; **Figure 4B**). Participants with MH were more likely to experience VMA release (0.58, 95% CI: 0.50–0.65; $I^2 = 53\%$; $P_{het} < 0.01$; **Figure 4D**) than those without MH (0.48, 95% CI: 0.43–0.52; $I^2 = 57\%$; $P_{het} < 0.01$; **Figure 4C**). Moreover, we found that the proportion of VMA release in participants with or without ERM potentially increased with time, especially in ERM participants after 6 months (**Supplementary Figure 2**).

The overall proportion for MH closure was 0.36 (95% CI: 0.32–0.39; $I^2 = 0\%$; $P_{het} = 0.91$; **Figure 5A**). The proportion in participants with MH diameter ≤ 250 μm (0.48, 95% CI: 0.41–0.55; $I^2 = 0\%$; $P_{het} = 0.62$; **Figure 5B**) was higher than those with MH diameter of 250–400 μm (0.27, 95% CI: 0.21–0.34; $I^2 = 0\%$; $P_{het} = 1.00$; **Figure 5C**).

Approximately, 40% of participants showed at least 1-line improvement in BCVA after ocriplasmin treatment (95% CI: 0.37–0.45; $I^2 = 53\%$; $P_{het} = 0.09$; **Figure 6A**) and 28 or 25% of participants with at least 2-line (95% CI: 0.21–0.35; $I^2 = 76\%$;

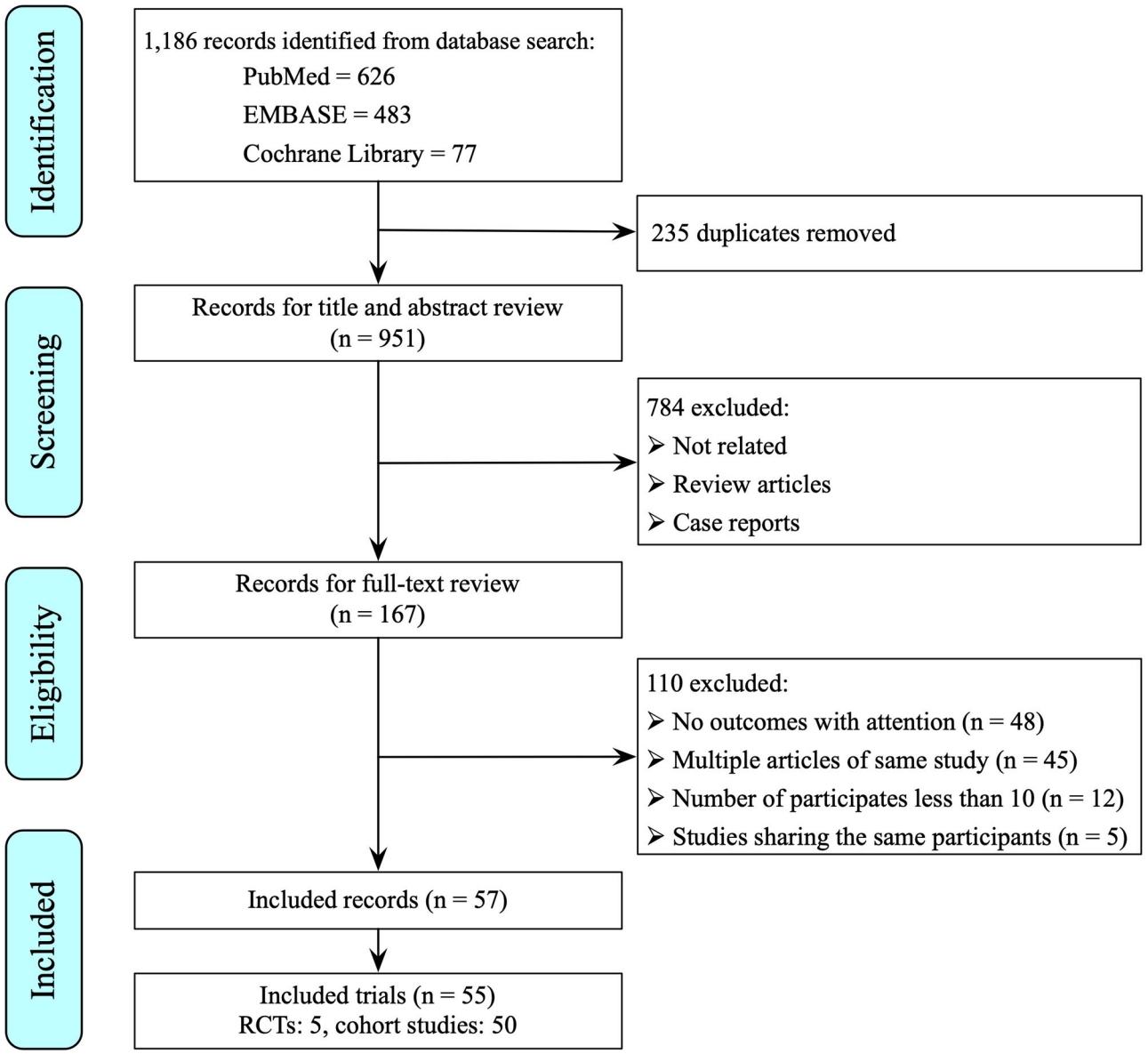

FIGURE 1 | Flow diagram describing the literature screening process.

$P_{het} < 0.01$; **Figure 6B**) or 3-line (95% CI: 0.18–0.34; $I^2 = 66\%$; $P_{het} = 0.03$; **Figure 6C**) improvement in BCVA, respectively. Mean improvement was −0.13 logarithm of the minimum angle of resolution (logMAR) (95% CI: −0.17 to −0.08; $I^2 = 79\%$; $P_{het} < 0.01$; **Supplementary Figure 3**).

Analysis of Potential Factors Affecting VMA Release and MH Closure

We further explored factors with potential to affect the rate of VMA release (VMAR) and MH closure including 556 participants from 14 studies. Participants who achieved VMAR were more likely to be female, without ERM, at a younger age, and with lower VMA diameter (**Supplementary Table 2**). Between participants with and without MH closure, MH closure was more likely to be achieved in participants with lower MH base diameter and minimum linear diameter (**Supplementary Table 3**).

In order to determine the optimal VMA profile of patient to receive ocriplasmin treatment, the ROC curve analysis was performed to find the predict ability of VMA diameter, age, ERM formation, and gender for VMA release in 5 studies including 120 participants (**Supplementary Table 4**). Cutoff values of VMA diameter and age were 506 μm (sensitivity: 81.13% and specificity: 56.41%) and 73 years (sensitivity: 66.18% and specificity: 57.69%; **Supplementary Table 5**), respectively. Specifically, the AUROC for VMA diameter < 506 μm, age < 73 years, without ERM formation, and

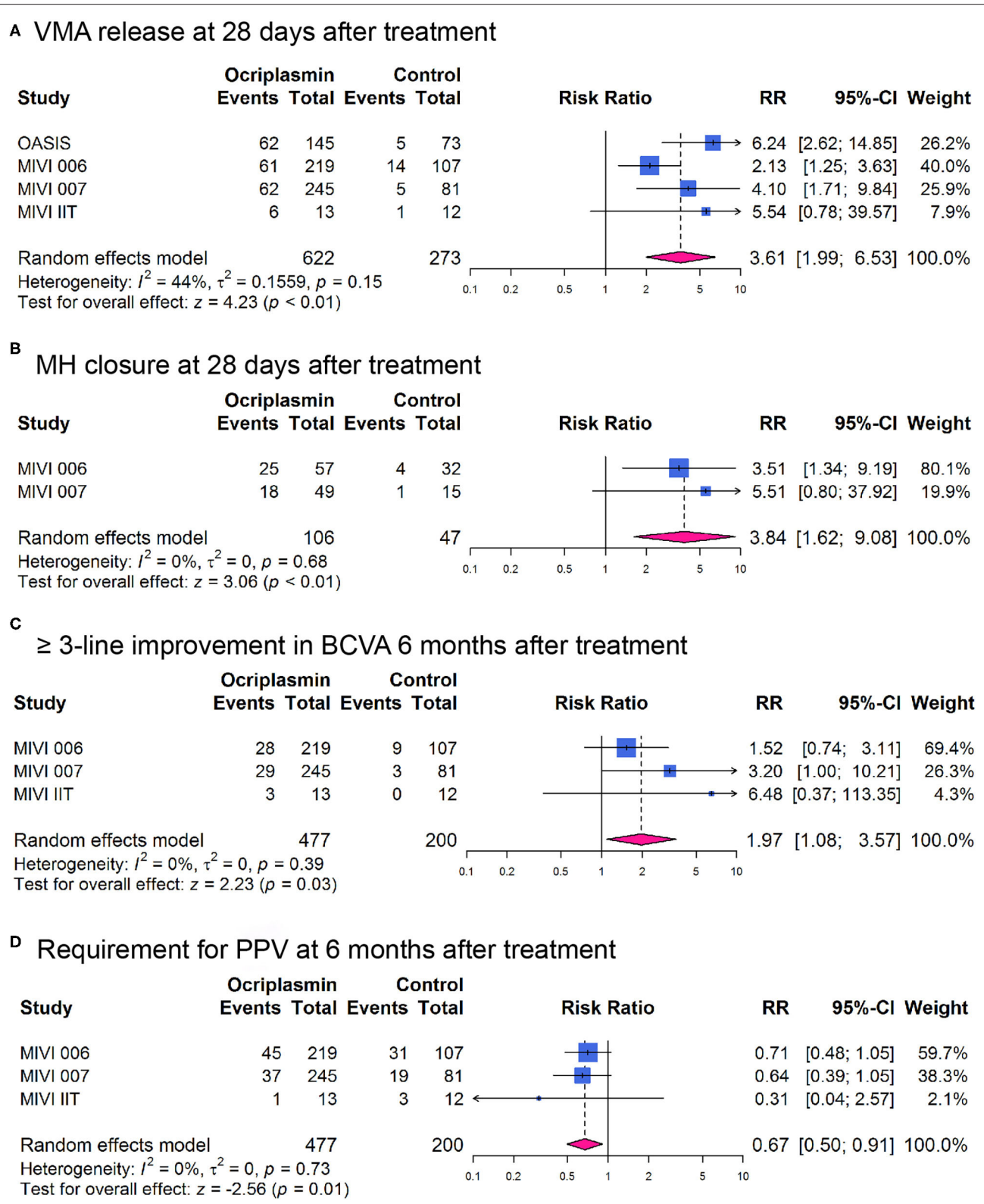

FIGURE 2 | Forest plots of therapeutic effect of ocriplasmin injection compared with controls in included randomized controlled trials. **(A)** Vitreomacular adhesion (VMA) release at 28 days after treatment; **(B)** Macular hole (MH) closure at 28 days after treatment; **(C)** At least 3-line improvement in best corrected visual acuity (BCVA) at 6 months after treatment; **(D)** Incidence of pars plana vitrectomy (PPV) at 6 months after treatment.

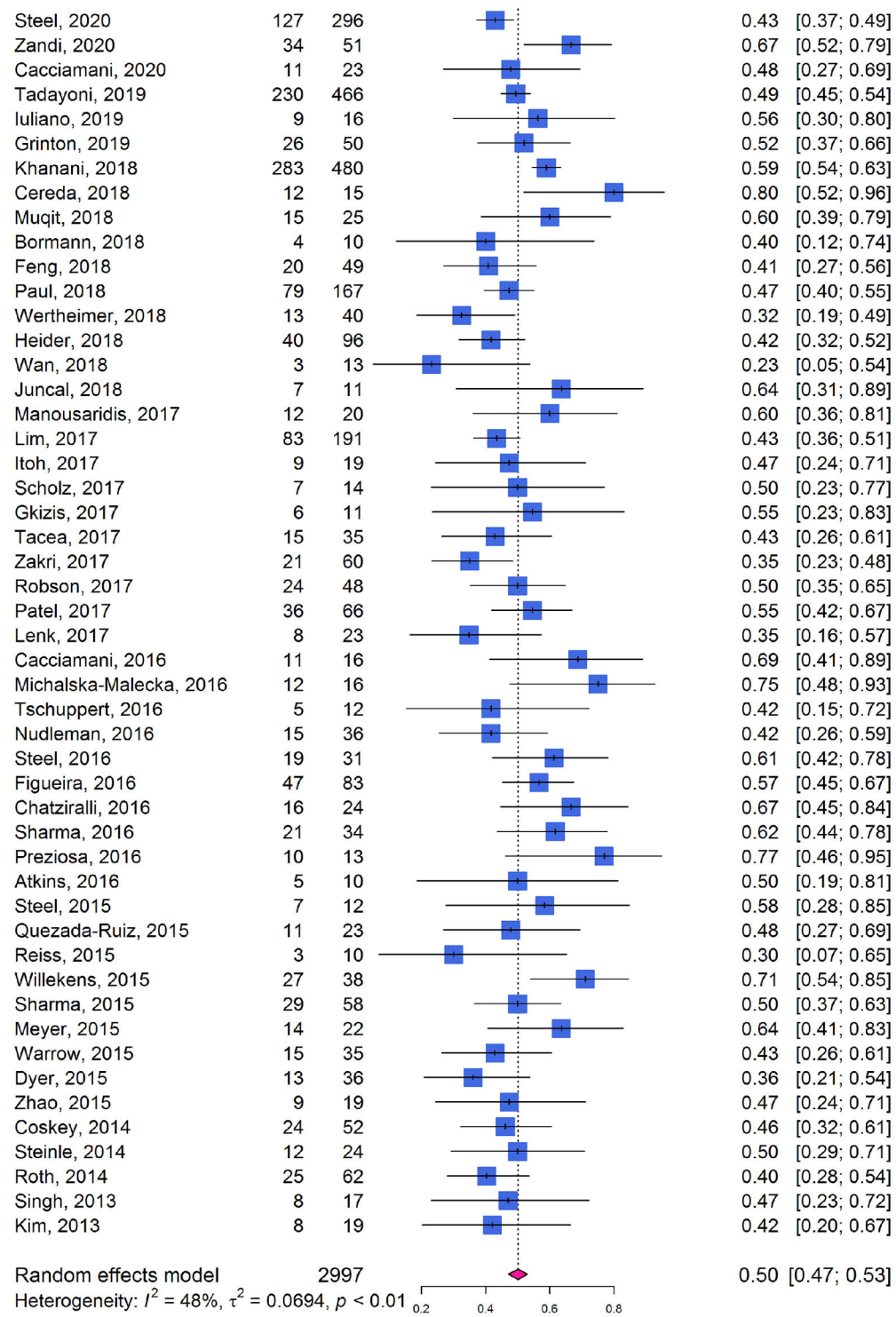

FIGURE 3 | Forest plots of proportion of VMA release in participants receiving ocriplasmin therapy in included cohort studies.

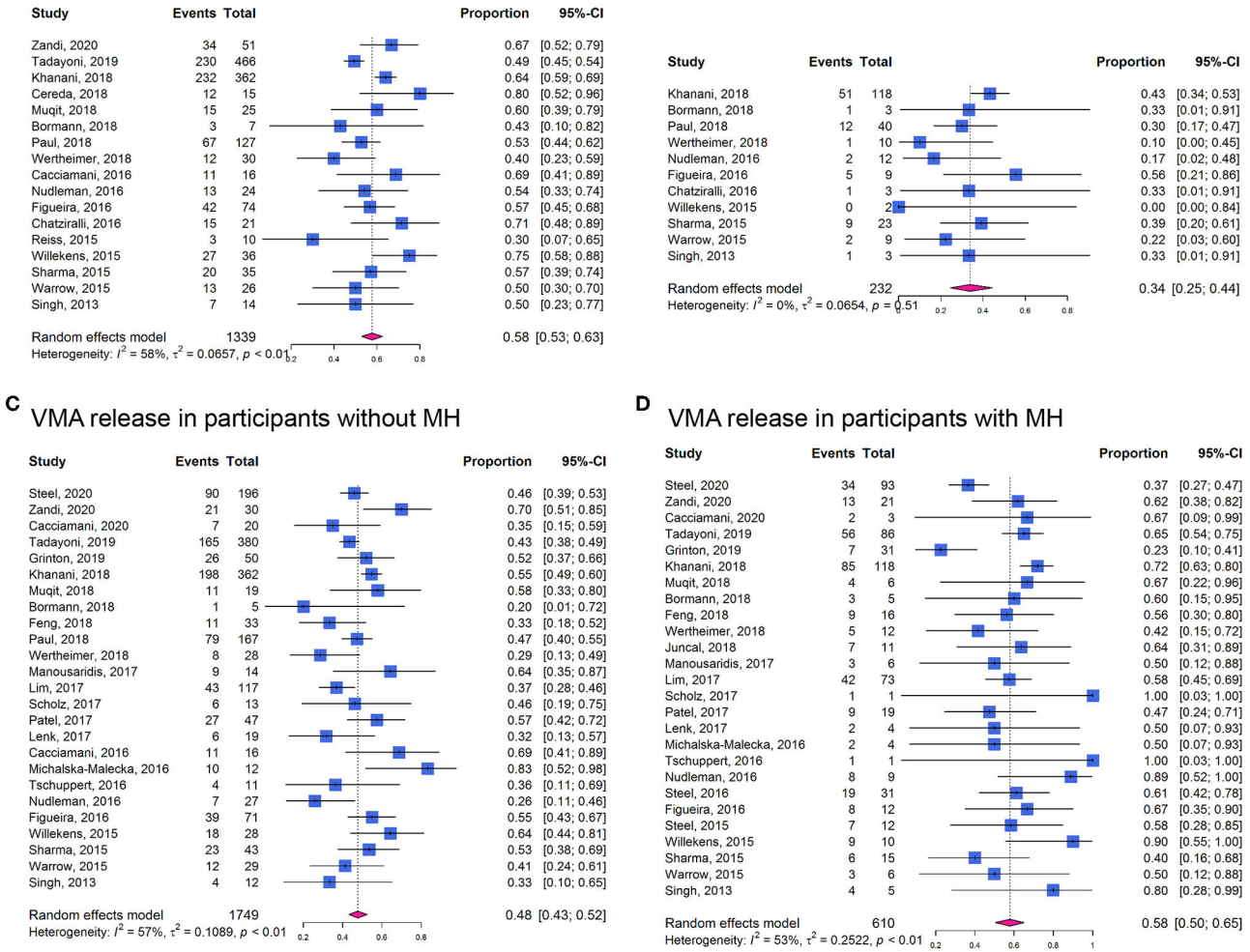

FIGURE 4 | Forest plots of proportion of VMA release in participants receiving ocriplasmin therapy in different groups. **(A)** In participants without epiretinal membrane (ERM); **(B)** In participants with ERM; **(C)** In participants without MH; **(D)** In participants with MH.

female participants to predict VMAR were 0.71, 0.62, 0.62, and 0.59, respectively. These characteristics were entered into the multivariable logistic regression model resulted in an AUROC and its 95% CI being 0.84 (0.74–0.92). We listed the formula of $P_{release}$ for calculating the estimated probability of VMAR using the character of patient including VMA diameter, sex, and ERM status. Also, we provided several examples and their $P_{release}$ value for reference (**Supplementary Table 6**).

It has been recognized that sVMA may be associated with other conditions such as AMD, DR, or RVO. In addition to the above factors that directly affect the therapeutic effect, we also analyzed the causes of secondary VMA. Subgroup analysis was performed and stratified by the median proportions of AMD, DR, and RVO, all of which were found not to affect the rate of VMA release after ocriplasmin injection (**Supplementary Table 7**).

Assessment of Study Quality and Publication Bias

Five RCTs were found to be of high quality. The OASIS trial (10) was found to have unclear risk of performance bias and the Novack et al. (18) study had unclear risk for selection, performance, and detection bias. The MIVI-IIT trial (9) showed unclear risk for selection and performance bias and the MIVI-TRUST trial (8) showed unclear risk for attrition bias (**Supplementary Figure 4**). In general, quality of the 50 cohort studies was found to be acceptable as shown in **Supplementary Table 8**. The included cohort studies showed relatively high quality in their objectives, statistical analyses, results, and conclusions (including follow-up and adverse events reporting), but performed less well on study design, intervention and cointervention, and outcome measures. No evidence of publication bias was found in analysis using the Begg's

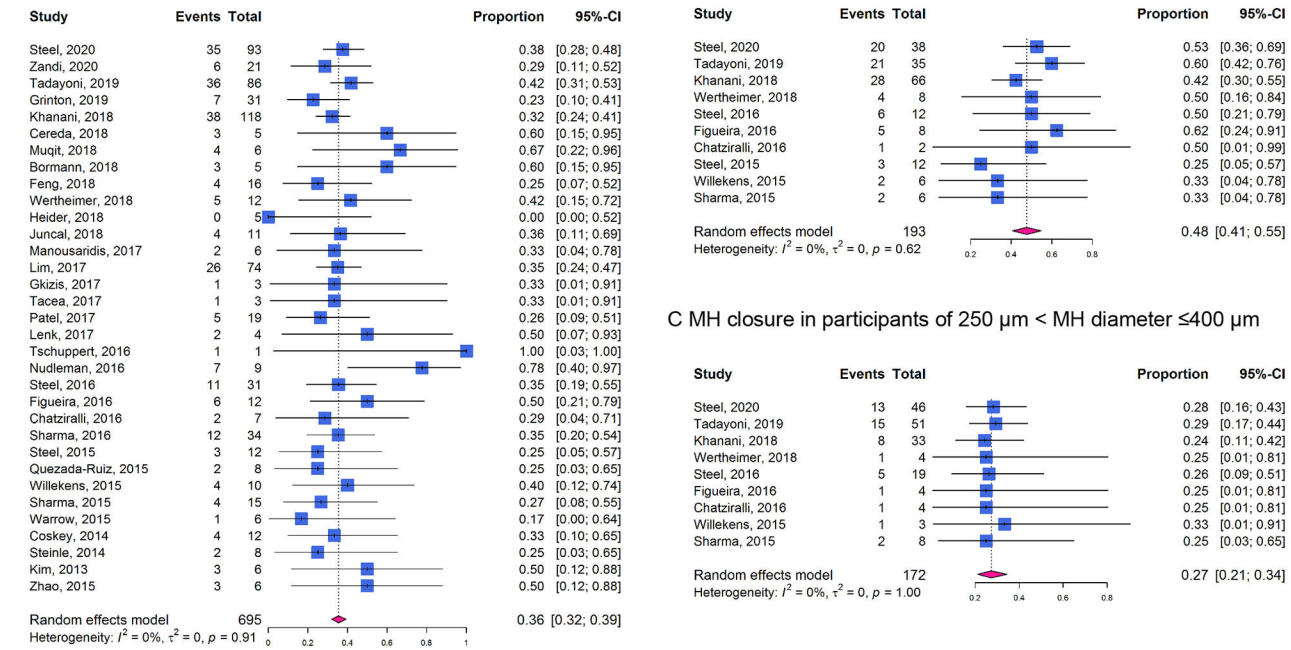

FIGURE 5 | Forest plots of proportion of MH closure in participants receiving ocriplasmin therapy in included cohort studies. **(A)** In all the participants; **(B)** In participants of MH diameter ≤ 250 μm; **(C)** In participants of MH diameter of 250–400 μm.

and Egger's tests and funnel plots (**Supplementary Table 9**; **Supplementary Figures 5**, **6**).

DISCUSSION

We identified 5 RCTs and 50 cohort studies including 4,159 participants. Our results demonstrated that treatment with ocriplasmin increased the likelihood of VMA release and MH closure and was associated with improvements in BCVA and questionnaire-assessed visual function. No increased risk in overall AEs was found between ocriplasmin treatment and control. The results also showed that VMAR was more likely in patients with absence of ERM. Patients with smaller MH diameter were more likely to achieve MH closure. Our findings have comprehensively demonstrated the effectiveness of ocriplasmin in VMA and MH treatment as well as patient-related factors affecting outcomes and included guidance on selection of suitable patients to receive ocriplasmin treatment in clinic.

Posterior vitreous detachment is a physiological age-related process and incomplete PVD could cause VMA due to the persistent adhesion of the vitreous to the macula, especially the fovea. Persistent asymptomatic VMA may progress to VMT, also known as sVMA, causing retinal structure deformation such as macular edema and MH and accompanied by metamorphopsia, decreased visual acuity, and other symptoms. The RCTs included in this study indicated that treatment with ocriplasmin was more likely than control intervention to result in VMA release and MH closure, reduce the requirement for PPV, and achieve visual improvement, consistent with a previous meta-analysis (19). One RCT study on wAMD (18), showed that the VMA release of patients with wAMD was lower than previously demonstrated by other RCT studies, suggesting that VMA secondary to wAMD may be less responsive to ocriplasmin. However, this study found that ocriplasmin treatment and its causing VMA release decreased the number of antivascular endothelial growth factor injection in patients with wAMD.

Furthermore, we analyzed VFQ-25 composite scores changes found in the OASIS and the MIVI-TRUST trials (20, 21). Ocriplasmin treatment was associated with visual function improvement not only in BCVA, but also in this participant-reported questionnaire-based outcome. These scores reflect the influence of visual disability and visual symptoms on generic health domains and indicate the effect of treatment on activities related to daily visual functions (22, 23). The findings are relevant to clinical decision-making, since outcomes reported by patients are powerful tools to verify the effects of a treatment on health and daily-life activities of patients, both in terms of benefits and potential adverse effects.

The strengths of this meta-analysis include the comprehensive search strategy and retrieval of all the relevant trials and the focus on detecting the optimal patient profile for ocriplasmin treatment. In the UK, the National Institute for Health and Care Excellence (NICE) guidance recommends the use of ocriplasmin for treating VMT in adults without ERM, who have a MH ≤ 400 μm diameter and/or severe symptoms (24). Several studies have demonstrated that ocriplasmin therapy might be more beneficial for patients with sVMA with specific characteristics such as relatively small adhesion diameter and absence of

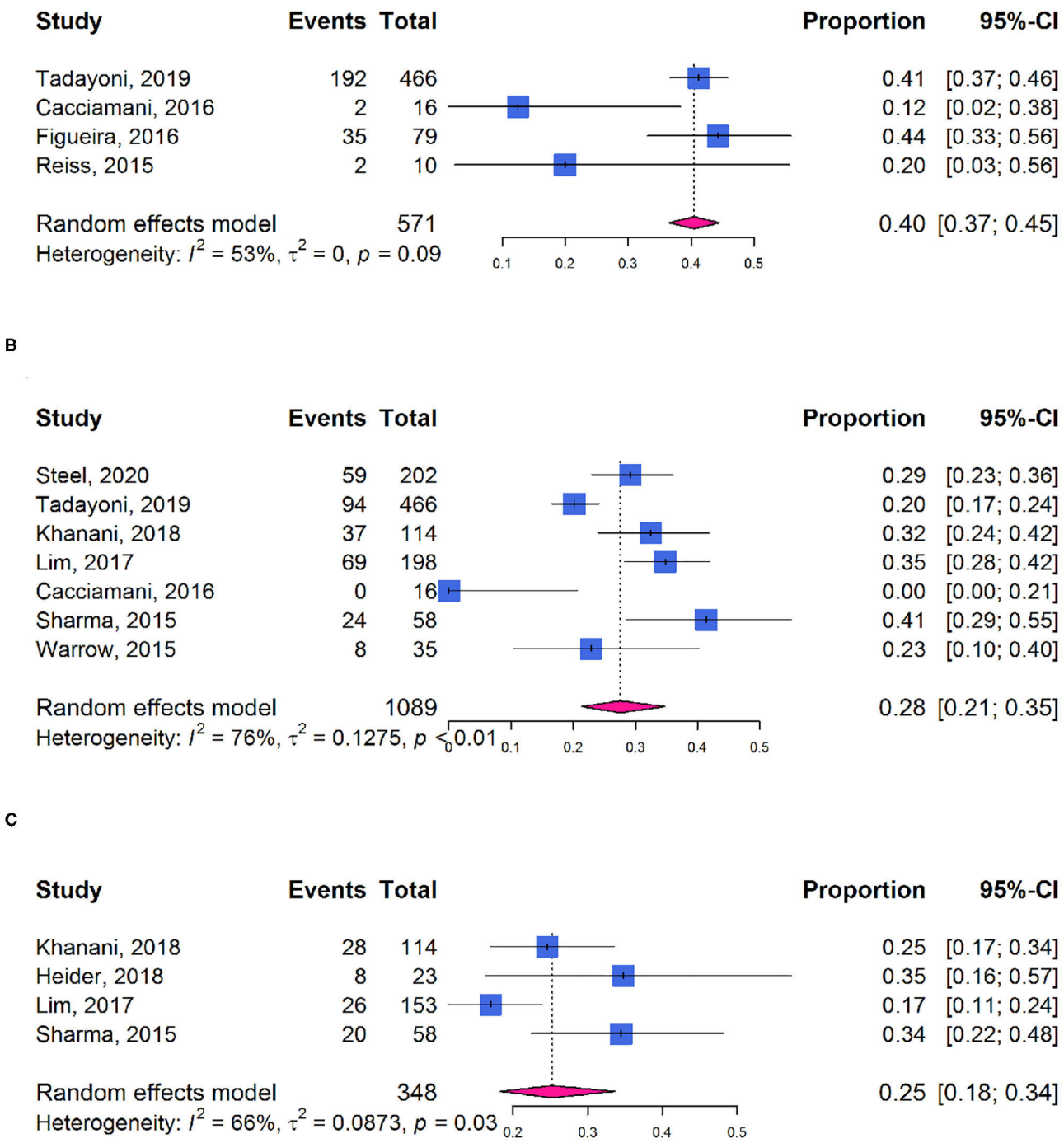

FIGURE 6 | Forest plots of proportion of visual acuity improvement in participants receiving ocriplasmin therapy. **(A)** ≥1-line improvement in BCVA; **(B)** ≥2-line improvement in BCVA; **(C)** ≥3-line improvement in BCVA.

ERM (25). More recently, Jackson et al. included 5 RCTs in an IPD meta-analysis and found that VMA release is more likely in younger, female patients and eyes with MH and less likely in the presence of ERM, broad VMA (>1,500 μm), DR, or pseudophakia (15). In this study, we also reported that patients with absence of ERM, the treatment of ocriplasmin

was more likely to induce VMA release (**Figure 4**). Patients with MH were more likely to experience VMA release after ocriplasmin injection, since ERM and large VMA adhesion diameters seemed to be rare in the presence of MH. However, even if a patient with MH achieves VMA release, without MH closure, PPV is subsequently required to close the MH, which would still be considered a treatment failure. For patients with MH, small diameter MH ($\leq$250 μm) was more likely to get nonsurgical closure (**Figure 5**). Therefore, as recommended by the NICE guidelines, patients with smaller MH may have a higher closure rate.

In this study, we extracted raw data from the included studies providing baseline characteristics of each participant and applied the ROC curves and the AUROCs analysis. By using the IPD of included studies, we estimated the cutoff values and evaluated the performance of these factors as predictors of VMA release after ocriplasmin therapy in a total of 120 patients. Further, the predict ability for female patients with VMA diameter <506 μm and without ERM was 0.84. So, in clinical practice, when we encounter patients with sVMA and consider whether to use ocriplasmin for them, the gender of patient, ERM formation, and VMA diameter were brought into the formula ($P_{Release}$). $P_{Release}$ represents the estimated probability of VMA release. If $P_{Release}$ is more than 0.68, the patient might probably achieve VMAR after with ocriplasmin therapy. We further provided several examples and their $P_{release}$ value in **Supplementary Table 6** for reference. These findings would help doctors about patient selection strategy.

It has been recognized that sVMA may be associated with other conditions such as AMD, DR, or RVO (18, 26, 27). These pathogenic factors may lead to an abnormally strong adhesion between the posterior vitreous cortex and macula. As mentioned earlier, the therapeutic effect of ocriplasmin for secondary VMA may be poorer than that for idiopathic VMA. In this study, we attempted to analyze whether AMD, DR, or RVO may affect the therapeutic effect of ocriplasmin, but a paucity of information on health status of patient in the included studies prevented this analysis.

Several other sVMA treatment modalities exist; observation often being the first approach. Studies report that 11 to 40% of sVMA cases resolve spontaneously (28, 29), with unpredictable timeframes. Moreover, sVMA may lead to anomalies of retinal morphology, being responsible for metamorphopsia or loss of visual acuity, which increases with duration. Previous meta-analyses evaluated VMA treatment by intravitreal gas injections and found VMAR in 84% and MH closure in 59% after perfluoropropane (C_3F_8) gas injection (30) or VMA resolution in 47% of cases with or without associated MH 1 month after the injection C_3F8 or SF_6 (31). Other studies have found VMA release in 36% of eyes treated with air injection (32). Recently, the first RCT for evaluating the safety and efficacy of intravitreal gas (C_3F_8) injection was terminated early because of safety concerns related to retinal detachments and retinal tears (33). So, the safety issue of intravitreal gas injection still requires great attention. More studies are needed to increase understanding of the benefits of different approaches to management of sVMA including observation, PPV, ocriplasmin, and intravitreal gas injections.

A potential limitation of this meta-analysis is that few trials compared different approaches of managing sVMA including PPV, intravitreal gas injection, ocriplasmin, and observation (32, 34, 35). It was, therefore, not possible for us to compare efficacy directly between these strategies. There might introduce some bias in the predict ability in IPD analysis for only based on 5 studies with limited sample size. Also, few studies observed recurrence after ocriplasmin therapy (36). In future studies, attention should be paid to recurrence rates and timeframes in ocriplasmin-induced patients with VMAR. In addition, highly myopic patients with VMA require special attention, since treatment may be challenging in this group (37). Insufficient study to date involves observation and follow-up after ocriplasmin treatment in this group of patients. Most of the existing study has been carried out in Europe and North America and the effects in other regions and races remain unclear. More long-term follow-up data and further analyses are needed to understand therapeutic effects in VMA induced by various etiologies.

CONCLUSION

Evidence from the 5 RCTs and 50 cohort studies included here suggests that ocriplasmin is a suitable approach for treating sVMA. As clinicians, we should be increasingly cognizant of appropriate patient selection for ocriplasmin treatment and should take into account various factors such as MH, ERM, VMA diameter, age, and sex.

DATA AVAILABILITY STATEMENT

The original contributions presented in the study are included in the article/**Supplementary Material**, further inquiries can be directed to the corresponding author/s.

AUTHOR CONTRIBUTIONS

XC contributed to the study design, manuscript writing, literature search, data abstraction, and finalization. ML contributed to the literature review, data abstraction, manuscript writing, and statistical analysis. RY contributed to the literature review and statistical analysis. WW contributed to the manuscript writing and review. YW contributed to the study design, manuscript writing, and review. All authors contributed to the article and approved the submitted version.

FUNDING

This study was supported by the National Natural Science Foundation of China under (Grant Nos. 82101128 and 81870686) and the Beijing Municipal Natural Science Foundation under (Grant No. 7184201). The funders had no role in the design or conduct of the study, collection, management, analysis, or interpretation of the data, preparation, review, or approval of the manuscript, or the decision to submit the manuscript for publication.

ACKNOWLEDGMENTS

We thank Prof Xiaoli Liu from Brigham and Women's Hospital and Harvard Medical School for valuable advice on project design.

SUPPLEMENTARY MATERIAL

The Supplementary Material for this article can be found online at: https://www.frontiersin.org/articles/10.3389/fmed.2021.759311/full#supplementary-material

REFERENCES

1. Mec-Slomska AE, Adamiec-Mroczek J, Kuzmicz E, Misiuk-Hojlo M. Intravitreal ocriplasmin: a breakthrough in the treatment of vitreomacular traction? *Adv Clin Exp Med.* (2017) 26:527–31. doi: 10.17219/acem/62122
2. Chan CK, Crosson JN, Mein CE, Daher N. Pneumatic vitreolysis for relief of vitreomacular traction. *Retina.* (2017) 37:1820–31. doi: 10.1097/IAE.0000000000001448
3. Morescalchi F, Gambicorti E, Duse S, Costagliola C, Semeraro F. From the analysis of pharmacologic vitreolysis to the comprehension of ocriplasmin safety. *Expert Opin Drug Saf.* (2016) 15:1267–78. doi: 10.1080/14740338.2016.1208169
4. Steel DH, Lotery AJ. Idiopathic vitreomacular traction and macular hole: a comprehensive review of pathophysiology, diagnosis, and treatment. *Eye.* (2013) 27 (Suppl. 1):S1–21. doi: 10.1038/eye.2013.212
5. Amoaku W, Cackett P, Tyagi A, Mahmood U, Nosek J, Mennie G, et al. Redesigning services for the management of vitreomacular traction and macular hole. *Eye.* (2014) 28 (Suppl. 1):S1–10. doi: 10.1038/eye.2014.125
6. U.S. Food Drug Administration. *JETREA (ocriplasmin) Intravitreal Injection, 2.5 mg/mL. Prescribing Information*. .S. Food Drug Administration (2012). Available online at: https://www.accessdata.fda.gov/drugsatfda_docs/label/2012/125422s000lbl.pdf (accessed October 17, 2012).
7. U.S. Food and Drug Administration. *JETREA (Ocriplasmin) Summary of Product Characteristics.* U.S. Food and Drug Administration (2018). Available online at: http://www.ema.europa.eu/docs/en_GB/document_library/EPAR_-_Product_Information/human/002381/WC500142158.pdf (accessed October 17, 2012).
8. Stalmans P, Benz MS, Gandorfer A, Kampik A, Girach A, Pakola S, et al. Enzymatic vitreolysis with ocriplasmin for vitreomacular traction and macular holes. *N Engl J Med.* (2012) 367:606–15. doi: 10.1056/NEJMoa1110823
9. Stalmans P, Delaey C, de Smet MD, van Dijkman E, Pakola S. Intravitreal injection of microplasmin for treatment of vitreomacular adhesion: results of a prospective, randomized, sham-controlled phase II trial (the MIVI-IIT trial). *Retina.* (2010) 30:1122–27. doi: 10.1097/IAE.0b013e3181e0970a
10. Dugel PU, Tolentino M, Feiner L, Kozma P, Leroy A. Results of the 2-Year ocriplasmin for treatment for symptomatic vitreomacular adhesion including macular hole (OASIS) randomized trial. *Ophthalmology.* (2016) 123:2232–47. doi: 10.1016/j.ophtha.2016.06.043
11. Steel DHW, Patton N, Stappler T, Karia N, Hoerauf H, Patel N, et al. Ocriplasmin for vitreomacular traction in clinical practice: the inject study. *Retina.* (2020) 41:266–76. doi: 10.1097/IAE.0000000000002862
12. Khanani AM, Duker JS, Heier JS, Kaiser PK, Joondeph BC, Kozma P, et al. Ocriplasmin treatment leads to symptomatic vitreomacular adhesion/vitreomacular traction resolution in the real-world setting: The phase IV ORBIT study. *Ophthalmol Retina.* (2019) 3:32–41. doi: 10.1016/j.oret.2018.07.011
13. Tadayoni R, Holz FG, Zech C, Liu X, Spera C, Stalmans P. Assessment of anatomical and functional outcomes with ocriplasmin treatment in patients with vitreomacular traction with or without macular holes: results of OVIID-1 trial. *Retina.* (2019) 39:2341–52. doi: 10.1097/IAE.0000000000002332
14. Zandi S, Freiberg F, Vaclavik V, Pfister IB, Traine PG, Kaya C, et al. Morphological reconstitution and persistent changes after intravitreal ocriplasmin for vitreomacular traction and macular hole. *J Ocul Pharmacol Ther.* (2020) 36:126–32. doi: 10.1089/jop.2019.0051
15. Jackson TL, Haller J, Blot KH, Duchateau L, Lescrauwaet B. Ocriplasmin for treatment of vitreomacular traction and macular hole: a systematic literature review and individual participant data meta-analysis of randomized, controlled, double-masked trials. *Surv Ophthalmol.* (2021). doi: 10.1016/j.survophthal.2021.08.003. [Online ahead of print].
16. Moher D, Liberati A, Tetzlaff J, Altman DG, Group P. Preferred reporting items for systematic reviews and meta-analyses: the PRISMA statement. *J Clin Epidemiol.* (2009) 62:1006–12. doi: 10.1016/j.jclinepi.2009.06.005
17. Guo B, Moga C, Harstall C, Schopflocher D. A principal component analysis is conducted for a case series quality appraisal checklist. *J Clin Epidemiol.* (2016) 69:199–207.e2. doi: 10.1016/j.jclinepi.2015.07.010
18. Novack RL, Staurenghi G, Girach A, Narendran N, Tolentino M. Safety of intravitreal ocriplasmin for focal vitreomacular adhesion in patients with exudative age-related macular degeneration. *Ophthalmology.* (2015) 122:796–802. doi: 10.1016/j.ophtha.2014.10.006
19. Neffendorf JE, Kirthi V, Pringle E, Jackson TL. Ocriplasmin for symptomatic vitreomacular adhesion. *Cochrane Database Syst Rev.* (2017) 10:CD011874. doi: 10.1002/14651858.CD011874.pub2
20. Mein C, Dugel PU, Feiner L, Drenser K, Miller D, Benz M, et al. Patient-reported visual function from the ocriplasmin for treatment for symptomatic vitreomacular adhesion, including macular hole (OASIS) study. *Retina.* (2020) 40:1331–38. doi: 10.1097/IAE.0000000000002599
21. Varma R, Haller JA, Kaiser PK. Improvement in patient-reported visual function after ocriplasmin for vitreomacular adhesion: results of the microplasmin for intravitreous injection-traction release without surgical treatment (MIVI-TRUST) trials. *JAMA Ophthalmology.* (2015) 133:997–1004. doi: 10.1001/jamaophthalmol.2015.1746
22. Wan Y, Zhao L, Huang C, Xu Y, Sun M, Yang Y, et al. Validation and comparison of the national eye institute visual functioning questionnaire-25 (NEI VFQ-25) and the visual function index-14 (VF-14) in patients with cataracts: a multicentre study. *Acta Ophthalmol.* (2021) 99:e480–8. doi: 10.1111/aos.14606
23. Potic J, Bergin C, Giacuzzo C, Konstantinidis L, Daruich A, Wolfensberger TJ. Application of modified NEI VFQ-25 after retinal detachment to vision-related quality of life. *Retina.* (2021) 41:653–60. doi: 10.1097/IAE.0000000000002894
24. National Institute for Health and Care Excellence. *Final Appraisal Determination—Ocriplasmin for Treating Vitreomacular Traction.* Available online at: https://www.nice.org.uk/guidance/ta297/documents/vitreomacular-traction-ocriplasmin-final-appraisal-determination-document2 (accessed October 23, 2013).
25. Chatziralli I, Theodossiadis G, Xanthopoulou P, Miligkos M, Sivaprasad S, Theodossiadis P. Ocriplasmin use for vitreomacular traction and macular hole: A meta-analysis and comprehensive review on predictive factors for vitreous release and potential complications. *Graefes Arch Clin Exp Ophthalmol.* (2016) 254:1247–56. doi: 10.1007/s00417-016-3363-5
26. Almeida DR, Chin EK. Spontaneous resolution of vitreomacular traction in two patients with diabetic macular edema. *Case Rep Ophthalmol.* (2014) 5:66–71. doi: 10.1159/000360219
27. Waldstein SM, Montuoro A, Podkowinski D, Philip AM, Gerendas BS, Bogunovic H, et al. Evaluating the impact of vitreomacular adhesion on anti-VEGF therapy for retinal vein occlusion using machine learning. *Sci Rep.* (2017) 7:2928. doi: 10.1038/s41598-017-02971-y
28. Theodossiadis GP, Grigoropoulos VG, Theodoropoulou S, Datseris I, Theodossiadis PG. Spontaneous resolution of vitreomacular traction demonstrated by spectral-domain optical coherence tomography. *Am J Ophthalmol.* (2014) 157:842–51.1. doi: 10.1016/j.ajo.2014.01.011

29. John VJ, Flynn HW Jr., Smiddy WE, Carver A, Leonard R, Tabandeh H, et al. Clinical course of vitreomacular adhesion managed by initial observation. *Retina.* (2014) 34:442–46. doi: 10.1097/IAE.0b013e3182a15f8b
30. Yu G, Duguay J, Marra KV, Gautam S, Le Guern G, Begum S, et al. Efficacy and safety of treatment options for vitreomacular traction: a case series and meta-analysis. *Retina.* (2016) 36:1260–70. doi: 10.1097/IAE.0000000000000909
31. Neffendorf JE, Simpson ARH, Steel DHW, Desai R, McHugh DA, Pringle E, et al. Intravitreal gas for symptomatic vitreomacular adhesion: a synthesis of the literature. *Acta Ophthalmologica.* (2018) 96:685–91. doi: 10.1111/aos.13547
32. Gruchociak S, Djerada Z, Afriat M, Chia V, Santorini M, Denoyer A, et al. Comparing intravitreal air and gas for the treatment of vitreomacular traction. *Retina.* (2020) 40:2140–47. doi: 10.1097/IAE.0000000000002733
33. Chan CK, Mein CE, Glassman AR, Beaulieu WT, Calhoun CT, Jaffe GJ, et al. Pneumatic vitreolysis with perfluoropropane for vitreomacular traction with and without macular hole: DRCR retina network protocols AG and AH. *Ophthalmology.* (2021) 128:1592–603. doi: 10.1016/j.ophtha.2021.05.005
34. Scholz P, Sitnilska V, Hess J, Becker M, Michels S, Fauser S. Comparison of resolution of vitreomacular traction after ocriplasmin treatment or vitrectomy. *Retina.* (2019) 39:180–5. doi: 10.1097/IAE.0000000000001926
35. Juncal VR, Chow DR, Vilà N, Kapusta MA, Williams RG, Kherani A, et al. Ocriplasmin versus vitrectomy for the treatment of macular holes. *Can J Ophthalmol.* (2018) 53:441–46. doi: 10.1016/j.jcjo.2018.01.017
36. Katsanos A, Gorgoli K, Asproudis I, Stefaniotou M. Recurrent vitreomacular traction in a patient treated with ocriplasmin: a case report. *Ophthalmol Ther.* (2021) 10:187–92. doi: 10.1007/s40123-020-00316-z
37. Goh LY, Motta L, Jackson TL. Myopic macular hole detachment associated with intravitreal ocriplasmin. *Am J Ophthalmol Case Rep.* (2020) 19:100697. doi: 10.1016/j.ajoc.2020.100697

Conflict of Interest: The authors declare that the research was conducted in the absence of any commercial or financial relationships that could be construed as a potential conflict of interest.

The Reviewer FL declared shared affiliation with the authors to the handling Editor at time of review.

Publisher's Note: All claims expressed in this article are solely those of the authors and do not necessarily represent those of their affiliated organizations, or those of the publisher, the editors and the reviewers. Any product that may be evaluated in this article, or claim that may be made by its manufacturer, is not guaranteed or endorsed by the publisher.

frontiers in Medicine

ORIGINAL RESEARCH
published: 04 February 2022
doi: 10.3389/fmed.2022.809787

Low Serum Vitamin D Is Not Correlated With Myopia in Chinese Children and Adolescents

Xiaoman Li[1†], *Haishuang Lin*[1,2†], *Longfei Jiang*[1], *Xin Chen*[1], *Jie Chen*[1*] *and Fan Lu*[1*]

[1] *The Eye Hospital, School of Ophthalmology and Optometry, Wenzhou Medical University, Wenzhou, China,* [2] *Wenzhou Medical University, Wenzhou, China*

Purpose: This cross-sectional study investigated the association between serum 25-hydroxyvitamin D [25(OH)D] concentration and myopia in two groups of Chinese children aged 6–14 years from different geographic and economic locations.

Methods: A total of 294 children from a lowland area and 89 from a highland area were enrolled as two groups of study subjects. The visual acuity, ocular biometry, and automated refraction were measured. The serum level of 25(OH)D was determined by chemiluminescence immunoassay. Near vision and outdoor exposure durations were assessed with a questionnaire interview. Data were analyzed for differences using Chi-square and Wilcoxon rank sum tests. The risk factors were evaluated using logistic regression analysis.

Results: We found that the serum level of 25(OH)D of the subjects from lowland area was 20.9 ng/mL which was higher than that of subjects from highland area (16.9 ng/mL). The median spherical equivalent refraction (SER) was −0.25 diopters(D) in lowland subjects and −0.63D in highland subjects. The prevalence of myopia was 45.2% in lowland subjects and 55.1% in highland subjects. The average axial length was similar, 23.6 mm and 23.1 mm in lowland and highland subjects, respectively. We found no statistical difference between the average SER and serum 25(OH)D concentration in subjects of either lowland or highland area. The ratio of myopia to non-myopia was also similar in subjects with three levels (sufficient, deficient, and insufficient) of serum 25(OH)D in these two areas.

Conclusions: There is no association between serum 25(OH)D concentration and myopia in the 6–14 years old Chinese children.

Keywords: myopia, serum 25(OH)D, children, lowland, highland

OPEN ACCESS

Edited by:
Menaka Chanu Thounaojam, Augusta University, United States

Reviewed by:
Carla Costa Lanca, Escola Superior de Tecnologia da Saúde de Lisboa (ESTeSL), Portugal
Dong-Hua Yang, St. John's University, United States

***Correspondence:**
Jie Chen
cj@mail.eye.ac.cn
Fan Lu
lufan62@mail.eye.ac.cn

[†] *These authors have contributed equally to this work*

Specialty section:
This article was submitted to Ophthalmology, a section of the journal Frontiers in Medicine

Received: *05 November 2021*
Accepted: *10 January 2022*
Published: *04 February 2022*

Citation:
Li X, Lin H, Jiang L, Chen X, Chen J and Lu F (2022) Low Serum Vitamin D Is Not Correlated With Myopia in Chinese Children and Adolescents. Front. Med. 9:809787. doi: 10.3389/fmed.2022.809787

INTRODUCTION

In the past 10 years, the prevalence of myopia has increased by 23% in East Asians (1). In Chinese children, the prevalence was 51.4% in Anyang (2), 34.9% in Guangzhou (3), 60.9% in Beijing (4) and these numbers are still rising (5). The prevalence of myopia in Haidian District, Beijing, increased from 55.9 to 65.5% from 2005 to 2015 (6). Myopia is now a worldwide public health problem affecting more and more young children (4, 7). However, the reasons for this multifactorial disease and its mechanism are still unclear (8, 9).

More outdoor exposure is known to slow the onset and progression of myopia (9–12). The seasonal effect on the progression of the axial length (AL) in children is confirmed. Increase in AL slows down with longer duration of sunlight exposure and high sunlight intensity (11, 13). Myopia progression is known to be slower in summer than in winter (14, 15). In Tibetan highlands, myopia prevalence is lower than that in lowland areas, presumably attributed to less education pressure, more sunlight exposure and higher sunlight intensity (16). The notion that sunlight exposure prevents myopia progression remains a controversy (17). Dopamine decrease AL growth is the most convincing hypothesis (18, 19), although there is not enough research in humans. A more uniform refraction pattern (20), longer depth of field and fewer high order aberrations (21) in an outdoor visual environment are factors that contribute to a sharper retina image, and these factors might contribute to slower AL growth.

The internal homeostasis of human body, especially serum vitamin D, is closely associated with outdoor activities. Serum vitamin D is composed of vitamin D_3 and vitamin D_2. Vitamin D_3, the main source of vitamin D in the body, is formed in the skin though sunlight exposure. Vitamin D_2 is absorbed through diary intake. Vitamin D_3 and vitamin D_2 are transformed into serum 25-hydroxyvitamin D [25(OH)D_3] and 25(OH)D_2, respectively, in the liver, and the serum level of 25(OH)D is the most reliable indicator of total vitamin D in the body (22).

Previous studies have investigated the relationship between the serum level of Vitamin D and myopia. Choi et al. investigated 2,038 adolescents aged 13 to 18 years old in Korea and found that serum 25(OH)D concentrations were 16.3 ± 0.3 ng/mL in the non-myopia group, 16.4 ± 0.3 ng/mL in the mild-myopia group, 16.0 ± 0.3 ng/mL in the moderate-myopia group, and 15.2 ± 0.4 ng/mL in the high-myopia group ($P = 0.054$) (23). A meta-analysis showed that the myopia group had lower 25(OH)D concentration than the non-myopia group (standard mean difference = −0.27 nmol/L, $P = 0.001$) (24). Researchers showed that lower Vitamin D is associated with increased risk of myopia (25–30). Besides refractive error, the change of AL was also reported in literature. A comprehensive cross-sectional study conducted by Tideman et al. in Netherlands showed that vitamin D was correlated with a longer AL in 6-year-old children (31). However, some of the other studies did not show any correlation between Vitamin D and refractive error (32–35). Hung-Da et al. found that the mean serum 25(OH)D concentrations were similar between the myopic and non-myopic groups (49.7 ± 13.6 and 48.8 ± 14.0 nmol/mL; $P = 0.806$) in 99 children with a mean age of 6.8 years (36). The prevalence of vitamin D deficiency and insufficiency is more than 80% in some age groups in China, a value much higher than those for other countries (37). Vitamin D deficiency in China is commonly seen even in developed regions like Guangzhou and Beijing (37–39). Whether vitamin D concentration, especially a relatively low concentration vitamin D, has an impact on the development of myopia is uncertain.

Vitamin D is generated in the body through light exposure and diary intake. In this study, we selected two groups of subjects from locations with substantially different diets and exposure to sunlight. Our intention was to test whether vitamin D is associated with myopia in these two groups of subjects with different levels of vitamin D concentration.

MATERIALS AND METHODS

Study Population

The study subjects were children aged 6–14 years old in both lowland and highland areas. Lowland subjects were enrolled from the Health Examination Center of the Second Affiliated Hospital of Wenzhou Medical University (WMU) (Sept 2011–Mar 2016). Their counterparts were subjects from the Highland Eye Study conducted in Tibet by the Eye Hospital of WMU (July 2013 to Aug 2013). Their inclusion criteria were: (1) Aged 6–14 years. (2) No metabolic or congenital systemic diseases. (3) No eye diseases, such as cataract, glaucoma, amblyopia, and others. (4) No history of orthokeratology contact lens wear or any other myopia control treatments such as atropine within 3 months. (5) No mental illness. (6) Children and their guardians were able to understand the aim and procedures of the study and sign the informed consent forms. The study was approved by the Ethics Committee of the Eye Hospital of Wenzhou Medical University (KYK[2014]26). Written informed consent was obtained from all subjects prior to participating in the program. The study followed the tenets of the Declaration of Helsinki.

Eye Examinations

Eye exams included slit lamp tests, refraction and biometry. Distance visual acuity was examined with an ETDRS visual chart at 4 m. Slit lamp was used to examine anterior eye structures. Auto-refraction (Topcon RT 8900) was tested several times until the readings of the refractive error became stable and the final reading was recorded. Biometry measurements were tested with Lenstar optical biometry (Lenstar 900). At least three stable tests were obtained and the readings of AL, anterior chamber depth, lens thickness, central corneal thickness, corneal diameter, corneal curvature, corneal astigmatism were recorded. If the subject and his/her guardian agreed to cycloplegia, 1% cyclopentolate hydrochloride would be used twice with a 5 min interval. Among 352 subjects in the lowland groups, 294 subjects (83.5%) who underwent cycloplegic refraction were included in the study. Subjects in the highland groups did not undergo cycloplegic refraction.

Blood Sample Collection and Vitamin D Detection

Three milliliter- fast blood sample was drawn and kept away from light for 30 min, then centrifuged (3,000 r/min) for 10 min. The blood serum was separated and frozen at −80°C refrigerator for 25(OH) D detection. Total vitamin D assay kit (SIMENS,100T) was used to detect 25(OH)D through the automatic chemiluminescence immunoassay analyzer Chemiluminescence (SIMENS, ADVIA Centaur XP, IRL26391136).

Questionnaire Interview

Demographic information, near vision duration, and outdoor duration were sought in the questionnaire. Near vision and

TABLE 1 | Demographic information of subjects in lowland and highland area*.

	Total			Lowland			Highland		
	Lowland (*n* = 294)	**Highland (*n* = 89)**	***P***	**Non-myopia (*n* = 161)**	**Myopia (*n* = 133)**	***P***	**Non-myopia (*n* = 40)**	**Myopia (*n* = 49)**	***P***
Age (year)	9.4 (3.3)	12.0 (3.0)	<0.001	8.5 (2.7)	10.6 (2.7)	<0.001	12.0 (3.0)	13.0 (4.0)	0.456
Gender, *n* (%)									
Boys	183 (62.2)	38 (42.7)	<0.001	102 (63.4)	81 (60.9)	0.378	16 (40.0)	22 (44.9)	0.826
Girls	111 (37.8)	51 (57.3)		59 (36.6)	52 (39.1)		24 (60.0)	27 (55.1)	
BMI (kg/m^2)	17.4 (6.1)	16.7 (3.6)	0.010	17.4 (5.9)	17.4 (7.4)	0.664	17.1 (3.1)	16.4 (4.9)	0.488
Outdoor time (h/w)	6.2 (5.9)	14.0 (7.0)	<0.001	6.6 (6.2)	5.5 (5.5)	0.009	–	–	
Near vision time (h/w)	16.6 (14.6)	28.0 (17.5)	<0.001	15.4 (13.8)	18.0 (15.3)	0.010	–	–	
25(OH)D (ng/mL)	20.9 (11.6)	16.9 (6.5)	<0.001	19.6 (12.2)	22.5 (11.2)	0.878	17.6 (8.8)	16.7(6.6)	0.216
Sufficient, *n* (%)	56 (19.0)	3 (3.4)	<0.001	33 (20.5)	23 (17.3)	0.158	1 (2.5)	2 (4.1)	0.295†
Insufficient, *n* (%)	100 (34.0)	22 (24.7)		47 (29.2)	53 (39.8)		13 (32.5)	9 (18.4)	
Deficient, *n* (%)	138 (46.9)	64 (71.9)		81 (50.3)	57 (42.9)		26 (65.0)	38 (77.6)	
SER(D)	−0.25 (1.7)	−0.63 (3.1)	0.163	0.25 (0.5)	−1.6 (1.9)	–	0.25 (1.3)	−2.5 (3.4)	–
Myopia, *n* (%)	133 (45.2)	49 (55.1)	0.066	–	–		–	–	
Non-myopia, *n* (%)	161 (54.8)	40 (44.9)		–	–		–	–	
AL (mm)	23.6 (1.3)			23.2 (1.0)	24.2 (1.1)	<0.001			

**Median (interquartile range) was used to describe continuous variables. Chi-square test was used in classification variable comparisons. Wilcoxon rank sum test was used in continuous variable comparisons.*

† Fisher's exact test.

outdoor duration were recorded for 3 conditions: on weekdays, during weekends and during summer/winter vacation.

Definitions

Myopia was defined as non-cycloplegic spherical equivalent refraction (SER) ≤-0.50 diopters(D) (40). Serum 25(OH)D concentration higher or equal to 30 ng/mL was defined as a sufficient level. Concentrations less or equal to 20 ng/mL were defined as deficient serum 25(OH)D and the concentrations between these extremes were defined as insufficient serum 25(OH)D (41).

Quality Control

Procedures for testing the subjects from both lowland and highland areas followed the same protocol. Questionnaire interviews were conducted by investigators who had good communication skills, knew local dialect and received training by the supervisors (CJ, LF) before the project began. A prior test was conducted to adjust improper procedures. The 25(OH)D detection was conducted by professional laboratory staff of the Eye Hospital of WMU.

Statistical Analysis

SER, 25(OH)D, AL and age were described as median (interquartile range) and Wilcoxon *t*-test was used for comparisons. Chi-square test and Fisher exact test were used for classical variables. A multivariable logistic regression model was constructed to assess the association between myopia and 25(OH)D concentration and adjusting for age, gender, and other covariates identified as being significant in univariable analysis. $P < 0.05$ was considered as statistically significant. Because SER and AL of both eyes were highly correlated, only data of the right eye was used in the analysis. Epidata (version 3.1.2701.2008, Chinese) was used for double-blinded data entry. SPSS (version 22.0, Chinese) was used for analysis.

RESULTS

Demographic Information and Myopia

A total of 383 subjects were enrolled in this analysis, including 294 lowland and 89 highland subjects. Compared with the lowland subjects, highland subjects were about 3 years older (12 vs. 9, $P < 0.001$), more girls (57.3 vs. 37.8%, $P < 0.001$), with lower BMI (16.7 vs. 17.4, $P = 0.010$), had longer duration for both near vision (28.0 vs. 16.6 h/w, $P < 0.001$) and outdoor activities (14.0 vs. 6.2 h/w, $P < 0.001$; **Table 1**). The median SER was −0.25 D in lowland subjects and −0.63 D in highland subjects ($P = 0.163$). Lowland myopia subjects were 2 years older than non-myopia subjects, with shorter outdoor duration (5.5 vs. 6.6 h/w, $P = 0.009$) and longer near vision duration (15.4 vs. 18.0 h/w, $P = 0.010$). Highland myopia subjects were 1 year older than non-myopia subjects, and their near vision and outdoor duration were similar. The AL of myopia subjects was 24.2 and 23.2 mm in non-myopia subjects in the lowland area (**Table 1**).

Relationships Between Serum 25(OH)D and Myopia

The serum level of 25(OH)D in highland subjects was lower than that in lowland subjects (16.9 vs. 20.9 ng/mL, $P < 0.001$) and the rate of deficiency in highland group was higher than that in the lowland group (71.9 vs. 46.9%, **Table 1**). We found no difference in serum 25(OH)D concentration between myopia

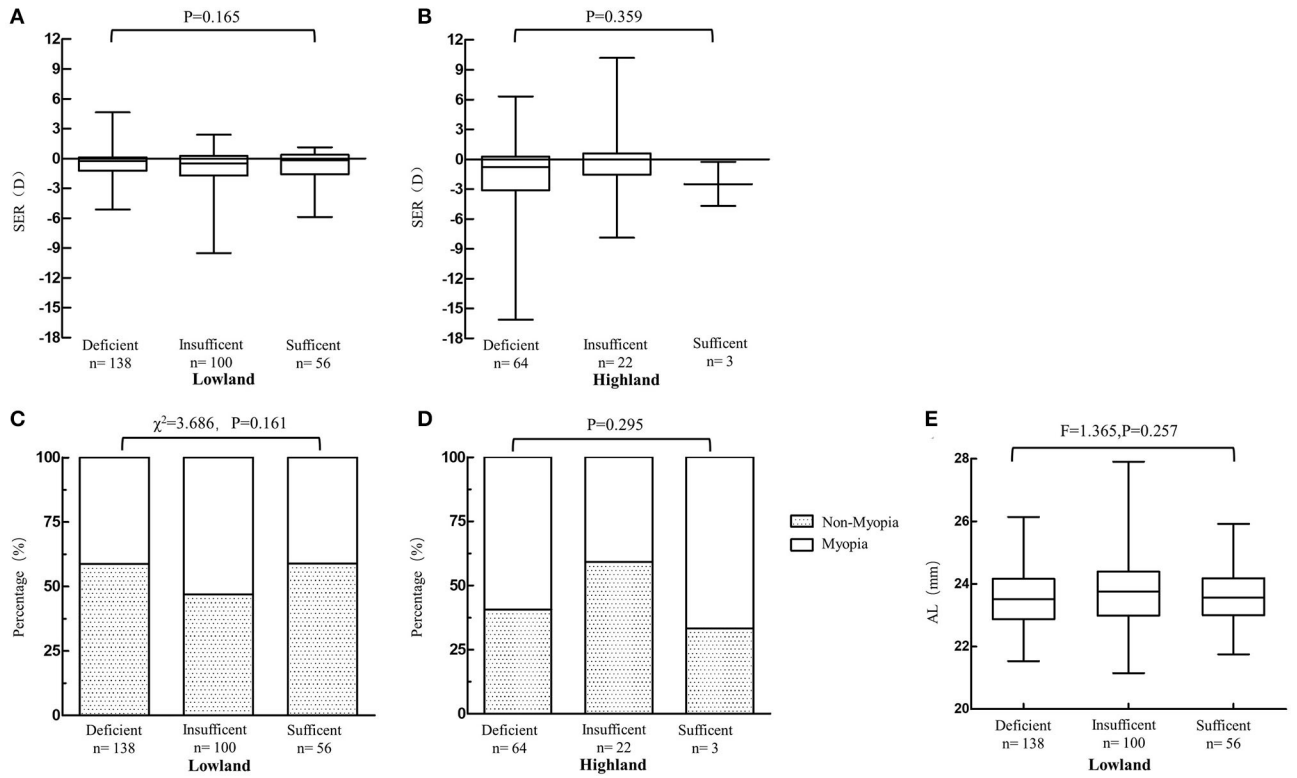

FIGURE 1 | Myopia related parameters among groups with different serum vitamin D [25(OH)D] concentration in both areas. **(A,B)** Average SER among groups with different serum vitamin D concentration in both areas (Wilcoxon rank sum test). **(C,D)** Percentage of myopia and non-myopia among groups with different serum vitamin D concentration in both areas (Lowland: Chi-square test; Highland: Fisher exact test). **(E)** Axial length among groups with different serum vitamin D concentration in lowland subjects (Wilcoxon rank sum test).

TABLE 2 | Multiple logistic regression of the myopia risk factors in lowland and highland area.

Factors	Lowland†		Highland‡		Total§	
	OR (95%CI)	***P***	**OR (95%CI)**	***P***	**OR (95%CI)**	***P***
Age (year)	**1.72 (1.46–2.03)**	**<0.001**	1.13 (0.90–1.41)	0.306	**1.55 (1.36–1.76)**	**<0.001**
Gender						
Boys	Reference		Reference		Reference	
Girls	1.30 (0.73–2.32)	0.373	1.02 (0.39–2.65)	0.969	1.20 (0.75–1.91)	0.456
BMI (kg/m^2)	0.94 (0.88–1.00)	0.066	0.90 (0.76–1.06)	0.208	**0.94 (0.88–0.99)**	**0.029**
25(OH)D (ng/mL)	1.01 (0.98–1.04)	0.706	0.94 (0.87–1.02)	0.141	0.99 (0.97–1.02)	0.676
Outdoor time (h/w)	0.95 (0.90–1.01)	0.120	–	–	–	–
Near vision time (h/w)	1.02 (0.99–1.04)	0.273	–	–	–	–
Region						
Highland	–	–	–	–	Reference	
Lowland	–	–	–	–	**2.13 (1.10–4.15)**	**0.026**

OR with statistically significance were listed in bold.
†Adjustment for age, gender, BMI, outdoor time and near vision time.
‡Adjustment for age, gender, and BMI.
§Adjustment for age, gender, BMI and region.

TABLE 3 | Children's vitamin D level in different regions of China.

Year	Region	Age	Detection method	Detection rate of Sufficiency %	Mean ± SD (ng/mL)
2011–2013	Guangzhou (37)	0–14	ELISA†	36.6	28.3 ± 8.4
		7–14		11.5	23.0 ± 5.9
2012–2013	Beijing (39)	0–14	MS-MS‡	12.9	22.1 ± 8.5
2017	Jiaxing of Zhejiang (43)	3–6	MS-MS	–	23.0 ± 7.7
2013	Shaoxing of Zhejing (44)	0–9	CLIA§	45.8	29.8 ± 12.8
2017	Shanxi (45)	9–16	CLIA	34.6	18.0 ± 6.4
2012	Guangxi (46)	6–13	ELISA	22.5	22.9 ± 0.4
2017–2018	Mianyang of Sichuan (47)	0–8	MS-MS	17.1	18.6
2016	Shenmu of Shanxi (48)	0–14	ELISA	14.8	13.3 ± 6.0
2015–2016	Heilongjiang (49)	0–6	MS-MS	–	24.2 ± 10.0
2011–2016	Wenzhou of Zhejiang*	6–14	CLIA	19.0	22.3 ± 8.9
2013	Tibetan Highland*	6–14	CLIA	3.37	18.2 ± 6.0

†*ELISA stands for enzyme-linked immunosorbent assay.*
‡*MS-MS stands for tandem mass spectrometry.*
§*CLIA stands for chemiluminescence immunoassay.*
**Children in our study.*

subjects and non-myopia subjects in either lowland or highland areas (lowland: 19.6 vs. 22.5, $P = 0.878$; highland:17.6 vs. 16.7, $P = 0.216$). There was no statistical difference in the percentage of subjects with sufficient, insufficient or deficient 25(OH)D in both myopia and non-myopia groups in both areas (lowland: $P = 0.158$, highland: $P = 0.295$) (**Table 1**). The average SER was similar among subjects with different levels of 25(OH)D concentrations in both areas (**Figure 1A**). The percentage of myopia and non-myopia also showed no difference among the three levels of 25(OH)D of subjects in either location (**Figure 1B**). When refractive error was considered in terms of AL, no significant difference was found. The results were the same in the lowland area ($F = 1.365$, $P = 0.257$) (**Figure 1C**). We obtained AL measurements for only 13 subjects in the highland group and only three subjects showed 25(OH)D higher than 30 ng/ml. The medians (interquartile) of AL in the deficient group ($n = 8$) and the insufficient group ($n = 4$) were 22.8(1.17) and 23.4(1.19) respectively ($P = 0.214$).

Multiple logistic regression analysis revealed that the serum level of 25(OH)D was not significantly associated with myopia in either lowland area ($P = 0.706$) or highland area ($P = 0.141$) after adjusting age, body mass index (BMI) and gender (**Table 2**). Older age (odds ratio [OR]: 1.72; 95% confident interval [CI]: 1.46, 2.03) was an independent risk factor for myopia in lowland subjects. A higher BMI [OR(95%CI = 0.94(0.88, 1.00)] seems to be a protective factor for myopia. For the highland subjects, none of the factors mentioned above was statistically significant in multiple logistic regression analysis. The results were similar to the lowland group when all subjects were included. Older age [OR(95%CI) = 1.55(1.36–1.76)] and living in lowland area [OR(95%CI) = 2.13(1.10, 4.15)] were independent risk factors of myopia after adjustment, whereas higher BMI [OR(95%CI) = 0.94(0.88, 0.99)] was independent protective factor (**Table 2**).

The SER of lowland subjects before and after cycloplegia was −0.78 ± 1.68D and −0.26 ± 1.85D, respectively, a difference of about a 0.5D. In order to know whether cycloplegia could affect the accuracy of these results, we conducted the same analysis using cycloplegic refraction data for our lowland group. Results were similar as using non-cycloplegic SER. These results demonstrated that non-cycloplegia had no confounding effect on the regression models.

DISCUSSION

The results in our study revealed that the serum vitamin D concentration does not show any protective effect toward myopia. Outdoor exposure is one of the protective factors of myopia, but its mechanism is controversial (17). One hypothesis is that vitamin D prevents myopia progression because the body synthesizes more vitamin D when outdoor exposure to sunlight increases (26). Our study involved subjects from a relatively high vitamin D concentration area and a relatively low vitamin D concentration area, yet results showed that serum vitamin D was not associated with either myopia or AL. The results of our study was similar to previous studies such as meta-analyses and prospective cohort studies (33–35). Neither vitamin D_3 which formed from sunlight in the skin nor vitamin D_2 from diary intake correlated with myopia, however, serum level of vitamin D was positively correlated with outdoor duration. There were also opposite results showing that subjects with higher vitamin D had shorter AL or positive SER (24, 31, 42).

In this study, the incidence of insufficient and deficient serum vitamin D of children was similar to or higher than that found in other studies (**Table 3**) (38, 39, 43–48). Serum vitamin D was 20.9 ng/mL in lowland subjects and 16.9 ng/mL in highland subjects. Only 19.0 and 3.4% of these subjects had optimal vitamin D level in lowland and highland areas, respectively. Thus, whether serum vitamin D didn't show its protective effect on myopia because of a relatively low concentration is worth to thinking about. To fully consider this possibility, two locations were chosen to understand the relationship between myopia and vitamin D. Subjects in highland areas came from Seda, Litang and Rangtang, small towns in the Tibetan highland, Sichuan, where both daily sunlight duration and sunlight intensity are higher than that of lowland area (**Table 4**). And serum vitamin D was not related to SER nor AL in either area. This result indicated

TABLE 4 | Comparisons of regional characteristics of lowland and highland area.

Characteristics	Lowland	Highland
Location	Southeast of Zhejiang Province, China. Lowland area.	Northwestern of Sichuan Province, Tibetan Plateau in Southwest China.
Altitude	10 meters.	More than 3,300 meters.
Climate	Central Asian tropical monsoon climate zone, with four distinct seasons and abundant rainfall.	Continental plateau monsoon type. No summer. Frost and snow occur in fourth seasons, and the atmospheric oxygen content is <60% of the standard.
Sunshine	Annual sunshine between 1,442 and 2,264 h.	Average annual sunshine about 2,451.1 h.
Time of sunrise and sunset		
Summer solstice	Sunrise at 5:01 sunset at 18:56.	Sunrise at 6:12 sunset at 20:28.
Winter solstice	Sunrise at 6:44 sunset at 17:06.	Sunrise at 8:16 sunset at 18:18.
Temperature	Annual average temperature is 17.3–19.4°C. Average temperature in January is 4.9–9.9°C. Average temperature in July is 26.7–29.6°C.	Annual average temperature is −0.16°C. Average temperature in January is −11.1°C. Average temperature in July is 9.9°C.
Rainfall	Annual precipitation between 1,113 and 2,494 mm. Raining season comes at the end of spring and early summer. Tropical cyclone happens between July and September. Frost-free period is 241–232 days.	Average precipitation 65.4 mm, and mostly happens during June to September. Average frost-free period is 21 days. Areas with higher altitude has no absolute frost-free period.

that maybe for Chinese children, serum vitamin D concentration does not show any association with myopia.

Although average daily sunshine duration is longer, the light intensity is higher in highland area, and highland subjects spent more time outdoors, their average total vitamin D level was lower than that in lowland subjects which was quite surprising. This phenomenon might be due to an increase in the amount of skin pigment and Tibetan robes covering most of the skin of the body, that may result in an increase in the sun-protection permitting less of the UVB radiation to reach the epidermal cells, and reduce cutaneous production of vitamin D3 (50). In addition, it is speculated that rare vitamin D_2 from daily intake may also contribute to the lower total vitamin D level of highland subjects. The three highland area are all National-level Poor Counties in China. Residents living here mainly live on Zanba (made of a cereal power specially seen in Tibetan highland areas), milk tea, handmade yogurt and yak meat. These foods comprise 90% of their daily intake, and deep sea fish and animal viscera are very uncommon in their diet. Tibetan Buddhism is a prevailing religion in Tibetan highland areas and many of the residents are vegetarians who do not eat yak meat. Our lowland area was Wenzhou city, a coastal city with abundant rainfall in eastern China (**Table 4**). Subjects of Wenzhou came from a health examination center and patients with any health problems were excluded from participation. The average family income of these Wenzhou children was higher than the per capita income of urban residents in Wenzhou in 2016 (51). The mean BMI was higher in these lowland subjects than highland counterparts (17.4 vs. 16.7, $P = 0.010$, **Table 1**). It could be speculated that the nutritional status of the subjects in the lowland area were better than those of their highland peers. These two reasons may explain why serum vitamin D was lower in highland subjects.

The prevalence of myopia in China is reported to be lower in Tibetan highland areas than lowland areas (52). The reason why myopia rate in the highland area was higher than lowland area may be because of age. The subjects in our highland areas are on average 3 years older than lowland subject. Age as a contributing factor of myopia must be considered in the group comparisons. The lowland subjects with an average age of 9 years old probably were in the third grade. The highland subjects with an average age of 12 years old were probably in the sixth grade. The myopia of grade 6 students was about 65% in lowland areas (53), which is much higher than the highland results in this study.

Duration of near vision and outdoor activity did not show a relationship with myopia compared with results from previous studies. Perhaps this is because of our highly selected samples. Lowland subjects were recruited from a health examination center where 74.2% of them were studying in downtown schools or key elementary schools, schools that demanded more homework and extracurricular tutoring. Most highland subjects were Buddhists in a Buddhist college with daily intensive reading courses. From **Supplementary Figure**, the distributions of both near vision and outdoor duration show high kurtosis and skewness. A significant correlation with myopia is difficult to obtain given the small sample size. Literatures reported that outdoor time is not significant risk to myopia. And the explanation is that the outdoor time per day was far <2 h/day and could not show its protecting effect (54, 55). This was exactly the fact in this study.

The merits of our study were the selection of subjects from two regions with significant contrasts, taking sunlight exposure and diary intake into account, and both refraction and AL were measured. The limitations were that the sample in our highland group was not large enough. A validated sun exposure questionnaire was not used to account for factors such as sun cream used and clothing worn. There are many other environmental and economical difference between lowland and highland areas that may impact the prevalence of myopia and should be considered in future studies. Compared to highland area, lowland area was risk toward myopia in this study. This maybe because subjects on the highland areas were from rural areas, the multi-effect of education pressure and modern urbanization affected the progression of myopia (52, 56, 57).

In summary, the total serum vitamin D concentration has no significant effect on myopia in Chinese children and adolescents. The mechanism of outdoor exposure affecting the progression of myopia should be further explored.

DATA AVAILABILITY STATEMENT

The original contributions presented in the study are included in the article/**Supplementary Material**, further inquiries can be directed to the corresponding authors.

ETHICS STATEMENT

The studies involving human participants were reviewed and approved by Ethics Committee of the Eye Hospital of Wenzhou Medical University. Written informed consent to participate in this study was provided by the participants' legal guardian/next of kin.

AUTHOR CONTRIBUTIONS

XL contributed to the formal analysis and original draft writing. HL contributed to the investigation, formal analysis, validation, and data curation. LJ contributed to the data collection. XC contributed to the investigation. JC contributed to the investigation, resources, and draft revision. FL contributed to supervision, methodology, funding acquisition, and draft revision. All authors contributed to the article and approved the submitted version.

FUNDING

This study was funded by the National Key Research and Development Program of China (2020YFC2008200), the Natural Science Foundation of China (Grant No. 81570880), and the Wenzhou Science and Technology Bureau Basic Research Funding (Grant No. Y20190166).

ACKNOWLEDGMENTS

The authors would like to thank Peining Liu for nutrition study part and transfer subjects. The authors would also like to thank Prof. Frank Thorn and Prof. Alan Johnston for his advices in writing this article.

SUPPLEMENTARY MATERIAL

The Supplementary Material for this article can be found online at: https://www.frontiersin.org/articles/10.3389/fmed.2022.809787/full#supplementary-material

Supplementary Figure | The distribution of near vision time and outdoor time. **(A)** The distribution of near vision time in lowland area. **(B)** The distribution of near vision time in highland area. **(C)** The distribution of outdoor time in lowland area. **(D)** The distribution of outdoor time in highland area.

REFERENCES

1. Ngo CS, Pan CW, Finkelstein EA, Lee CF, Wong IB, Ong J, et al. A cluster randomised controlled trial evaluating an incentive-based outdoor physical activity programme to increase outdoor time and prevent myopia in children. *Ophthalmic Physiol Opt.* (2014) 34:362–8. doi: 10.1111/opo.12112
2. Sun YY, Li SM, Li SY, Kang MT, Liu LR, Meng B, et al. Effect of uncorrection versus full correction on myopia progression in 12-year-old children. *Graefes Arch Clin Exp Ophthalmol.* (2016) 255:1–7. doi: 10.1007/s00417-016-3529-1
3. Zhou Z, Morgan IG, Chen Q, Jin L, He M, Congdon N. Disordered sleep and myopia risk among Chinese children. *PLoS ONE.* (2015) 10:e0121796. doi: 10.1371/journal.pone.0121796
4. Guo Y, Duan JL, Liu LJ, Sun Y, Tang P, Lv YY, et al. High myopia in greater Beijing school children in 2016. *PLoS ONE.* (2017) 12:e0187396. doi: 10.1371/journal.pone.0187396
5. Zhai LL, Wu XY, Xu SJ, Wan UH, Zhang SC, Xu L, et al. Study on relationship between outdoor activities and self-reported myopia among middle school students. *Chin J Prevent Med.* (2017) 51:801–6. doi: 10.3760/cma.j.issn.0253-9624.2017.09.006
6. Yan L, Jia L, Qi P. The increasing prevalence of myopia in junior high school students in the Haidian District of Beijing, China: a 10-year population-based survey. *BMC Ophthalmol.* (2017) 17:88. doi: 10.1186/s12886-017-0483-6
7. Ma Y, Qu X, Zhu X, Xu X, Zhu J, Sankaridurg P, et al. Age-specific prevalence of visual impairment and refractive error in children aged 3-10 years in Shanghai, China. *Invest Ophthalmol Visual Sci.* (2016) 57:6188. doi: 10.1167/iovs.16-20243
8. Flitcroft DI, Loughman J, Wildsoet CF, Williams C, Guggenheim JA, for the CC. Novel Myopia genes and pathways identified from Syndromic forms of myopia. *Invest Ophthalmol Vis Sci.* (2018) 59:338–48. doi: 10.1167/iovs.17-22173
9. Wu PC, Tsai CL, Wu HL, Yang YH, Kuo HK. Outdoor activity during class recess reduces myopia onset and progression in school children. *Ophthalmology.* (2013) 120:1080–5. doi: 10.1016/j.ophtha.2012.11.009
10. Jin JX, Hua WJ, Jiang X, Wu XY, Yang JW, Gao GP, et al. Effect of outdoor activity on myopia onset and progression in school-aged children in northeast china: the sujiatun eye care study. *BMC Ophthalmol.* (2015) 15:73. doi: 10.1186/s12886-015-0052-9
11. Cui D, Trier K, Munk Ribel-Madsen S. Effect of day length on eye growth, myopia progression, and change of corneal power in myopic children. *Ophthalmology.* (2013) 120:1074–9. doi: 10.1016/j.ophtha.2012.10.022
12. Kearney S, O'Donoghue L, Pourshahidi LK, Richardson P, Laird E, Healy M, et al. Conjunctival ultraviolet autofluorescence area, but not intensity, is associated with myopia. *Clin Exp Optom.* (2019) 102:43–50. doi: 10.1111/cxo.12825
13. Read SA, Collins MJ, Vincent SJ. Light exposure and physical activity in myopic and emmetropic children. *Optom Vis Sci.* (2014) 91:330–41. doi: 10.1097/OPX.0000000000000160
14. Rusnak S, Salcman V, Hecova L, Kasl Z. Myopia progression risk: seasonal and lifestyle variations in axial length growth in Czech children. *J Ophthalmol.* (2018) 2018:5076454. doi: 10.1155/2018/5076454
15. Donovan L, Sankaridurg P, Ho A, Chen X, Lin Z, Thomas V, et al. Myopia progression in Chinese children is slower in summer than in winter. *Optom Vis Sci.* (2012) 89:1196–202. doi: 10.1097/OPX.0b013e3182640996
16. Qian X, Liu B, Wang J, Wei N, Qi X, Li X, et al. Prevalence of refractive errors in Tibetan adolescents. *BMC Ophthalmol.* (2018) 18:118. doi: 10.1186/s12886-018-0780-8
17. Ngo C, Saw SM, Dharani R, Flitcroft I. Does sunlight. (bright lights) explain the protective effects of outdoor activity against myopia? *Ophthalmic Physiol Opt.* (2013) 33:368–72. doi: 10.1111/opo.12051
18. Zhou X, Pardue MT, Iuvone PM, Qu J. Dopamine signaling and myopia development: what are the key challenges. *Prog Retin Eye Res.* (2017) 61:60–71. doi: 10.1016/j.preteyeres.2017.06.003
19. Feldkaemper M, Schaeffel F. An updated view on the role of dopamine in myopia. *Exp Eye Res.* (2013) 114:106–19. doi: 10.1016/j.exer.2013.02.007
20. Flitcroft DI. The complex interactions of retinal, optical and environmental factors in myopia aetiology. *Progr Retinal Eye Res.* (2012) 31:622–60. doi: 10.1016/j.preteyeres.2012.06.004
21. Ramamurthy D, Lin Chua SY, Saw SM. A review of environmental risk factors for myopia during early life, childhood and adolescence. *Clin Exp Optom.* (2015) 98:497–506. doi: 10.1111/cxo.12346

22. Holick MF. Vitamin D deficiency. *N Engl J Med*. (2007) 357:266–81. doi: 10.1056/NEJMra070553
23. Choi JA, Han K, Park Y-M, La TY. Low serum 25-Hydroxyvitamin D is associated with myopia in Korean adolescents. *Invest Opthalmol Visual Sci*. (2014) 55:2041. doi: 10.1167/iovs.13-12853
24. Tang SM, Lau T, Rong SS, Yazar S, Chen LJ, Mackey DA, et al. Vitamin D and its pathway genes in myopia: systematic review and meta-analysis. *Br J Ophthalmol*. (2019) 103:8–17. doi: 10.1136/bjophthalmol-2018-312159
25. Kwon JW, Choi JA, La TY, Epidemiologic survey committee of the Korean ophthalmological S. Serum 25-hydroxyvitamin D level is associated with myopia in the Korea national health and nutrition examination survey. *Medicine*. (2016) 95:e5012. doi: 10.1097/MD.0000000000005012
26. Laval J. Vitamin D and myopia. *Arch Ophthalmol*. (1938) 19:612. doi: 10.1001/archopht.1938.00850160138010
27. Mutti DO, Marks AR. Blood levels of vitamin D in teens and young adults with myopia. *Optom Vis Sci*. (2011) 88:377–82. doi: 10.1097/OPX.0b013e31820b0385
28. Jung BJ, Jee D. Association between serum 25-hydroxyvitamin D levels and myopia in general Korean adults. *Indian J Ophthalmol*. (2020) 68:15–22. doi: 10.4103/ijo.IJO_760_19
29. Lingham G, Mackey DA, Zhu K, Lucas RM, Black LJ, Oddy WH, et al. Time spent outdoors through childhood and adolescence - assessed by 25-hydroxyvitamin D concentration - and risk of myopia at 20 years. *Acta Ophthalmol*. (2021) 99:679–87. doi: 10.1111/aos.14709
30. Gao F, Li P, Liu YQ, Chen Y. Association study of the serum 25(OH)D concentration and myopia in Chinese children. *Medicine*. (2021) 100:e26570. doi: 10.1097/MD.0000000000026570
31. Tideman JW, Polling JR, Voortman T, Jaddoe VW, Uitterlinden AG, Hofman A, et al. Low serum vitamin D is associated with axial length and risk of myopia in young children. *Eur J Epidemiol*. (2016) 31:491–9. doi: 10.1007/s10654-016-0128-8
32. Lingham G, Yazar S, Lucas RM, Walsh JP, Zhu K, Hunter M, et al. Low 25-hydroxyvitamin D concentration is not associated with refractive error in middle-aged and older Western Australian adults. *Transl Vision Sci Tech*. (2019) 8:13. doi: 10.1167/tvst.8.1.13
33. Williams KM, Bentham GC, Young IS, McGinty A, McKay GJ, Hogg R, et al. Association between myopia, ultraviolet b radiation exposure, serum vitamin D concentrations, and genetic polymorphisms in vitamin D metabolic pathways in a multicountry European study. *JAMA Ophthalmol*. (2017) 135:47–53. doi: 10.1001/jamaophthalmol.2016.4752
34. Guggenheim JA, Williams C, Northstone K, Howe LD, Tilling K, St Pourcain B, et al. Does vitamin D mediate the protective effects of time outdoors on myopia? Findings from a prospective birth cohort. *Invest Ophthalmol Vis Sci*. (2014) 55:8550–8. doi: 10.1167/iovs.14-15839
35. Cuellar-Partida G, Williams KM, Yazar S, Guggenheim JA, Hewitt AW, Williams C, et al. Genetically low vitamin D concentrations and myopic refractive error: a Mendelian randomization study. *Int J Epidemiol*. (2017) 46:1882–90. doi: 10.1093/ije/dyx068
36. Chou HD, Yao TC, Huang YS, Huang CY, Yang ML, Sun MH, et al. Myopia in school-aged children with preterm birth: the roles of time spent outdoors and serum vitamin D. *Br J Ophthalmol*. (2021) 105:468–72. doi: 10.1136/bjophthalmol-2019-315663
37. Zhang PP, Li YT, Li XF, Li ZB, Chen ZG. Analysis of 25-hydroxy vitamin D levels in children aged 0 to 14 years old in Guangzhou city. *Chin J Child Health Care*. (2014) 22:856–9. doi: 10.11852/zgetbjzz2014-22-08-23
38. Sheng XY. Epidemiological data on vitamin D and calcium nutrition in Chinese children. *Chin J Practical Pediatr*. (2012) 27:180–2.
39. Wang H, Lan CZ, Ma SJ, Bi YW, Luo S. Leves of vitamin A and 2 5-OH vitamin D in children in Beijing. *Chin J Microcirculation*. (2014) 2014:48–51.
40. Morgan IG, Ohno-Matsui K, Saw SM. Myopia. *Lancet*. (2012) 379:1739–48. doi: 10.1016/S0140-6736(12)60272-4
41. Ganmaa D, Uyanga B, Zhou X, Gantsetseg G, Delgerekh B, Enkhmaa D, et al. Vitamin D supplements for prevention of tuberculosis infection and disease. *N Engl J Med*. (2020) 383:359–68. doi: 10.1056/NEJMoa1915176
42. Shen L, Yang CH. Serum levels of vitamin D in children with myopia. *Chin J Ophthalmol Otorhinolaryngol*. (2015) 15:94–7. doi: 10.14166/j.issn.1671-2420.2015.02.005
43. Tang HM, Sun XY, Wang F, Xiao X, Gu YY. Serum vitamin A, D and E levels in children aged 3-6 years. *J Prevent Med*. (2018) 30:1116–9. doi: 10.19485/j.cnki.issn2096-5087.2018.11.009
44. Zhang JW, Wang ZY. An investigation on 25 -hydroxyvitamin D level among children aged 0–9 years. *Zhejiang J Prevent Med*. (2015) 27:229–31.
45. Yan YQ, Li YH, Bai ZH, Wang J, Zhang H, Dong JP, et al. Analysis of vitamin D status in 353 children and adolescents aged 9–16. *Chin Remedies Clin*. (2018) 18:1911–3. doi: 10.11655/zgywylc2018.11.014
46. Jiang YY, Tang ZZ, Su B. Relation between vitamin D status and growth in school children. *J Appl Prevent Med*. (2013) 19:135–7. doi: 10.3969/j.issn.1673-758X.2013.03.004
47. Shi R. Investigation on serum 25-hydroxyvitamin D3 and vitamin E levels of children less than 8 years old in Mianyang. *J Front Med*. (2018) 8:56–7. doi: 10.3969/j.issn.2095-1752.2018.32.035
48. Liu J, Liu YL. Analysis of the levels of serum 25-hydroxy vitamin D in autumn and winter among children of Shenmu city,Shaanxi province. *Chin J Primary Med Pharmacy*. (2019) 26:279–81. doi: 10.3760/cma.j.issn.1008-6706.2019.03.007
49. Wang LM, Zhang XL, Wang WJ, Wang HY, Huo MX, Yuan XH, YuanBY. Levels of serum vitamin A,25-hydroxyvitamin D and vitamin E of children under 6 years old in Jiamusi. *Lab Med*. (2017) 32:276–9. doi: 10.3969/j.issn.1673-8640.2017.04.007
50. Wacker M, Holick MF. Sunlight and Vitamin D: a global perspective for health. *Dermato-Endocrinol*. (2013) 5:51–108. doi: 10.4161/derm.24494
51. Lin HS, Zhou H, Li XM, Jiang LF, Li KK, Lin Z, et al. The distribution of astigmatism in children and adolescents in wenzhou area and risk factor analysis. *Chin J Optometr Ophthalmol Visual Sci*. (2017) 19:369–75. doi: 10.3760/cma.j.issn.1674-845X.2017.06.010
52. Lee YY, Lo CT, Sheu SJ, Lin JL. What factors are associated with myopia in young adults? A survey study in Taiwan Military Conscripts. *Invest Ophthalmol Vis Sci*. (2013) 54:1026–33. doi: 10.1167/iovs.12-10480
53. Xu L, Zhuang Y, Zhang G, Ma Y, Yuan J, Tu C, et al. Design, methodology, and baseline of whole city-million scale children and adolescents myopia survey. (CAMS) in Wenzhou, China. *Eye Vision*. (2021) 8:31. doi: 10.1186/s40662-021-00255-1
54. Yotsukura E, Torii H, Inokuchi M, Tokumura M, Uchino M, Nakamura K, et al. Current prevalence of myopia and association of myopia with environmental factors among schoolchildren in Japan. *JAMA Ophthalmol*. (2019) 137:1233–9. doi: 10.1001/jamaophthalmol.2019.3103
55. Terasaki H, Yamashita T, Yoshihara N, Kii Y, Sakamoto T. Association of lifestyle and body structure to ocular axial length in Japanese elementary school children. *BMC Ophthalmol*. (2017) 17:123. doi: 10.1186/s12886-017-0519-y
56. Cordain L, Eaton SB, Brand Miller J, Lindeberg S, Jensen C. An evolutionary analysis of the aetiology and pathogenesis of juvenile-onset myopia. *Acta Ophthalmol Scand*. (2002) 80:125–35. doi: 10.1034/j.1600-0420.2002.800203.x
57. Ip JM, Rose KA, Morgan IG, Burlutsky G, Mitchell P. Myopia and the urban environment: findings in a sample of 12-year-old Australian school children. *Invest Ophthalmol Vis Sci*. (2008) 49:3858–63. doi: 10.1167/iovs.07-1451

Conflict of Interest: The authors declare that the research was conducted in the absence of any commercial or financial relationships that could be construed as a potential conflict of interest.

frontiers in Medicine

CASE REPORT
published: 14 February 2022
doi: 10.3389/fmed.2022.697030

Case Report: Multiple Retinal Astrocytic Hamartomas in Congenital Disorder of Glycosylation-Ia

Giulia Midena[1] *and Elisabetta Pilotto*[2,3]*

[1] IRCCS—Fondazione Bietti, Rome, Italy, [2] Department of Ophthalmology, University of Padova, Padua, Italy, [3] ERN-EYE Center, Padova University Hospital, Padua, Italy

Congenital disorder of glycosylation-Ia (CDG-Ia) is a rare autosomal recessive genetic disorder, characterized by systemic and ophthalmological abnormalities. Here, we report multiple retinal astrocytic hamartomas as a new retinal finding in an adolescent affected by congenital disorder of CDG-Ia. A 15-year-old boy affected by CDG-Ia underwent full ophthalmic examination, full field electroretinography (ERG) evaluation and retinal multimodal imaging, including: fundus photography, spectral domain optical coherence tomography (SD-OCT) and blue fundus autofluorescence (FAF). Blue FAF showed multiple papillary and iuxtapapillary bilateral hyper-FAF lesions, corresponding to hyperreflective thickening of the retinal nerve fiber layer, with internal optical empty spaces and posterior dense optical shadowing at SD-OCT. These imaging findings were consistent with retinal astrocytic hamartomas. Scotopic ERG response was significantly reduced in both eyes. Macular edema and absence of the retinal outer segments layer were also detectable. Retinal multi-modal imaging provides additional insights about retinal involvement of patients affected by CDG-Ia. In particular, this case shows the presence of multiple retinal astrocytic hamartomas.

Keywords: congenital disorder of glycosylation-Ia, astrocytic hamartoma, retinal dystrophy, multimodal imaging, OCT, autofluorescence, metabolic disease

OPEN ACCESS

Edited by:
Yasuo Yanagi, Yokohama City University Medical Center, Japan

Reviewed by:
Maria Vittoria Cicinelli, San Raffaele Scientific Institute (IRCCS), Italy
Carlo Gesualdo, Università della Campania Luigi Vanvitelli, Italy

***Correspondence:**
Elisabetta Pilotto
elisabetta.pilotto@unipd.it

Specialty section:
This article was submitted to Ophthalmology, a section of the journal Frontiers in Medicine

Received: *18 April 2021*
Accepted: *21 January 2022*
Published: *14 February 2022*

Citation:
Midena G and Pilotto E (2022) Case Report: Multiple Retinal Astrocytic Hamartomas in Congenital Disorder of Glycosylation-Ia. Front. Med. 9:697030. doi: 10.3389/fmed.2022.697030

INTRODUCTION

Congenital disorder of glycosylation (CDG) Ia, also known as phosphomannomutase 2 (PMM2)-CDG, is a rare autosomal recessive genetic disorder, characterized by neurometabolic abnormalities (1–3). Main clinical features are: facial dysmorphism, abnormal fat distribution, various coagulation and endocrine defects. Neurologic, cardiac, gastrointestinal, hepatic, renal, immunologic, and skeletal abnormalities may be also present (1, 2). High myopia, abnormal eye movements, squint, cataract, nystagmus and retinal dystrophy have been reported (3–7).

CASE REPORT

A 15-year-old boy affected by, genetically confirmed, CDG-Ia complaining progressive high myopia, visual acuity impairment and night blindness, was referred to our pediatric low vision unit. His systemic history was characterized by: hypotonia, abnormal fat distribution, joint contracture, developmental delay and feeding difficulties. Eye examination showed: bilateral high myopia (−8.0 diopters), best-corrected visual acuity of 20/40 in both eyes, exotropia and hypertropia. Fundus biomicroscopy of the right eye revealed vitreous disorganization and, only in the right eye, a iuxtapapillary, white,

gliotic tissue. Optic disc of the left eye appeared normal. Blue fundus autofluorescence (FAF) of the right eye showed multiple intensely hyper-FAF spots corresponding to the gliotic tissue, and an isolated hyper-FAF spot on the optic nerve head. Blue FAF of the left eye showed a mild hyper-FAF spot on the optic nerve head. Spectral domain optical coherence tomography (SD-OCT) of these lesions showed hyperreflective thickening of the retinal nerve fiber layer (RNFL) with internal moth-eaten optical empty spaces and posterior dense optical shadowing. The combined imaging techniques were diagnostic for multiple, bilateral, calcific retinal astrocytic hamartomas (**Figure 1**). In particular, according to the SD-OCT findings, we excluded the diagnosis of optic disc drusen. SD-OCT also showed convex scleral profile, foveal and perifoveal retinal thickening with intraretinal cysts, retinoschisis, and the absence of the retinal outer segments, outside the fovea (**Figure 2**). Full field electroretinography (ERG) evaluation according to ISCEV standards revealed a significant reduction of scotopic response with mild reduction in photopic response in both eyes. Brain magnetic resonance imaging and specific genetic blood tests excluded the diagnosis of tuberous sclerosis and neurofibromatosis type 1, systemic syndromes typically characterized by multiple, bilateral, calcific retinal astrocytic hamartomas.

DISCUSSION/CONCLUSION

CDG-Ia is the most common congenital disorder of N-glycosylation. Mutations in the PMM2 gene, located on chromosome 16p13, cause a deficiency of PMM. This cytoplasmic enzyme has an essential role in the N-glycosylation process and in the synthesis of glycosylphosphati-dylinositol, which is used to anchor proteins to the cell membrane (1, 6, 7). Immunohistochemical studies of the mammalian retina have established that N-linked glycans are represented in all retinal layers: this may explain the previously known retinal manifestation of CDG in the human retina, namely retinal dystrophy (8, 9). The peculiarity of this case is the previously unreported combination of CDG-Ia and the presence of multiple, bilateral, calcific retinal astrocytic hamartomas. These benign retinal lesions are glial tumors located in the RNFL, arising from retinal astrocytes (10). Clinically they appear as cream-white, well-circumscribed, non-calcified or calcified, elevated lesions that may present multiple or solitary. These lesions are commonly calcified and multilobulated in appearance, as in our case, but may also present flat and semitraslucent. Multiple and bilateral retinal astrocytic hamartomas are most frequently associated with tuberous sclerosis and neurofibromatosis type 1, and rarely, retinitis pigmentosa (10, 11). In our case, any other phacomatosis were excluded. Retinal astrocytic hamartomas originate from the astrocytes in the RNFL. These cells are characteristic star-shaped glial cells located in the retina, and also in the brain and spinal cord (12). Recent findings revealed that central nervous system astrocytoma progression is correlated with the constant decrease of total N-glycosylation. In particular, Padhiar et al. demonstrated that brain astrocytoma is characterized by the loss of overall N-glycosylation (12). Since brain astrocytoma and retinal astrocytic hamartoma share the same originating cell, we hypothesize that the abnormal proliferation of retinal astrocytes may be due to the deficit of N-glycosylation. Concerning the outer retinal layers, Andreasson et al. hypothesized that in the CDG-Ia retinal disease opsin and interphotoreceptor retinoid-binding protein, the two major glycosylated proteins associated with photoreceptors, are affected (13). Therefore, the lack of PMM determines the inefficacy of these proteins and a progressive photoreceptor degeneration, which may cause, as late phenomenon, a pigmentary retinopathy (5–7). Pigment accumulation is a late stage clinical sign, reported only after significant photoreceptor cell death and migration of the retinal pigment epithelium cells toward the inner layers of the retina (5–7). Jensen et al. rarely noted pigment deposition in a series of 23 pediatric patients with CDG-Ia, but it was described by Krasnewich et al. in his adult patients (7, 13).

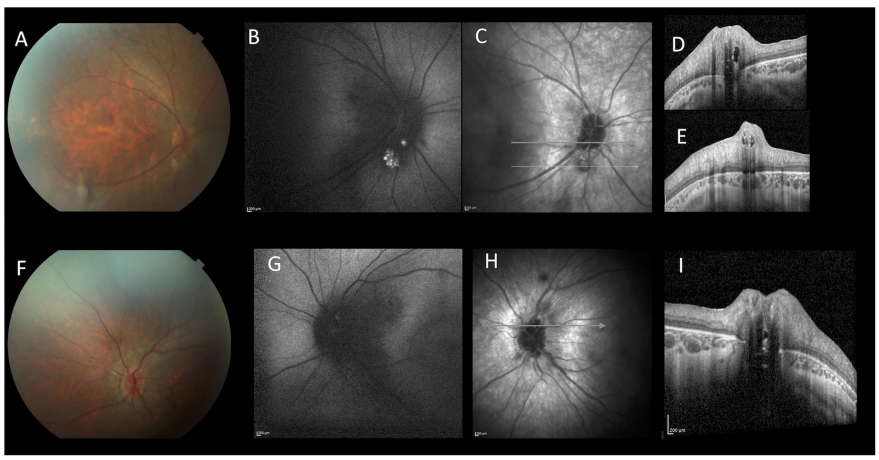

FIGURE 1 | Multimodal imaging of a 15-year-old patient affected by CDG-Ia. Color fundus photograph of the right **(A)** and left **(F)**. Blue-autofluorescence (FAF, **B,G**) shows hyperautofluorescent spots. Linear SD-OCT **(C–E,H,I)** shows hyperreflective thickening of the retinal nerve fiber layer RNFL with internal moth-eaten optical empty spaces and posterior dense optical shadowing. These aspects are diagnostic for multiple, bilateral, calcific retinal astrocytic hamartomas.

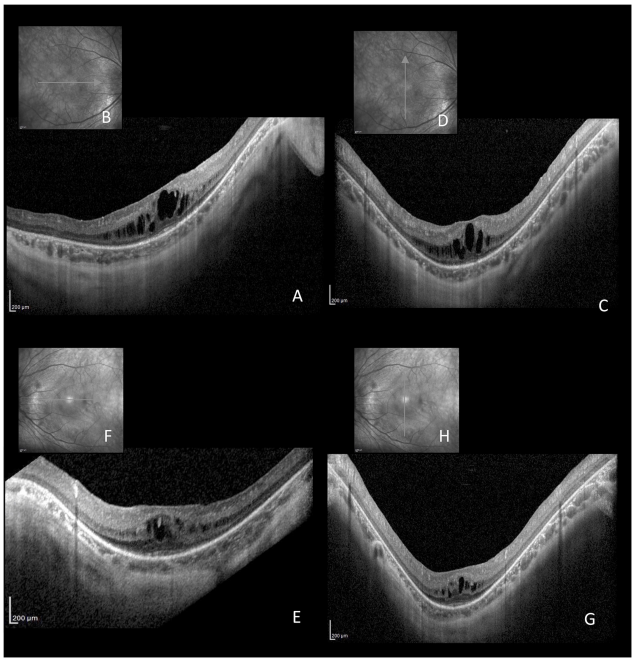

FIGURE 2 | Horizontal **(A,B,E,F)** and vertical **(C,D,G,H)** linear SD-OCT passing through the fovea of the same patient affected by CDG-Ia. Cystoid macular edema with foveal and perifoveal retinal thickening, intraretinal cysts, retinoschisis, and absence of the retinal outer segment, outside the fovea, are evident.

Marked pigmentary fundus changes were undetectable in our patient, however, both SD-OCT and ERG findings were consistent with rod dystrophy. This might indicate that the patient was young or, probably, CDG-Ia retinal disease was at an early stage, and therefore the diagnosis of retinitis pigmentosa cannot be excluded.

In conclusion, the present case confirms the essential role of retinal multimodal imaging which provides, in a non-invasive way, new insights in the retinal involvement of patients affected by CDG-Ia. In particular, retinal multimodal imaging was instrumental to document the association, never reported before, between CDG-Ia and multiple, bilateral, calcific retinal astrocytic hamartomas. These new findings should be considered in the multidisciplinary evaluation of children within CDG, and retinal and/or brain astrocytic hamartoma, which share the same originating cell, should be excluded.

DATA AVAILABILITY STATEMENT

The original contributions presented in the study are included in the article/supplementary material, further inquiries can be directed to the corresponding author.

ETHICS STATEMENT

Written informed consent was obtained from the minor(s)' legal guardian/next of kin for the publication of any potentially identifiable images or data included in this article.

AUTHOR CONTRIBUTIONS

GM and EP: data research, case design, drafting and revising, final approval, and agreement to be accountable for all aspects of the work.

ACKNOWLEDGMENTS

The authors are grateful to the European Reference Network dedicated to Rare Eye Diseases (ERN-EYE). The contribution of the Fondazione Bietti in this paper was supported by Ministry of Health and Fondazione Roma.

REFERENCES

1. Grünewald S. The clinical spectrum of phosphomannomutase 2 deficiency (CDG-Ia). *Biochim Biophys Acta.* (2009) 1792:827–34. doi: 10.1016/J.BBADIS.2009.01.003
2. Verheijen J, Tahata S, Kozicz T, Witters P, Morava E. Therapeutic approaches in congenital disorders of glycosylation (CDG) involving N-linked glycosylation: an update. *Genet Med.* (2020) 22:268–79. doi: 10.1038/s41436-019-0647-2
3. Morava E, Wosik HN, Sykut-Cegielska J, Adamowicz M, Guillard M, Wevers RA, et al. Ophthalmological abnormalities in children with congenital disorders of glycosylation type I. *Br J Ophthalmol.* (2009) 93:350–4. doi: 10.1136/bjo.2008.145359
4. Krasnewich D, O'Brien K, Sparks S. Clinical features in adults with congenital disorders of glycosylation type Ia (CDG-Ia). *Am J Med Genet C Semin Med Genet.* (2007) 145C:302–6. doi: 10.1002/ajmg.c.30143
5. Thompson DA, Lyons RJ, Russell-Eggitt I, Liasis A, Jägle H, Grünewald S. Retinal characteristics of the congenital disorder of glycosylation PMM2-CDG. *J Inherit Metab Dis.* (2013) 36:1039–47. doi: 10.1007/s10545-013-9594-2
6. Thompson DA, Lyons RJ, Liasis A, Russell-Eggitt I, Jägle H, Grünewald S. Retinal on-pathway deficit in congenital disorder of glycosylation due to phosphomannomutase deficiency. *Arch Ophthalmol.* (2012) 130:712–9. doi: 10.1001/archophthalmol.2012.130
7. Jensen H, Kjaergaard S, Klie F, Moller HU. Ophthalmic manifestations of congenital disorder of glycosylation type 1a. *Ophthalmic Genet.* (2003) 24:81–8. doi: 10.1076/opge.24.2.81.13994
8. Wu WC, Lai CC, Liu JH, Singh T, Li LM, Peumans WJ, et al. Differential binding to glycotopes among the layers of three mammalian retinal neurons by man-containing N-linked glycan, T(alpha) (Galbeta1-3GalNAcalpha1), Tn (GalNAcalpha1-Ser/Thr) and I (beta)/II (beta) (Galbeta1-3/4GlcNAcbeta-) reactive lectins. *Neurochem Res.* (2006) 31:619–28. doi: 10.1007/s11064-006-9060-8
9. Tam BM, Moritz OL. The role of rhodopsin glycosylation in protein folding, trafficking, and light-sensitive retinal degeneration. *J Neurosci.* (2009) 29:15145–54. doi: 10.1523/JNEUROSCI.4259-09.2009
10. Shields CL, Say EAT, Fuller T, Arora S, Samara WA, Shields JA. Retinal astrocytic hamartoma arises in nerve fiber layer and shows "moth-eaten" optically empty spaces on optical coherence tomography. *Ophthalmology.* (2016) 123:1809–16. doi: 10.1016/j.ophtha.2016.04.011
11. Pichi F, Massaro D, Serafino M, Carrai P, Giuliari GP, Shields CL, et al. Retinal astrocytic hamartoma: optical coherence tomography classification

and correlation with tuberous sclerosis complex. *Retina.* (2016) 36:1199–208. doi: 10.1097/IAE.0000000000000829
12. Padhiar AA, Fan J, Tang Y, Yu J, Wang S, Liu L, et al. Upregulated β1-6 branch N-glycan marks early gliomagenesis but exhibited biphasic expression in the progression of astrocytic glioma. *Am J Cancer Res.* (2015) 5:1101–16.
13. Andreasson S, Blennow G, Ehinger B, Strömland K. Full-field 17 electroretinograms in patients with the carbohydrate-deficient glycoprotein syndrome. *Am J Ophthalmol.* (1991) 112:83–6. doi: 10.1016/S0002-9394(14)76218-X

Conflict of Interest: The authors declare that the research was conducted in the absence of any commercial or financial relationships that could be construed as a potential conflict of interest.

Publisher's Note: All claims expressed in this article are solely those of the authors and do not necessarily represent those of their affiliated organizations, or those of the publisher, the editors and the reviewers. Any product that may be evaluated in this article, or claim that may be made by its manufacturer, is not guaranteed or endorsed by the publisher.

frontiers | Frontiers in Medicine

ORIGINAL RESEARCH
published: 18 May 2022
doi: 10.3389/fmed.2022.855385

The Extent of Gender Gap in Citations in Ophthalmology Literature

Suqi Cao, Yue Xiong, Wenhua Zhang, Jiawei Zhou and Zhifen He**

Department of Ophthalmology, Eye Hospital, Wenzhou Medical University, Wenzhou, China

Purpose: To investigate the severity and causes of gender imbalance in the counts of ophthalmology citations.

Methods: The PubMed database was searched to identify cited papers that were published in four journals (*Prog Retin Eye Res*, *Ophthalmology*, *JAMA Ophthalmol*, and *Invest Ophthalmol Vis Sci*) between August 2015 and July 2020, and those that referenced these cited papers by 2021 July (i.e., citing papers). The gender category of a given paper is defined by the gender of the first and last author (MM, FM, MF, and FF; M means male and F means female). A generalized additive model to predict the expected proportion was fitted. The difference between the observed proportion and expected proportion of citations of a paper's gender category was the primary outcome.

Results: The proportion of female-led (MF and FF) papers slightly increased from 27% in 2015 to 30% in 2020. MM, FM, MF, and FF papers were cited as −9.3, −1.5, 13.0, and 23.9% more than expected, respectively. MM papers cited 13.9% more male-led (MM and FM) papers than female-led papers, and FF papers cited 33.5% fewer male-led papers than female-led papers. The difference between the observed proportion and expected proportion of MM citing papers within male-led and female-led cited papers grew at a rate of 0.13 and 0.67% per year.

Conclusion: The high frequency of citations of female-led papers might narrow the gender gap in the citation count within ophthalmology. These findings show that papers by female-led are less common, so the gender gap might still exist even with their high citation count.

Keywords: gender, equity, ophthalmology, citation, generalized additive model

OPEN ACCESS

Edited by:
Menaka Chanu Thounaojam, Augusta University, United States

Reviewed by:
Bharat Gurnani, Aravind Eye Hospital and Post Graduate Institute of Ophthalmology, India
Andy Wai Kan Yeung, The University of Hong Kong, Hong Kong SAR, China

****Correspondence:***
Jiawei Zhou
zhoujw@mail.eye.ac.cn
Zhifen He
zhifen0821@163.com

Specialty section:
This article was submitted to Ophthalmology, a section of the journal Frontiers in Medicine

Received: *15 January 2022*
Accepted: *19 April 2022*
Published: *18 May 2022*

Citation:
Cao S, Xiong Y, Zhang W, Zhou J and He Z (2022) The Extent of Gender Gap in Citations in Ophthalmology Literature. Front. Med. 9:855385. doi: 10.3389/fmed.2022.855385

INTRODUCTION

Women have faced societal pressures and barriers associated with gender (1–3) compared to men. For this reason, scientists have become concerned with the gender imbalance in academia (4), such as women have won fewer awards (5), published fewer papers (6), and accumulated fewer citation counts (7) even if they comprise of more than 50% Ph.D. holders in America. Accumulating evidence shows that women have been underrepresented (7), especially in the fields of science, technology, engineering, mathematics, and medicine (STEMM) (8).

Despite an increase in the proportion of female graduates in medical school (9) and the proportion of female authors in medicine (10), the representation of female ophthalmologists in academic medicine has been much lower than male ophthalmologists (11). Gender imbalance has manifested in the male/female proportion of authors in papers within ophthalmology. To illustrate, Heng Wong et al. (12) analyzed the top 100 cited papers in ophthalmology from 1975 to 2017 and found that 70% of the first authors were male. In addition, the gender imbalance can be observed not just in the proportion of authors in scientific papers but also in academic ranks, such as senior professorships (13), leadership positions (4, 9, 11), and participation in reputable conferences (14). Some have spearheaded efforts to mitigate the gender imbalance against women. For instance, Dr. Mariya Moosajee, Dr. Julie Daniels, and Dr. Maryse Bailly established the Women in Vision UK (WVUK) network to mitigate gender inequality (15).

Assessment criteria for performance in academia include academic ranks, peer-reviewed publications, salary, and funding (3, 16, 17). The number of peer-reviewed publications has been especially important in climbing up the ladder of academic ranks (9, 18–20) and securing funding for principal investigators. A recent study by Dworkin et al. (21) examines the severity of gender imbalance in the citation count of neuroscience papers. They analyzed 303,886 articles that were published in five top neuroscience journals between 1995 and 2018 and examined the link between authors' gender and citations. They revealed that female authors have received fewer citations than expected and that this gender imbalance might not be alleviated over time.

As mentioned above, several previous studies on gender bias in ophthalmology focus on the percentage of female authors, female academic ranks, and citation count, all of which mainly measure the passive consequences of gender behavior. Using the framework of the relationship between authors' gender and the gender makeup of their citation lists (21), one could directly measure the citation behavior itself. In our study, we were interested in investigating the severity of gender imbalance in the citation count of ophthalmology papers in ophthalmology citations. To do so, we analyzed papers published between August 2015 and July 2020 in four top ophthalmology journals (*Prog Retin Eye Res, Ophthalmology, JAMA Ophthalmol,* and *Invest Ophthalmol Vis Sci*), which had the highest h-index (22) in 2020.

MATERIALS AND METHODS

Data Collection

We have selected three research journals (*Ophthalmology*: 244 [h-index]; *Invest Ophthalmol Vis Sci*: 218; and *JAMA Ophthalmol*: 196) and one review journal (*Prog Retin Eye Res*: 152) with the highest h-index in the ophthalmology field in 2020 (**Figure 1**). We searched the PubMed database for papers published from August 2015 to July 2020 in these four journals and defined these papers as cited papers. Papers that referenced these cited papers by July 2021 were defined as citing papers (**Figure 2A**). We obtained the Author Full Name (AF), Source of Publication (SO), Document Type (DT), Publication Date (PD), and Published Year (PY) for each cited paper. We also searched PMID of Cited by lists (CL) and Times Cited Count (TC) of above-cited papers and obtained the AF, PD, and PY for each citing paper (the paper in CL) by July 2021.

Gender Determination

Similar to Dworkin et al. (21), gender was awarded using a publicly available probabilistic database (GenderAPI).[1] We attributed male (or female) to each author whose name had at least 85% probability of belonging to someone labeled as male (or female) according to the GenderAPI. We randomly selected 100 unique authors involved in the aforementioned dataset that we collected from PubMed for the manual gender verification and found that the accuracy of GenderAPI program was 98% (see **Supplementary Material**). In the current study, the gender of both the first and last author of 86% of the papers (both cited and citing papers) could be determined by using GenderAPI. Subsequently, we manually determined the gender of the authors by visiting lab websites for the remaining 14% papers.

Self-Citations Removal

We defined self-citation papers where either the first or last author of the citing paper was the first or last author of the cited paper. In this study, self-citations were eliminated from all analyses of gender citation behavior.

Statistical Analysis

To obtain an expected proportion that accounts for various characteristics that might be associated with gender, we fitted the same generalized additive model (GAM) as Dworkin et al. (21) on the multinomial outcome [MM (first and last authors are male), FM (first author is female and last author is male), MF (first author is male and last author is female), and FF (first and last authors are female)]. This model includes the following explanatory variables: (1) date (PD and PY), (2) team size (The number of authors), (3) source of publication (SO), (4) team seniority estimated with (TC), and (5) document type (DT). Then, we applied the model to each paper using the *mgcv* package in R (23), which returned the expected proportions of citing papers (MM, FM, MF, and FF) for a given cited paper. We then compared this expected proportion with the observed proportion of citations of the paper. If the expected proportion does not match, it means that the gender gap still exists after the consideration of the abovementioned variables of each paper.

In this study, we presented all estimations with a CI (95% confidence interval), a *p*-value, or both. The CIs were computed by bootstrapping the cited papers (e.g., randomly sampling 500 cited papers each time to get the average expected proportion for each iteration). Randomization was conducted by probabilistically drawing new gender categories for each paper according to their estimated gender probabilities by GAM. The statistical significance was adjusted for multiple comparisons; *p*-values were corrected according to the Holm–Bonferroni method (24).

[1] http://genderapi.io/

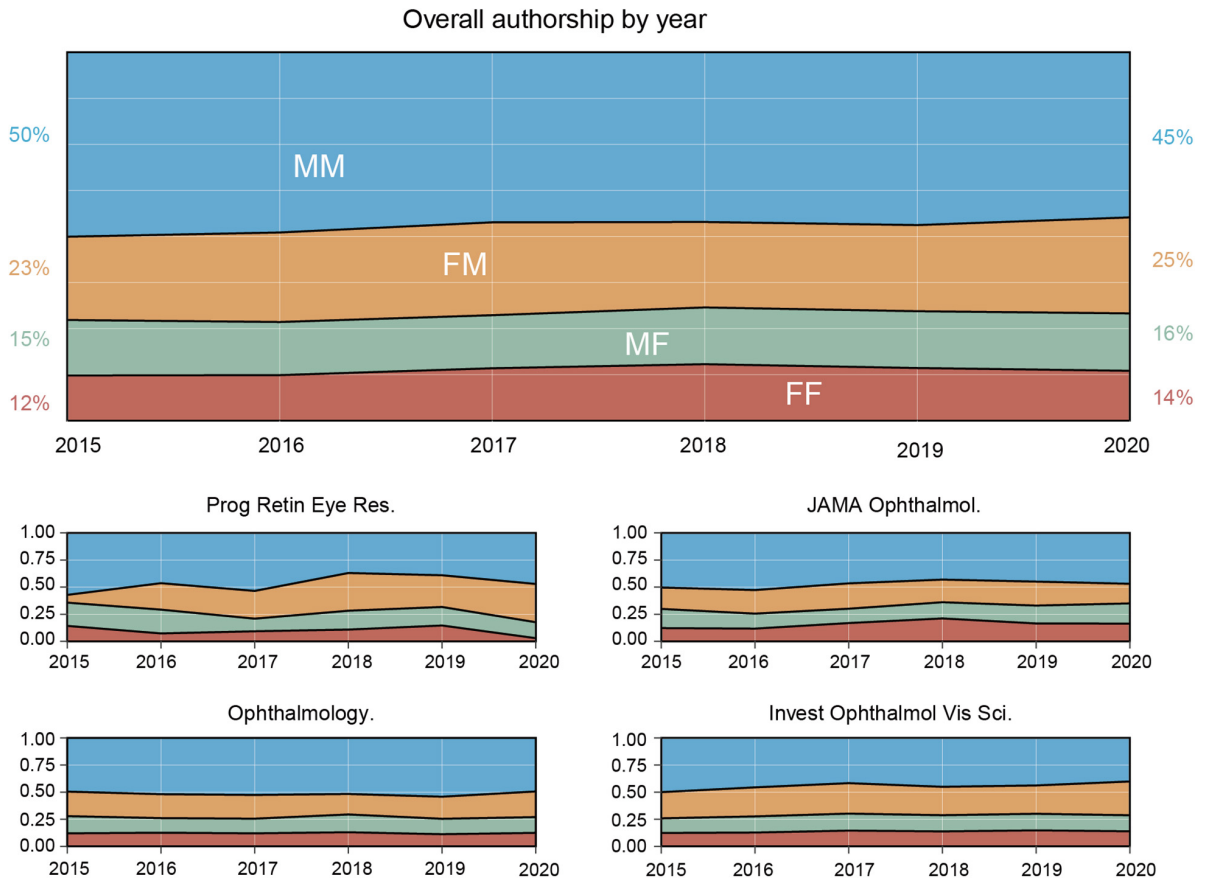

FIGURE 1 | Trends of gender among authors within the four ophthalmology journals between August 2015 and July 2020. Proportions of published papers with male as first and last authors (MM, blue), female as the first author and male as the last author (FM, yellow), male as the first author and female as the last author (MF, green), and female as the first and last authors (FF, red) are plotted as a function of time (between August 2015 and July 2020) in four ophthalmology journals: *Prog Retin Eye Res*, *Ophthalmology*, *JAMA Ophthalmol,* and *Invest Ophthalmol Vis Sci*. The overall trend of these four journals is also plotted (top panel).

Generally, the last author of a paper was considered the senior investigator. We defined a female-led (MF and FF) paper as the article in which the last author is female and a male-led (MM and FM) paper as the article in which the last author is male.

Hypotheses

In this study, we tested four hypotheses:

Hypothesis 1: The citation rate of female-led papers is lower than expected.

To verify this assumption, we first estimated the expected proportion of citations given to each category of authors. This expectation was calculated by summing the probabilities estimated by the GAM for all papers from 2015 to 2020. These values were compared by calculating the percentage difference between observed and expected proportions for each author's gender group. If the hypothesis is true, the percentage difference of female-led papers will be less than 0.

Hypothesis 2: The citation of female-led papers occurs to a fewer degree in MM papers.

We used a similar method to those described above to test the second hypothesis. The primary difference is that, instead of calculating the observed and expected proportion by summing over the citations within all citing papers, we performed those summations separately for lists in papers with male-led papers and female-led papers. If this hypothesis is true, MM papers will be citing more male-led papers than female-led papers.

Hypothesis 3: The proportion of MM citations of female-led papers will be decreasing more than that of male-led papers over time.

The changes in male-led papers and female-led papers over time were estimated using linear regression. The CIs of this estimate was obtained using the article bootstrap procedure, and significance was assessed using the graph-preserving null model (21). If the hypothesis is true, the annual growth rate of MM citation count from female-led papers will be lower than that of male-led papers.

Hypothesis 4: A relationship exists between local co-authorship networks and citation behavior.

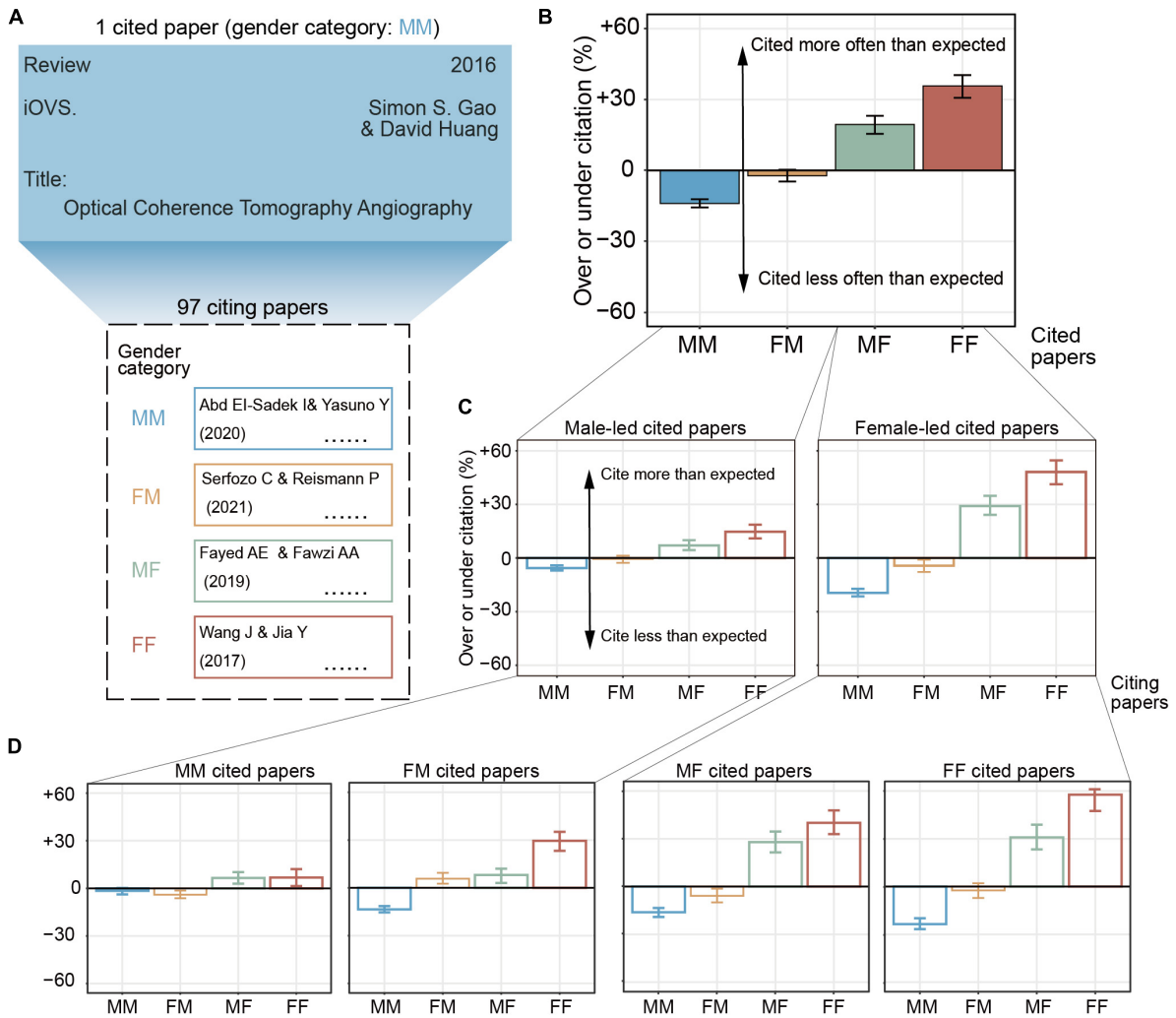

FIGURE 2 | The gender gap in citation counts. **(A)** Definition of cited paper and citing papers. Gender category of a given paper is defined by the gender of the first and last author. In the example we provide here, a review paper from Dr. Simon was published in iOVS in 2016. We defined it as an MM cited paper using the GenderAPI database. This cited paper has been cited by 97 citing papers. **(B)** The degree of over- or under-citation of different gender category of cited paper. MM papers were cited 9.3% less than expected (95% CI, –10.6 to –8.0%), FM papers were cited 1.5% less than expected (95% CI, –3.1 to 0.5%), MF papers were cited 13.0% more than expected (95% CI, 10.5–15.2%), and FF papers were cited 23.9% more than expected (95% CI, 20.5–27.2%). **(C)** The degree of over- or under-citation after separating cited papers by the more common (i.e., led) gender and **(D)** by full gender. Bars represent overall over-citation and under-citation, calculated from 53,962 total citation counts (MM, 24,058, FM, 13,742, MF, 8,384, and FF, 7,778). Error bars represent the 95% of CI of each citation estimate, calculated from 1,000 bootstrap resampling iterations.

A co-authorship network of first and last authors is defined as where they established a connection by co-authoring a paper with another author before a given date. We examined how the citation behavior was affected by the co-authorship network. If the hypothesis is true, there will be a consistent citation behavior between with co-authorship networks and without networks.

RESULTS

Data Description

Our data included 8,084 cited papers, which were published in *Prog Retin Eye Res* (219 papers), *Ophthalmology* (2,265 papers), *JAMA Ophthalmol* (1,918 papers), and *Invest Ophthalmol Vis Sci* (3,682 papers) from August 2015 to July 2020 (data from the PubMed database). From those, 3,813 were MM papers (47.17%), 1,950 were FM papers (24.12%), 1,209 were MF papers (14.95%), and 1,112 were FF papers (13.76%).

Authorship's Trends

The proportion of female-led papers slightly increased from 27% in 2015 to 30% in 2020. On one hand, this trend of female-led papers varied across journals. To illustrate, *Prog Retin Eye Res* decreased from 35 to 18%; *Ophthalmology* hardly changed (from 28 to 27%); *JAMA Ophthalmol* increased from 30 to 34%, and *Invest Ophthalmol Vis Sci* increased from 26 to 29%. On the other

hand, the overall proportion of articles that had females as first or last authors slightly increased from 50% in 2015 to 55% in 2020 (**Figure 1**).

Citation Imbalance

To test the extent of the gender gap in the number of citations, we narrowed the 8,084 cited papers to 5,864, which were either research or review articles (with at least 1 citation count) that were published in the four ophthalmology journals. We found that these 5,864 papers had been cited by 53,962 times before August 2021. We then obtained the observed proportion in each gender category for all 5,864 papers [e.g., a given cited paper was cited by 97 (47 MM, 27 FM, 22 MF, and 1 FF) citing papers, the observed proportion was 0.48, 0.28, 0.23, and 0.01, respectively; **Figure 2A**].

We studied whether there were any relationships between gender and paper characteristics (e.g., date, journal, team size, author seniority, and document type). We modeled the multinomial gender category (MM, FM, MF, and FF) as a function of the above characteristics by fitting a GAM, by which we estimated the expected proportion of citing papers for a given cited paper (**Figure 2B**). For all 5,864 cited papers, MM papers received 42.4% citations of observed proportion, compared to 25.9% for FM papers, 17.3% for MF papers, and 14.4% for FF papers. According to the relevant proportion of paper, the expected proportions were 46.8% (MM), 26.3% (FM), 15.3% (MF), and 11.6% (FF). Therefore, MM papers were cited 9.3% less than expected (95% CI, −10.6 to −8.0%), FM papers were cited 1.5% less than expected (95% CI, −3.1 to 0.5%), MF papers were cited 13.0% more than expected (95% CI, 10.5–15.2%), and FF papers were cited 23.9% more than expected (95% CI, 20.5–27.2%). The over-citation of MF papers and FF papers does not support the hypothesis that the citation rate of female-led papers is lower than expected (*Hypothesis 1*).

The Effect of Author Gender on Citation Behavior

Among the abovementioned 5,864 cited papers that we screened, there were roughly 71% male-led papers and 29% female-led papers. In this section, after separating cited papers by gender, we found that, within male-led cited papers (TC: 37800), MM citing papers were cited 5.6% less than expected (95% CI, −7.0 to −4.1%, $p < 0.001$), FM papers were cited 0.5% less than expected (95% CI, −2.7 to 1.3%, $p = 0.61$), MF papers were cited 7.1% more than expected (95% CI, 4.5–10.0%, $p < 0.001$), and FF papers were cited 14.7% more than expected (95% CI, 11.0–18.7%, $p < 0.001$); within female-led cited papers (TC: 16162), MM papers were cited 19.5% less than expected (95% CI, −21.5 to −17.3%, $p < 0.001$), FM papers were cited 4.3% less than expected (95% CI, −7.8 to −1.0%, $p = 0.01$), MF papers were cited 29.1% more than expected (95% CI, 24.2–34.8%, $p < 0.001$), and FF papers were cited 48.2% more than expected (95% CI, 41.3–54.6%, $p < 0.001$; **Figure 2C**). Our results indicate that MM papers tended to cite fewer female-led papers (*Hypothesis 2*), whereas FF papers tended to cite more female-led papers.

Within the male-led group and female-led group, the citation proportion of MM and FM and MF and FF subgroups are plotted in **Figure 2D**. Specifically, the over-citation degrees of MM, FM, MF, and FF citing papers that cite MM cited papers gradually decreased, whereas those of MF and FF cited papers gradually increased.

Time-Trends of Citation Imbalance

In addition to the overall citation behavior, we also quantified temporal trends of citation imbalance. We examined the yearly gap between the observed and expected proportions of MM citing papers.

After splitting by gender of cited author, we found that the gaps between observed and expected proportions of MM citing papers were increasing at a rate of 0.13% per year within male-led cited papers, compared to 0.67% within female-led cited papers (**Figure 3A**; observed and expected proportion across citing groups are shown in **Figure 3B**). In fact, the gaps in MM citation within female-led papers over time have been increasing faster than that within male-led papers. This finding is in contrast with *Hypotheses 3*, i.e., the proportion of MM citations of female-led papers will be increasing faster than that of male-led papers over time.

The Relationship Between Social Network and Citation Behavior

So far, we have shown that MF and FF citing papers cite female-led cited papers more often than expected (i.e., prediction from our model), whereas MM and FM papers cite less frequently than expected. One question is whether researchers are more likely to work with others of their own gender in the ophthalmology area as the findings by Ghiasi et al. (25) indicate. This could be addressed by examining the social network analytics and co-author relationship networks (26).

For a given paper f, we defined FF paper's overrepresentation as the difference between the FF papers within f's paper neighborhood and the overall proportion of FF papers within the network at the time of f's publication. Specifically, the number of papers published before the given paper f is n, where the number of FF papers is FF_{all}; the number of papers forming a co-author network with f is m, the number of FF papers is FF_{net}, and the FF paper overrepresentation means $\frac{FF_{net}}{m} - \frac{FF_{all}}{n}$. As shown in **Figure 4A**, co-authorship networks tended to include fewer FF papers than the base rate in the field, and overrepresentation of FF papers also differed based on the author's gender and time. Co-authorship networks tended to cite fewer FF papers than the base rate in the overall field, but this underrepresentation phenomenon has improved over time. In this case, the median FF papers were roughly overrepresented relative to the field's base rate within the networks of MM teams (− 0.04; 95% CI, − 0.09 to 0.02), FM teams (− 0.04; 95% CI, − 0.09 to 0.00), FM teams (− 0.03; 95% CI, − 0.08 to 0.02), and FF teams (0.01; 95% CI, − 0.03 to 0.04).

Furthermore, we checked whether the composition of the author's social networks accounts for the citation behavior of women. We utilized the absolute difference of FF citations

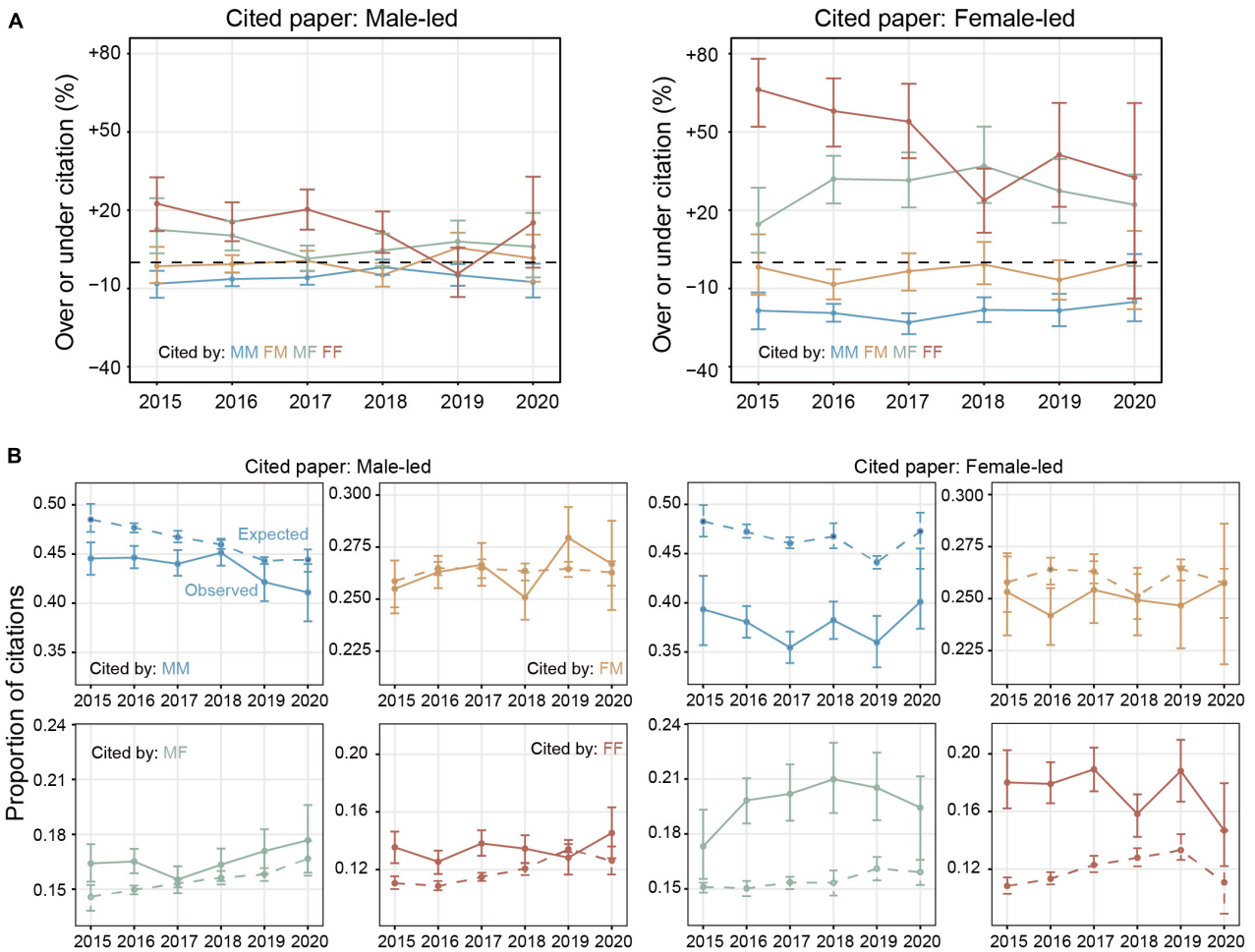

FIGURE 3 | Time-trends in citation rates across gender of the cited and citing author. **(A)** The degree of over-citation and under-citation of male-led and female-led papers over time. The gaps of MM, FM, MF, and FF citations between observed and expected proportions were increasing at a rate of 0.13, 0.60, –1.31, and –1.47% per year within male-led cited papers compared to 0.67, 0.39, 1.45, and –6.74% per year within female-led cited papers. The points represent overall over-citation and under-citation. **(B)** The observed (solid line) and expected (dashed line) proportions of citation within male-led and female-led citing papers over time. The points represent the observed or expected citation rates during a given year. Error bars represent the 95% CI of each rate, which were calculated from 1,000 bootstrap resampling iterations.

between the observed proportion and the expected proportion based on the GAM. We found that, without social network, the median MM teams cited fewer FF papers by 0.1% (95% CI, − 0.8 to 1.2%, $p = 0.84$), whereas they cited more FF papers by 2.4% for FM teams (95% CI, 1.2–3.3%, $p < 0.001$), 4.4% for MF teams (95% CI, 2.8–5.8%, $p < 0.001$), and 7.1% for FF teams (95% CI, 4.8–7.8%, $p < 0.001$; **Figure 4B**).

However, after the social networks have been accounted for, the gender citation patterns remain. Specifically, the median MM teams still cited FF papers less by around 0.38% (95% CI, − 1.4 to 0.8%, $p = 0.47$), whereas they cited FF papers more by 2.2% for FM teams (95% CI, 1.33.7%, $p = 0.001$), 4.3% for MF teams (95% CI, 2.7–5.6%, $p < 0.001$), and 7.1% for FF teams (95% CI, 4.3–7.9%, $p < 0.001$). The citation behavior of women by other women remains after accounting for social networks ($p = 0.93$). These two results do support *Hypothesis 4*: There seems to be a relationship between local co-authorship networks and citation behavior.

DISCUSSION

We found that the overall proportion of female-led papers increased slightly from 2015 to 2020, but the proportion was only 30% in 2020. Detailed analyses indicate that our finding does not confirm *Hypothesis 1:* The citation rate of female-led papers is lower than expected. In fact, after considering the related characteristics of papers, we found that the proportions of citation of male-led papers were lower than expected and that of female-led papers were higher than expected. However, we found that MM papers cited other MM, FM, MF, and FF papers less by 1.6, 13.5, 16.1, and 23.5%, respectively, compared

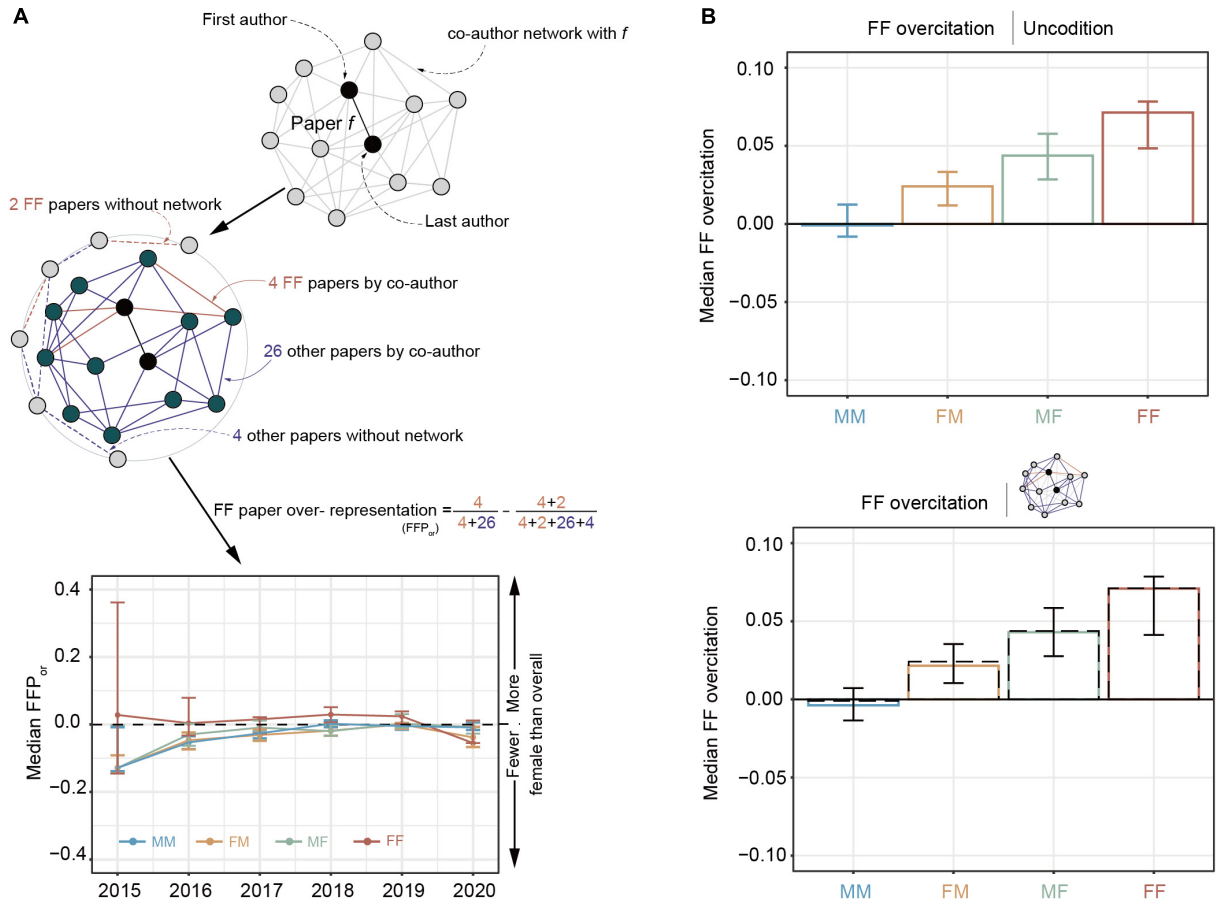

FIGURE 4 | Display of the composition measurement of the co-author network. **(A)** Examples of calculation of the FF paper overrepresentation (FFP_{or}) for the specific paper, and the median FF papers in the local network composition based on author gender from 2015 to 2020. **(B)** Over-citation of FF papers without network (the bar graph above and the dashed graph below) and after accounting for network (the bar graph below) influence. The bar graphs represent median FF papers of different gender groups (MM, FM, MF, and FF). The error bars represent the 95% CI of each estimation, which was calculated from 1,000 bootstrap resampling iterations There is only a slight median difference in the citation behavior (MM, –0.001 and –0.004; FM, 0.024 and 0.022; MF, 0.044 and 0.043; and FF, 0.071 and 0.071).

to their expected proportions. For FF papers, these values were, respectively + 6.8, +29.5, +40.0, and +57.7%. It means that MM papers have under-citation compared to female-led papers. This finding agrees with *Hypothesis 2:* The citation of female-led papers occurs to a fewer degree in MM citing papers. The over-citation rate of male-led papers will be growing slower than that of female-led papers over time, which is contrary to *Hypothesis 3:* The proportion of MM citations of female-led papers will be decreasing more than that of male-led papers over time. Our findings also agree with *Hypothesis 4:* A relationship exists between local co-authorship networks and citation behavior.

Our conclusions regarding *Hypotheses 1 and 3* are different from those in a previous study that investigates citation behavior in the field of neuroscience field (21). It may be because scientists have put more effort into balancing the gender gap in the field of ophthalmology. For example, the proportion of women as first or last authors (10, 27), the number of women holding important positions (4, 13, 14), and the number of women winning awards (28) have increased. A comparison of the findings with those of other studies confirms that men are less likely to cite papers written by women (29–31). Similarly, we found that female scientists in the field of ophthalmology also tended to cite papers written by male authors less frequently. The result of co-authorship networks analysis may provide some support that women may consciously look for and cite work by other women to fight gender imbalance. These findings might explain how our conclusions regarding *Hypotheses 2 and 4* are the same as those in the previous study that investigates citation behavior in the field of neuroscience (21).

As we all know, gender equity is not a short-term job. Since the proportion of FF papers is much lower than that of MM papers, even if the FF papers cited more female-led papers, the gender gap in citation behavior might not be alleviated. It is an important step to improve the willingness of researchers, especially men, to address the existing gender imbalance. Furthermore, addressing the current gender imbalance in ophthalmology can appropriately increase the proportion of women in senior positions and then encourage women to publish more scientific

creations (32). It has also been pointed out women are consistent with men in publishing papers early in their careers (33), but women still contend with an excessive burden of family responsibilities (15, 34), resulting in reduced outcomes after they get married. To address these identified imbalances, society should encourage men to bear family responsibilities.

Limitation and Future Work

Although our study reduces the confound of journal prestige, we still agree that it does not capture the entirety of the field as we selected only four journals. We aimed to evaluate the extent of gender differences in citations to the ophthalmology literature, so the h-index of the journal was the main index for selecting target journals (35, 36). Based on the similar study in this area (21) and limited by resources, we only selected three research journals (*Ophthalmology*: 244; *Invest Ophthalmol Vis Sci*: 218; and *JAMA Ophthalmol*: 196) and one review journal (*Prog Retin Eye Res:* 152) with the highest h-index in the ophthalmology field in 2020. Furthermore, we collected more than 8,000 cited papers from these four journals, and more than 50,000 papers citing them across the whole PubMed database. Even though we believed that these datasets could be a good representation of the question we asked, we agree that an ideal way should be to consider all the journals. Further studies should explore the gender gap in citation behavior by examining more ophthalmology journals.

The previous studies on the gender bias in ophthalmology focus mainly on authors' characteristics, such as the percentage of female authors (10, 27), female academic ranks (9, 14), and citation count (12). These previous reports provide valuable information on the consequences of gender behavior. In this study, we used the framework of the relationship between authors' gender and the gender makeup of their cited-by lists to directly measure the citation behavior itself. Limited by the resources we collected from PubMed, we did not include the author's characteristics (i.e., authors' publication count, age, and academic rank) into our GAM model. We conducted citation gender analysis through papers' characteristics rather than authors' characteristics, not only because it has been validated in the neuroscience area but also because we used the same model for analyzing the gender bias as Dworkin et al. (21). On the other hand, it is also hard to clearly define authors' characters through the PubMed database. To illustrate, an author might have cross-academic backgrounds; therefore, we do not have an ideal way of determining whether he/she belongs to ophthalmology or other fields. Early studies define the research disciplines of authors based on departmental affiliations (37). However, given the development of interdisciplinary collaboration, particularly to the diversity of researchers' backgrounds, authors may not be easily classified by a single field (38). Nevertheless, we believe that the citers (people who cited the references) might not really look into the author's gender before deciding to cite it or not. Thus, the citation bias that we found in the current study could be a reflection of women facing more gender-related obstacles in career development.

There are multiple avenues by which future works could be undertaken based on our study. For example, the paper citation might differ in different ophthalmology subfields, such as retina, cataract, glaucoma, and strabismus. Therefore, it would be interesting to further assess the difference between the ophthalmic sections in the gender gap in citation counts. Limited by the resources we got from the PubMed database, we were not able to extract the keywords and classify the papers into these different categories. Future work may combine other databases into the GAM model to address it.

CONCLUSION

In summary, despite the increase in the proportion of female-led papers from August 2015 to July 2020, the proportion was still found to be much lower than that of the male-led papers. Since the proportion of FF papers is much lower than that of MM papers, even if the FF papers cited more female-led papers, the gender gap in citation behavior might not be alleviated; this phenomenon might be related to social co-authorship networks.

DATA AVAILABILITY STATEMENT

The raw data supporting the conclusions of this article will be made available by the authors, without undue reservation.

AUTHOR CONTRIBUTIONS

SC and JZ designed the study. SC, YX, and WZ collected the data. SC, ZH, and JZ contributed to the interpretation of the results and critical revision of the manuscript for important intellectual content and approved the final version of the manuscript. All authors have read and approved the final manuscript.

FUNDING

This work was supported by the Project of State Key Laboratory of Ophthalmology, Optometry and Vision Science, Wenzhou Medical University (Grant No. J02-20210203), the Zhejiang Basic Public Welfare Project (Grant No. LGJ20H120001), and the Wenzhou Medical University (Grant No. QTJ16005). The sponsor or funding organizations had no role in the design or conduct of this research.

ACKNOWLEDGMENTS

We would like to thank Seung Hyun Min for his help in manuscript editing.

SUPPLEMENTARY MATERIAL

The Supplementary Material for this article can be found online at: https://www.frontiersin.org/articles/10.3389/fmed.2022.855385/full#supplementary-material

REFERENCES

1. Zhuge Y, Kaufman J, Simeone DM, Chen H, Velazquez OC. Is there still a glass ceiling for women in academic surgery? *Ann Surg.* (2011) 253:637–43. doi: 10.1097/SLA.0b013e3182111120
2. Moss-Racusin CA, Dovidio JF, Brescoll VL, Graham MJ, Handelsman J. Science faculty's subtle gender biases favor male students. *Proc Natl Acad Sci USA*. (2012) 109:16474–9. doi: 10.1073/pnas.1211286109
3. Reddy AK, Bounds GW, Bakri SJ, Gordon LK, Smith JR, Haller JA, et al. Representation of women with industry ties in ophthalmology. *JAMA Ophthalmol.* (2016) 134:636–43. doi: 10.1001/jamaophthalmol.2016.0552
4. Colby K. Sex diversity in ophthalmology leadership in 2020-a call for action. *JAMA Ophthalmol.* (2020) 138:458–9. doi: 10.1001/jamaophthalmol.2020.0188
5. Lincoln AE, Pincus S, Koster JB, Leboy PS. The matilda effect in science: awards and prizes in the US, 1990s and 2000s. *Soc Stud Sci.* (2012) 42:307–20. doi: 10.1177/0306312711435830
6. De Kleijn M, Jayabalasingham B, Falk-Krzesinski HJ, Collins T, Kuiper-Hoyng L, Cingolani I, et al. *The Researcher Journey Through a Gender Lens: An Examination of Research Participation, Career Progression and Perceptions Across the Globe*. Amsterdam: Elsevier (2020).
7. Huang J, Gates AJ, Sinatra R, Barabási AL. Historical comparison of gender inequality in scientific careers across countries and disciplines. *Proc Natl Acad Sci USA*. (2020) 117:4609–16. doi: 10.1073/pnas.1914221117
8. Holman L, Stuart-Fox D, Hauser CE. The gender gap in science: how long until women are equally represented? *PLoS Biol.* (2018) 16:e2004956. doi: 10.1371/journal.pbio.2004956
9. Svider PF, D'Aguillo CM, White PE, Pashkova AA, Bhagat N, Langer PD, et al. Gender differences in successful national institutes of health funding in ophthalmology. *J Surg Educat.* (2014) 71:680–8. doi: 10.1016/j.jsurg.2014.01.020
10. Mimouni M, Zayit-Soudry S, Segal O, Barak Y, Nemet AY, Shulman S, et al. Trends in authorship of articles in major ophthalmology journals by gender, 2002–2014. *Ophthalmology.* (2016) 123:1824–8. doi: 10.1016/j.ophtha.2016.04.034
11. Camacci ML, Lu A, Lehman EB, Scott IU, Bowie E, Pantanelli SM. Association between sex composition and publication productivity of journal editorial and professional society board members in ophthalmology. *JAMA Ophthalmol.* (2020) 138:451–8. doi: 10.1001/jamaophthalmol.2020.0164
12. Heng Wong MY, Tan NYQ, Sabanayagam C. Time trends, disease patterns and gender imbalance in the top 100 most cited articles in ophthalmology. *Br J Ophthalmol.* (2019) 103:18. doi: 10.1136/bjophthalmol-2018-312388
13. Tuli SS. Status of women in academic ophthalmology. *J Acad Ophthalmol.* (2019) 11:e59–64. doi: 10.1055/s-0039-3401849
14. Patel SH, Truong T, Tsui I, Moon J-Y, Rosenberg JB. Gender of presenters at ophthalmology conferences between 2015 and 2017. *Am J Ophthalmol.* (2020) 213:120–4. doi: 10.1016/j.ajo.2020.01.018
15. Khan H, Moosajee M. Facing up to gender inequality in ophthalmology and vision science. *Eye.* (2018) 32:1421–2. doi: 10.1038/s41433-018-0147-7
16. Inoue K, Blumenthal DM, Elashoff D, Tsugawa Y. Association between physician characteristics and payments from industry in 2015-2017: observational study. *BMJ Open.* (2019) 9:e031010. doi: 10.1136/bmjopen-2019-031010
17. Chiam M, Camacci ML, Lehman EB, Chen MC, Vora GK, Pantanelli SM. Sex differences in academic rank, scholarly productivity, national institutes of health funding, and industry ties among academic cornea specialists in the United States. *Am J Ophthalmol.* (2021) 222:285–91. doi: 10.1016/j.ajo.2020.09.011
18. Sanfey H, Hollands C. Career development resource: promotion to associate professor. *Am J Surg.* (2012) 204:130–4. doi: 10.1016/j.amjsurg.2012.04.004
19. Eloy JA, Svider P, Chandrasekhar SS, Husain Q, Mauro KM, Setzen M, et al. Gender disparities in scholarly productivity within academic otolaryngology departments. *Otolaryngol Head Neck Surg.* (2013) 148:215–22. doi: 10.1177/0194599812466055
20. Eloy JA, Svider PF, Cherla DV, Diaz L, Kovalerchik O, Mauro KM, et al. Gender disparities in research productivity among 9952 academic physicians. *Laryngoscope.* (2013) 123:1865–75. doi: 10.1002/lary.24039
21. Dworkin JD, Linn KA, Teich EG, Zurn P, Shinohara RT, Bassett DS. The extent and drivers of gender imbalance in neuroscience reference lists. *Nat Neurosci.* (2020) 23:918–26. doi: 10.1038/s41593-020-0658-y
22. Jones T, Huggett S, Kamalski J. Finding a way through the scientific literature: indexes and measures. *World Neurosurg.* (2011) 76:36–8. doi: 10.1016/j.wneu.2011.01.015
23. Wood SN. *Generalized Additive Models:An Introduction with R*. London: Chapman and Hall (2017).
24. Chalmers S. Board of the foundation of the scandinavian journal of statistics a simple sequentially rejective multiple test procedure. *Scand J Statist.* (2008) 6:65–70.
25. Ghiasi G, Larivière V, Sugimoto CR. On the compliance of women engineers with a gendered scientific system. *PLoS One.* (2015) 10:e0145931. doi: 10.1371/journal.pone.0145931
26. Fonseca Bde P, Sampaio RB, Fonseca MV, Zicker F. Co-authorship network analysis in health research: method and potential use. *Health Res Policy Syst.* (2016) 14:34. doi: 10.1186/s12961-016-0104-5
27. Shah DN, Huang J, Ying G-S, Pietrobon R, O'Brien JM. Trends in female representation in published ophthalmology literature, 2000-2009. *DJO.* (2013) 19:50–5. doi: 10.5693/djo.01.2013.07.002
28. Chao DL, Schiffman JC, Gedde SJ. Characterization of a clinician–scientist cohort in ophthalmology: a demographic analysis of K grant awardees in ophthalmology. *Ophthalmology.* (2013) 120:2146–50. doi: 10.1016/j.ophtha.2013.02.021
29. Ferber MA, Brün M. The gender gap in citations: does it persist? *Feminist Econom.* (2011) 17:151–8. doi: 10.1080/13545701.2010.541857
30. Maliniak D, Powers R, Walter BF. The gender citation gap in international relations. *Int Organiz.* (2013) 67:889–922. doi: 10.1017/S0020818313000209
31. Caplar N, Tacchella S, Birrer S. Quantitative evaluation of gender bias in astronomical publications from citation counts. *Nat Astronomy.* (2017) 1:0141. doi: 10.1038/s41550-017-0141
32. Ceci SJ, Ginther DK, Kahn S, Williams WM. Women in academic science: a changing landscape. *Psychol Sci Public Interest.* (2014) 15:75–141. doi: 10.1177/1529100614541236
33. Okafor S, Tibbetts K, Shah G, Tillman B, Agan A, Halderman AA. Is the gender gap closing in otolaryngology subspecialties? An analysis of research productivity. *Laryngoscope.* (2020) 130:1144–50. doi: 10.1002/lary.28189
34. Carr PL, Helitzer D, Freund K, Westring A, McGee R, Campbell PB, et al. A summary report from the research partnership on women in science careers. *J Gen Intern Med.* (2019) 34:356–62. doi: 10.1007/s11606-018-4547-y
35. Grech V, Rizk DEE. Increasing importance of research metrics: journal Impact Factor and h-index. *Int Urogynecol J.* (2018) 29:619–20. doi: 10.1007/s00192-018-3604-8
36. Cheung M, Leung P. Who is citing your work? journals with impact factor and h-index in social work and related fields. *Res Soc Work Pract.* (2021) 31:115–37. doi: 10.1177/1049731520963770
37. Qin J, Lancaster FW, Allen B. Types and levels of collaboration in interdisciplinary research in the sciences. *J Am Soc Informat Sci.* (1997) 48:893–916. doi: 10.1002/(sici)1097-4571(199710)48:10<893::aid-asi5>3.0.co;2-x
38. Feng S, Kirkley A. Mixing Patterns in Interdisciplinary Co-Authorship Networks at Multiple Scales. *Sci Rep.* (2020) 10:7731–7731. doi: 10.1038/s41598-020-64351-3

Conflict of Interest: The authors declare that the research was conducted in the absence of any commercial or financial relationships that could be construed as a potential conflict of interest.

frontiers | Frontiers in Medicine

ORIGINAL RESEARCH
published: 19 May 2022
doi: 10.3389/fmed.2022.867884

Whitecoat Adherence in Patients With Primary Open-Angle Glaucoma

Shervonne Poleon[1], *Nouran Sabbagh*[2] *and Lyne Racette*[3]*

[1] Department of Optometry and Vision Science, School of Optometry, University of Alabama at Birmingham, Birmingham, AL, United States, [2] Department of Internal Medicine, University of Alabama at Birmingham, Montgomery, AL, United States, [3] Department of Ophthalmology and Visual Sciences, School of Medicine, University of Alabama at Birmingham, Birmingham, AL, United States

Purpose: Whitecoat adherence refers to improved medication adherence in the days surrounding clinic visits. This may lead to clinical measures that are not representative of those outside of clinical encounters. In glaucoma, whitecoat adherence to prescribed hypotensive therapy may lead to intraocular pressure readings within the target range, which may impact clinical decision-making. We aimed to quantify and identify factors associated with whitecoat adherence.

Methods: In this cohort study, patients with primary open-angle glaucoma were selected from an ongoing longitudinal NIH-funded study if they used hypotensive eyedrops, had a clinic visit during the parent study, and had adherence data during the 28 days evenly bracketing the clinic visit. Adherence within the implementation phase was measured using Medication Event Monitoring System (MEMS) caps. Wilcoxon tests were used to compare mean adherence between the following periods: Pre_{14-4} (days 14 to 4 preceding the clinic visit) and Pre_{3-1} (days 3 to 1 preceding the visit); $Post_{1-3}$ (days 1 to 3 following the clinic visit) and $Post_{4-14}$ (days 4 to 14 following the visit). Analyses were performed in the full sample and in patients with optimal (≥80%, $n = 49$) and suboptimal adherence (<80%, $n = 17$).

Results: Sixty-six patients were included, of which 51.5% were female. Mean age was 70.8 ± 8.1 years. In the 6 months evenly bracketing the clinic visit, mean and median adherence were 86.3% (standard deviation = 17.7) and 95.6% (interquartile range = 21.2), respectively. Overall, mean adherence increased from Pre_{14-4} to Pre_{3-1} (85.5% ± 21.2 to 88.5% ± 23.2, $p = 0.01$) and decreased from $Post_{1-3}$ to $Post_{4-14}$ (87.0 ± 23.9 to 84.9 ± 23.3, $p = 0.02$). In patients with optimal adherence, adherence increased from Pre_{14-4} to Pre_{3-1} (94.0 ± 11.7 to 97.7 ± 7.4, $p = 0.001$) and from $Post_{1-3}$ to $Post_{4-14}$ (95.2 ± 12.0 to 95.4 ± 5.7, $p = 0.007$). Whitecoat adherence was not observed in patients with suboptimal adherence.

Conclusion: We documented the presence of whitecoat adherence in this cohort. Due to its potential impact on clinical outcomes and decisions, providers should remain vigilant for this phenomenon and prioritize it during patient-provider discussions.

Keywords: glaucoma, medication, whitecoat, adherence, implementation phase

OPEN ACCESS

Edited by:
Menaka Chanu Thounaojam, Augusta University, United States

Reviewed by:
Altaf A. Kondkar, King Saud University, Saudi Arabia
Sara Mucherino, University of Naples Federico II, Italy

***Correspondence:**
Lyne Racette
lracette@uabmc.edu

Specialty section:
This article was submitted to Ophthalmology, a section of the journal Frontiers in Medicine

Received: *01 February 2022*
Accepted: *26 April 2022*
Published: *19 May 2022*

Citation:
Poleon S, Sabbagh N and Racette L (2022) Whitecoat Adherence in Patients With Primary Open-Angle Glaucoma. Front. Med. 9:867884. doi: 10.3389/fmed.2022.867884

INTRODUCTION

Primary open-angle glaucoma (POAG) is a progressive eye disease that is distinguished by connective tissue remodeling at the optic nerve head and characteristic patterns of vision loss. POAG has an estimated global prevalence of over 70 million, and is the leading cause of irreversible blindness worldwide (1). Elevated intraocular pressure (IOP) is the sole modifiable risk factor for glaucoma progression, and daily instillation of hypotensive eyedrops can lower IOP and reduce pressure-induced optic nerve damage. However, despite the effectiveness of ocular hypotensive medications, research indicates that as few as 20% of patients are adherent to prescribed therapy (2). Later investigations by Friedman et al. reported a median adherence rate of 64% based on the analysis of pharmacy claims data for over 13,000 POAG patients (3). These findings are concerning as poor adherence has been associated with faster glaucoma progression (4, 5).

Whitecoat adherence describes patients' tendency to improve their adherence in the days surrounding clinic visits (6). This effect has been documented in several chronic conditions including asthma (7), diabetes (8), and epilepsy (9). In glaucoma, whitecoat adherence is clinically relevant because it can lead to IOP measurements that are unrepresentative of those outside of clinical encounters. IOP readings within the target range may lead clinicians to overestimate treatment effectiveness, which may bias the interpretation of other clinical measures (e.g., visual field imaging results). Furthermore, the obtention of IOP readings within the target range may preclude recommendations for indicated adjunctive therapy or surgical intervention. In this study, we sought to assess whitecoat adherence in patients with POAG and identify factors associated with this phenomenon. We hypothesized that there would be an increase in adherence preceding the clinic visit and a decrease following this visit.

MATERIALS AND METHODS

Study Participants

Ancillary adherence data were obtained from patients enrolled in an NIH-funded longitudinal study (NIH grant EY025756) at the University of Alabama at Birmingham (henceforth referred to as the parent study). Participants in the parent study were required to have a POAG diagnosis, visual acuity better than 20/40, mean deviation better than −12 dB, spherical and cylindrical refraction within 5D and 3D, respectively, and be above age 18 at baseline. Participants with a history of secondary glaucoma, diseases affecting the visual field, intraocular surgery (except uncomplicated cataract or glaucoma surgery), or cognitive impairment were excluded. The parent study was approved by the University of Alabama at Birmingham Institutional Review Board and patients received standard clinical care throughout. All aspects of the study complied with HIPAA regulations and adhered to the tenets of the Declaration of Helsinki.

Medication Adherence

Medication adherence describes the degree to which actual medication use corresponds with prescribed medication use. The Medication Adherence Reporting Guideline (EMERGE) was developed by the International Society for Medication Adherence (ESPACOMP), and aims to standardize the measurement, analysis, and reporting of medication adherence. EMERGE recognizes three phases of adherence: initiation—when the patient takes the first dose of a prescribed drug, discontinuation—which marks the end of therapy, and implementation—which describes the degree to which patients use their medication as prescribed from treatment initiation to discontinuation (10). In this study, medication adherence was recorded using Medication Event Monitoring System (MEMS) caps (Aardex; Liège, Belgium) during the implementation phase (10, 11). Participants were given one MEMS per prescribed medication and were instructed to store their medication inside the MEMS containers. With this bottle-in-bottle approach, patients were required to open the larger MEMS container to retrieve their medication, replace the medication in the MEMS container after use, and carefully resecure the MEMS caps. Each opening of the MEMS container is logged by the MEMS cap and the electronic measurement serves as a proxy for an instilled eyedrop. Although this method is imperfect, it has been reliably used in previous studies (12, 13). Participants did not receive reminders or feedback on their adherence but were informed at the start of the parent study that the MEMS caps recorded the date and time at which the containers were opened. During research visits, data from the MEMS caps were uploaded into MedAmigo—a web platform for data analysis and visualization—using a MEMS universal serial bus near-field communication reader. Daily adherence was calculated using the following formula:

$$\frac{\textit{Number of doses taken}}{\textit{Number of doses prescribed}}\ \textit{X 100\%}$$

No penalties were applied for taking doses that exceeded the prescribed number, and extra doses were excluded from the calculations. For patients with multiple medications, daily adherence was calculated per medication and averaged across the total number of medications. Adherence data were downloaded from MedAmigo and reviewed to ensure that all changes in regimen during the parent study were accounted for. Adherence data for the first 2 months of the parent study were excluded from this analysis to minimize the influence of the Hawthorne effect, which is more marked at the start of the monitoring period (9).

Clinic Visits

To be included in this analysis, participants from the parent study needed to have attended at least one clinic visit with their eye care provider between May 10, 2018 (the start of the parent study) and March 13, 2020 (date of the declaration of the Covid-19 pandemic). We excluded clinic visits after March 13, 2020, as research indicates that adherence in glaucoma was negatively affected during the COVID-19 pandemic (14, 15). We reviewed participants' clinical charts to identify eligible clinic visit dates. To limit the influence of whitecoat adherence associated with research visits during the parent study, we excluded clinic visits that occurred within 14 days of a research visit (16). For each

patient, we selected the first eligible clinic visit date and calculated mean daily adherence for each of the days in the 28-day period evenly bracketing this date.

Factors Associated With Whitecoat Adherence

To identify factors associated with whitecoat adherence, we included the demographic, clinical, and psychological data collected during the parent study. Demographic factors included patients' self-reported age, race, gender, education level, marital status, employment level, and income level. Clinical factors included mean adherence, number of prescribed ocular medications, and regimen complexity. We operationalized regimen complexity as the number of daily eyedrop instillations multiplied by the number of prescribed ocular medications (17). Mean adherence was computed for each participant over the 180-day period evenly bracketing the date of the clinic visit. Psychological factors included patients' perceptions of glaucoma, which were assessed using the Brief Illness Perception Questionnaire (BIPQ) (18). The BIPQ uses a 0–10 Likert-type scale to assess eight domains related to illness perception: consequences, timeline, personal control, treatment control, identity, concern, emotional representation, and coherence. Subscale and total BIPQ scores were computed.

Statistical Analysis

Based on previous work showing an increase in adherence within the 3-day period preceding the clinic visit (9, 19), we used Wilcoxon signed-rank test to identify significant differences in mean adherence between the following study periods: Pre_{14-4} (days 14 to 4 preceding the clinic visit) and Pre_{3-1} (days 3 to 1 preceding the clinic visit); $Post_{1-3}$ (days 1 to 3 following the clinic visit) and $Post_{4-14}$ (days 4 to 14 following the clinic visit). **Figure 1** depicts the study design and study periods. As research indicates that whitecoat adherence may vary by adherence level (20), we stratified participants using an 80% threshold (21), where adherence <80% was deemed to be suboptimal and adherence ≥80% was deemed to be optimal. Wilcoxon signed-rank test was repeated in each adherence group. Lastly, we performed univariate linear regression to identify factors associated with whitecoat adherence, which we operationalized as an increase in adherence from Pre_{14-4} to Pre_{3-1} or a decrease in adherence from $Post_{1-3}$ to $Post_{4-14}$. Analyses were performed in JMP Pro (version 16), and alpha was set at 0.05.

RESULTS

A total of 66 participants were included in this analysis. **Table 1** presents participant characteristics. Mean age was 70.8 ± 8.1 years and mean number of prescribed hypotensive medications was 1.6 ± 0.7. Approximately 51.5% of participants were female and 57.6% self-reported as White. Fifty-nine percent of participants attained a baccalaureate degree or higher, and approximately 30% reported a household income of $60,000 or more. Mean adherence was 86.3% ± 17.7 compared to the median value of 95.6% (interquartile range, IQR = 21.2) Median BIPQ total score was 27 (IQR = 12). The maximum possible BIPQ total score was 80, with higher BIPQ total scores indicating a more daunting outlook on glaucoma.

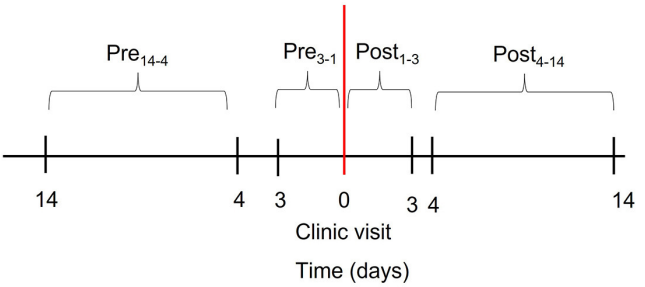

FIGURE 1 | Study design. Study periods within the 28 days evenly bracketing the clinic visit (red line) are depicted by black brackets.

Table 2 presents mean adherence during each study period in the overall sample, as well as in patients with optimal and suboptimal adherence. As depicted in **Figure 2**, patients with optimal adherence showed an increase in adherence both prior to and after the clinic visit (Pre_{14-4} to Pre_{3-1}: 94.0 ± 11.7 to 97.7 ± 7.4, $p = 0.001$; $Post_{1-3}$ to $Post_{4-14}$: 95.2 ± 12.0 to 95.4 ± 5.7, $p = 0.007$). There was no significant change from Pre_{14-4} to Pre_{3-1} ($p = 0.69$) or from $Post_{1-3}$ to $Post_{4-14}$ ($p = 0.32$) in patients with suboptimal adherence. In the entire sample, mean adherence increased from Pre_{14-4} to Pre_{3-1} (85.5% ± 21.2 to 88.5% ± 23.2, $p = 0.01$) and decreased from $Post_{1-3}$ to $Post_{4-14}$ (87.0 ± 23.9 to 84.9 ± 23.3, $p = 0.02$). Overall, there was a small but significant increase of 3.0% ± 15.2 (range = −36.4 to 63.64%) prior to the clinic visit and a decrease of 2.0% ± 15.0 (range = −36.4 to 54.5%) afterwards. Among only patients with whitecoat adherence prior to the clinic visit ($n = 29$), there was an increase of 13.4% ± 14.0 (range = 1.5 to 64%). Among patients with whitecoat adherence after the clinic visit ($n = 27$), there was a decrease of 13.4% ± 13.0 (range = −0.7 to −54%).

In the full sample, no clinical or demographic variables were associated with whitecoat adherence before or after the clinic visit. This was also true in patients with suboptimal adherence. In patients with optimal adherence, lower education level was associated with whitecoat adherence after the clinic visit (B = −4.0, $p = 0.046$). **Table 3** presents the associations between whitecoat adherence and BIPQ scores. In the full sample, a significant negative association was observed between whitecoat adherence before the clinic visit and BIPQ total score (B = −0.40, $p = 0.01$). This was also true in the optimal adherence group (B = −0.39, $p = 0.03$). The personal control and treatment control subscales of the BIPQ were negatively associated with whitecoat adherence prior to the clinic visit in the full sample (B = −1.41, $p = 0.02$ and B = −1.96, $p = 0.048$, respectively). Similar associations were observed in patients with optimal adherence (Personal control: B = −1.52, $p = 0.02$, Treatment control: B = −2.06, $p = 0.04$).

In the period following the clinic visit, no significant associations were observed between BIPQ subscale scores and whitecoat adherence in the full sample. Among patients with

TABLE 1 | Participants clinical, demographic, and psychological characteristics.

Study variable	
Age (years) mean ± SD	70.8 ± 8.1
Number of ocular medications, mean ± SD	1.6 ± 0.7
Medication adherence, mean ± SD (median, IQR)	Percentage (%)
Overall	86.3 ± 17.7 (95.6, 21.2)
Optimal ($N = 49$)	95.1 ± 5.5 (97.8, 6.8)
Suboptimal ($N = 17$)	60.7 ± 15.9 (64.6, 18.2)
Gender	Percentage (%)
Female	51.5
Male	48.5
Race	Percentage (%)
White	57.6
Black	42.4
Education level	Percentage (%)
High school/Some college	40.9
Baccalaureate	31.8
Graduate	27.3
Marital status	Percentage (%)
Married	65.2
Not married	34.8
Employment level	Percentage (%)
Employed full-time	28.8
Not employed full-time	71.2
Household income	Percentage (%)
$60,000 or less	42.5
Above $60,000	30.3
Declined to answer or unknown	27.2
BIPQ subscale scores	Median (IQR)
Total BIPQ score	27 (12)
Consequences	1 (2.3)
Timeline	10 (0.25)
Personal control	2 (4.3)
Treatment control	1 (2)
Identity	0.5 (3.3)
Concern	8 (5)
Emotional representation	1 (2)
Coherence	1 (2.3)

optimal adherence, there was a positive association between BIPQ total score and whitecoat adherence (B = 0.29, $p = 0.04$), as well as between the concern subscale score and whitecoat adherence (B = 1.26, $p = 0.01$). Among patients with suboptimal adherence, there was a negative association between the concern subscale score and whitecoat adherence (B = −5.46, p = 0.01), as well as between the consequences subscale score and whitecoat adherence (B = −3.89, $p = 0.05$).

DISCUSSION

Whitecoat adherence has previously been documented in several chronic conditions (7, 8, 22). In this study, we reported the presence of whitecoat adherence in patients with POAG, which supported our hypothesis. We documented higher adherence within 3 days of the clinic visit, consistent with findings by Modi et al. (9) who reported a significant increase in the use of anti-epileptic drugs in the 3 days preceding the clinic visit. A similar finding was documented by Zueger et al. (19) who found that a significantly higher number of insulin boluses were administered in the 3 days prior to clinic visits. In glaucoma, Kass et al. also observed a significant increase in adherence, specifically within 24 h of the clinic visit (23).

We observed whitecoat adherence within 3 days of the clinic visit in the overall sample as well as in patients with adherence ≥80%. This suggests that patients with higher adherence may also have higher levels of healthcare engagement, which would prompt them to place greater emphasis on their adherence, particularly prior to the clinic visit. However, Okeke et al. reported a whitecoat effect in patients with adherence below 75% (20). This discrepancy could be due to differences in the characteristics of the two cohorts. Patients included in our analysis were also participants in a 2.5-year longitudinal study, and may have higher levels of healthcare engagement compared to patients not engaged in clinical research. In this study, whitecoat adherence was not observed in patients with suboptimal adherence. This could potentially be due to the small size of this group. Although there was a large decrease in adherence after the clinic visit, high variability in adherence measurements in this group reduced our ability to detect a significant effect. Overall, there was a mean increase of 3% prior to the clinic visit and a mean decrease of 2% afterwards. Among only patients who demonstrated a whitecoat effect, there was a mean change of ±13.4% before and after the clinic visit. The magnitude of this change is sufficiently large to be of concern clinically.

Medication adherence is a complex and dynamic behavior as up to five distinct patterns have been observed in POAG (24–27). During a given period for instance, highly adherent patients may take drug holidays. As such, metrics such as mean and median adherence may not adequately capture gaps in medication use, resulting in undetected periods of uncontrolled IOP. Hypotensive eyedrops lower IOP per 12 or 24-h, which can mask periods of uncontrolled IOP prior to the clinic visit. In the absence of regular visual field testing—which may not be requested if IOP appears to be controlled—glaucomatous vision loss may not be easily detected. This line of thought is consistent with reports of progressive worsening of the visual field with IOP levels seemingly at or below the target when measured in the clinic (20). As suboptimal adherence has also been associated with faster rates of vision loss (5), it also has a significant negative impact on clinical and patient-reported outcomes. Poor and non-adherence may go undetected by providers, and the opportunity to prescribe alternative therapies or deliver interventions that could improve adherence and delay further worsening of the visual field may also be missed.

Whitecoat adherence can be attributed to several factors. For instance, increasing proximity to the clinic visit likely serves as a reminder for patients to instill their medication and prevent disease progression. Additionally, the impending clinic visit signals imminent face-to-face contact with the eye

TABLE 2 | Mean adherence per study time point.

	Pre_{14-4}	Pre_{3-1}	P value	$Post_{1-3}$	$Post_{4-14}$	*P*-value
Overall	85.5 ± 21.2	88.5 ± 23.2	0.01	87.0 ± 23.9	84.9 ± 23.3	0.02
Optimal	94.0 ± 11.7	97.7 ± 7.4	0.001	95.2 ± 12.0	95.4 ± 5.7	0.007
Suboptimal	60.9 ± 23.7	61.8 ± 31.7	0.69	63.2 ± 33.1	54.7 ± 28.0	0.32

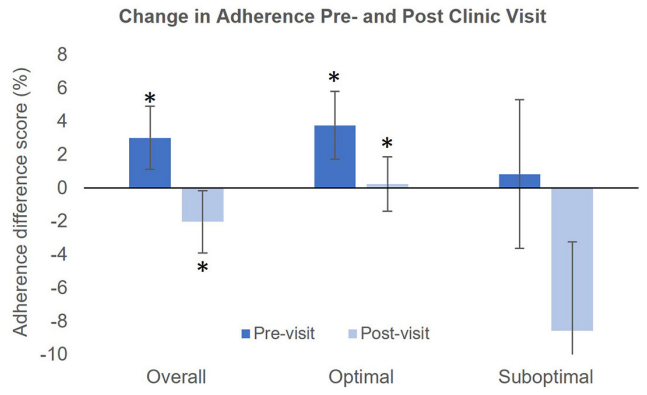

FIGURE 2 | Magnitude of the change in adherence pre- and post-clinic visit in the study population. Asterisks indicate significant differences between the Pre_{14-4} and Pre_{3-1} or between $Post_{1-3}$ and $Post_{4-14}$.

care provider. This may motivate patients to increase their adherence in an effort to avoid providers' disapproval (20). In the clinic, medication adherence is often assessed via patient reports and is frequently overestimated (28). Whitecoat adherence may contribute to this effect as patients' assessments may be biased in favor of more recent adherence behavior. As research indicates that the whitecoat effect may be more marked at the beginning of treatment (9), newly diagnosed patients should monitored more closely for poor adherence and more objective methods should be employed where possible. In addition to increased monitoring, poor adherence may be addressed in the clinic by improving the patient-provider relationship. Research conducted in a cohort of hypertensive patients suggests that patients who engaged in active vs. passive decision-making had higher adherence (29). Providers may employ a shared decision-making approach that encourages patients to become more involved in their care. This may strengthen and lengthen the patient-provider relationship, which has also been associated with higher adherence (29). The patient-provider relationship has been identified as a facilitator of good adherence (30), and research has shown that non-adherent patients were less likely to believe that their eye doctors spent sufficient time talking with them about their eye condition (31). Increased focus on patient education regarding the clinical impact of poor adherence may also help to increase engagement in eye care and improve adherence to prescribed medical therapy.

In this analysis, we found that lower BIPQ total score was associated with whitecoat adherence prior to clinic visits. Patients with a less daunting view of glaucoma (lower BIPQ total score) may experience lower levels of psychological stress, which may lead to higher levels of engagement in eye care and ultimately higher adherence. This is consistent with the finding of Jiang et al. (32) who reported that BIPQ total score was inversely associated with medication adherence The personal control and treatment control subscales of the BIPQ describe patients' perceived level of control over their illness and degree to which treatment can help their illness, respectively. These scales are inverted, with lower scores representing higher perceived ability. Lower scores were associated with whitecoat adherence prior to the clinic visit. This finding may be explained by patients' higher levels of confidence in their control of the disease and the effectiveness of treatment, which may motivate them to improve their adherence as the clinic visit approaches. Lower scores on both subscales are analogous to higher self-efficacy and treatment efficacy, which have been linked with higher adherence (33, 34).

The illness concern subscale measures patients' level of concern about their condition. Lower scores were associated with lower adherence after the clinic visit in the optimal adherence group compared to higher adherence after the visit in the suboptimal adherence group. Thus, the clinic visit may have a different impact on these patient groups. Patients with optimal adherence and low levels of concern about glaucoma may feel secure in their management of the condition and may not be driven to improve their adherence after the clinic visit. However, for patients with suboptimal adherence, the clinic visit may reinforce the need to control IOP and prevent vision loss, leading to higher adherence after the visit. This could also explain the positive association between illness consequences score—which describes the perceived impact of illness on one's life—and whitecoat adherence after the clinic visit. Given the ramifications of whitecoat adherence on clinical outcomes, prioritizing this topic during patient-provider discussions is critical for helping patients to maintain high levels of adherence throughout the course of treatment.

This study has several strengths. We assessed adherence using electronic monitoring, which provides objective measurements. A drawback of this approach is that patients using electronic monitors are susceptible to the Hawthorne effect, which can produce artificially high measurements. However, we guarded against this by excluding the first 2 months of monitoring data. We were also able to identify psychological factors associated with whitecoat adherence, providing potential insight into this phenomenon. This study is not without limitations, which include the surrogate nature of the adherence data collected with MEMS. However, this method has been shown to yield more accurate data than self-report. While direct observation

TABLE 3 | Coefficients for the relationship between BIPQ scores and whitecoat adherence.

BIPQ Scores	Pre_{14-4} to Pre_{3-1} estimate			$Post_{1-3}$ to $Post_{4-14}$ estimate		
	Overall	Optimal	Suboptimal	Overall	Optimal	Suboptimal
Total BIPQ Score	**−0.40**	**−0.39**	−0.48	0.11	**0.29**	−0.81
Consequences	−1.13	−1.00	−1.29	−0.54	1.24	**−3.89**
Timeline	−0.21	−0.04	−0.65	0.97	0.94	1.34
Personal control	**−1.41**	**−1.52**	−1.12	0.76	0.33	1.42
Treatment control	**−1.96**	**−2.06**	−1.48	−0.68	0.18	−4.97
Identity	−1.08	−1.16	−0.80	0.05	1.13	−3.56
Concern	−0.47	−0.47	−0.28	0.38	**1.26**	**−5.46**
Emotion	−1.16	−1.46	−0.49	0.57	−0.53	3.26
representation	−0.64	−0.56	−0.73	−0.08	0.71	−2.52
Coherence						

Bolded values represent statistically significant estimates.

would be more accurate, it is not practical in glaucoma where patients instill eyedrops daily. A second limitation associated with the longitudinal cohort used in this study was our inability to assess whitecoat adherence over multiple clinic visits. This was not possible as the number of research visits during the parent study reduced the number of eligible clinic visits for our analysis. Another limitation is the possible presence of a whitecoat effect throughout the parent study. Participants enrolled in the parent study were required to complete 12 research visits over a 2.5-year period. This may have contributed to a consistent whitecoat effect throughout the parent study which could have minimized the magnitude of the effect detected during the period of our analysis. We minimized this limitation by ensuring that no research visits occurred within the 28-day period evenly bracketing the clinic visit. Nonetheless, our ability to detect whitecoat adherence in this cohort suggests that the effect may be even more marked in the wider patient population. Lastly, the relatively small number of patients with suboptimal adherence reduced our ability to detect a whitecoat effect in this group.

In this study, we documented a significant increase in adherence within 3 days of the clinic visit. This supported our hypothesis. Beliefs about personal control, treatment control, illness concern, and illness consequences were associated with whitecoat adherence. Providers should remain vigilant for these factors and prioritize discussions regarding medication adherence during clinic visits. Future research should assess whitecoat adherence using electronic monitoring to determine whether this finding is consistent in the wider patient population.

DATA AVAILABILITY STATEMENT

The raw data supporting the conclusions of this article will be made available by the authors, without undue reservation.

ETHICS STATEMENT

The studies involving human participants were reviewed and approved by University of Alabama at Birmingham Institutional Review Board. The patients/participants provided their written informed consent to participate in this study.

AUTHOR CONTRIBUTIONS

SP: study design, data analysis, and manuscript preparation. NS: data preparation, and manuscript preparation. LR: study design, data analysis, manuscript preparation, and supervision of all aspects of research. All authors contributed to the article and approved the submitted version.

FUNDING

This study was supported by the National Eye Institute of the National Institutes of Health (Bethesda) under award numbers R01EY025756 and P30EY003039. The study was also supported by an unrestricted grant from Research to Prevent Blindness. The sponsors had no role in the design or conduct of this research.

REFERENCES

1. Tham YC Li X, Wong TY, Quigley HA, Aung T, Cheng CY. Global prevalence of glaucoma and projections of glaucoma burden through 2040: a systematic review and meta-analysis. *Ophthalmology.* (2014) 121:2081–90. doi: 10.1016/j.ophtha.2014.05.013
2. Olthoff CMG, Schouten JSAG, van de Borne BW, Webers CAB. Noncompliance with ocular hypotensive treatment in patients with glaucoma or ocular hypertension: an evidence-based review. *Ophthalmology.* (2005) 112:953–61.e7. doi: 10.1016/j.ophtha.2004.12.035
3. Friedman DS, Quigley HA, Gelb L, Tan J, Margolis J, Shah SN, et al. Using pharmacy claims data to study adherence to glaucoma medications: methodology and findings of the Glaucoma adherence and persistency study (GAPS). *Invest Ophthalmol Vis Sci.* (2007) 48:5052–7. doi: 10.1167/iovs.07-0290
4. Sleath B, Blalock S, Covert D, Stone JL, Skinner AC, Muir K, et al. The relationship between glaucoma medication adherence, eye drop technique, and visual field defect severity. *Ophthalmology.* (2011) 118:2398–402. doi: 10.1016/j.ophtha.2011.05.013
5. Newman-Casey PA, Niziol LM, Gillespie BW, Janz NK, Lichter PR, Musch DC. The association between medication adherence and visual field progression in the collaborative initial glaucoma treatment study. *Ophthalmology.* (2020) 127:477–83. doi: 10.1016/j.ophtha.2019.10.022

6. Cook P, Schmiege S, McClean M, Aagaard L, Kahook M. Practical and analytic issues in the electronic assessment of adherence. *West J Nurs Res.* (2012) 34:598–620. doi: 10.1177/0193945911427153
7. Keemink Y, Klok T, Brand P. White coat adherence in children with asthma enrolled in a comprehensive asthma management program. *Eur Respir J.* (2014) 44:P1161. doi: 10.1002/ppul.23138
8. Driscoll KA, Wang Y, Bennett Johnson S, Lynch R, Stephens H, Willbur K, et al. White coat adherence in pediatric patients with type 1 diabetes who use insulin pumps. *J Diabetes Sci Technol.* (2016) 10:724–9. doi: 10.1177/1932296815623568
9. Modi AC, Ingerski LM, Rausch JR, Glauser TA, Drotar D. White coat adherence over the first year of therapy in pediatric epilepsy. *J Pediat.* (2012) 161:695–9.e1. doi: 10.1016/j.jpeds.2012.03.059
10. Helmy R, Zullig LL, Dunbar-Jacob J, Hughes DA, Vrijens B, Wilson IB, et al. ESPACOMP medication adherence reporting guidelines (EMERGE): a reactive-Delphi study protocol. *BMJ Open.* (2017) 7:e013496. doi: 10.1136/bmjopen-2016-013496
11. Vrijens B, De Geest S, Hughes DA, Przemyslaw K, Demonceau J, Ruppar T, et al. A new taxonomy for describing and defining adherence to medications. *Br J Clin Pharmacol.* (2012) 73:691–705. doi: 10.1111/j.1365-2125.2012.04167.x
12. Cook PF, Schmiege SJ, Mansberger SL, Kammer J, Fitzgerald T, Kahook MY. Predictors of adherence to glaucoma treatment in a multisite study. *Ann Behav Med*. (2015) 49:29–39. doi: 10.1007/s12160-014-9641-8
13. Cook PF, Schmiege SJ, Mansberger SL, Sheppler C, Kammer J, Fitzgerald T, et al. Motivational interviewing or reminders for glaucoma medication adherence: results of a multi-site randomised controlled trial. *Psychol Health.* (2017) 32:145–65. doi: 10.1080/08870446.2016.1244537
14. Subathra GN, Rajendrababu SR, Senthilkumar VA, Mani I, Udayakumar B. Impact of COVID-19 on follow-up and medication adherence in patients with glaucoma in a tertiary eye care centre in south India. *Indian J Ophthalmol.* (2021) 69:1264–70. doi: 10.4103/ijo.IJO_164_21
15. Racette L, Abu SL, Poleon S, Thomas T, Sabbagh N, Girkin CA. The impact of the coronavirus disease 2019 pandemic on adherence to ocular hypotensive medication in patients with primary open-angle glaucoma. *Ophthalmology.* (2021) 129:258–66. doi: 10.1016/j.ophtha.2021.10.009
16. Muir K, Lee P. Glaucoma medication adherence: room for improvement in both performance and measurement. *Arch Ophthalmol.* (2011) 129:243–5. doi: 10.1001/archophthalmol.2010.351
17. Odegard PS, Carpinito G, Christensen DB. Medication adherence program: adherence challenges and interventions in type 2 diabetes. *J Am Pharm Assoc.* (2013) 53:267–72. doi: 10.1331/JAPhA.2013.12065
18. Broadbent E, Petrie KJ, Main J, Weinman J. The brief illness perception questionnaire. *J Psychosom Res.* (2006) 60:631–7. doi: 10.1016/j.jpsychores.2005.10.020
19. Zueger T, Gloor M, Lehmann V, Melmer A, Kraus M, Feuerriegel S, et al. White coat adherence effect on glucose control in adult individuals with diabetes. *Diabetes Res Clin Pract.* (2020) 168:108392. doi: 10.1016/j.diabres.2020.108392
20. Okeke CO, Quigley HA, Jampel HD. Ying G-s, Plyler RJ, Jiang Y, et al. Adherence with topical glaucoma medication monitored electronically: the travatan dosing aid study. *Ophthalmology.* (2009) 116:191–9. doi: 10.1016/j.ophtha.2008.09.004
21. Dreer LE, Girkin C, Mansberger SL. Determinants of medication adherence to topical glaucoma therapy. *J Glaucoma.* (2012) 21:234–40. doi: 10.1097/IJG.0b013e31821dac86
22. Blair CS, Beymer MR, Kofron RM, Bolan RK, Jordan WC, Haubrich RH, et al. PrEP Non-adherence, white coat dosing, and HIV risk among a cohort of MSM. *Open Forum Infect Dis.* (2020) 7:ofaa329. doi: 10.1093/ofid/ofaa329
23. Kass MA, Meltzer DW, Gordon M, Cooper D, Goldberg J. Compliance with topical pilocarpine treatment. *Am J Ophthalmol.* (1986) 101:515–23. doi: 10.1016/0002-9394(86)90939-6
24. Beckers HJ, Webers CA, Busch MJ, Brink HM, Colen TP, Schouten JS, et al. Adherence improvement in Dutch glaucoma patients: a randomized controlled trial. *Acta Ophthalmol.* (2013) 91:610–8. doi: 10.1111/j.1755-3768.2012.02571.x
25. Ajit RR, Fenerty CH, Henson DB. Patterns and rate of adherence to glaucoma therapy using an electronic dosing aid. *Eye.* (2010) 24:1338–43. doi: 10.1038/eye.2010.27
26. Cate H, Bhattacharya D, Clark A, Holland R, Broadway DC. Patterns of adherence behaviour for patients with glaucoma. *Eye.* (2013) 27:545–53. doi: 10.1038/eye.2012.294
27. Newman-Casey PA, Blachley T, Lee PP, Heisler M, Farris KB, Stein JD. Patterns of glaucoma medication adherence over 4 years of follow-up. *Ophthalmology.* (2015) 122:2010–21. doi: 10.1016/j.ophtha.2015.06.039
28. Lam WY, Fresco P. Medication adherence measures: an overview. *Biomed Res Int.* (2015) 2015:217047. doi: 10.1155/2015/217047
29. Schoenthaler A, Rosenthal DM, Butler M, Jacobowitz L. Medication adherence improvement similar for shared decision-making preference or longer patient-provider relationship. *J Am Board Family Med.* (2018) 31:752–60. doi: 10.3122/jabfm.2018.05.180009
30. Poleon S, Racette L, Fifolt M, Schoenberger-Godwin YM, Abu SL, Twa MD. Patient and provider perspectives on glaucoma treatment adherence: a delphi study in Urban Alabama. *Optom Vis Sci.* (2021) 98:1085–93. doi: 10.1097/OPX.0000000000001776
31. Stryker JE, Beck AD, Primo SA, Echt KV, Bundy L, Pretorius GC, et al. An exploratory study of factors influencing glaucoma treatment adherence. *J Glaucoma.* (2010) 19:66–72. doi: 10.1097/IJG.0b013e31819c4679
32. Jiang H, Zhao L, Yang L, Cai HY. Relationships among illness perceptions, medication beliefs and medication adherence in primary angle closure glaucoma patients. *Zhonghua Yan Ke Za Zhi.* (2017) 53:109–14. doi: 10.3760/cma.j.issn.0412-4081.2017.02.008
33. Sleath B, Blalock SJ, Stone JL, Skinner AC, Covert D, Muir K, et al. Validation of a short version of the glaucoma medication self-efficacy questionnaire. *Br J Ophthalmol.* (2012) 96:258–62. doi: 10.1136/bjo.2010.199851
34. Sleath B, Blalock SJ, Carpenter DM, Sayner R, Muir KW, Slota C, et al. Ophthalmologist-patient communication, self-efficacy, and glaucoma medication adherence. *Ophthalmology.* (2015) 122:748–54. doi: 10.1016/j.ophtha.2014.11.001

Conflict of Interest: LR is a scientific advisor for Olleyes, Inc.

The remaining authors declare that the research was conducted in the absence of any commercial or financial relationships that could be construed as a potential conflict of interest.

Publisher's Note: All claims expressed in this article are solely those of the authors and do not necessarily represent those of their affiliated organizations, or those of the publisher, the editors and the reviewers. Any product that may be evaluated in this article, or claim that may be made by its manufacturer, is not guaranteed or endorsed by the publisher.

frontiers | Frontiers in Medicine

ORIGINAL RESEARCH
published: 25 May 2022
doi: 10.3389/fmed.2022.873483

Putative Biomarkers in Tears for Diabetic Retinopathy Diagnosis

*Madania Amorim[1,2], Beatriz Martins[1,2], Francisco Caramelo[1,2], Conceição Gonçalves[3], Grimalde Trindade[3], Jorge Simão[3], Patrícia Barreto[4], Inês Marques[4], Ermelindo Carreira Leal[2,5], Eugénia Carvalho[2,5], Flávio Reis[1,2,6], Teresa Ribeiro-Rodrigues[1,2,6], Henrique Girão[1,2,6], Paulo Rodrigues-Santos[1,2,5,6], Cláudia Farinha[1,3,4,6], António Francisco Ambrósio[1,2,4,6], Rufino Silva[1,2,3,4,6] and Rosa Fernandes[1,2,4,6]**

[1] Coimbra Institute for Clinical and Biomedical Research, Faculty of Medicine, University of Coimbra, Coimbra, Portugal, [2] Center for Innovative Biomedicine and Biotechnology, University of Coimbra, Coimbra, Portugal, [3] Coimbra University Hospital, Coimbra, Portugal, [4] Association for Innovation and Biomedical Research on Light and Image, Coimbra, Portugal, [5] Center for Neuroscience and Cell Biology, University of Coimbra, Coimbra, Portugal, [6] Clinical Academic Center of Coimbra, Coimbra, Portugal

OPEN ACCESS

Edited by:
Menaka Chanu Thounaojam, Augusta University, United States

Reviewed by:
Lei Zhou, Singapore Eye Research Institute (SERI), Singapore
Claudio Bucolo, University of Catania, Italy

***Correspondence:**
Rosa Fernandes
rcfernandes@fmed.uc.pt

Specialty section:
This article was submitted to Ophthalmology, a section of the journal Frontiers in Medicine

Received: *10 February 2022*
Accepted: *19 April 2022*
Published: *25 May 2022*

Citation:
Amorim M, Martins B, Caramelo F, Gonçalves C, Trindade G, Simão J, Barreto P, Marques I, Leal EC, Carvalho E, Reis F, Ribeiro-Rodrigues T, Girão H, Rodrigues-Santos P, Farinha C, Ambrósio AF, Silva R and Fernandes R (2022) Putative Biomarkers in Tears for Diabetic Retinopathy Diagnosis. Front. Med. 9:873483. doi: 10.3389/fmed.2022.873483

Purpose: Tear fluid biomarkers may offer a non-invasive strategy for detecting diabetic patients with increased risk of developing diabetic retinopathy (DR) or increased disease progression, thus helping both improving diagnostic accuracy and understanding the pathophysiology of the disease. Here, we assessed the tear fluid of nondiabetic individuals, diabetic patients with no DR, and diabetic patients with nonproliferative DR (NPDR) or with proliferative DR (PDR) to find putative biomarkers for the diagnosis and staging of DR.

Methods: Tear fluid samples were collected using Schirmer test strips from a cohort with 12 controls and 54 Type 2 Diabetes (T2D) patients, and then analyzed using mass spectrometry (MS)-based shotgun proteomics and bead-based multiplex assay. Tear fluid-derived small extracellular vesicles (EVs) were analyzed by transmission electron microscopy, Western Blotting, and nano tracking.

Results: Proteomics analysis revealed that among the 682 reliably quantified proteins in tear fluid, 42 and 26 were differentially expressed in NPDR and PDR, respectively, comparing to the control group. Data are available via ProteomeXchange with identifier PXD033101. By multicomparison analyses, we also found significant changes in 32 proteins. Gene ontology (GO) annotations showed that most of these proteins are associated with oxidative stress and small EVs. Indeed, we also found that tear fluid is particularly enriched in small EVs. T2D patients with NPDR have higher IL-2/-5/-18, TNF, MMP-2/-3/-9 concentrations than the controls. In the PDR group, IL-5/-18 and MMP-3/-9 concentrations were significantly higher, whereas IL-13 was lower, compared to the controls.

Conclusions: Overall, the results show alterations in tear fluid proteins profile in diabetic patients with retinopathy. Promising candidate biomarkers identified need to be validated in a large sample cohort.

Keywords: diabetic retinopathy, tear fluid, inflammatory cytokines, metalloproteinases, proteome, exosomes

INTRODUCTION

Diabetic retinopathy (DR) is the most common complication of diabetes (1). It is the leading cause of significant vision loss and blindness in the working-age population, with significant socio-economic and quality-of-life implications (1–4). DR incidence increases with the duration of Type 2 Diabetes (T2D), the most common form of diabetes, and within 20 years of diagnosis, almost two thirds of people with T2D will have some degree of retinopathy. Based on the typical retinal microvascular lesions that become fundoscopically detectable, DR can be diagnosed and classified into two main classes: nonproliferative (NPDR) and proliferative (PDR) (5). DR is a progressive pathology, with a dynamic and varied nature from individual to individual, characterized by a set of complex changes in several key signaling pathways that coordinate communication between different retinal cells (6–8). Regular follow-up of diabetic patients could result in early detection and treatment of vision-threatening DR, enabling the prevention of up 98% of vision impairment to this condition (9). However, due to a lack of reliable markers, its diagnosis in asymptomatic patients is insufficient.

Besides neurovascular changes in the retina, a high percentage of diabetic patients develop complications in the anterior segment of the eye, including dry eye syndrome, corneal erosion, and impaired wound healing of the cornea (10). Diabetic patients can have decreased corneal sensitivity and decreased tear function. It has been reported that the impaired blood flow seen in DR can modulate the composition of tear fluid, suggesting that tears can reflect retinal changes even though there is no direct contacts between retina and tear fluid (11, 12). These alterations found in ocular surface are usually associated with inflammation, which can increase susceptibility to corneal infection and blindness (10, 13). The production of antimicrobial peptides (AMPs), which normally protect the ocular surface from bacterial infection and aid corneal wound healing by acting as anti-inflammatory mediators, is altered in tears from DR patients (13). Patients with PDR are more susceptible to impaired tear functions (14). A growing body of evidence links inflammation with diabetes-associated retinal perturbations. Upregulation of various proinflammatory cytokines, including TNF, has been reported in the vitreous/aqueous samples of diabetic patients with retinopathy (15–17). It seems that chronic inflammatory processes may also occur at the ocular surface of diabetic patients. Dysregulated inflammatory cytokine levels (MCP-1, IP-10, TNF) and decreased ratios of antiangiogenic and angiogenic cytokines were reported in T2D patients without or with DR (18, 19). Chronic hyperglycemia also triggers ocular surface changes (10). Several studies have found evidence of proteome changes in tear fluid of DR patients (12, 20, 21). Increased levels of lysozyme and low levels of lipocalin in the tear fluid were found in patients with DR (22). On the onset of PDR, lower amounts of lactoferrin and lipocalin, as well as a decrease in tear film function, were reported (22). It was also reported that diabetic and DR patients have increased levels of apolipoprotein A-1 (22). However, these studies did not assess the progression of DR or the assessment was made in a pool of tear samples prepared with different amounts of each sample (19). Therefore, tears may provide important information, namely biomarkers such as AMPs and inflammatory mediators, with clinical relevance for the diagnosis, staging and monitoring of DR.

To the best of our knowledge, a detailed examination of changes in the proteins, including AMPs, and inflammatory mediators from ocular surface of patients with diabetes and their relationship to DR has not been performed to date. In the present study, we investigated the impact of chronic hyperglycemia on ocular surface AMPs and inflammation-related proteins present in the tear fluid in diabetic humans with NPDR and PDR.

Abbreviations: DR, Diabetic retinopathy; NPDR, nonproliferative diabetic retinopathy; PDR, proliferative diabetic retinopathy; T2D, Type 2 Diabetes; GO, Gene ontology; AMPs, antimicrobial peptides; MMP, matrix metalloproteinase; LFQ, label-free quantification; SDS, sodium dodecyl sulphate; FDR, false discovery rate.

MATERIALS AND METHODS

Patient Enrollment

This cross-sectional, non-interventional study was approved by the Ethics Committee of Centro Hospitalar e Universitário de Coimbra (CHUC; Coimbra, Portugal), with the identification CHUC-059-18. An informed consent from all participants was obtained after a detailed description of the aim and design of the study, as well as the possible complications. All procedures used in this study adhere to the tenets of the Declaration of Helsinki.

Patients with T2D, without or with DR (NPDR or PDR), as well as healthy subjects (control group) aged 40-75 years-old were included in this study. The exclusion criteria were as follows: cataract, glaucoma, or other eye diseases compromising visual acuity; systemic diseases potentially associated with tears abnormalities including rheumatoid arthritis, lupus, Sjögren's syndrome, thyroid related disorders such as Grave's disease, Hashimoto's and thyroiditis, asthma, allergies; use of anti-inflammatory, anti-bacterial or immunomodulatory drugs in the last 3 months; previous punctal plug; ocular surgery or trauma; active ocular infections or inflammations; use of contact lens within the previous 3 months; eyelid problems such as entropion, ectropion, Meibomian gland dysfunction and other anterior segment disorders and, kerato-refractive procedures (LASIK, LASEK, PRK) in the last year.

Fifty-four T2D patients with more than 5 years of diabetes duration and, under insulin therapy and/or other oral antidiabetic agents, were included in the study: 13 patients without DR, 25 patients with NPDR, and 16 patients with PDR. Twelve healthy subjects were in the control group. All criteria-satisfying control and patient groups underwent an ophthalmic examination. This ensured that inclusion and exclusion criteria were met and confirmed the stage of DR. We collected data and tear samples from both eyes of each subject whenever possible.

Schirmer Test Type 1 and Tear Sample Collection

To measure total tear secretion and collect tear samples, a Schirmer test type 1, using Schirmer filter paper strips (Dina strip Schirmer-Plus, Dina-Hitex, Bucovice, Czech Republic), was

performed. From each eye, sterile Schirmer filter paper strips were placed without anesthetic at the junction of the lateral and middle thirds of the lower eyelid and kept in place for 5 min, while subjects closed their eyes. The wet length of Schirmer strips (in mm) was registered. After tears collection, the wet portion of the strip was immediately soaked in 200 μl of 0.9% NaCl for 1 h to elute tear proteins, as previously reported (23). Eluted protein fractions were aliquoted and frozen at −80°C until analysis. Total tear protein concentration of each sample was determined by the Pierce BCA Protein Assay kit (Pierce Biotechnology Inc.), using bovine serum albumin as standard.

Tear Film Breakup Time

TBUT test was assessed for tear film stability. Fluorescein (0.5%) was instilled into participant's tear film and the interval between instillation and appearance of the first dry spots on the cornea was measured using a broad beam of slit lamp with a blue filter. A TBUT of <10 s was considered abnormal, indicative of tear instability.

Proteomics Analysis

Sample Preparation

Protein levels changes in tear samples were evaluated using mass spectrometry (MS)-based shotgun proteomics. A total of 32 samples was prepared for LC-MS/MS analyses. Proteins were denatured by addition of urea to a final concentration of 8 M in 20 mM HEPES, reduced by addition of 15 mM dithiothreitol (DTT) and incubation for 30 min at 55°C. Then proteins were alkylated by addition of 30 mM iodoacetamide (IAA) for 15 min at room temperature in the dark. Samples were diluted with 20 mM HEPES pH 8.0 to a final urea concentration of 4 M and proteins were digested with 1 μg lysyl endopeptidase (Wako) (1/100, w/w) for 4 h at 37°C. Samples were again diluted to 2 M urea and digested with 1 μg trypsin (Promega) (1/100, w/w) overnight at 37°C. The resulting peptide mixture was acidified by the addition of 1% trifluoroacetic acid (TFA) and desalted on a reversed phase (RP) C18 OMIX tip (Agilent). The tip was first washed 3 times with 100 μl pre-wash buffer [0.1% trifluoroacetic acid (TFA) in water/acetonitrile (ACN, 20:80, v/v)] and pre-equilibrated 5 times with 100 μl of washing buffer (0.1% TFA in water) before loading the sample on the tip. After peptide binding, the tip was washed 3 times with 100 μl of wash buffer and peptides were eluted twice with 100 μl elution buffer [0.1% TFA in water/ACN (40:60, v/v)]. The combined elutions were dried in a vacuum concentrator.

LC-MS/MS Analysis

Peptides were re-dissolved in 20 μl loading solvent A [0.1% TFA in water/ACN (98:2, v/v)] of which 2 μg were injected for LC-MS/MS analysis on an Ultimate 3000 RSLCnano system in-line connected to a Q Exactive HF mass spectrometer (Thermo). Trapping was performed at 10 μl/min for 4 min in loading solvent A on a 20 mm trapping column [made in-house, 100 μm internal diameter (I.D.), 5 μm beads, C18 Reprosil-HD, Dr. Maisch, Germany]. The peptides were separated on a 250 mm Waters nanoEase M/Z HSS T3 Column, 100Å, 1.8 μm, 75 μm inner diameter (Waters Corporation) kept at a constant temperature of 45°C. Peptides were eluted by a non-linear gradient starting at 1% MS solvent B [0.1% formic acid (FA) in water/ACN (2:8, v/v)] reaching 33% MS solvent B in 63 min, 55% MS solvent B in 87 min, 99% MS solvent B in 90 min followed by a 10-min wash at 99% MS solvent B and re-equilibration with MS solvent A (0.1% FA in water). The mass spectrometer was operated in data-dependent mode, automatically switching between MS and MS/MS acquisition for the 16 most abundant ion peaks per MS spectrum. Full-scan MS spectra (375-1,500 m/z) were acquired at a resolution of 60,000 in the Orbitrap analyzer after accumulation to a target value of 3,000,000. The 16 most intense ions above a threshold value of 15,000 were isolated with a width of 1.5 m/z for fragmentation at a normalized collision energy of 28% after filling the trap at a target value of 100,000 for maximum 50 ms. MS/MS spectra (200-2,000 m/z) were acquired at a resolution of 15,000 in the Orbitrap analyzer.

Data Analysis

Analysis of the mass spectrometry data was performed with MaxQuant (version 1.6.11.0) with mainly default search settings including a false discovery rate set at 1% on PSM, peptide and protein level. Spectra were searched against the human proteins in the Reference proteins database (database release version of January 2020 containing 20,365 human protein sequences, downloaded from http://www.uniprot.org). The mass tolerance for precursor and fragment ions was set to 4.5 and 20 ppm, respectively, during the main search. Enzyme specificity was set as C-terminal to arginine and lysine, also allowing cleavage at proline bonds with a maximum of two missed cleavages. Variable modifications were set to oxidation of methionine residues, acetylation of protein N-termini. Matching between runs was enabled with a matching time window of 0.7 min and an alignment time window of 20 min. Only proteins with at least one unique or razor peptide were retained. Proteins were quantified by the MaxLFQ algorithm integrated in the MaxQuant software. A minimum ratio count of two unique or razor peptides was required for quantification. A total of 312,428 peptide-to-spectrum matches (PSMs) were performed, resulting in 9,707 identified unique peptides, corresponding to 1,407 identified proteins. Further data analysis of the results was performed with the Perseus software (version 1.6.2.1) after loading the protein groups file from MaxQuant. Reverse database hits were removed, LFQ intensities were log2 transformed and replicate samples were grouped. Proteins with less than three valid values in at least one group were removed and missing values were imputed from a normal distribution around the detection limit leading to a list of 682 quantified proteins that was used for further data analysis.

Multiplex Analyses of Matrix Metalloproteinases and Cytokines in Tears

A set of three matrix metalloproteinases (MMP-2, MMP-3 and MMP-9) and eleven cytokines (GM-CSF, IFNγ, TNF, IL-1β, IL-2, IL-4, IL-5 and IL-6, IL-12p70, IL-13, IL-18,) were analyzed using a preconfigured panel ProcartaPlex Human MMP Panel II 3plex (Thermo Fisher Scientific, Vienna, Austria) and ProcartaPlex Human TH1 TH2 11plex (Thermo Fisher Scientific), respectively. These analyses were performed

using xMAP-based technology (Luminex) at the Laboratory of Immunology and Oncology (CNC-UC) and at the Blood and Transplantation Center of Coimbra (IPST). After thawing, tear samples were mixed firstly by vortex and then centrifuged at 10,000xg for 10 min, to remove eventual particulates. After, the supernatants were transferred to new Eppendorf microcentrifuge tubes. The assay workflow was performed according to the manufacturer's manual. Briefly, after 120 min incubation at room temperature of the magnetic beads with standards or samples, the wells were incubated for 30 min with detection antibody mixture and subsequently 30 min with streptavidin bound phycoerythrine solution. Between incubation times, thorough washing steps were performed. After adding reading buffer, the beads were analyzed with the Luminex instrument. Standard curves were generated by using the reference cytokine samples supplied by the manufacturer. Raw data were analyzed by ProcartaPlex Analyst 1.0 Software to obtain analyte concentrations in tear samples.

Isolation of Small Extracellular Vesicles From Tear Fluid

Small EVs were isolated using the total Exosome Isolation Reagent (Invitrogen, Thermo Fisher Scientific, Vilnius, Lithuania), according to the manufacturer. Briefly, after an overnight incubation at 4°C of the mixture of tear fluid with isolation reagent (2:1), samples were centrifuged at 10,000xg at 4°C for 1 h. The pellet was suspended in 50 µl of filtered phosphate-buffered saline (PBS) or 150 mM NaCl, 50 mM Tris (pH 7.5), 5 mM ethylene glycol tetraacetic acid, 1% Triton X-100 (Tx-100), 0.5% sodium deoxycholate and 0.1% sodium dodecyl sulphate (SDS), supplemented with 1× protease inhibitor cocktail (Roche, Indianapolis, IN, USA), 2 mM of phenylmethylsulfonyl fluoride and 2 mM of iodoacetamide (IAD) for Nanoparticle Tracking Analysis (NTA) or Western Blotting, respectively.

Nanoparticle Tracking Analysis

Small EVs were analyzed by performing NTA using a NanoSight NS300 instrument (Malvern Panalytical Limited, Malvern, UK). NTA acquisition settings were optimized, and the videos were used to perform the analysis and estimate the mean size and modal size and concentration of particles. Data were processed using NTA 3.3 analytical software (Malvern Panalytical Limited, Malvern, UK).

Transmission Electron Microscopy

An aliquot of small EVs resuspended in PBS were fixed with 2% paraformaldehyde (PFA) for TEM. After deposition of PFA-fixed small EVs on Formvar-carbon coated grids (TAAB Laboratories Equipment, Berkshire, UK), grids were contrasted with uranyl acetate for 5 min. Observations were carried out under TECNAI G2 Spirit BioTWIN electron microscope (FEI) at 100 kV.

Western Blot Analysis

Tear samples or small EVs were denatured with Laemmli buffer 5x without reducing agents (125 mM Tris-HCl (pH 6.8), 5% SDS, 20% glycerol and 0.01% bromophenol blue). Samples were loaded on polyacrylamide gels and proteins were separated by SDS-PAGE and transferred to polyvinylidene difluoride Amersham™ Hybond™ membranes (GE Healthcare, Cleveland, Ohio, USA). The membranes were blocked in 5% (m/v) nonfat milk in TBS-T (20 mM Tris, 150 mM NaCl, Tween 0.2%, pH 7.6) and probed with antibody against exosome markers CD63 (1:500; SICGEN, Cantanhede, Portugal) and flotillin-1 (1:250; Santa Cruz Biotechnology, Dallas, Texas) overnight at 4°C. After washing, the membranes were incubated with secondary anti-goat IgG-HRP-linked antibody (1:10,000; Bio-Rad, Hercules, California, USA) or anti-mouse IgG-HRP-linked antibody (1:10,000; Bio-Rad). The immunoreactive bands were detected by enhanced chemiluminescence (ECL) substrate using an imaging system (LAS500, GE Health Life Sciences, Chicago, Illinois, USA).

Bioinformatics and Statistical Analysis

Using the Gene Ontology (GO) knowledgebase (http://geneontology.org/), a database that until 2022-01-13 had 43,786 GO terms, 7,965,896 annotations, 1,566,018 gene products, 5,128 species, a GO enrichment analysis with the 682 quantified proteins as input list was carried out. Through the database, the input list was connected to an analyzing tool of the PANTHER Classification System. A PANTHER Overrepresentation Test (Released at 2021-02-24) with Homo sapiens as reference list was performed and molecular, biological processes and cellular components annotations data set were available considering Fisher's Exact test with FDR correction (FDR $p < 0.05$). From a reference list containing 20,595 protein IDs, a total of 624 proteins were mapped, remaining 38 proteins unmapped (24, 25). Protein-protein interactome analysis was performed using STRING (https:// string-db.org, version 11.5), a database that currently covers 24,584,628 proteins from 5,090 organisms (26–37). The analysis considered both functional and physical protein associations with 0.700 (high confidence) as minimum required interaction score. Before statistical analysis, MS data were log2 transformed.

Statistical Analysis

GraphPad Prism version 8.00 was used to perform data analysis. A *t*-test was performed (FDR = 0.05 and s0 = 1) to compare tear samples between control group and T2D, NPDR and PDR groups, and between NDPR and PDR groups, and a volcano plot was generated. For multiple comparison analysis, parameters were checked for normal distribution, given a $p < 0.05$ of the Shapiro-Wilk test. For normal distribution, one-way ANOVA followed by *post-hoc* analysis (Tukey test) was carried out to test for significance for a specific protein or analyte. Whenever a variable did not reach the normality assumption the non-parametric Kruskal-Wallis test followed by Dunn-Sidak test *post-hoc* test was performed. Differences between groups were considered significant at $p < 0.05$. The diagnostic power of biomarkers was evaluated with receiver operating characteristics (ROC) curves (AUC, confidence interval).

RESULTS

Characterization of the Study Population

The subjects enrolled in this study were 42-75 years old in the nondiabetic control group and 40-75 years old in the T2D group, with an average age of 62 years for the entire study population. Out of 66 participants, 42 (62.1 %) were males and 24 (37.9 %) were females. Between them, 12 were healthy, nondiabetic controls (control group) and 54 T2D patients, with 13 having no DR, 25 having NPDR, and 16 having PDR (**Table 1**). To investigate if tear secretion and tear stability were altered, we performed Schirmer's I test and TBUT, respectively. In T2D, the Schirmer I test values reduced significantly ($p < 0.05$), with 68% of diabetic individuals having values < 10 mm/5 min. Also, 61% of T2D with NPDR and 74% with PDR had a Schirmer test < 10 mm/5 min, with Schirmer values also significantly reduced compared to the control group ($p < 0.001$) (**Figures 1A,B**).

Compared with the control group, TBUT values in the NPDR and PDR groups were significantly decreased ($p < 0.05$) (**Figure 1C**). The results of the TBUT test indicate that individuals with DR (NPDR and PDR) have an average value below 10 s, reflecting changes in tear stability compared to controls.

Comprehensive Global Proteome Profiling of Tear Fluid

To investigate whether tear fluid proteomic composition in DR is altered, we performed LC-MS/MS of 8 samples/group. Spectra against human protein sequences were searched in the Swiss-Prot database after LC-MS/MS runs. In all 32 samples, 312,428 peptide-to-spectrum matches (PSMs), 9,707 peptides, and 1,407 protein groups were identified in the tear fluid with a FDR at 1% at the protein and peptide spectrum match levels (**Supplementary Table S1**), and a total of 682 protein groups were reliably quantified (**Supplementary Table S2**). We checked for well-known tear markers such lipocalin-1, serum albumin, lysozyme, lactotransferrin and lactoperoxidase to guarantee the quality of our samples.

The number of proteins in each tear sample was then determined. Although there was a trend toward an increased number of proteins in tears from T2D patients with DR compared to nondiabetic control group, there were no significant differences (**Supplementary Figure S1**).

To analyze what biological processes, molecular functions and cellular components got overrepresented, GO enrichment analysis was performed with the quantified proteins (**Figures 2A–F; Supplementary Tables S3A–C**), using bioinformatics tools of the PANTHER Classification System. From a reference list containing 20,595 protein IDs, 624 proteins were identified from a list created with 682 proteins, remaining 58 unidentified. Biological process analysis revealed that "small molecule metabolic process" and "regulation of biological activity" were the most significant terms. For molecular functions, proteins were mainly enriched in "protein binding" and "cadherin binding." The cellular components most populated were "extracellular exosome" and "extracellular vesicle" (**Figures 2A–C**).

Regardless of the statistical degree of enrichment analysis, for each of the GO categories, a representation of GO terms that were considered related or relevant to the physiology and/or pathogenesis of diabetes and/or DR was made. This analysis of enriched significant Biological processes, Molecular functions and Cellular components of 682 quantified proteins, revealed that highly expressed proteins might be related to response to glucose and to the retina, being involved in retina homeostasis, gliogenesis, retinoic metabolic process, regulation of endothelial cell migration and maintenance of blood vessels homeostasis by renin-angiotensin (**Figures 2D–F**). Moreover, the highly expressed proteins were mainly associated with regulation of proteolysis, innate and humoral immune responses, oxidative stress, and response to cytokine, among others (**Figures 2D–F**).

Since the cellular components were most populated with exosomal proteins, we next assessed the presence of small EVs in the tear fluid. Transmission electron microscopy of tear fluid from nondiabetic healthy controls revealed the presence of "non-vesicles" and "vesicles." Tear fluid-derived small EVs were shown to be cup-shaped or spherical vesicles, surrounded by a well-defined membrane (**Figures 2G,H**). NTA revealed that these vesicles were present in the tear fluid in a high concentration ($2.26 \times 10^9 \pm 1.65 \times 10^8$ particles/ml), where the modal size was 152.42 ± 10.81 nm, which is characteristic of small EVs (**Figure 2I**). Moreover, the exosome markers CD63 and Flotillin-1 were detectable in our samples, as revealed by Western blot analysis (**Figure 2J**).

Protein Composition Changes in Tear Fluid of T2D Patients Without or With DR

To assess whether there were statistically significant differences in expression levels of each protein between the nondiabetic healthy control group and the experimental groups, a Student's *t*-test (with a correction by Benjamin and Hochberg, with FDR = 0.05 and S0 = 1) was performed. For this analysis, all the quantified proteins were considered ($n = 682$), in which a comparison was made between the samples of each group in relation to the control group. Volcano plots show the $\log_{10}$ *p*-values for each protein *vs.* the respective $\log_2$ fold-change. These values, as well as the statistical significance, given as a value -log p, for each protein, were plotted on a volcano graph, with fold change values shown on the X axis and –log *p*-values on the Y-axis (**Figures 3A–C**). Only one protein [hemoglobin subunit beta (HBB)] was upregulated in T2D tear samples, according to the volcano plot analysis (**Figure 3A**, **Supplementary Table S4A**). The volcano plot of comparison between NPDR samples and control samples, revealed 38 proteins (CALML5, EEF1B2, TXNL1, GLUL, SET/SETSIP, ALCAM, APOBEC3A, KRT8, GLRX, GGCT, AHNAK, NAMPT, VCL, SH3BGRL, ABHD14B, GRHPR, TFF3, HNRNPA2B1, PDIA3, CRIP1, DDT/DDTL, NAPRT, AKR7A2, CAPS, GSTO1, TPT1, TMSB4X, GFPT1, CRYZ, PPP2R1A, TALDO1, GOT1, CAST, IQGAP1, RNPEP, CALML3, ADH1C, PPA1) significantly downregulated (**Figure 3C**, **Supplementary Table S4B**).

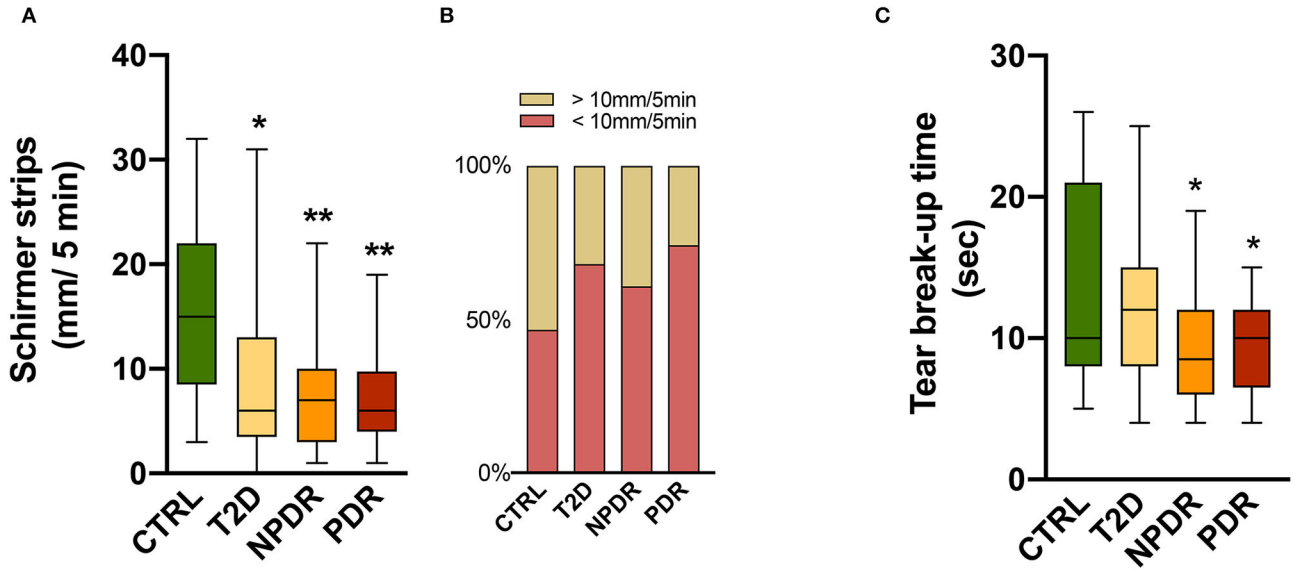

FIGURE 1 | (A,B) Tear function tests in healthy, nondiabetic controls and T2D patients without DR or with NPDR or PDR. **(A)** Schirmer test I showing significantly reduced scores in diabetics compared to controls (Kruskal-Wallis test). **(B)** Above 60% of diabetics have <10 mm/5 min of tears volume, suggesting impairment of tears secretion or production. **(C)** Tear break-up time (TBUT) showing significantly decreased (One-way ANOVA) values in NPDR and PDR subjects, reflecting changes in tear stability in DR. Values are expressed as mean ± S.D. $^{*}p < 0.05$, $^{**}p < 0.001$ vs. CTRL. CTRL, healthy, nondiabetic control; T2D, type 2 diabetes; NPDR, nonproliferative DR; PDR, proliferative DR.

TABLE 1 | Clinical characteristics in control subjects (CTRL), T2D patients without DR, T2D patients with NPDR and T2D patients with PDR.

Variables	Control ($n = 12$)	Diabetic ($n = 54$)		
	Healthy subjects	Without DR ($n = 13$)	NPDR ($n = 25$)	PDR ($n = 16$)
Age (years)	54 ± 11	59 ± 11	65 ± 9*	66 ± 6
Gender (male/female)	3/9	7/6	18/7	13/3
Diabetes duration (years mean ± SD)	not applicable	12 ± 7.5	19 ± 9.2#	22 ± 8.7##
Diabetes treatment type				
Oral medication	not applicable	82%	30%	17%
Insulin	not applicable	9%	35%	25%
Oral medication + insulin	not applicable	9%	35%	58%
HbA1c values (mean ± SEM)	-	7.1 ± 0.3	7.6 ± 0.2	7.9 ± 0.3

*$p < 0.05$ vs CTRL, #$p < 0.05$ vs Diabetic without DR, ##$p < 0.001$ vs Diabetic without DR.

In PDR samples, the volcano plot showed 24 proteins (NUTF2, APOBEC3A, HBB, NCCRP1, NAMPT, SET/SETSIP, ABHD14B, DEFA3/DEFA1, GLRX, PDIA3, CAST, TYMP, GLUL, PPP2R1A, RAB1A, TXNRD1, CALML5, IGKV3D-11, IGKV2-24/IGKV2D-24, CALR, LAP3, WARS, CALML3, PPA1) significantly upregulated and 2 proteins (SERPINF2 and CTSL) significantly downregulated compared to those in control group (**Figure 3C**, **Supplementary Table S4C**). Interestingly, we did not find differences in proteins expression between the PDR and NPDR groups (**Supplementary Figure S3**). Heatmaps of all proteins identified to be differentially expressed are shown in **Figures 3D,E**. To further examine the differentially expressed proteins, GO enrichment analyses were performed. Enrichment analysis for the cellular component term, demonstrated that these proteins were mainly located in extracellular vesicles, including small EVs in NPDR group (**Supplementary Table S5B**, **Figure 3F**), or associated to MHC class I peptide loading complex and endocytic vesicle lumen in PDR group (**Supplementary Table S6B, Figure 3G**). In both groups, the proteins overexpressed are mainly associated with disulfide-reductase activity (**Supplementary Tables S5A, S6A**).

To identify the significant differences in the proteomics profile of the different groups, we compared all the groups with each other, performing an ANOVA test (using S0 = 0 and FDR = 0.05). In this analysis, 32 proteins were significantly changed (**Supplementary Figure S4**; **Supplementary Table S4D**; **Figure 4A**). Nine proteins (S100A13, CSTB, SERPINF2, MTPN, GSN, PGD, NQO2, CFL1, and IMPA1) were differentially regulated in T2D patients with NPDR and PDR, compared

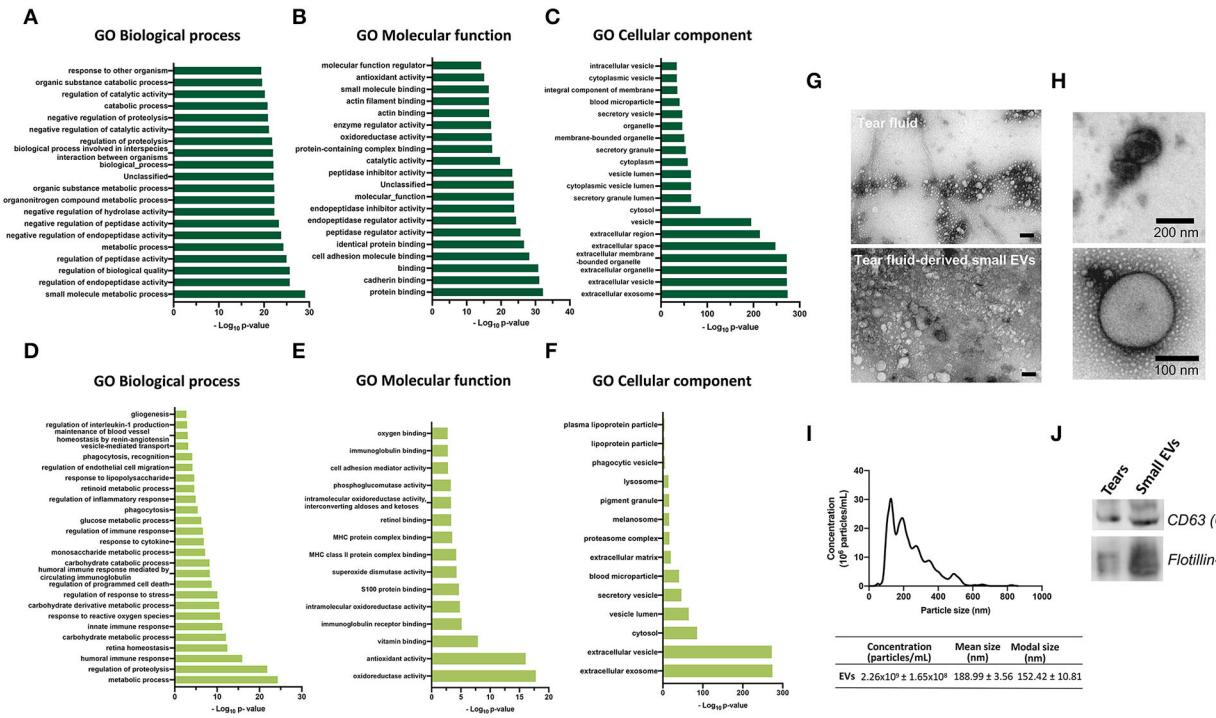

FIGURE 2 | (A–F) Gene Ontology enrichment analysis for GO biological process, molecular function and cellular component terms. Each diagram displays the bar plot of GO category terms along the y-axis and the corresponding degree of enrichment by the $-\log_{10}$ (p-value) on x-axis. Top-ranked 20 enriched significant **(A)** Biological processes, **(B)** Molecular functions and **(C)** Cellular components of quantified proteins by LC-MS/MS. **(D–F)** Enriched significant biological processes, molecular functions and cellular components of 682 quantified proteins by LC-MS/MS that might be associated with the retina. [Fischer's exact test (FDR $p < 0.05$)]. **(G–J)** Tear fluid and tear-derived small EVs from healthy, nondiabetic subjects. **(G,H)** Transmission electron microscopy images showing small EVs. Small EVs were obtained using Total Exosome Isolation Reagent. Scale bar of panel G: 100 nm. **(I)** Nanoparticle tracking analysis, showing the small EVs size distributions, mean size, modal size and concentration of particles. **(J)** Western blot analysis of small EVs using antibodies against CD63 and Flotilin-1.

with T2D patients without signs of DR. Significant changes in the levels of two proteins (NQO2 and IMPA1) were found in the PDR group compared with the NPDR group (**Supplementary Figure S4**). After differentially expressed proteins being identified between all groups, it was possible to found that 10 proteins (CALML3, CALML5, GLUL, SET/SETSIP, APOBEC3A, CTSL, GLRX, NAMPT, ABHD14B, and PDIA3) were common among NPDR and PDR, when performed a comparison between each diabetic subgroup to the control group or in multiple comparison, and 13 proteins are common to NPDR and PDR groups (**Figure 4B**). CALML3 and CALML5, like TXNDC17, TXNRD1, GLRX, PGD, and PDIA3, show a significant relationship, according to STRING analysis of the differentially regulated proteins (**Supplementary Tables S8A,B; Figure 4C**). In GO analysis of the 32 regulated proteins, we found that "glutathione oxidoreductase activity" and "regulated exocytosis" occurred significantly more frequently in the GO annotations (for molecular function and biological process, respectively) (**Supplementary Tables S8C,D, Figure 4D**), and "myelin sheath" and "ficolin-1-rich granule lumen" as the most enriched GO cellular components (**Supplementary Table S8E**, **Figure 4E**).

To understand how diabetes and DR progression affect the levels of inflammation related cytokines, we assessed the concentrations of inflammatory mediators in tears of controls and T2D patients without retinopathy and with NPDR or NPDR by multiplex immunoassays (**Figure 5**). We found an upregulation of pro-inflammatory cytokines, in particular IL-2, IL-18, IL-5 and TNF in NPDR group compared to nondiabetic control group (**Figures 5E,F,H,J**). To validate these inflammatory mediators as potential biomarkers able to differentiate NPDR group from control group, calculation of ROC was performed. High AUC revealed that IL-2 (AUC = 0.7519; CI 95% [0.5957; 0.9081]), IL-5 (AUC = 0.9218; CI 95% [0.8335; 1.000]), IL-18 (AUC = 0.8324; CI 95% [0.7024; 0.9624]) and TNF (AUC = 0.7724; CI 95% [0.6245; 0.9203]) show specificity and selectivity for NPDR group, when comparing to these tear inflammatory mediators measured in control individuals.

IL-4 and TNF were also significantly increased in this group compared to the T2D without retinopathy group (**Figures 5G,J**). ROC analysis revealed that IL-4 (AUC = 0.7848; CI 95% [0.6375; 0.9322] and TNF (AUC = 0.7908; CI 95% [0.6449; 0.9367]) enabled the identification of NPDR patients when compared to T2D patients without signs of DR.

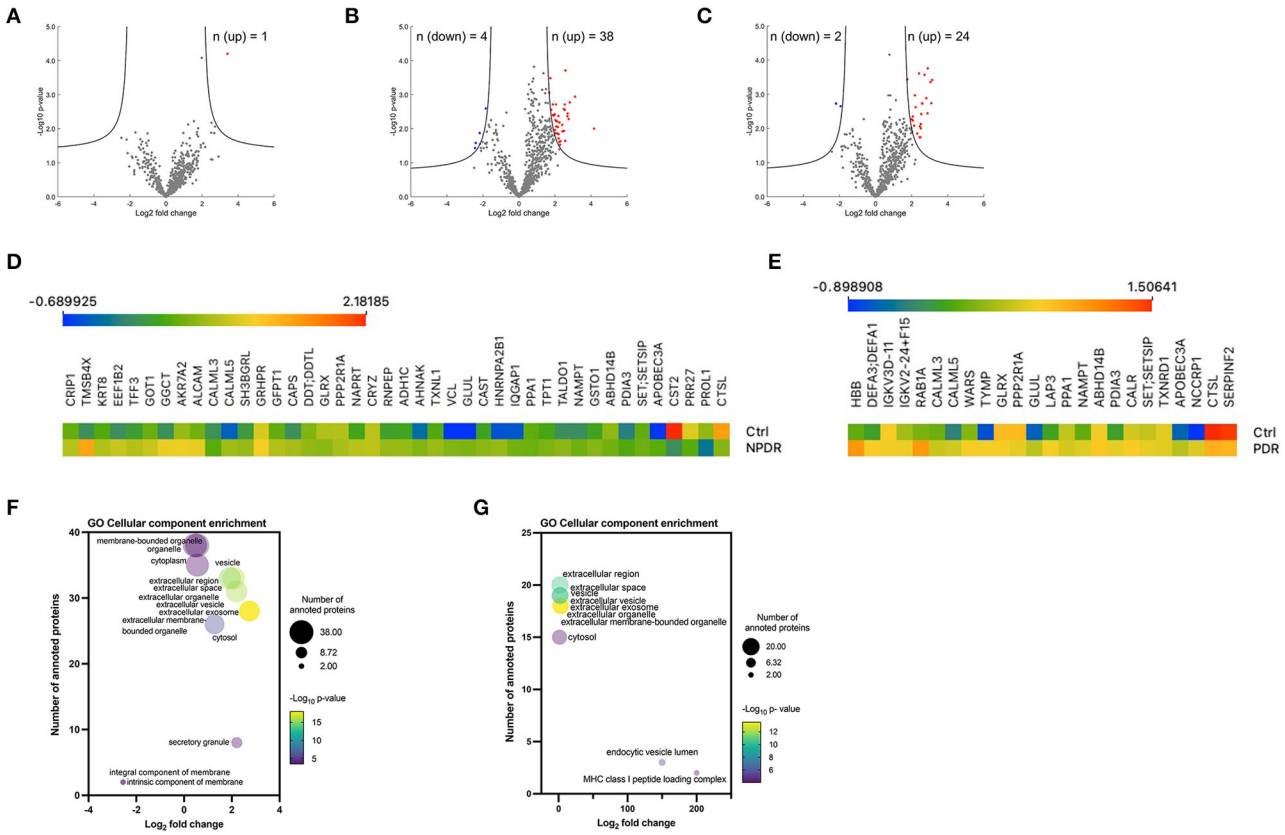

FIGURE 3 | Overview of significantly regulated proteins in diabetic subgroups compared to control group. **(A–C)** Volcano plots of proteomic data. Volcano plots were generated in the software Perseus, comparing the differential protein expression in tear fluid between nondiabetic healthy controls and **(A)** T2D group, **(B)** T2D with NPDDR, and **(C)** T2D with PDR. The points indicate different proteins that display magnitude fold-changes (Log_2; x-axis) and the *p*-values ($–Log_{10}$; y axis) of all proteins quantified in control group and each one of the other groups (two-sample *t*-test; FDR = 0.05, S0 = 1). Proteins with significant increases are indicated by red circles. Proteins with significant decreases are depicted by blue circles. **(D,E)** Heatmaps of the differentially expressed proteins. Protein expression values were log_2 normalized. Data corresponding to the proteins differentially expressed when comparing **(D)** NPDR and **(E)** PDR with the controls. Red indicates a high expression level; blue indicates a low expression level. **(F,G)** Bubble plots showing the enrichment for GO cellular component terms for the significantly expressed proteins in NPDR and PDR groups. The log_2 (fold change) in x-axis represents the ratio of total proteins identified and the different proteins expected to be related to each cellular component; the size of the bubble represents the number of proteins for each cellular component and color represents the $–log_{10}$ (*p*-value), which indicates the statistical significance. No statistically significant enrichment was found in biological process (not presented).

Interestingly, we found that only IL-18 and IL-5 were regulated in the same way in both PDR group and NPDR groups, and for TNF and IL-13, a decrease in these cytokines was observed compared to NPDR group (**Figures 5E,H,J,L,M**). High AUC of IL-5 (AUC = 0.9323; CI 95% [0.853; 1.000]) and IL-18 (AUC = 0.8158; CI 95% [0.6740; 0.9575]) was obtained allowing the identification of PDR group, when compared to AUC of IL-5 and IL-18 of control group. ROC analysis revealed that IL-13 (AUC = 0.8209; CI 95% [0.684; 0.9569]) and TNF (AUC = 0.7724; CI 95% [0.6245; 0.9203]) levels predicted the classification of NPDR, when comparing to the PDR group.

MMP-2,−3 and−9 protein concentrations were also assessed. We found increased MMP-2,−3 and−9 protein levels in the tear fluid from T2D patients without or with DR compared to nondiabetic healthy controls (**Figures 5N–Q**). ROC analysis revealed that MMP-3 (AUC = 0.8930; CI 95% [0.7904; 0.9956] for NPDR and (AUC = 0.9500; CI 95% [0.8747; 1.000] for PDR) and MMP-9 (AUC = 0.7919; CI 95% [0.6473; 0.9366] for NPDR and (AUC = 0.8609; CI 95% [0.7306; 0.9912] for PDR) tear levels predicted the identification of NPDR and PDR groups, when comparing to the control group. MMP-2 showed a lower AUC (AUC = 0.5711; CI 95% [0.3844; 0.7577], and so cannot be considered a reliable biomarker to identify the NPDR group, when compared to the control group.

DISCUSSION

In recent years, the interest in tear fluid as a potential source of biomarkers to diagnose several diseases has been increasing, due to its relatively easy non-invasive access and simple composition compared to other body fluids, such as blood and serum. Besides that, a gentle collection of tears, such as the one used in this study (with Schirmer test strips), enables the assessment of

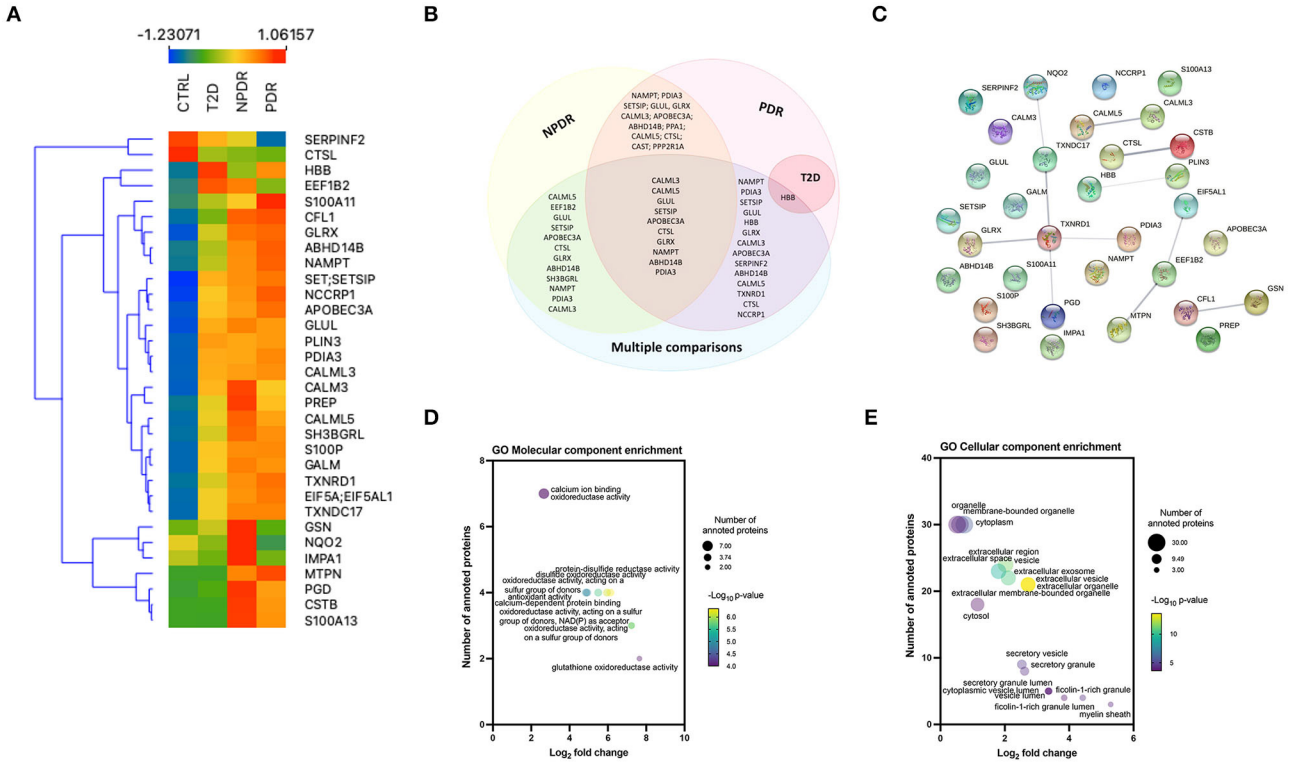

FIGURE 4 | Multiple comparison analysis between the diabetic subgroups and the control group. **(A)** Heatmap of the 32 significantly expressed proteins across replicates among diabetic subgroups and control group, showing a clear distinction between all the groups, and NPDR and PDR subgroups compared to control group. **(B)** Venn diagram displaying the overlapping statistically significant proteins between each diabetic subgroup vs. control group and, the comparison of the different groups with each other (multiple comparison). **(C)** STRING network interactome analysis of statistically significant proteins in multiple comparison. PPI enrichment *p*-value: 0.00357. Each node represents the 32 statistically significant proteins, the 11 edges represent the protein-protein associations (functionally or physically) and each edge strength represents the confidence of interaction. **(D)** Bubble plot displaying the significantly enriched GO Molecular function terms for significantly expressed proteins. The $\log_2$ fold change in x-axis represents the ratio of proteins; the size of the bubble represents the number of proteins and color represents the statistical significancy. **(E)** Bubble plot displaying the significantly enriched GO Cellular component terms for the differentially expressed proteins in multiple comparison analysis. Extracellular vesicle and extracellular organelle represented by overlapping yellow bubbles, are the most significant cellular component. No statistically significant enrichment was obtained in biological process (data not shown).

tear components (proteins/AMPs and inflammatory mediators) that eventually may be associated with DR. Herein, we designed a cross sectional, non-interventional study comprising nondiabetic, healthy controls, patients with T2D without retinopathy, with NPDR and PDR to investigate whether the tear fluid can be a source of biomarkers for diagnosis of DR.

According to several studies, dry eye syndrome is more common in diabetic individuals, which might be explained by reduced tear production or secretion mainly due to autonomic nervous system dysfunction (13, 38–42). In the population studied, with an average of 62 years, we found a significant proportion of individuals with decreased tear secretion, even in the healthy group. This is consistent with the fact that tear production declines with age due to the involution of the lacrimal and Meibomian glands and nerve activities that regulate them (43). Even though we did not conduct a comprehensive study, including a McMonnies' dry eye questionnaire or other questionnaires (44–47), to validate some of the symptoms associated with dry eye, such as foreign body sensation or itching, we detected dry eye using Schirmer's test. In addition, we performed another tear function assay, the TBUT. Schirmer and TBUT values were significantly reduced in NPDR and PDR groups, meaning a dysfunction of tear fluid production and stability in DR. These results are corroborated by some reports (39, 48) which suggest that diabetic individuals are more likely to suffer from dry eye syndrome than their age-matched peers and that with the progression of diabetes and DR, the risk is even greater. A study reported that autonomic neuropathy is present in 75% of diabetic patients with PDR (49). Chronic hyperglycemia, peripheral autonomic neuropathy, reduced insulin levels, and microvascular dysfunction, are risk factors for dry eye, that in diabetic subjects cause the decreased density of neuronal fibers of lacrimal glands and cornea, modifications of the cornea and conjunctiva epithelium, and increased osmolarity of the tear film (42). Altogether, they contribute to an inflammatory environment. These results suggest that dysfunction of the lacrimal functional unit may be related to the progression to dry eye disease in T2D patients.

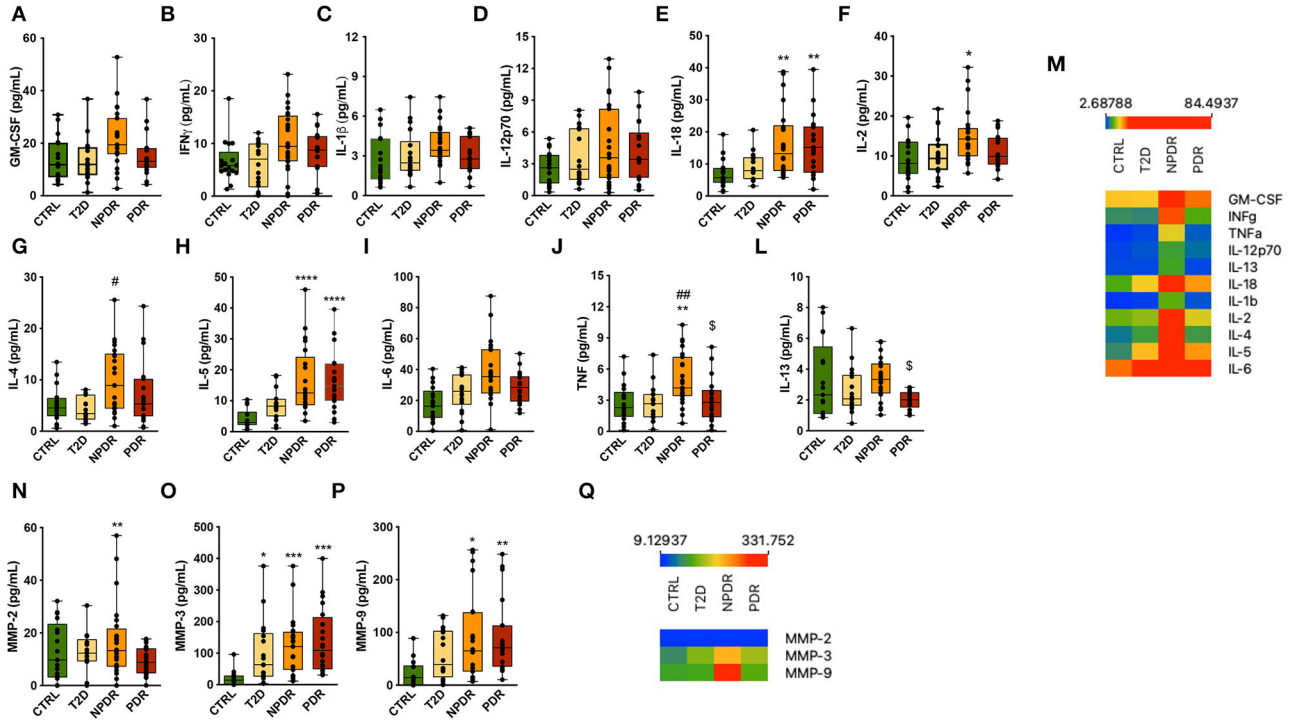

FIGURE 5 | Inflammation-related mediators in nondiabetic controls and T2D patients having no DR or with NPDR or PDR. **(A–L)** Th1- and Th2-type cytokines (GM-CSF, IFNγ, IL-1β, IL-12p70, IL-18, IL-2, IL-4, IL-5, IL-6, TNF, IL-13) were measured in the tear fluid by multiplex immunoassays. The concentrations of IL-2,−4,−5,−13,−18 and TNF were significantly changed. Increased concentrations of IL-18 and IL-5 were found in NPDR and PDR groups compared to control group, and TNF and IL-2 were found to be increased only in NPDR group. IL-4 and TNF concentrations were also significantly increased in NPDR compared to T2D group. Interestingly, the concentrations of TNF and IL-13 were significantly decreased in PDR group compared to NPDR group. **(M)** Heatmap of the expression of Th1/Th2 cytokines across replicates among control group and diabetic subgroups. **(N–P)** Multiplex analysis of MMPs in tear fluid. The concentration of MMP-2 was higher in NPDR group compared to control group. Increased concentrations of MMP-3 and−9 were also found in NPDR and PDR groups. MMP-3 concentration was found to be significantly increased in T2D group. **(Q)** Heatmap of the MMP's expression across replicates among control group and diabetic subgroups**.** (n = 17-26 samples/group; Kruskal-Wallis test; $^{*}p < 0.05$, $^{**}p < 0.01$, $^{***}p < 0.001$ vs. CTRL. ****p<0.0001 vs. Control, #p<0.05 vs T2D, ##p<0.001 vs T2D.

However, we should be cautious and should not discard that most of the diabetic patients take drugs, such as beta blockers and diuretics, commonly used to treat hypertension, which can also inhibit the production of tears.

In this study, we used Schirmer test strips to collect tear samples for proteomics analysis and assessed proteins of interest by a bead-based multiplexed immunoassay. We performed label-free quantitative proteomics analysis to compare the tear fluid of nondiabetic, healthy controls with T2D diabetic patients with no retinopathy, T2D patients with NPDR or PDR. There have been a few proteomics studies on the tear fluid in DR, however, most of them did not compare the four groups as we did (20, 21, 50–55). Overall, we identified 1,407 protein groups from tear fluid, being 682 proteins reliably quantified. In general, many of these proteins have already been described to be present in tear fluid in previous proteomics studies (56–58). However, a complex analysis involving healthy, diabetic patients without retinopathy and diabetic individuals with the main stages of retinopathy, to our knowledge, had not yet been performed.

We used gene enrichment analysis to find the enrichment of expressed proteins in biological processes, cellular components, and molecular function. We noticed that the proteomics profile of our enriched results indicated that significantly high expressed proteins in tear fluid are involved in key processes for the preservation of retinal homeostasis, including regulation of endothelial cell migration (fibroblast growth factor (A0A2I2YE38), annexin (G3QPT3), fibroblast growth factor (G3QIJ1), multifunctional fusion protein (FGF1), PRCP isoform 3 (PRCP)] and maintenance of vessel diameter [(transforming protein RhoA (RHOA), angiotensinogen (AGT) and alpha-1-antiplasmin (SERPINF2)]. The retinal vascular network is arranged hierarchically and plays a key role in homeostasis and disease. Endothelial cells form a single cell layer that lines all blood vessels and can respond to a variety of biomechanical stimuli in their environment, leading them to migrate and promote vascular morphogenesis or angiogenesis (59). The retina is a complex structure with intricate anatomical connections between the microvasculature, neurons, and glia. The local renin-angiotensin system (present in retinal microvessels, macroglial Müller cells, and ganglion cells) (60) has a key role in systemic

vascular control and electrolyte homeostasis, and dysfunction in this system is often associated with diseases of retinal vasculature, such as DR (61). Moreover, other proteins that are highly enriched in tear fluid are related to the processing of antigens (MHC II molecules), regulation of proteolysis, oxidative stress, and response to cytokine, which are critical modulators of innate immune responses in DR (62, 63).

Among the 682 proteins, we identified 13 proteins that were commonly changed among diabetic subjects with different stages of retinopathy, implying that the amounts of proteins in tear fluid might indicate the presence of DR. Moreover, this knowledge can be used to better understand the molecular mechanisms underlying DR and identify target candidates of the disease. In the multiple comparisons between the four groups, 32 proteins were found to be differentially expressed, with 10 of them [Calmodulin-like protein 5 (CALML5), Glutamine synthetase (GLUL), Protein SET; Protein SETSIP (SET/SETSIP), DNA dC->dU-editing enzyme APOBEC-3A (APOBEC3A), Cathepsin L1 (CTSL), Glutaredoxin-1 (GLRX), Nicotinamide phosphoribosyltransferase (NAMPT), Alpha/beta hydrolase domain-containing protein 14B (ABHD14B), Protein disulfide-isomerase A3 (PDIA3), and Calmodulin-like protein 3 (CALML3)] not known to be highly expressed in tear fluid. These immunomodulatory proteins are associated with oxidative stress response and are relevant in angiogenesis and the healing process (13). For example, the proteins Thymidine phosphorylase (TYMP), Glutamine synthetase (GLUL), Alpha-2-antiplasmin (SERPINF2), and Tryptophan–tRNA ligase (WARS1) form a cluster related to blood vessel morphogenesis and development. These proteins significantly changed in the PDR group compared to the control group. With this information, we can infer a probable implication in the pathogenesis of retinopathy. Cathepsin L1 (CTSL), Thymidine phosphorylase (TYMP), DNA dC->dU-editing enzyme APOBEC-3A (APOBEC3A) and F-box only protein 50 (NCCRP1) form a cluster related to carbohydrate derivative catabolic process, while Cathepsin L1 (CTSL), Ras-related protein Rab-1A (RAB1A) and F-box only protein 50 (NCCRP1) form a cluster related to glycoprotein metabolic process. These findings are relatively attractive because the levels of these proteins were shown to be significantly changed when a multiple comparison test was performed between the four groups, implying a relation with diabetes progression and microvascular complications such as DR. Ig kappa chain V-III region VG (IGKV3D-11) and Immunoglobulin kappa variable 2-24 (IGKV2D-24) are involved in the production of molecular mediators of immune response, immunoglobulin production and adaptive immune response processes, with the first two proteins being significantly changed only in the PDR group compared to the control group.

A previous study reported 20 proteins differently expressed in tears from diabetic individuals compared to healthy individuals by the ESI-Q-TOF MS/MS analysis (21). Among these, 2 were up-regulated (beta-2 microglobulin and DJ-1 protein) and the others were down-regulated (S100A4/A8/A9, adenine phosphoribosyl transferase isoform, envelop protein, keratin 31, SAP1 protein, lipocalin 1-like-1, lipocalin, cytokeratin 4, lipocalin 1 precursor, HSP27, beta globin phosphohistidine phosphatase, phosphohistidine phosphatase). In other studies, NPDR patients had reduced levels of lipocalin-1, HSP27, beta-microglobulin in tears and increased levels of endothelin and neuron-specific enolase, while PDR subjects had increased levels of nerve growth factor, APOA1, lipocalin 1, lactotransferrin, lacritin, lipophilin A and Immunoglobulin lambda chain (21). Some of these proteins were also identified in our study, although without statistically significant differences, probably due to the small sample size. This might limit the interpretation of the results obtained. Nevertheless, these proteins are described as being involved in immune processes, inflammatory and oxidative stress processes. Although they are described as abundant proteins in the tear fluid, it is not yet known if they have a direct implication in DR pathophysiology. However, certain aspects such as the type of study and groups involved, as well as, the type of tears collected, the extraction procedures, and the proteomics techniques chosen for each type of study, must be considered in this comparative analysis between the present study and those previous studies. Furthermore, before being translated into clinical practice, proteomic findings must be confirmed using a larger cohort of samples and other methodologies.

Currently, there are a few promising circulating biomarkers for which verification evidence is now available (64). HbA1c levels, for example, have been shown to be a good predictor of DR risk and a useful clinical indicator when combined with other markers (65). Besides HbA1c, other protein biomarkers identified in circulation, saliva, vitreous or tears include basement membrane and extracellular matrix turnover markers [Collagen IV, Matrix metalloproteinases (MMPs)], enzyme inhibitors [cystatin C, α-2-macroglobulin (A2MG)], plasma protein transport regulators [afamin (AFM), apolipoproteins, retinol binding protein 4 (RBP4)], coagulation cascade mediators (complement cascade proteins and serpinA4), inflammatory mediators such as lipoprotein-associated phospholipase A2 (Lp-PLA2), leucine-rich alpha-2-glycoprotein (LRG1), Interleukin-6, TNF, and other circulating factors such as advanced glycation end products and vascular endothelial growth factor (VEGF). Some of them were reported to be elevated in early and intermediate phases of NPDR (for example, IL-6, VEGF, and AGES) (64). Serum levels of transforming growth factor β (TGF- β1) have been recently shown to be predictive of DR progression from NPDR to PDR (66). Moreover, recent evidence has shown a correlation between specific miRNA and intraretinal hyper-reflective spots, assessed by optical coherence tomography (67).

One of the enrichments analyses, the GO cellular component, showed that most of the quantified proteins are associated with the extracellular space and are present in extracellular vesicles, including exosomes. These data corroborate a study that states that proteins enriched in tear fluid (from principal and accessories lacrimal glands, as well as from cells of the ocular surface) are mostly from the extracellular region, whereas proteins from the lacrimal fluid (exclusively from lacrimal gland) are mostly cytosolic, followed by the extracellular proteins. Considering that the tears were collected using the Schirmer test, the samples contain proteins secreted not only by the tear glands but also by the epithelial cells of the ocular surface, stromal immune cells and meibomian and gland acinar cells,

justifying the results obtained. Although we found that tear fluid is enriched in small EVs, we did not investigate whether their number or the levels of small EVs proteins are altered in the tear fluid of subgroups of T2D patients. Furthermore, we found the presence of structures with typical characteristics of small EVs both in the total tear fluid and in samples of isolated small EVs. Interestingly, other distinct structures were also observed. It was previously reported that exosome isolation using a precipitation-based approach, such as the one used in this work, can result in the presence of contaminating structures such as "non vesicles," microparticles, cell debris, and macroaggregates (68). In this work, the isolation method consists of the use of the polymer polyethylene glycol, to dehydrate and precipitate the vesicles. However, besides their precipitation, other extracellular vesicles, protein aggregates, and extracellular proteins can also be concomitantly isolated. To unveil the biological information these vesicles can be conveying, and the cells implicated in their production, further studies are required to carefully test and characterize the extracellular vesicles-derived tear fluid, not just from a physical standpoint but primarily from a composition one.

Studies indicate that the inflammatory environment associated with lacrimal functional unit dysfunction, and the pathophysiological of diabetes/ DR, are mediated by changes in inflammatory mediators (7, 8, 69–73). In this study, we analyzed 11 cytokines, from which, IL-2, IL-1b, TNF, IL-12p70, GM-CSF, and IFNγ are produced primarily by human CD4+ T-helper (Th) 1 cells, and IL-4, IL-5, IL-6, IL-13, IL-12p70, and IL-18 are mainly produced by Th2 cells. Th1 and Th2 cells are linked to inflammation and hypersensitivity and enhance both cellular and humoral immune responses. Previous reports demonstrated the presence of Th1 and Th2 cytokines in vitreous samples (74). We assessed the levels of these cytokines in our study to get a better understanding of the inflammatory process in T2D with DR. We found increased concentrations of various inflammatory cytokines (IL-2,−4,−5,−18, and TNF) in T2D patients with NPDR. The diagnostic power of biomarkers evaluated with ROC curves revealed that tears IL-2 and TNF present in tears can be considered acceptable biomarkers, and IL-18 and IL-5 can be excellent biomarkers for the discrimination of NPDR patients from control individuals.

We also found increased concentrations of IL-4 and TNF in the NPDR group compared to the T2D group. In this case, IL-4 and TNF can be considered acceptable biomarkers to discriminate NPDR group from T2D patients without signs of DR. Although no statistically significant changes in GM-CSF, IFNγ, IL2p70 and IL-6, there was a trend toward an increase in their concentrations in the NPDR group compared to control group. As a result, it is plausible that a disruption of the balance of pro-inflammatory and anti-inflammatory factors, required for retinal homeostasis, underly NPDR. Activated microglia, endothelial cells, macroglia, and neurons can produce increased levels of pro-inflammatory cytokines in the early stages of DR and contribute to exacerbating inflammatory response throughout all cell types of the retina. It has been reported that these mediators, with exception of IL-18, are also increased in serum and ocular (aqueous or vitreous samples) of both diabetic patients with NPDR and PDR. Interestingly, we did not find gradual increases in concentrations with the degree of DR, and we only found significantly higher concentrations of IL-5 and IL-18 in the PDR group than in the control group. Like in the NPDR group, the two interleukins revealed to be potential biomarkers for the discrimination of PDR patients from control individuals. IL-18 has been associated with retinal degenerative diseases, playing a critical role in angiogenesis (75). In the samples of tear fluid from the PDR group, there was a down-regulation of the anti-inflammatory cytokine IL-13 compared to the NPDR group, suggesting a decrease of anti-inflammatory activity in the tears of individuals with PDR. We also found decreased levels of TNF in the PDR group compared to the NPDR group, while other authors have detected higher TNF levels in the tear fluid of the PDR group (50). To understand the association between the lowered levels of protein factors and DR, more research into the precise roles of TNF- and other cytokines in the development of DR is needed.

Based on previous findings showing the role of MMPs on pathological processes related to DR (76, 77), we analyzed MMP-2,−3, and−9 in the tear fluid of control subjects, diabetic patients without signs of DR and diabetic patients with NPDR or PDR. We found increased levels of MMP-3 and−9 in the tear fluid of diabetic individuals with DR, which were shown to be promising biomarkers of DR, having an AUC close to 1. Although MMP-2 levels were also increased in the tear fluid of the NPDR group, it did not present a high AUC value in the ROC curve, meaning that it is not a good predictive biomarker for DR. Elevated levels of MMP-2 and−9 were previously reported in the vitreous and retina in patients with DR and animal models of the disease (76, 78, 79). Moreover, they were shown to act as pro-apoptotic, accelerating the apoptosis of retinal neuronal and endothelial cells (76, 79). Additionally, they were shown to play an important role in the development of DR, more specifically, their increased levels in the diabetic retina facilitate the increase in vascular permeability, through proteolytic degradation of the tight junction complexes (76). MMPs have also been reported to act on pro-inflammatory mediators, playing an important role in the switch in acute and chronic inflammation (77). MMPs also facilitate neovascularization in the advanced stages (77).

Although inflammatory mediators were not detected in proteomics analysis, some of the proteins that were identified by proteomics as significantly differentially expressed in multiple comparisons have been described as related to inflammation in DR. For example, S100A13 was significantly upregulated in diabetic individuals with NPDR. It has been reported to be involved in angiogenesis and cell apoptosis and has a moderately strong binding to receptors for advanced glycation end products (RAGE) which are involved in inflammatory processes of diabetes (80). Another example is GLRX, which was significantly increased in both stages of retinopathy. It was previously reported an increase in GLRX in the retinas of diabetic rats and retinal Müller glial cells cultured in high glucose. GLRX regulates NF-κB activation and induction of the inflammatory mediator intercellular adhesion molecule-1 (ICAM-1) (81). In the multiplex bead immunoassay, the quantification of inflammatory mediators allowed us to verify this trend, with an increase of the pro-inflammatory cytokines

IL-2, IL-18, IL-5 and TNF particularly in diabetic individuals with NPDR.

The proteomic study and multiplex immunoassay of the tears from patients with DR revealed valuable molecular information regarding already identified and novel proteins that are changed in tears in the context of this disease. After validating proteomics data using a larger cohort of individuals and a different methodological approach, a set of biomarkers can be identified and validated for DR diagnosis. These changes could also contribute to gaining a better understanding of DR.

CONCLUSIONS

In this study, we identified several proteins in tear fluid that are changed in the context of DR. Our findings not only confirm the presence of dry eye syndrome in patients with DR, but also unveil specific protein profile changes that are not present in DR patients. The altered proteins in tear fluid are associated with various biological processes, such as oxidative stress, immune response, and inflammation, characteristic of DR. Although a major limitation of this study is the small number of samples, the information presented here offers a foundation for future research into biomarkers in tear fluid and eventually in tear fluid-derived extracellular vesicles. A study with a larger sample size should be performed to validate our results. The identification of a set of biomarkers can improve the early diagnosis of DR and ensure prompt treatment for this vision-threatening disease.

DATA AVAILABILITY STATEMENT

The mass spectrometry proteomics data have been deposited to the ProteomeXchange Consortium via the PRIDE (82) partner repository with the dataset identifier PXD033101 and 10.6019/PXD033101.

ETHICS STATEMENT

The studies involving human participants were reviewed and approved by Comissão de Ética para a Saúde do CHUC, E.P.E. - Centro Hospitalar e Universitário de Coimbra, Praceta Prof. Mota Pinto 3000-075 Coimbra. The patients/participants provided their written informed consent to participate in this study.

AUTHOR CONTRIBUTIONS

EC, EL, FR, AFA, and RF: study design. GT, CG, JS, PB, IM, CF, and RS: clinical management. MA, BM, TR-R, PR-S, FC, and RF: data collection and analysis. MA, HG, and RF: data curation. MA and RF: writing—original draft preparation. HG, AFA, and RF: writing—review and editing. RS, and RF: supervision. RF: funding acquisition and project administration. All authors have read and agreed to the published version of the manuscript.

FUNDING

This study was funded by Faculty of Medicine, University of Coimbra/Santander-Totta (PEPITA Program), Study Group In Fundamental and Translational Research (GIFT) of the Portuguese Society of Diabetology (SPD), Portuguese National Funding Agency for Science and Technology (FCT) and Strategic Projects UIDB/04539/2020 and UIDP/04539/2020 (CIBB), and COMPETE-FEDER (POCI-01-0145-FEDER-007440); Centro 2020 Regional Operational Program: BRAINHEALTH 2020 (CENTRO-01-0145-FEDER-000008).

ACKNOWLEDGMENTS

The authors acknowledge the VIB Proteomics Core, Gent, Belgium, for the support in Proteomics study. The authors would like to thank Mónica Zuzarte of iLAB—Microscopy and Bioimaging Lab, Faculty of Medicine, University of Coimbra, a node of PPBI (Portuguese Platform of BioImaging, POCI-01-0145-FEDER-022122) for technical assistance in transmission electron microscopy. The authors would also like to thank the help of António Martinho and the Blood and Transplant Center of Coimbra (IPST, Portugal) with xMAP-based technology analyses.

SUPPLEMENTARY MATERIAL

The Supplementary Material for this article can be found online at: https://www.frontiersin.org/articles/10.3389/fmed.2022.873483/full#supplementary-material

REFERENCES

1. Biswas S, Sarabusky M, Chakrabarti S. Diabetic retinopathy, lncrnas, and inflammation: a dynamic, interconnected network. *J Clin Med.* (2019) 8:1033. doi: 10.3390/jcm8071033
2. Cheung N, Mitchell P, Wong TY. Diabetic retinopathy. *Lancet* (2010) 376:124–36. doi: 10.1016/S0140-6736(09)62124-3
3. Rodriguez ML, Perez S, Mena-Molla S, Desco MC, Ortega AL. Oxidative stress and microvascular alterations in diabetic retinopathy: future therapies. *Oxid Med Cell Longev.* (2019) 2019:4940825. doi: 10.1155/2019/4940825
4. Youngblood H, Robinson R, Sharma A, Sharma S. Proteomic biomarkers of retinal inflammation in diabetic retinopathy. *Int J Mol Sci.* (2019) 20:4755. doi: 10.3390/ijms20194755
5. Duh EJ, Sun JK, Stitt AW. Diabetic retinopathy: current understanding, mechanisms, and treatment strategies. *JCI Insight.* (2017) 2:e93751. doi: 10.1172/jci.insight.93751
6. Aboualizadeh E, Ranji M, Sorenson CM, Sepehr R, Sheibani N, Hirschmugl CJ. Retinal oxidative stress at the onset of diabetes determined by synchrotron Ftir widefield imaging: towards diabetes pathogenesis. *Analyst.* (2017) 142:1061-72. doi: 10.1039/C6AN02603F

7. Barrett EJ, Liu Z, Khamaisi M, King GL, Klein R, Klein BEK, et al. Diabetic microvascular disease: an endocrine society scientific statement. *J Clin Endocrinol Metab.* (2017) 102:4343-410. doi: 10.1210/jc.2017-01922
8. Santiago AR, Boia R, Aires ID, Ambrosio AF, Fernandes R. Sweet stress: coping with vascular dysfunction in diabetic retinopathy. *Front Physiol.* (2018) 9:820. doi: 10.3389/fphys.2018.00820
9. Solomon SD, Chew E, Duh EJ, Sobrin L, Sun JK, VanderBeek BL, et al. Diabetic retinopathy: a position statement by the American Diabetes Association. *Diabetes Care.* (2017) 40:412-8. doi: 10.2337/dc16-2641
10. Han SB, Yang HK, Hyon JY. Influence of diabetes mellitus on anterior segment of the eye. *Clin Interv Aging.* (2019) 14:53-63. doi: 10.2147/CIA.S190713
11. Sherwin JC, Kokavec J, Thornton SN. Hydration, Fluid regulation and the eye: in health and disease. *Clin Exp Ophthalmol.* (2015) 43:749-64. doi: 10.1111/ceo.12546
12. von Thun Und Hohenstein-Blaul N, Funke S, Grus FH. Tears as a source of biomarkers for ocular and systemic diseases. *Exp Eye Res.* (2013) 117:126-37. doi: 10.1016/j.exer.2013.07.015
13. Csosz E, Deak E, Kallo G, Csutak A, Tozser J. Diabetic retinopathy: proteomic approaches to help the differential diagnosis and to understand the underlying molecular mechanisms. *J Proteomics.* (2017) 150:351-8. doi: 10.1016/j.jprot.2016.06.034
14. Lv H, Li A, Zhang X, Xu M, Qiao Y, Zhang J, et al. Meta-analysis and review on the changes of tear function and corneal sensitivity in diabetic patients. *Acta Ophthalmol.* (2014) 92:e96-104. doi: 10.1111/aos.12063
15. Funatsu H, Yamashita H, Noma H, Mimura T, Nakamura S, Sakata K, et al. Aqueous humor levels of cytokines are related to vitreous levels and progression of diabetic retinopathy in diabetic patients. *Graefes Arch Clin Exp Ophthalmol.* (2005) 243:3-8. doi: 10.1007/s00417-004-0950-7
16. Demircan N, Safran BG, Soylu M, Ozcan AA, Sizmaz S. Determination of vitreous interleukin-1 (Il-1) and tumour necrosis factor (Tnf) levels in proliferative diabetic retinopathy. *Eye.* (2006) 20:1366-9. doi: 10.1038/sj.eye.6702138
17. Schwartzman ML, Iserovich P, Gotlinger K, Bellner L, Dunn MW, Sartore M, et al. Profile of lipid and protein autacoids in diabetic vitreous correlates with the progression of diabetic retinopathy. *Diabetes.* (2010) 59:1780-8. doi: 10.2337/db10-0110
18. Liu J, Shi B, He S, Yao X, Willcox MD, Zhao Z. Changes to tear cytokines of type 2 diabetic patients with or without retinopathy. *Mol Vis.* (2010) 16:2931-8.
19. Hagan S, Martin E, Enriquez-de-Salamanca A. Tear fluid biomarkers in ocular and systemic disease: potential use for predictive, preventive and personalised medicine. *EPMA J.* (2016) 7:15. doi: 10.1186/s13167-016-0065-3
20. Csosz E, Boross P, Csutak A, Berta A, Toth F, Poliska S, et al. Quantitative analysis of proteins in the tear fluid of patients with diabetic retinopathy. *J Proteomics.* (2012) 75:2196-204. doi: 10.1016/j.jprot.2012.01.019
21. Kim HJ, Kim PK, Yoo HS, Kim CW. Comparison of tear proteins between healthy and early diabetic retinopathy patients. *Clin Biochem.* (2012) 45:60-7. doi: 10.1016/j.clinbiochem.2011.10.006
22. Nguyen-Khuong T, Everest-Dass AV, Kautto L, Zhao Z, Willcox MD, Packer NH. Glycomic characterization of basal tears and changes with diabetes and diabetic retinopathy. *Glycobiology.* (2015) 25:269-83. doi: 10.1093/glycob/cwu108
23. Cruz A, Queiros R, Abreu CM, Barata C, Fernandes R, Silva R, et al. Electrochemical immunosensor for Tnfalpha-mediated inflammatory disease screening. *ACS Chem Neurosci.* (2019) 10:2676-82. doi: 10.1021/acschemneuro.9b00036
24. Ashburner M, Ball CA, Blake JA, Botstein D, Butler H, Cherry JM, et al. Gene ontology: tool for the unification of biology. The Gene Ontology Consortium. *Nat Genet.* (2000) 25:25-9. doi: 10.1038/75556
25. Gene Ontology C. The gene ontology resource: enriching a gold mine. *Nucleic Acids Res.* (2021) 49:D325-34.
26. Szklarczyk D, Gable AL, Nastou KC, Lyon D, Kirsch R, Pyysalo S, et al. The string database in 2021: customizable protein-protein networks, and functional characterization of user-uploaded gene/measurement sets. *Nucleic Acids Res.* (2021) 49:D605-12. doi: 10.1093/nar/gkaa1074
27. Szklarczyk D, Gable AL, Lyon D, Junge A, Wyder S, Huerta-Cepas J, et al. String V11: protein-protein association networks with increased coverage, supporting functional discovery in genome-wide experimental datasets. *Nucleic Acids Res.* (2019) 47:D607-13. doi: 10.1093/nar/gky1131
28. Szklarczyk D, Morris JH, Cook H, Kuhn M, Wyder S, Simonovic M, et al. The string database in 2017: quality-controlled protein-protein association networks, made broadly accessible. *Nucleic Acids Res.* (2017) 45:D362-8. doi: 10.1093/nar/gkw937
29. Szklarczyk D, Franceschini A, Wyder S, Forslund K, Heller D, Huerta-Cepas J, et al. String V10: protein-protein interaction networks, integrated over the tree of life. *Nucleic Acids Res.* (2015) 43:D447-52. doi: 10.1093/nar/gku1003
30. Franceschini A, Lin J, von Mering C, Jensen LJ. Svd-Phy: improved prediction of protein functional associations through singular value decomposition of phylogenetic profiles. *Bioinformatics.* (2016) 32:1085-7. doi: 10.1093/bioinformatics/btv696
31. Franceschini A, Szklarczyk D, Frankild S, Kuhn M, Simonovic M, Roth A, et al. String V9.1: protein-protein interaction networks, with increased coverage and integration. *Nucleic Acids Res.* (2013) 41:D808-15. doi: 10.1093/nar/gks1094
32. Szklarczyk D, Franceschini A, Kuhn M, Simonovic M, Roth A, Minguez P, et al. The string database in 2011: functional interaction networks of proteins, globally integrated and scored. *Nucleic Acids Res.* (2011) 39:D561-8. doi: 10.1093/nar/gkq973
33. Jensen LJ, Kuhn M, Stark M, Chaffron S, Creevey C, Muller J, et al. String 8–a global view on proteins and their functional interactions in 630 organisms. *Nucleic Acids Res.* (2009) 37:D412-6. doi: 10.1093/nar/gkn760
34. von Mering C, Jensen LJ, Kuhn M, Chaffron S, Doerks T, Kruger B, et al. String 7–recent developments in the integration and prediction of protein interactions. *Nucleic Acids Res.* (2007) 35:D358-62. doi: 10.1093/nar/gkl825
35. von Mering C, Jensen LJ, Snel B, Hooper SD, Krupp M, Foglierini M, et al. String: known and predicted protein-protein associations, integrated and transferred across organisms. *Nucleic Acids Res.* (2005) 33:D433-7. doi: 10.1093/nar/gki005
36. von Mering C, Huynen M, Jaeggi D, Schmidt S, Bork P, Snel B. String: a database of predicted functional associations between proteins. *Nucleic Acids Res.* (2003) 31:258-61. doi: 10.1093/nar/gkg034
37. Snel B, Lehmann G, Bork P, Huynen MA. String: a web-server to retrieve and display the repeatedly occurring neighbourhood of a gene. *Nucleic Acids Res.* (2000) 28:3442-4. doi: 10.1093/nar/28.18.3442
38. He F, Zhao Z, Liu Y, Lu L, Fu Y. Assessment of ocular surface damage during the course of type 2 diabetes mellitus. *J Ophthalmol.* (2018) 2018:1206808. doi: 10.1155/2018/1206808
39. Sandra Johanna GP, Antonio LA, Andres GS. Correlation between type 2 diabetes, dry eye and meibomian glands dysfunction. *J Optom.* (2019) 12:256-62. doi: 10.1016/j.optom.2019.02.003
40. Kern TS. Contributions of inflammatory processes to the development of the early stages of diabetic retinopathy. *Exp Diabetes Res.* (2007) 2007:95103. doi: 10.1155/2007/95103
41. Messmer EM, Schmid-Tannwald C, Zapp D, Kampik A. *In Vivo* confocal microscopy of corneal small fiber damage in diabetes mellitus. *Graefes Arch Clin Exp Ophthalmol.* (2010) 248:1307-12. doi: 10.1007/s00417-010-1396-8
42. Zhang X, Zhao L, Deng S, Sun X, Wang N. Dry eye syndrome in patients with diabetes mellitus: prevalence, etiology, and clinical characteristics. *J Ophthalmol.* (2016) 2016:8201053. doi: 10.1155/2016/8201053
43. Rolando M, Cantera E, Mencucci R, Rubino P, Aragona P. The correct diagnosis and therapeutic management of tear dysfunction: recommendations of the P.I.C.A.S.S.O. Board. *Int Ophthalmol.* (2018) 38:875-95. doi: 10.1007/s10792-017-0524-4
44. Wolffsohn JS, Arita R, Chalmers R, Djalilian A, Dogru M, Dumbleton K, et al. Tfos Dews Ii diagnostic methodology report. *Ocul Surf.* (2017) 15:539-74. doi: 10.1016/j.jtos.2017.05.001
45. Guo Y, Peng R, Feng K, Hong J. Diagnostic performance of mcmonnies questionnaire as a screening survey for dry eye: a multicenter analysis. *J Ophthalmol.* (2016) 2016:6210853. doi: 10.1155/2016/6210853
46. Methodologies to diagnose and monitor dry eye disease: report of the diagnostic methodology subcommittee of the international dry eye workshop 2007. *Ocul Surf.* (2007) 5:108-52. doi: 10.1016/S1542-0124(12)70083-6
47. The definition and classification of dry eye disease: report of the definition and classification subcommittee of the international dry eye workshop 2007. *Ocul Surf.* (2007) 5:75-92. doi: 10.1016/S1542-0124(12)70081-2

48. DeMill DL, Hussain M, Pop-Busui R, Shtein RM. Ocular surface disease in patients with diabetic peripheral neuropathy. *Br J Ophthalmol.* (2016) 100:924-8. doi: 10.1136/bjophthalmol-2015-307369
49. Clark CV. Autonomic neuropathy in proliferative diabetic retinopathy. *Eye.* (1987) 1:496-9. doi: 10.1038/eye.1987.74
50. Costagliola C, Romano V, De Tollis M, Aceto F, dell'Omo R, Romano MR, et al. Tnf-alpha levels in tears: a novel biomarker to assess the degree of diabetic retinopathy. *Mediators Inflamm.* (2013) 2013:629529. doi: 10.1155/2013/629529
51. Amil-Bangsa NH, Mohd-Ali B, Ishak B, Abdul-Aziz CNN, Ngah NF, Hashim H, et al. Total protein concentration and tumor necrosis factor alpha in tears of nonproliferative diabetic retinopathy. *Optom Vis Sci.* (2019) 96:934-9. doi: 10.1097/OPX.0000000000001456
52. Torok Z, Peto T, Csosz E, Tukacs E, Molnar A, Maros-Szabo Z, et al. Tear fluid proteomics multimarkers for diabetic retinopathy screening. *BMC Ophthalmol.* (2013) 13:40. doi: 10.1186/1471-2415-13-40
53. Matsumura T, Takamura Y, Tomomatsu T, Arimura S, Gozawa M, Takihara Y, et al. Changes in matrix metalloproteinases in diabetes patients' tears after vitrectomy and the relationship with corneal epithelial disorder. *Invest Ophthalmol Vis Sci.* (2015) 56:3559-64. doi: 10.1167/iovs.15-16489
54. Grus FH, Sabuncuo P, Dick HB, Augustin AJ, Pfeiffer N. Changes in the tear proteins of diabetic patients. *BMC Ophthalmol.* (2002) 2:4. doi: 10.1186/1471-2415-2-4
55. Ghosh S, Ghosh S, Azharuddin M, Bera S, Datta H, Dasgupta A. Change in tear protein profile in diabetic retinopathy with duration of diabetes. *Diabetes Metab Syndr.* (2014) 8:233-5. doi: 10.1016/j.dsx.2014.09.019
56. Dor M, Eperon S, Lalive PH, Guex-Crosier Y, Hamedani M, Salvisberg C, et al. Investigation of the global protein content from healthy human tears. *Exp Eye Res.* (2019) 179:64-74. doi: 10.1016/j.exer.2018.10.006
57. Zhou L, Zhao SZ, Koh SK, Chen L, Vaz C, Tanavde V, et al. In-depth analysis of the human tear proteome. *J Proteomics.* (2012) 75:3877-85. doi: 10.1016/j.jprot.2012.04.053
58. Jung JH, Ji YW, Hwang HS, Oh JW, Kim HC, Lee HK, et al. Proteomic analysis of human lacrimal and tear fluid in dry eye disease. *Sci Rep.* (2017) 7:13363. doi: 10.1038/s41598-017-13817-y
59. Fonseca CG, Barbacena P, Franco CA. Endothelial cells on the move: dynamics in vascular morphogenesis and disease. *Vasc Biol.* (2020) 2:H29-43. doi: 10.1530/VB-20-0007
60. Wilkinson-Berka JL, Agrotis A, Deliyanti D. The Retinal renin-angiotensin system: roles of angiotensin II and aldosterone. *Peptides.* (2012) 36:142-50. doi: 10.1016/j.peptides.2012.04.008
61. Phipps JA, Dixon MA, Jobling AI, Wang AY, Greferath U, Vessey KA, et al. The renin-angiotensin system and the retinal neurovascular unit: a role in vascular regulation and disease. *Exp Eye Res.* (2019) 187:107753. doi: 10.1016/j.exer.2019.107753
62. Schmalen A, Lorenz L, Grosche A, Pauly D, Deeg CA, Hauck SM. Proteomic phenotyping of stimulated muller cells uncovers profound pro-inflammatory signaling and antigen-presenting capacity. *Front Pharmacol.* (2021) 12:771571. doi: 10.3389/fphar.2021.771571
63. Xu H, Chen M. Diabetic retinopathy and dysregulated innate immunity. *Vision Res.* (2017) 139:39-46. doi: 10.1016/j.visres.2017.04.013
64. Frudd K, Sivaprasad S, Raman R, Krishnakumar S, Revathy YR, Turowski P. Diagnostic circulating biomarkers to detect vision-threatening diabetic retinopathy: potential screening tool of the future? *Acta Ophthalmol.* (2021) 100:e648-68. doi: 10.1111/aos.14954
65. Blighe K, Gurudas S, Lee Y, Sivaprasad S. Diabetic retinopathy environment-wide association study (Ewas) in Nhanes 2005-2008. *J Clin Med.* (2020) 9:3643. doi: 10.3390/jcm9113643
66. Bonfiglio V, Platania CBM, Lazzara F, Conti F, Pizzo C, Reibaldi M, et al. Tgf-Beta serum levels in diabetic retinopathy patients and the role of anti-Vegf therapy. *Int J Mol Sci.* (2020) 21:9558. doi: 10.3390/ijms21249558
67. Trotta MC, Gesualdo C, Platania CBM, De Robertis D, Giordano M, Simonelli F, et al. Circulating mirnas in diabetic retinopathy patients: prognostic markers or pharmacological targets? *Biochem Pharmacol.* (2021) 186:114473. doi: 10.1016/j.bcp.2021.114473
68. Grigor'eva AE, Dyrkheeva NS, Bryzgunova OE, Tamkovich SN, Chelobanov BP, Ryabchikova EI. [Contamination of exosome preparations, isolated from biological fluids]. *Biomed Khim.* (2017) 63:91-6. doi: 10.18097/PBMC20176301091
69. Chung YR, Kim YH, Ha SJ, Byeon HE, Cho CH, Kim JH, et al. Role of inflammation in classification of diabetic macular edema by optical coherence tomography. *J Diabetes Res.* (2019) 2019:8164250. doi: 10.1155/2019/8164250
70. Rossino MG, Casini G. Nutraceuticals for the treatment of diabetic retinopathy. *Nutrients.* (2019) 11:771. doi: 10.3390/nu11040771
71. He M, Long P, Guo L, Zhang M, Wang S, He H. Fushiming capsule attenuates diabetic rat retina damage via antioxidation and anti-inflammation. *Evid Based Complement Alternat Med.* (2019) 2019:5376439. doi: 10.1155/2019/5376439
72. Kitamura H. Effects of propolis extract and propolis-derived compounds on obesity and diabetes: knowledge from cellular and animal models. *Molecules.* (2019) 24:4394. doi: 10.3390/molecules24234394
73. Fresta CG, Fidilio A, Caruso G, Caraci F, Giblin FJ, Leggio GM, et al. A new human blood-retinal barrier model based on endothelial cells, pericytes, and astrocytes. *Int J Mol Sci.* (2020) 21:1636. doi: 10.3390/ijms21051636
74. Rubsam A, Parikh S, Fort PE. Role of inflammation in diabetic retinopathy. *Int J Mol Sci.* (2018) 19:942. doi: 10.3390/ijms19040942
75. Song Z, Sun M, Zhou F, Huang F, Qu J, Chen D. Increased intravitreous interleukin-18 correlated to vascular endothelial growth factor in patients with active proliferative diabetic retinopathy. *Graefes Arch Clin Exp Ophthalmol.* (2014) 252:1229-34. doi: 10.1007/s00417-014-2586-6
76. Giebel SJ, Menicucci G, McGuire PG, Das A. Matrix metalloproteinases in early diabetic retinopathy and their role in alteration of the blood-retinal barrier. *Lab Invest.* (2005) 85:597-607. doi: 10.1038/labinvest.3700251
77. Kowluru RA, Zhong Q, Santos JM. Matrix metalloproteinases in diabetic retinopathy: potential role of Mmp-9. *Expert Opin Investig Drugs.* (2012) 21:797-805. doi: 10.1517/13543784.2012.681043
78. Joussen AM, Poulaki V, Le ML, Koizumi K, Esser C, Janicki H, et al. A central role for inflammation in the pathogenesis of diabetic retinopathy. *FASEB J.* (2004) 18:1450-2. doi: 10.1096/fj.03-1476fje
79. Mohammad G, Kowluru RA. Diabetic retinopathy and signaling mechanism for activation of matrix metalloproteinase-9. *J Cell Physiol.* (2012) 227:1052-61. doi: 10.1002/jcp.22822
80. Rani SG, Sepuru KM, Yu C. Interaction of S100a13 with C2 domain of receptor for advanced glycation end products (Rage). *Biochim Biophys Acta.* (2014) 1844:1718-28. doi: 10.1016/j.bbapap.2014.06.017
81. Shelton MD, Kern TS, Mieyal JJ. Glutaredoxin regulates nuclear factor Kappa-B and intercellular adhesion molecule in muller cells: model of diabetic retinopathy. *J Biol Chem.* (2007) 282:12467-74. doi: 10.1074/jbc.M610863200
82. Perez-Riverol Y, Bai J, Bandla C, Hewapathirana S, García-Seisdedos D, Kamatchinathan S, et al. The PRIDE database resources in 2022: A Hub for mass spectrometry-based proteomics evidences. *Nucleic Acids Res.* (2022) 50:D543–52. doi: 10.1093/nar/gkab1038

Conflict of Interest: The authors declare that the research was conducted in the absence of any commercial or financial relationships that could be construed as a potential conflict of interest.

Publisher's Note: All claims expressed in this article are solely those of the authors and do not necessarily represent those of their affiliated organizations, or those of the publisher, the editors and the reviewers. Any product that may be evaluated in this article, or claim that may be made by its manufacturer, is not guaranteed or endorsed by the publisher.

frontiers | Frontiers in Medicine

ORIGINAL RESEARCH
published: 01 June 2022
doi: 10.3389/fmed.2022.848776

Defining an Optimal Sample Size for Corneal Epithelial Immune Cell Analysis Using *in vivo* Confocal Microscopy Images

*Xin Yuan Zhang, Mengliang Wu, Holly R. Chinnery and Laura E. Downie**

Department of Optometry and Vision Sciences, University of Melbourne, Parkville, VIC, Australia

Purpose: *In vivo* confocal microscopy (IVCM) images are frequently used to quantify corneal epithelial immune cell (IC) density in clinical studies. There is currently limited evidence to inform the selection of a representative image sample size to yield a reliable IC density estimate, and arbitrary numbers of images are often used. The primary aim of this study was to determine the number of randomly selected, unique IVCM images required to achieve an acceptable level of accuracy when quantifying epithelial IC density, in both the central and peripheral cornea. The secondary aim was to evaluate the consistency and precision of an image selection approach where corneal epithelial IC density was quantified from "three representative images" selected independently by three experienced observers.

Methods: All combinations of two to 15 non-overlapping IVCM images were used for deriving IC density estimates, for both the central and peripheral cornea, in 20 healthy participants; the density value from averaging quantifications in the 16 images was defined as the "true mean". IC density estimates were compared with the true mean in each corneal region using a mean ratio. Intraclass correlation coefficients (ICCs) were used to evaluate the consistency of the mean ratios of IC density estimates derived from the method involving the manual selection of "three representative images" by the observers. The precision of the IC density estimates was compared to a scenario involving three randomly selected images.

Results: A total of 12 randomly selected, non-overlapping IVCM images were found to be required to produce a corneal epithelial IC density estimate that was within 30% of the true mean, 95% of the time, for the central cornea; seven such images produced an equivalent level of precision in the peripheral cornea. Mean ratios of corneal IC density estimates derived from "three representative images" methods had poor consistency between observers (ICC estimates <0.5) and similar levels of precision when compared with using three randomly selected images ($p > 0.05$ for all comparisons), in both the central and peripheral cornea.

Conclusions: Data presented in this study can inform image selection methods, and the sample size required for a preferred level of accuracy, when quantifying IC densities in the central and peripheral corneal epithelium using IVCM images.

Keywords: cornea, immune cell, confocal, IVCM, dendritic cell, image, sample size, combinations

OPEN ACCESS

Edited by:
Menaka Chanu Thounaojam, Augusta University, United States

Reviewed by:
Fabio Scarpa, University of Padua, Italy
Rayaz A. Malik, Weill Cornell Medicine – Qatar, Qatar

****Correspondence:***
Laura E. Downie
ldownie@unimelb.edu.au

Specialty section:
This article was submitted to Ophthalmology, a section of the journal Frontiers in Medicine

Received: *05 January 2022*
Accepted: *29 April 2022*
Published: *01 June 2022*

Citation:
Zhang XY, Wu M, Chinnery HR and Downie LE (2022) Defining an Optimal Sample Size for Corneal Epithelial Immune Cell Analysis Using in vivo Confocal Microscopy Images. Front. Med. 9:848776. doi: 10.3389/fmed.2022.848776

INTRODUCTION

In vivo confocal microscopy (IVCM) is a high-resolution tool for non-invasively capturing images of the cornea in living humans. Corneal immune cells (ICs) can be visualized in IVCM images as bright, typically dendriform bodies at the level of the basal epithelium (1). These corneal epithelial ICs are generally considered to represent resident dendritic cells (2), which are involved in immune surveillance, initiating adaptive immune responses (3) and maintaining tissue homeostasis (4). The quantification of epithelial IC density from IVCM images is frequently performed in clinical studies, as a means for considering corneal immune status, particularly in the context of disease (5–12). For example, central corneal epithelial IC density has been described to increase in corneal infections (13), contact lens wear (14) and dry eye disease (15).

A single IVCM image has a relatively small field-of-view, typically 400 μm × 400 μm (i.e., 0.16 mm^2), equating to approximately 0.2% of the entire corneal area. Due to this limited capture area, it is generally recognized that more than one IVCM image needs to be acquired and analyzed to derive a representative estimate of the corneal epithelial IC density in a particular corneal region. However, there has not yet been a study investigating the optimal IVCM image sample size required to derive a valid estimate of corneal epithelial IC density for a particular individual. Kheirkhah et al. proposed that averaging findings from "three representative images, chosen by an experienced observer," could accurately estimate central corneal epithelial IC density in a clinical population (16). However, a human observer, experienced or otherwise, may have unconscious biases in image selection, particularly if they are not masked to a participant's health status; such biases could affect the validity of the epithelial IC density measures (17). Another approach has been to analyze IVCM images with the highest IC density (8, 18), which is likely also problematic as it could overestimate absolute values and/or the effect of an inflammatory overlay.

Previous corneal IVCM studies have used a variety of sample sizes, including quantifications from three (9, 15, 19–22), five (6), eight (23), or twelve (24) non-overlapping images, to derive an estimate of central corneal epithelial IC density for a single participant. Using a larger sample would be expected to yield a more accurate estimate, as a larger portion of the corneal region is directly quantified; the trade-off is that more time and effort is required for the image acquisition, selection and analysis (25). Using randomly selected images, rather than images selected by an observer, would be expected to reduce biases in image selection. However, the optimal image sample size for quantifying corneal epithelial IC density from randomly selected IVCM images is yet to be determined. The effect of corneal eccentricity on the required sample size also requires consideration. Corneal epithelial IC density is eccentricity dependent, with approximately threefold more cells in the peripheral cornea relative to the central region (26). Therefore, different image sample sizes might be required for reliable estimations of central and peripheral corneal IC densities.

Vagenas et al. described a method for determining the optimal sample size of IVCM images for quantifying central corneal sub-basal nerve parameters (27). This study concluded that eight randomly chosen images, overlapping by less than 20%, were needed per participant to produce an estimated value within 30% of the true mean, 95% of the time. The aim of the present study was to use a similar approach to determine the optimal image sample sizes for quantifying epithelial IC density from IVCM images in healthy individuals, for both the central and peripheral cornea. This study also considered whether quantifying the mean number of cells using "three representative images," by different observers, led to a different corneal epithelial IC density estimate relative to the derived true density.

MATERIALS AND METHODS

Participants

This retrospective study involved the analysis of corneal IVCM images, acquired at the level of the basal epithelium, from 20 randomly selected, heathy adult participants who had participated in research studies in the Downie laboratory at the University of Melbourne from 2017 to 2019. The studies were approved by the University of Melbourne Human Research Ethics Committees (ID #1749830 and #1749836). All participants provided written informed consent to participate. The number of participants was chosen to align with the analysis set defined by Vagenas et al. (27), which adopted a similar methodological approach.

Eligible participants had self-reported no underlying health conditions that could affect eye health (including dry eye disease), were not pregnant or breastfeeding, had not undergone ocular surgery within the 6 months prior to the study visit, and did not have a history of contact lens wear. Dry eye disease symptom screening was conducted using the McMonnies dry eye questionnaire (28); potential participants with a score exceeding 14.5 were ineligible to participate.

Corneal *in vivo* Confocal Microscopy Image Acquisition and Selection

Participants underwent laser-scanning IVCM (Heidelberg Retina Tomograph-3 with the Rostock Corneal Module, Heidelberg Engineering, Germany) using our established protocols (29). IVCM images (400 μm × 400 μm) were acquired from the right corneal apex (central region) and 2 mm above the inferior limbus (peripheral region) using the device sequence scan mode, at the level of the basal epithelium. Capturing the relevant regions of interest was achieved by having the contralateral (left) eye focus on a series of fixation targets, involving a grid to ensure the capture of multiple non-overlapping IVCM regions. In total, at least 600 IVCM images were captured per participant, from which 16 unique corneal images from each of the central and peripheral cornea were randomly selected for inclusion in this study. Images that had variable focus, imaging artifacts, compression lines or vignetting effects, and images that captured the same or overlapping corneal regions, were excluded from the analysis set. A total of 640 unique high quality IVCM images

comprised the analysis set. This analysis set involved 16 images of corneal areas (defined by <20% overlap with any other image in the analysis set) in both the central and peripheral cornea for each participant. To confirm that images were not overlapping, they were processed using the Photomerge function in Photoshop (Adobe Photoshop Version: 23.0.0) with images that were unable to merge regarded as non-overlapping.

Image Analysis

For each IVCM image, the number of corneal epithelial ICs was manually counted by one experienced observer using the Cell Counter plugin in ImageJ (30) (**Figure 1**). ICs that were only partially visible at the edge of an image were excluded. Corneal IC density (cells/mm^2) was calculated for each image. For each participant, the average epithelial IC density from the 16 images (quantified corneal area: 2.56 mm^2), in both the central and peripheral cornea, was regarded as the reference standard and "true" mean value based on the method used by Vagenas et al. (27).

To evaluate whether this experienced observer's IC counts were representative of other observers, two other experienced observers also independently performed IC counts in 100 randomly selected IVCM images, comprising 50 from the central cornea and 50 from the peripheral cornea; this subset represents one sixth of the total number of images analyzed for the study. The level of inter-observer agreement was analyzed using the intraclass correlation coefficient (ICC), with 95% confidence intervals, using a single-rating, absolute-agreement, two-way random-effects model.

The analysis also considered how the estimate of corneal epithelial IC density from "three representative images," selected manually by observers, compared with the estimate derived from random image selection. Three experienced observers were instructed to select three IVCM images, from both the central and peripheral cornea, that they considered to "best represent" the 16 images for each participant. The epithelial IC density estimate for each participant, in each corneal region, was then calculated by averaging the IC densities from the "three representative images" selected by each of the three observers.

Statistical Analysis

The statistical approach for the current study was based on the methodology described by Vagenas et al. (27). The sampling technique involved creating mathematical combinations of IVCM image sets, comprising two to 15 unique images (k) from the 16 image reference set (n), in both the central and peripheral regions, for each participant. A combination was defined as an unordered selection of k items, from a set of n items without repetition ($k \leq n$). Estimates of corneal IC density, determined by sampling different numbers of randomly selected images, were then compared to the "true" mean value in order to determine the minimum number of images that would provide an acceptable estimate, defined as less than 30% different to the "true mean" value; this level of precision was defined as acceptable based on the criterion used for corneal nerve parameter estimates by Vagenas et al. (27). The estimated IC density is presented as the "relative mean," also termed the "mean ratio," defined as the ratio between the estimated and "true" IC density, for each participant. Mean ratios were plotted relative to the number of images (two to 15) used to derive the estimates. The same process was followed for both the central and peripheral corneal regions.

Given the large number of estimates generated from each combination level, the mean ratios were considered to approximate a normal distribution, based on the Central Limit Theorem. The confidence intervals (CIs) of the mean ratio data were calculated using the formula $CI = \mu \pm (t \times SD)$ at confidence levels of 80, 85, 90, and 95% (where μ is the mean of the distribution, SD is the standard deviation of the distribution, and t is the value that corresponds to 80, 85, 90, and 95% levels of confidence in a t-distribution).

The level of consistency between estimates of corneal epithelial IC density derived from the "three representative images" selected by three independent observers was analyzed separately for the central and peripheral regions using the ICC. ICC estimates and their 95% CIs were calculated using a single-rating, consistency-agreement, two-way random-effects model. The three observers were selected randomly and therefore the results are expected to be generalizable to the whole observer population. The difference in mean estimates of IC density ratio between each observer and a random combination of three IVCM images was analyzed using a Student's t-test, with Bonferroni adjustment for multiple comparisons. To evaluate whether the 95% CI estimations for corneal IC density from the observers were narrower (i.e., had better precision) than the 95% CIs derived from a random combination of three IVCM images, variance equality was evaluated using an F-test, with Bonferroni adjustment for multiple comparisons.

All statistical analyses were performed, and figures constructed, using R software (Version 4.1.2, R Development Core Team).[1] A p-value less than 0.05 was considered statistically significant.

RESULTS

Corneal Immune Cell Density

Overall, the mean ($\pm$ SD) epithelial IC density for the 20 healthy participants, calculated from the "true" mean quantified from 16 images by a single expert observer for each participant was 21.7 $\pm$ 17.7 cells/mm^2 (range: 2.7 to 63.3 cells/mm^2) for the central cornea, and 62.0 $\pm$ 26.1 cells/mm^2 (range: 17.2 to 104.7 cells/mm^2) for the peripheral cornea.

Confirming the validity of the single expert observer's epithelial IC counts, the ICCs for counts performed independently by three observers in a subset of 100 randomly selected IVCM images was: central cornea: 0.91 (95% CI: 0.85 to 0.95), and peripheral cornea: 0.90 (95% CI: 0.83 to 0.94). These ICCs indicate a high level of agreement in the quantification of corneal epithelial ICs from IVCM images by three experienced observers.

[1] https://www.r-project.org/

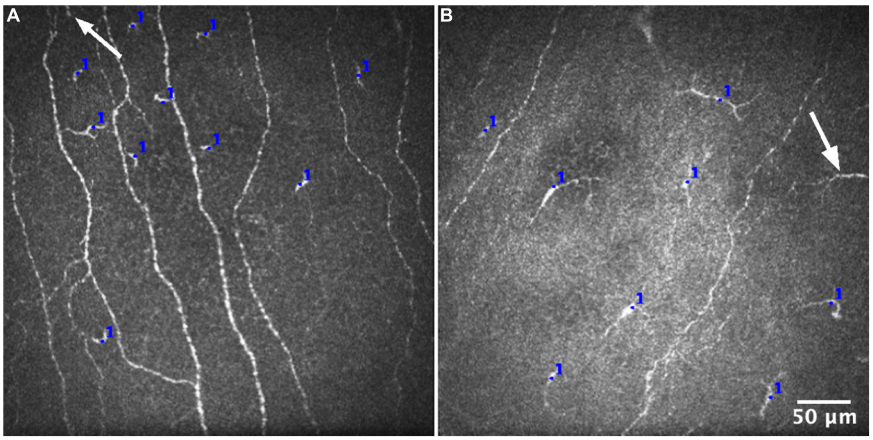

FIGURE 1 | Representative IVCM images for quantifying epithelial immune cell density from the central **(A)** and peripheral **(B)** corneal regions. The number of cells was manually counted in each IVCM image, using the Cell Counter plugin in ImageJ (blue marks). Cells that were only partially visible at the edge of an image (white arrows) were consistently excluded from the analysis.

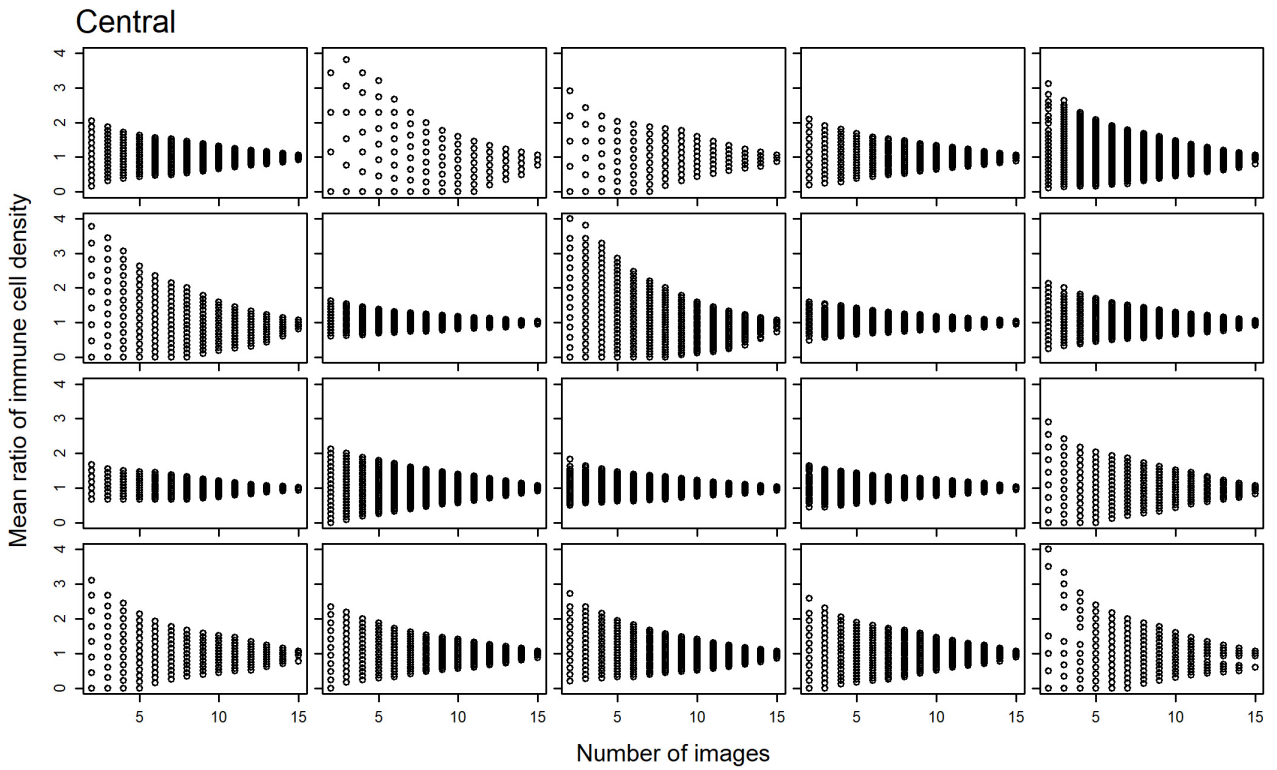

FIGURE 2 | Scatterplots of the mean ratio for corneal epithelial immune cell (IC) density relative to the number of randomly selected, non-overlapping IVCM images used for the density estimate for each participant, in the central cornea.

Optimal *in vivo* Confocal Microscopy Image Sample Size for Estimating Corneal Epithelial Immune Cell Density

Scatterplots of the mean ratios for IC density estimates derived from all image combinations, for all study participants, are shown for the central (**Figure 2**) and peripheral (**Figure 3**) cornea; as the number of sampled images increases, the spread of the mean ratio data decreases.

Plots of the CIs (80, 85, 90, and 95%) for the epithelial IC density mean ratios, relative to the number of images used to derive the estimate, are shown for the central (**Figure 4**) and peripheral (**Figure 5**) cornea. In both regions, the CIs narrow

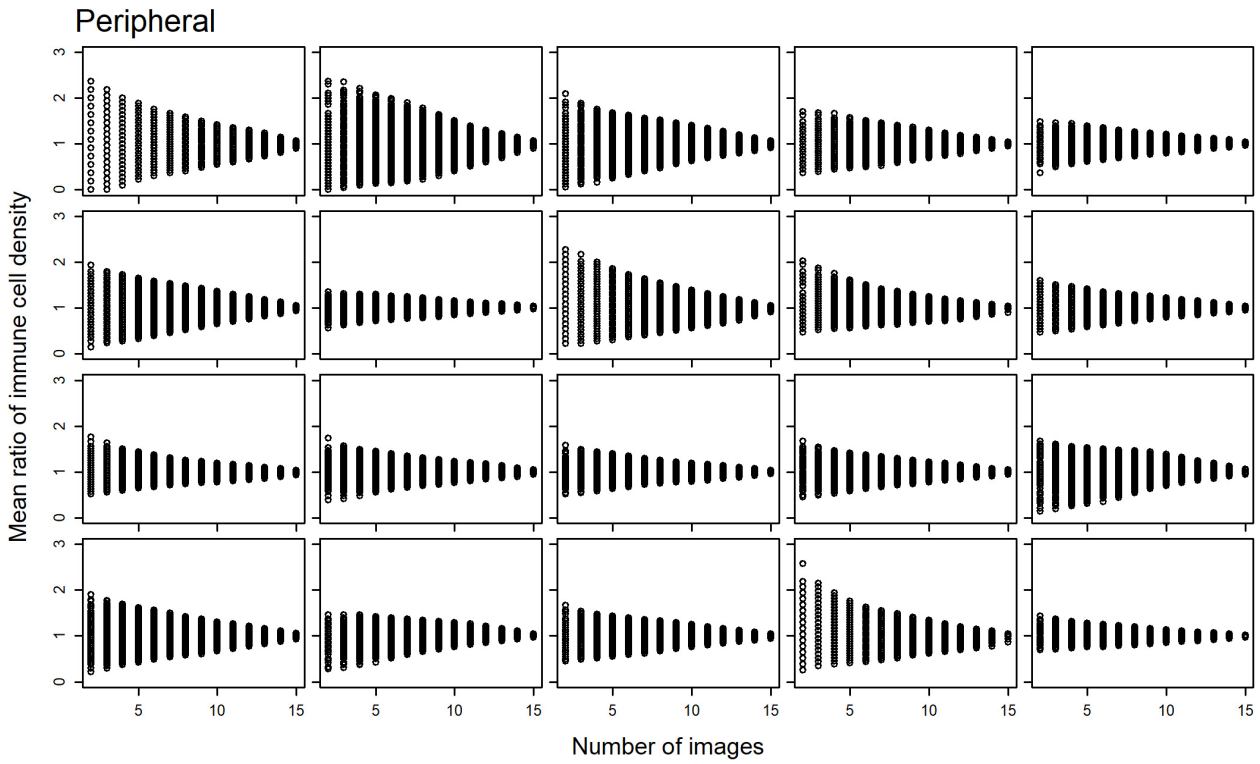

FIGURE 3 | Scatterplots of the mean ratio for corneal epithelial immune cell (IC) density relative to the number of randomly selected, non-overlapping IVCM images used for the density estimate for each participant, in the peripheral cornea.

as the number of images used to derive the estimate increases. An optimal IVCM image sample size to estimate the true corneal epithelial IC density was determined from the plots, using a pre-specified level of precision (mean ratio) and level of confidence. The estimated mean was considered acceptable if it was not more than 30% different from the true mean at a 95% confidence level (27). Using this criterion, 12 randomly selected, non-overlapping images of the central cornea, and seven such images of the peripheral cornea, were found to be required, per participant, for accurate quantification and averaging.

Evaluation of the Method Involving Selection of the "Three Representative" *in vivo* Confocal Microscopy Images

The ICC for the mean ratio of the epithelial IC density estimates derived from the three images selected as "representative" by three independent observers was −0.21 (95% CI: −0.35 to 0.04) for the central cornea, and 0.17 (95% CI: −0.08 to 0.48) for the peripheral cornea. Given that poor reliability is defined by ICC values less than 0.50 (31), this result indicates poor consistency among the mean ratio estimates of IC density between the three observers.

The mean ratio and corresponding 95% CIs for epithelial IC density estimates derived from the "representative" images selected by each observer are shown for the central (**Figure 6**) and peripheral (**Figure 7**) cornea. Comparing the mean ratio estimates calculated from all combinations of three randomly sampled images, two of the three observers selected images that significantly overestimated central corneal epithelial IC density (rater 2: $p = 0.010$; rater 3: $p = 0.047$), while one observer selected images that overestimated the peripheral corneal IC density (rater 3: $p = 0.003$). The size of the 95% CIs around the epithelial IC density mean ratio for any of the raters was not significantly narrower than the estimate derived from three randomly selected images, in both the central and peripheral cornea ($p > 0.05$ for all comparisons). This finding indicates that there was similar precision in the IC density estimate when three images were subjectively selected by observers and when any random three images were used in the analysis.

DISCUSSION

This is the first study to investigate the optimal number of IVCM images required to accurately estimate IC density in a healthy individual, in both the central and peripheral corneal epithelium. The analysis also considered the validity of using "three representative images" selected by experienced observers to derive corneal epithelial IC density estimates. The main finding was that to derive a corneal epithelial IC density estimate that is at most 30% different from the "true mean," 95% of the time, quantifications need to be performed and averaged for 12 randomly selected, non-overlapping IVCM images in the

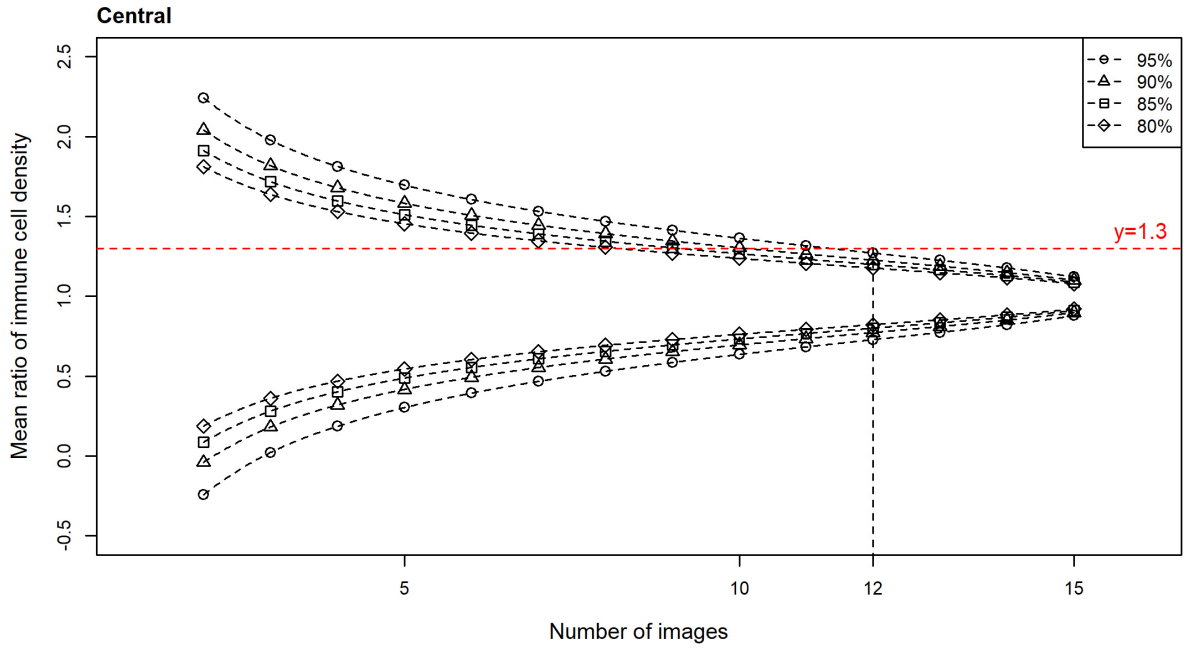

FIGURE 4 | Confidence intervals (CIs) with 80, 85, 90, and 95% levels of confidence for the mean ratio for corneal epithelial immune cell (IC) density relative to the number of randomly selected, non-overlapping images used for the density estimate, for all participants for the central cornea. Horizontal line (mean ratio = 1.3) indicates the location where the estimated mean is 30% different from the true mean in the distributions. Vertical line (number of images = 12) indicates the number of images that is predicted to produce estimated means that are 30% different from the true mean (i.e., mean ratio = 1.3 or 0.7), at a confidence level of 95%, for the central cornea.

central cornea, and for seven such images in the peripheral cornea, per participant. The study also identified that corneal IC density estimates derived from cell quantifications in "three representative images," by experienced observers, had poor reliability; overall, the level of precision was similar to using three random images. These findings can inform future IVCM studies that include corneal epithelial IC density calculations, both with respect to the required image sample size and the methods used for image selection.

Quantifying corneal epithelial IC density from IVCM images is frequently used to evaluate corneal inflammation in clinical studies (5–12). Although it is generally accepted that inflamed corneas have higher epithelial IC densities relative to control (healthy) conditions, a recent meta-analysis reported high levels of heterogeneity (I^2 value: 94.5% for the central cornea and 96.1% for the peripheral cornea) among studies that had quantified corneal epithelial IC density from IVCM images in healthy eyes (26). In this analysis, and similar to the data in the present study, the pooled estimate for central corneal epithelial IC density was 26.4 ± 13.6 cells/mm^2 (from 1203 participants in 38 studies) for the central cornea and 74.9 ± 22.7 cells/mm^2 (from 466 participants in 9 studies) for the peripheral inferior cornea. The study by Mobeen et al. also investigated whether specific factors, including participant sex, the definition of ICs and whether three or five IVCM images were sampled, contributed to the observed heterogeneity. Age was reported to be the only significant factor, with peripheral corneal epithelial IC density decreasing with advancing age (26). The lack of significance of sample size as a contributing factor in this analysis likely reflects the dichotomous consideration of this variable, and that both categories are relatively under-sampled based on the findings in the present study. Other aspects of the IVCM image analysis approach, such as selection method (e.g., random or observer-selected) may also contribute to the unexplained heterogeneity.

The selection of a subset of images for analysis, from a larger raw acquisition set, is a necessary initial step in IVCM studies. This step has not been consistently performed in previous studies, both in terms of the number of images selected or the method of selection. First, in terms of sample size, it is important to consider whether the number of unique images (each covering 0.16 mm^2 of corneal area) selected for analysis sufficiently represents the corneal region; under-sampling may lead to inaccurate estimates. The present study identified that to ensure a level of precision such that an estimate was no more than 30% different from the true mean, 95% of the time, at least 12 randomly selected, non-overlapping IVCM images should be used to quantify epithelial IC densities in the central cornea of an individual. Consistent with epithelial ICs being more populous in the peripheral cornea, seven such images were found to be required to achieve the same level of precision in this region. In the absence of evidence to inform optimal image sampling methods, prior clinical studies have used a wide variety of image sample sizes, ranging from three (9, 15, 19–22) to twelve (24) non-overlapping images. The analyses in the current study indicate that central corneal epithelial IC density estimates derived from eight randomly sampled images only reach the above accepted level of precision

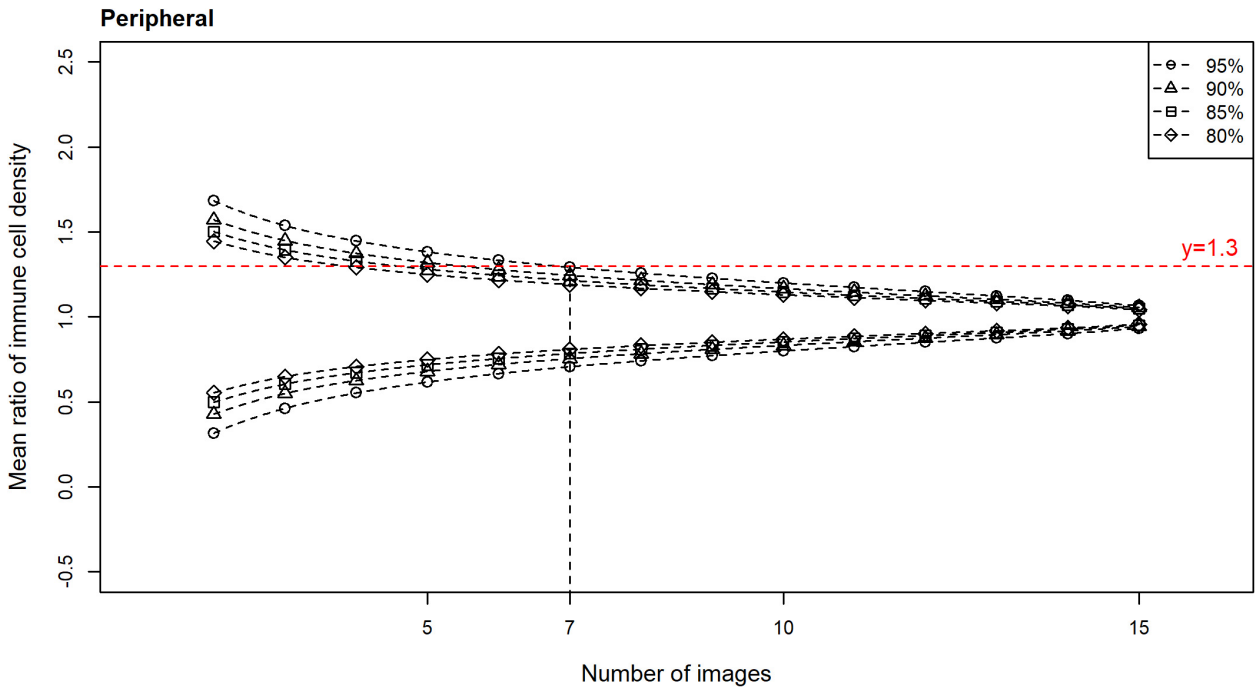

FIGURE 5 | Confidence intervals (CIs) with 80, 85, 90, and 95% levels of confidence for the mean ratio for corneal epithelial immune cell (IC) density relative to the number of randomly selected, non-overlapping images used for IC density estimate, for all participants for the peripheral cornea. Horizontal line (mean ratio = 1.3) indicates the location where the estimated mean is 30% different from the true mean in the distributions. Vertical line (number of images = 7) indicates the number of images that is predicted to produce estimated means that are 30% different from the true mean (i.e., mean ratio = 1.3 or 0.7), at a confidence level of 95%, for the peripheral cornea.

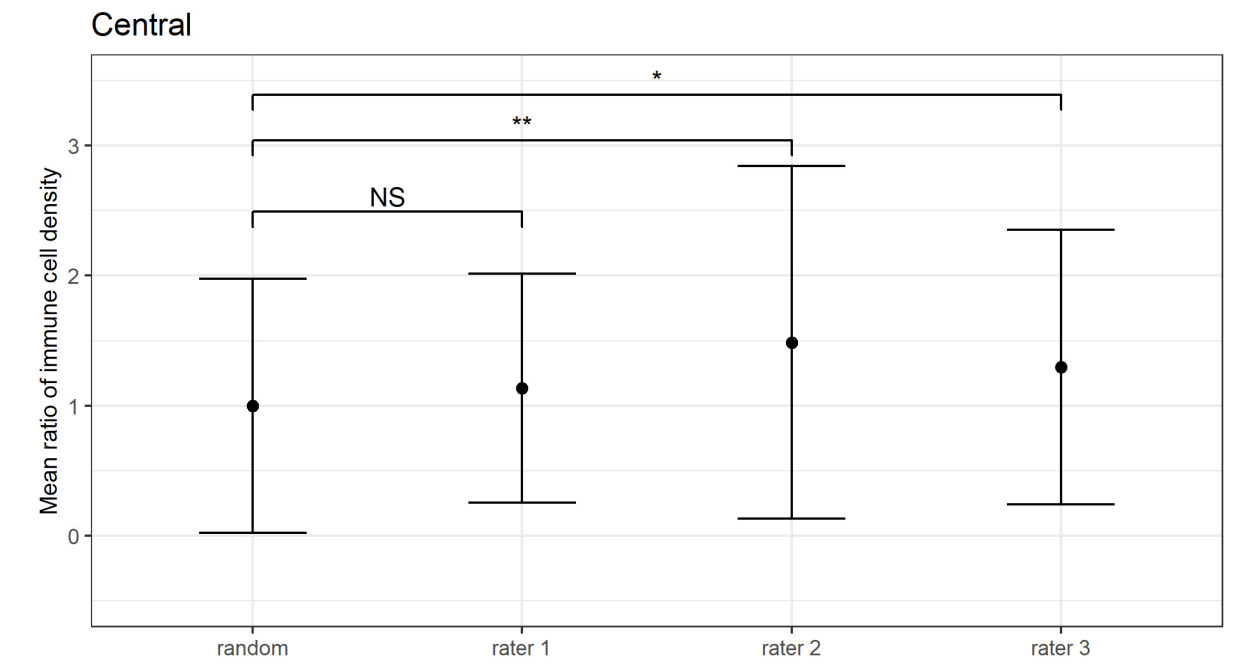

FIGURE 6 | Central corneal epithelial immune cell (IC) density mean ratios, and corresponding 95% CIs, obtained when IC density estimates derived from all combinations of three randomly sampled images (random), and when the "three representative images" were independently selected by three observers (i.e., raters 1 to 3). Mean ratios of IC density estimates derived from images selected by rater 2 and rater 3 were significantly higher in comparison to 3 randomly sampled images (**$p = 0.01$; *$p < 0.05$; NS: $p > 0.05$).

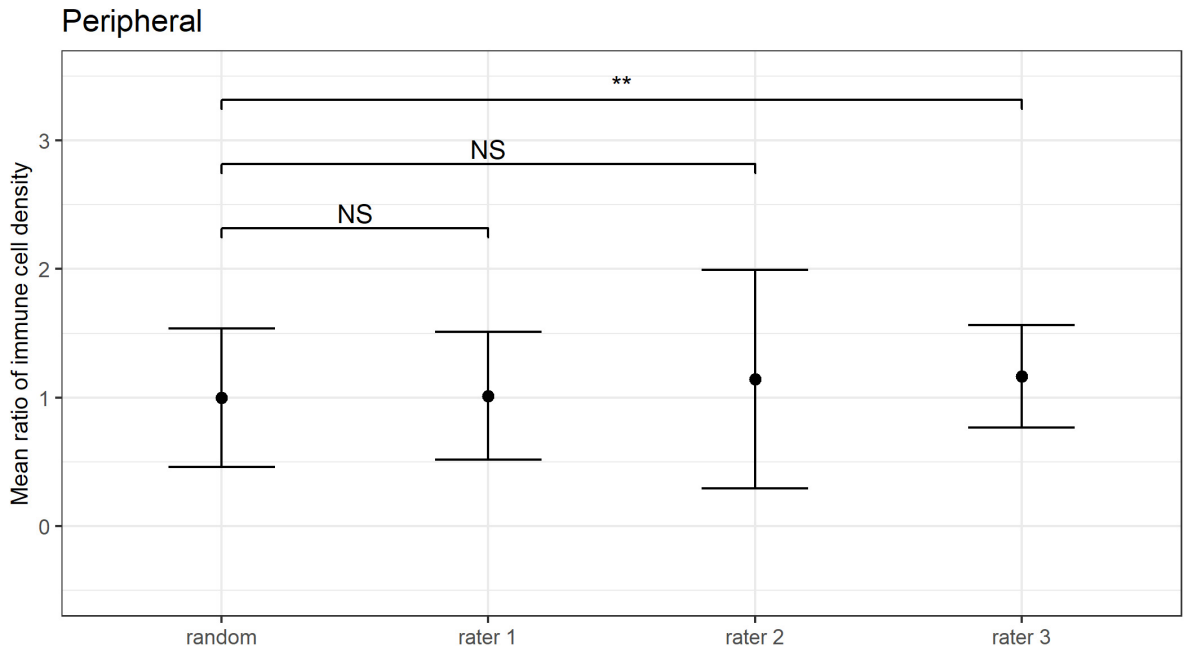

FIGURE 7 | Peripheral corneal epithelial immune cell (IC) density mean ratios, and corresponding 95% CIs, obtained when IC density estimates derived from all combinations of three randomly sampled images (random), and when the "three representative images" were independently selected by three observers (i.e., raters 1 to 3). Mean ratios of IC density estimates derived from images selected by rater 3 were significantly higher in comparison to 3 randomly selected images (**$p < 0.01$; NS: $p > 0.05$).

80% of the time; with the use of five randomly selected images, the IC density estimates are predicted to only achieve the precision level of not being more than 50% different from the true mean, 80% of the time. Together, these findings suggest studies using less than the determined minimum image sample sizes are at risk of unreliable estimates of corneal epithelial IC density, and report findings should be interpreted in view of this limitation.

Considerations relating to IVCM image sample sizes have also been investigated by Vagenas et al. for quantifying central corneal nerve parameters. These authors concluded that averaging data from at least eight unique IVCM images, per participant, was required to yield an estimate with the same level of precision used in the present study (27). That a larger sample size is required for corneal IC density estimates, relative to nerve density parameters, likely reflects that the healthy central corneal epithelium has high nerve density with relatively low inter-image parameter variability (32), but a sparse epithelial IC population. The use of images from healthy individuals in the present study was in recognition that the cornea has fewer epithelial ICs under physiological vs. inflammatory conditions. The image sample sizes determined in the present study are thus based on homeostatic corneal epithelial IC levels and provide a conservative estimate of the required sample size when relatively few ICs are present; the reported sample sizes are thus expected to remain robust when analyzing IVCM images with more ICs, such as diseased corneas. Although, this ideally should be confirmed in different disease states, acknowledging that corneal epithelial IC density may vary both in relation to absolute numbers and the region examined, dependent on the condition etiology. A further reason for the approach taken in the current paper is that healthy individuals often serve as controls in disease or intervention studies, and it is important to have reliable estimates in both participant populations.

In terms of image selection methods, a frequent approach involves an observer manually identifying a designated number of "representative images" for analysis; the use of three such images is common (9, 15, 19–22). However, observer bias might be expected to affect the validity of corneal epithelial IC density estimates derived from a small, subjectively curated image set (17). To consider this question, Kheirkhah et al. evaluated the mean corneal epithelial IC density calculated from "three representative images" selected by one observer with the value obtained from quantifying ICs in a wide-view composite image of the central cornea (covering 1.29 ± 0.64 mm^2 of corneal area) (16). Although these authors reported no overall significant difference in the estimated values across the study population, they noted considerable differences between the methods as a function of cell density in individual participants (16). Furthermore, the average corneal area used to derive the benchmark value from the composite images was approximately half of that in the current study (and likely equivalent to about eight non-overlapping IVCM images). The present study focused on analyses at the participant (rather than study population) level, evaluating both the inter-observer consistency of the "three representative images" selection approach, and the level of precision relative to using three random IVCM images, in both central and peripheral cornea. These analyses identified poor

inter-observer consistency for epithelial IC density estimates (as determined using the ICC), and a similar level of precision to three randomly selected images (as determined by assessing variance equality). These findings were conserved across the central and peripheral cornea. Together, these findings indicate that using "three representative images," selected by experienced observers, to quantify corneal epithelial IC densities is likely to be inconsistent and suboptimal with respect to the level of sampling, and imprecise when compared to the "true mean".

Considerations relevant to the interpretation of the current study include that, based on the prior work of Vagenas et al. (27), the "true mean" IC density has been taken as the average cell density calculated from 16 random, non-overlapping images, per participant, in each corneal region. The optimal image sample size was based on a pre-specified acceptable level of accuracy (27) for the estimated values of corneal epithelial IC density, which is an estimate within 30% of the true mean, 95% of the time. In the current study, only images of right eyes were acquired and analyzed, based on previous findings that corneal sub-basal nerve plexus parameters are highly correlated between eyes in an individual (33, 34). As such, we could not evaluate potential inter-eye asymmetries. We would expect, although could not identify direct evidence for, corneal epithelial IC densities also being similar between right and left eyes in healthy corneas (33, 34). Some indirect evidence for this relationship derives from research in unilateral corneal infection, where it has been shown that contralaterally clinically unaffected eyes show increased corneal epithelial IC densities; this was suggested to result from coordinated, bilateral interactions between the nervous and immune systems (35). Central corneal epithelial IC density measures similar to those reported in the present study have also been described in two recently published studies that analyzed a total of six images (i.e., three per eye) in healthy populations (36, 37).

We also acknowledge that the level of consistency between observers in the current study may not be generalizable, but instead represents the extent of agreement within this group of observers. All corneal epithelial ICs were quantified in the density calculations; morphological subtypes, which may represent either distinct cell populations or cells at different states of maturation, were not considered separately. It would be predicted that higher optimal image sample sizes may be required if distinct cell populations intend to be quantified. Some recent studies have assessed the infero-central corneal whorl region and noted that it is an area where round-shaped "globular" cells congregate (38–40). The current study determined optimal image sample sizes for deriving epithelial IC estimates in the central and peripheral corneal regions; the whorl region was not evaluated. This could be a topic for future research, noting that the corneal whorl will be inherently limited in its potential sampling area as it is a relatively small anatomical region of the cornea.

In conclusion, the present study finds that to minimize the likelihood of under-sampling at the participant level of a study, the average cell density value from quantifying 12 random, non-overlapping IVCM images (400 μm $\times$ 400 μm) should be used for corneal epithelial IC density estimates for the central cornea, and seven equivalent images should be used for the peripheral cornea. This study also finds that using "three representative images," selected by experienced observers, to derive corneal epithelial IC density estimates from IVCM images has poor inter-observer consistency, and leads to imprecise estimates that are similar to random under-sampling.

DATA AVAILABILITY STATEMENT

The datasets presented in this article are not readily available because our current Ethics Approval does not permit data sharing, even on anonymised data. If there was as external request for access to the raw, anonymised data, the corresponding author could seek approval of an Ethics Amendment from the Ethics approval for this purpose. Requests to access the datasets should be directed to LD, ldownie@unimelb.edu.au.

ETHICS STATEMENT

The studies involving human participants were reviewed and approved by the University of Melbourne Human Research Ethics Committee. The patients/participants provided their written informed consent to participate.

AUTHOR CONTRIBUTIONS

LD and HC conceived and designed the study and revised the manuscript. XZ collected the data. MW performed the data analyses. XZ and MW drafted the manuscript. All authors contributed to the interpretation of data, agreed to be accountable for all aspects of the work, and approved the final submitted version of the manuscript.

FUNDING

This study was internally funded by the research team.

REFERENCES

1. Zhivov A, Stave J, Vollmar B, Guthoff R. In vivo confocal microscopic evaluation of Langerhans cell density and distribution in the normal human corneal epithelium. *Graefes Arch Clin Exp Ophthalmol.* (2005) 243:1056–61. doi: 10.1007/s00417-004-1075-8
2. Mayer WJ, Mackert MJ, Kranebitter N, Messmer EM, Grüterich M, Kampik A, et al. Distribution of antigen presenting cells in the human cornea: correlation of in vivo confocal microscopy and immunohistochemistry in different pathologic entities. *Curr Eye Res.* (2012) 37:1012–8. doi: 10.3109/02713683.2012.696172
3. Forrester JV, Xu H, Kuffová L, Dick AD, McMenamin PG. Dendritic cell physiology and function in the eye. *Immunol Rev.* (2010) 234:282–304. doi: 10.1111/j.0105-2896.2009.00873.x
4. Gao N, Yin J, Yoon GS, Mi QS, Yu FS. Dendritic cell-epithelium interplay is a determinant factor for corneal epithelial wound

repair. *Am J Pathol.* (2011) 179:2243–53. doi: 10.1016/j.ajpath.2011.07.050
5. Tavakoli M, Boulton AJ, Efron N, Malik RA. Increased Langerhan cell density and corneal nerve damage in diabetic patients: role of immune mechanisms in human diabetic neuropathy. *Cont Lens Anterior Eye.* (2011) 34:7–11. doi: 10.1016/j.clae.2010.08.007
6. Marsovszky L, Resch MD, Németh J, Toldi G, Medgyesi E, Kovács L, et al. In vivo confocal microscopic evaluation of corneal Langerhans cell density, and distribution and evaluation of dry eye in rheumatoid arthritis. *Innate Immun.* (2013) 19:348–54. doi: 10.1177/1753425912461677
7. Yamaguchi T, Calvacanti BM, Cruzat A, Qazi Y, Ishikawa S, Osuka A, et al. Correlation between human tear cytokine levels and cellular corneal changes in patients with bacterial keratitis by in vivo confocal microscopy. *Invest Ophthalmol Vis Sci.* (2014) 55:7457–66. doi: 10.1167/iovs.14-15411
8. Wu L-Q, Cheng J-W, Cai J-P, Le Q-H, Ma X-Y, Gao L-D, et al. Observation of corneal Langerhans cells by in vivo confocal microscopy in thyroid-associated ophthalmopathy. *Curr Eye Res.* (2016) 41:927–32. doi: 10.3109/02713683.2015.1133833
9. Cavalcanti BM, Cruzat A, Sahin A, Pavan-Langston D, Samayoa E, Hamrah P. In vivo confocal microscopy detects bilateral changes of corneal immune cells and nerves in unilateral herpes zoster ophthalmicus. *Ocul Surf.* (2018) 16:101–11. doi: 10.1016/j.jtos.2017.09.004
10. Khan A, Li Y, Ponirakis G, Akhtar N, Gad H, George P, et al. Corneal immune cells are increased in patients with multiple sclerosis. *Transl Vis Sci Technol.* (2021) 10:19. doi: 10.1167/tvst.10.4.19
11. Stettner M, Hinrichs L, Guthoff R, Bairov S, Petropoulos IN, Warnke C, et al. Corneal confocal microscopy in chronic inflammatory demyelinating polyneuropathy. *Ann Clin Transl Neurol.* (2016) 3:88–100. doi: 10.1002/acn3.275
12. Dehghani C, Frost S, Jayasena R, Fowler C, Masters CL, Kanagasingam Y, et al. Morphometric changes to corneal dendritic cells in individuals with mild cognitive impairment. *Front Neurosci.* (2020) 14:556137. doi: 10.3389/fnins.2020.556137
13. Cruzat A, Witkin D, Baniasadi N, Zheng L, Ciolino JB, Jurkunas UV, et al. Inflammation and the nervous system: the connection in the cornea in patients with infectious keratitis. *Invest Ophthalmol Vis Sci.* (2011) 52:5136–43. doi: 10.1167/iovs.10-7048
14. Zhivov A, Stave J, Vollmar B, Guthoff R. In vivo confocal microscopic evaluation of Langerhans cell density and distribution in the corneal epithelium of healthy volunteers and contact lens wearers. *Cornea.* (2007) 26:47–54. doi: 10.1097/ICO.0b013e31802e3b55
15. Aggarwal S, Kheirkhah A, Cavalcanti BM, Cruzat A, Jamali A, Hamrah P. Correlation of corneal immune cell changes with clinical severity in dry eye disease: an in vivo confocal microscopy study. *Ocul Surf.* (2021) 19:183–9. doi: 10.1016/j.jtos.2020.05.012
16. Kheirkhah A, Muller R, Mikolajczak J, Ren A, Kadas EM, Zimmermann H, et al. Comparison of standard versus wide-field composite images of the corneal subbasal layer by in vivo confocal microscopy. *Invest Ophthalmol Vis Sci.* (2015) 56:5801–7. doi: 10.1167/iovs.15-17434
17. De Silva MEH, Zhang AC, Karahalios A, Chinnery HR, Downie LE. Laser scanning in vivo confocal microscopy (IVCM) for evaluating human corneal sub-basal nerve plexus parameters: protocol for a systematic review. *BMJ Open.* (2017) 7:e018646. doi: 10.1136/bmjopen-2017-018646
18. Wei Z, Cao K, Wang L, Baudouin C, Labbé A, Liang Q. Corneal changes in acanthamoeba keratitis at various levels of severity: an in vivo confocal microscopic study. *Transl Vis Sci Technol.* (2021) 10:10. doi: 10.1167/tvst.10.7.10
19. Levine H, Hwang J, Dermer H, Mehra D, Feuer W, Galor A. Relationships between activated dendritic cells and dry eye symptoms and signs. *Ocul Surf.* (2021) 21:186–92. doi: 10.1016/j.jtos.2021.06.001
20. Bitirgen G, Korkmaz C, Zamani A, Ozkagnici A, Zengin N, Ponirakis G, et al. Corneal confocal microscopy identifies corneal nerve fibre loss and increased dendritic cells in patients with long COVID. *Br J Ophthalmol.* (2021) bjophthalmol-2021-319450. doi: 10.1136/bjophthalmol-2021-319450 [Epub ahead of print].
21. Liu Q, Xu Z, Xu Y, Zhang J, Li Y, Xia J, et al. Changes in corneal dendritic cell and sub-basal nerve in long-term contact lens wearers with dry eye. *Eye Contact Lens.* (2020) 46:238–44. doi: 10.1097/icl.0000000000000691
22. Kheirkhah A, Rahimi Darabad R, Cruzat A, Hajrasouliha AR, Witkin D, Wong N, et al. Corneal epithelial immune dendritic cell alterations in subtypes of dry eye disease: a pilot in vivo confocal microscopic study. *Invest Ophthalmol Vis Sci.* (2015) 56:7179–85. doi: 10.1167/iovs.15-17433
23. Chinnery HR, Naranjo Golborne C, Downie LE. Omega-3 supplementation is neuroprotective to corneal nerves in dry eye disease: a pilot study. *Ophthalmic Physiol Opt.* (2017) 37:473–81. doi: 10.1111/opo.12365
24. Kamel JT, Zhang AC, Downie LE. Corneal epithelial dendritic cell response as a putative marker of neuro-inflammation in small fiber neuropathy. *Ocul Immunol Inflamm.* (2020) 28:898–907. doi: 10.1080/09273948.2019.1643028
25. Chinnery HR, Rajan R, Jiao H, Wu M, Zhang AC, De Silva MEH, et al. Identification of presumed corneal neuromas and microneuromas using laser-scanning in vivo confocal microscopy: a systematic review. *Br J Ophthalmol.* (2021) bjophthalmol-2020-318156. doi: 10.1136/bjophthalmol-2020-318156 [Epub ahead of print].
26. Mobeen R, Stapleton F, Chao C, Madigan MC, Briggs N, Golebiowski B. Corneal epithelial dendritic cell density in the healthy human cornea: a meta-analysis of in-vivo confocal microscopy data. *Ocul Surf.* (2019) 17:753–62. doi: 10.1016/j.jtos.2019.07.001
27. Vagenas D, Pritchard N, Edwards K, Shahidi AM, Sampson GP, Russell AW, et al. Optimal image sample size for corneal nerve morphometry. *Optom Vis Sci.* (2012) 89:812–7. doi: 10.1097/OPX.0b013e31824ee8c9
28. Gothwal VK, Pesudovs K, Wright TA, McMonnies CW. McMonnies questionnaire: enhancing screening for dry eye syndromes with Rasch analysis. *Invest Ophthalmol Vis Sci.* (2010) 51:1401–7. doi: 10.1167/iovs.09-4180
29. Britten-Jones AC, Kamel JT, Roberts LJ, Braat S, Craig JP, MacIsaac RJ, et al. Investigating the neuroprotective effect of oral omega-3 fatty acid supplementation in type 1 diabetes (nPROOFS1): a randomized placebo-controlled trial. *Diabetes.* (2021) 70:1794–806. doi: 10.2337/db21-0136
30. Schneider CA, Rasband WS, Eliceiri KW. NIH image to imageJ: 25 years of image analysis. *Nat Methods.* (2012) 9:671–5. doi: 10.1038/nmeth.2089
31. Koo TK, Li MYA. Guideline of selecting and reporting intraclass correlation coefficients for reliability research. *J Chiropr Med.* (2016) 15:155–63. doi: 10.1016/j.jcm.2016.02.012
32. Cruzat A, Qazi Y, Hamrah P. In vivo confocal microscopy of corneal nerves in health and disease. *Ocul Surf.* (2017) 15:15–47. doi: 10.1016/j.jtos.2016.09.004
33. Misra S, Craig JP, McGhee CN, Patel DV. Interocular comparison by in vivo confocal microscopy of the 2-dimensional architecture of the normal human corneal subbasal nerve plexus. *Cornea.* (2012) 31:1376–80. doi: 10.1097/ICO.0b013e31823f0b60
34. Parissi M, Karanis G, Randjelovic S, Germundsson J, Poletti E, Ruggeri A, et al. Standardized baseline human corneal subbasal nerve density for clinical investigations with laser-scanning in vivo confocal microscopy. *Invest Ophthalmol Vis Sci.* (2013) 54:7091–102. doi: 10.1167/iovs.13-12999
35. Cruzat A, Schrems WA, Schrems-Hoesl LM, Cavalcanti BM, Baniasadi N, Witkin D, et al. Contralateral clinically unaffected eyes of patients with unilateral infectious keratitis demonstrate a sympathetic immune response. *Invest Ophthalmol Vis Sci.* (2015) 56:6612–20. doi: 10.1167/iovs.15-16560
36. Klitsch A, Evdokimov D, Frank J, Thomas D, Saffer N, Meyer Zu Altenschildesche C, et al. Reduced association between dendritic cells and corneal sub-basal nerve fibers in patients with fibromyalgia syndrome. *J Peripher Nerv Syst.* (2020) 25:9–18. doi: 10.1111/jns.12360
37. Ferdousi M, Romanchuk K, Mah JK, Virtanen H, Millar C, Malik RA, et al. Early corneal nerve fibre damage and increased Langerhans cell density in children with type 1 diabetes mellitus. *Sci Rep.* (2019) 9:8758. doi: 10.1038/s41598-019-45116-z
38. Hao R, Liu Z, Chou Y, Huang C, Jing D, Wang H, et al. Analysis of globular cells in corneal nerve vortex. *Front Med (Lausanne).* (2022) 9:806689. doi: 10.3389/fmed.2022.806689
39. Colorado LH, Dando SJ, Harkin DG, Edwards K. Label-free imaging of the kinetics of round-shaped immune cells in the human cornea using in vivo confocal microscopy. *Clin Exp Ophthalmol.* (2021) 49:628–30. doi: 10.1111/ceo.13954

40. Badian RA, Andréasson M, Svenningsson P, Utheim TP, Lagali N. The pattern of the inferocentral whorl region of the corneal subbasal nerve plexus is altered with age. *Ocul Surf.* (2021) 22:204–12. doi: 10.1016/j.jtos.2021.08.015

Conflict of Interest: The authors declare that the research was conducted in the absence of any commercial or financial relationships that could be construed as a potential conflict of interest.

Publisher's Note: All claims expressed in this article are solely those of the authors and do not necessarily represent those of their affiliated organizations, or those of the publisher, the editors and the reviewers. Any product that may be evaluated in this article, or claim that may be made by its manufacturer, is not guaranteed or endorsed by the publisher.

Advantages of publishing in Frontiers

OPEN ACCESS
Articles are free to read for greatest visibility and readership

FAST PUBLICATION
Around 90 days from submission to decision

HIGH QUALITY PEER-REVIEW
Rigorous, collaborative, and constructive peer-review

TRANSPARENT PEER-REVIEW
Editors and reviewers acknowledged by name on published articles

Frontiers
Avenue du Tribunal-Fédéral 34
1005 Lausanne | Switzerland

Visit us: www.frontiersin.org
Contact us: frontiersin.org/about/contact

REPRODUCIBILITY OF RESEARCH
Support open data and methods to enhance research reproducibility

DIGITAL PUBLISHING
Articles designed for optimal readership across devices

FOLLOW US
@frontiersin

IMPACT METRICS
Advanced article metrics track visibility across digital media

EXTENSIVE PROMOTION
Marketing and promotion of impactful research

LOOP RESEARCH NETWORK
Our network increases your article's readership